Alfred-Wegener Institute for Polar and Marine Research
Global Change in the Marine Realm – Graduate School
University of Bremen

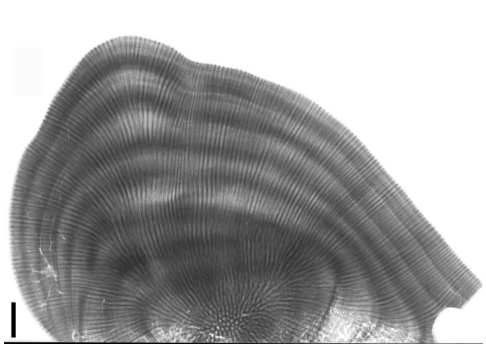

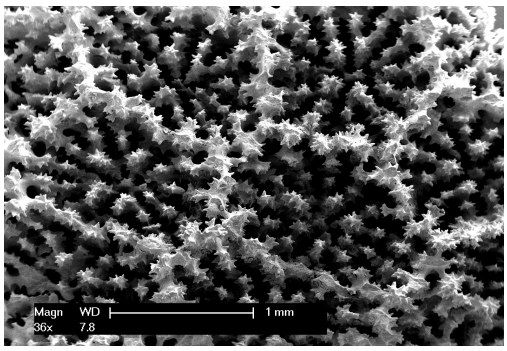

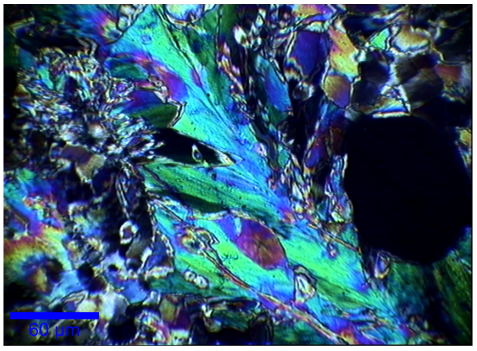

Patterns and controls of calcification in tropical reefs:
from the coral skeletal microstructure to reef framework scale

Marlene Wall
PhD Thesis, University Bremen
Bremen, September 2012

Alfred-Wegener Institute for Polar and Marine Research
Global Change in the Marine Realm – Graduate School
University of Bremen

Patterns and controls of calcification in tropical reefs:
from the coral skeletal microstructure to reef framework scale

Dissertation submitted by

Marlene Wall

In partial fulfillment of the requirements for the degree of Doctor of natural sciences
-Dr. rer. Nat. –

-Faculty of Biology/Chemistry
-University of Bremen

Bremen, September 2012

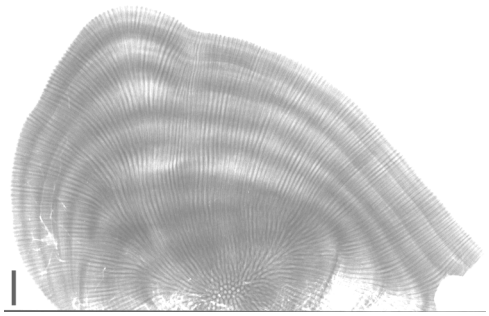

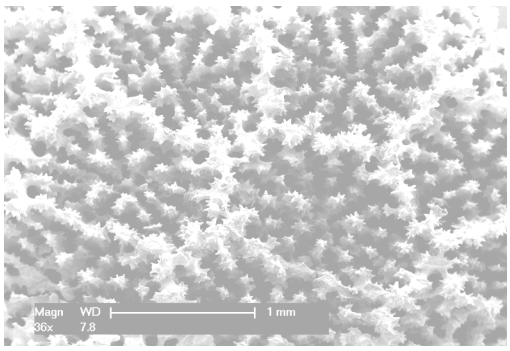

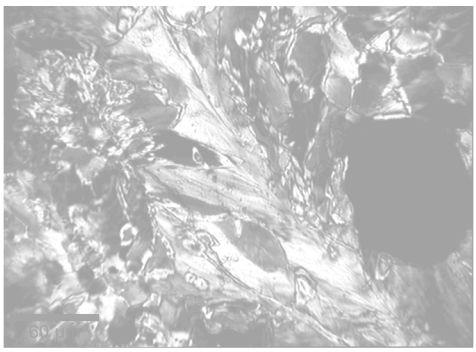

MARIE CURIE ACTIONS cal.mar.o AWI GLOMAR Universität Bremen

The present study has been realized at the Alfred-Wegener Institute (AWI), Bremerhaven, Germany and the Phuket Marine Biological Center (PMBC), Phuket, Thailand as part of the EU FP 7 Marie Curie International Training Network (ITN) CalMarO – Calcification by Marine Organisms – Workpackage II – Research Topic 5.

The project was mainly funded by the Marie Curie ITN CalMarO (FP7-PEOPLE-2007-1-1-ITN, grant number 215157). Additional financial support was provided by the German Federal Ministry of Education and Research (BMBF) project BIOACID (Grant Number 03F0608B, Bioacid 3.2.3 Coral calcification in marginal reefs), the AWI and PMBC.

Support was given by:

- the Bremen International Graduate School of Marine Sciences, funded by the German Research Foundation (DFG) within the frame of the Excellence Initiative by the German federal state governments to promote science and research at German universities and

- the CalMarO network of 12 research institutions and 4 commercial enterprises.

Examination committee

1st Examiner:	Prof. Dr. Claudio Richter Bentho-Pelagic Processes, Alfred Wegener Institute, Bremerhaven, Germany
2nd Examiner:	Prof. Dr. Christian Wild Coral Reef Ecology, Center for Tropical Marine Ecology, Bremen, Germany
1st Additional Examiner:	Prof. Dr. Kai Bischof Department of Marine Botany, University of Bremen, Bremen, Germany
2nd Additional Examiner:	Dr. Tim Rixen Department of Biogeochemistry, Center for Tropical Marine Ecology, Bremen, Germany
1st student member:	Laura Fillinger PhD student, Bentho-Pelagic Processes, Alfred Wegener Institute, Bremerhaven, Germany
2nd student member:	Franziska Kupperat MSc Marine Biology Student, University of Bremen, Bremen, Germany

Für meinen Opa!

Table of Content

List of Tables

List of Figures

SYNOPSIS

The global distribution of coral reefs is mainly limited by temperature and light; further factors controlling reef development include nutrients, salinity, oxygen concentration and aragonite saturation state. The most vigorous reef growth can be found within the tropics, where corals build a massive 3-dimensional carbonate framework. However, in some areas reefs are confronted with strongly fluctuating environmental conditions and they are subjected to marginal conditions. Both can hamper reef formation and prevent framework development. In such areas (i.e. upwelling regions, reefs close to run-off areas with high turbidity) coral growth and reef functioning can be studied under sub-optimal conditions. Investigating the potential of reefs to adapt to - and identifying the associated costs for living in - such unfavorable environmental conditions provides further insight on the fate of coral reefs in a changing climate.

An underexplored, but potentially important source of disturbance in coral reefs is the impact of internal waves. In contrast to surface waves internal waves travel along density gradients within the water column and can attain much larger amplitudes. They are a common hydrodynamic phenomenon in all ocean basins. In the Andaman Sea, internal waves show extraordinary large amplitudes of 60 m or higher and travel with speeds of up to 2 m s^{-1}. These large amplitude internal waves (LAIW) induce cold-water pulses that concomitantly change salinity, pH and oxygen in shallow reef areas of several offshore islands on the Thai continental shelf (→ Manuscript I). These offshore islands are additionally impacted by high surface waves due to the southwest (SW) monsoon. Both LAIW and SW monsoon affect the islands westerly sides. A previous study provided a good characterization of LAIW and SW monsoon exposed and sheltered reef coral community structure of the Similan Island chain close to the shelf break. The previous investigation particularly highlighted the reduced carbonate framework on the exposed sites. However, the limited spatial extent of this investigation, combined with the spatial covariance of the environmental factors, made it difficult to assess the relative contributions of monsoon and LAIW to the observed biological changes. Here the spatial scale of this previous study was extended and it was attempted to disentangle the effects of LAIW and SW monsoon on coral reefs. The reef framework height was determined and the environmental conditions monitored at an intermediate depth of 15 m on 5 offshore islands. Proxy values were used to characterize the environmental conditions due to LAIW and SW monsoon. For the examined depth the reef framework builder are subjected to surface waves-induced sedimentation, strong currents and LAIW impact. Temperature anomalies were used as surrogate for LAIW intensity, bottom grain size reflects the hydrodynamic conditions and sedimentation rate gives an indication of surface wave induced turbulences. In contrast to sedimentation the LAIW intensity and bottom sediment grain size both regressed with the reef framework height. It was a correlation found between reef framework height and a combination of grain size and LAIW intensity suggesting a combined impact of LAIW and monsoon affecting the intermediate depth. The observed relationship with LAIW intensity supports the previously observed decreased framework height in 20 m as LAIW intensity increases with depth. Hence, LAIW impact prevents a vertical extension of the framework as well as a lateral expansion of a dense coral community below the storm-accretion limit into deeper areas. (→ Manuscript I).

Additionally, skeletal properties were studied along this natural gradient on LAIW and SW monsoon impact. The results suggest that hydrodynamic processes (such as increased currents and waves) and LAIW, potentially influence skeletal density at these offshore islands. LAIW intensity increases with depth. Thus, more studies are necessary to reveal if the relationship between density and LAIW intensity persists with greater depth where LAIW become stronger. (→ Manuscript III)

The ongoing global climate change threatens coral reefs. Worldwide reported bleaching events due to elevated seawater temperature contribute significantly to coral reef degradation. Coral bleaching refers to the disruption of their symbiosis with microscopic algae, consequent symbiont expulsion and, thus, loss of coral coloration. Bleaching events are often associated with significant loss in live coral cover, and recovery to pre-bleaching states can take several years up to decades if at all possible. The fate of coral reefs and their adaptation potential to cope with rising seawater temperature cannot be clearly answered with our current knowledge. Moreover, thermal stress and bleaching response are highly heterogeneous

among locations and amongst species influenced by the interactions of local physical, chemical and biological conditions. Several conceptual environmental settings were hypothesized to help corals withstand thermal stress – i.e. upwelling regions, high-latitude settings, offshore reefs and deep reef regions. Internal wave induced cold-water pulses in shallow reef communities have so far not received strong attention as potential cooling agents during bleaching because they are short-lived in contrast to upwelling and cannot be captured by satellite monitored sea surface temperature data. The Andaman Sea experienced a severe bleaching event in 2010. The temperature and bleaching response was monitored *in situ* at several offshore islands. It was shown that LAIW induced cold-water pulses on exposed sites prevailed during the thermal stress period. During that time more bleached and recently dead corals were observed on the sheltered sides, in contrast to the exposed island sides. LAIW intensity differed between sites and decreased gradually. This gradual decrease in cooling intensity was reflected in an increase in bleaching response. It is also known that branching species are in general more susceptible than massive species, and even within growth morphologies the response can vary. The community composition differed between sites and hence, the susceptibility of the reef community to heat stress. Site-specific community composition and cumulative heat stress both together explained 75 % of the observed variability in bleaching response. The heat stress exceeded the stress limits of highly susceptible taxa and they vanished from the east side but survived in small numbers on the exposed sites. The study showed that Andaman Sea offshore island exposed sides provided protection from severe heat stress and that they can serve as refuge areas. (→ Manuscript II)

Coral skeletal annual growth cycles are displayed by the skeletal density pattern that form a high- and a low-density band each year. They are compared to tree rings and likewise record the environmental conditions they have grown in. Skeletal proxies are known to provide useful information of past environmental conditions (e.g. temperature, nutrients, currents) but are as well subjected to biological processes that potentially blur skeletal recording - the so-called 'vital effects'. Studying sites with strong environmental fluctuations can potentially provide new insights into the skeletal recording potential and constraints. Coral skeletons of *Porites lutea* were collected at LAIW-exposed and -sheltered island sides, where the temperature values were recorded close to the collected corals. Skeleton strontium to calcium (Sr/Ca) ratios – a temperature proxy - were determined at spatial scales representing sub-daily temporal resolution. Preliminary results suggest that Sr/Ca ratios do not resolve the high variability in the LAIW-exposed side. In accordance to other studies, this potentially implies that biological processes, which influence the calcification process, mask the recording potential of corals at daily to sub-daily scales. (→ Manuscript IV)

A better understanding of spatial coral skeletal growth patterns is desirable in order to improve the interpretation of high-resolution proxy data. Several growth concepts exist that link the incremental growth lines of the bulk skeleton (the skeletal fibers formed of layers of organic and mineral phase) with the arrangement of centers of calcification. These growth concepts indicate that tracing of individual growth lines potentially helps to improve proxy sampling. However, conventional sample treatment to make growth lines visible involves etching of skeletal surface at the expense of not being able to perform follow up analyses of trace elements or isotopes. The application of confocal Raman mapping (CRM) on coral skeletal surfaces has shown that it can be used to visualize coral crystal arrangement and trace growth layers without altering the sample surface. This allowed subsequent analysis of trace elements (magnesium (Mg), sulfur (S), Ca, Sr) on the same sample surface. Prominent low Mg growth lines were detected within the skeleton, a fact that potentially plays a role in the skeletal growth cyclicity. Hence, CRM is a highly valuable diagnostic tool, which enables tracing of growth lines over large skeletal areas, and relates centers of calcification and incremental growth lines and relates the skeletal organic to the mineral phase. This simultaneously obtained information definitively deepens our understanding of growth patterns in coral skeletons and helps to improve growth concepts above micrometer scale. (→ Manuscript V)

ZUSAMMENFASSUNG

Das Vorkommen von Korallenriffen, wie wir sie aus den Tropen kennen, wird maßgebend von Temperatur- und Lichtverhältnissen bestimmt. Jedoch können auch andere Faktoren, wie Nährstoffkonzentrationen, Salzgehalt, Sauerstoffkonzentrationen und die Aragonit-Sättigung des Meerwassers, limitierend auf das Korallenwachstum wirken. Korallenriffe zeichnen sich in den Tropen, wo die Umweltbedingungen für das Korallenwachstum grundsätzlich optimal sind, durch den Aufbau eines internen festen Gerüsts aus, das dreidimensional stark gegliedert und verbunden ist. Diese komplexe Riffstruktur bietet verschiedensten Organismen Lebensraum und ist unter anderem für eine hohe Artenvielfalt in Riffen verantwortlich. In manchen Gebieten können jedoch Umweltbedingungen vorherrschen, die Riffbildung verlangsamen oder unterbinden. In diesen Gebieten (z.B. Regionen mit Auftrieb von Tiefenwasser, Riffe in der Nähe einer Flussmündung mit hoher Wassertrübe) kann abseits von optimalen Bedingungen die Funktionalität von Riffen und deren Wachstum untersucht werden. Die Ergebnisse dieser Untersuchungen geben Aufschluss über mögliche Anpassungen und Kosten, die mit veränderten Umweltbedingungen einhergehen.

Interne Wellen sind ein häufiges ozeanographisches Phänomen sind, jedoch deren Auswirkung auf Ökosysteme weitgehend unerforscht ist. Im Unterschied zu Oberflächenwellen bewegen sich interne Wellen innerhalb der Wassersäule – entlang von Dichtesprungschichten – fort und können große Wellenamplituden erreichen. In der Andamanensee erreichen interne Wellen Amplituden von über 60m und bewegen sich mit einer Geschwindigkeit von 2 m s^{-1}. Aufgrund ihrer Wellenamplitude werden diese als interne Wellen mit großer Amplitude bezeichnet (engl. large amplitude internal waves (LAIW)). Wenn sich solche Wellen auf den Schelf zubewegen, transportieren sie Wasser aus der Tiefe in seichte Gebiete. Dabei verändern sich die Umweltbedingungen drastisch mit Temperaturabfällen bis zu 8°C und Senkung des pH-Wertes. Zusätzlich steigt auch der Salzgehalt und fällt die Sauerstoffkonzentration, wie für die untersuchten Inseln am Kontinentalschelf nachgewiesen wurde (→ Manuscript I). In der Andamanensee herrscht ein Monsunklima. Das Untersuchungsgebiet prägt vor allem der Südwest (SW) Monsun (Mai bis November), der sich durch starke Winde, hohe Wellen und intensiven Regen auszeichnet. Sowohl LAIW als auch SW Monsun kommen aus derselben Richtung und beeinflussen die Riffe auf den Westseiten der Inseln. Eine vorangegangene Studie beschrieb die Riffe der Similan Islands, einer Inselkette nahe der Schelfkante, und hob insbesondere den Unterschied in der Riffbildung mit geringer Riffentwicklung an den Westseiten hervor. Aufgrund der räumlichen Beschränkung dieser vorangegangenen Studie auf eine einzige Inselkette einerseits und der Tatsache, dass es sich um zwei Störungen, die aus der gleichen Richtung kommen, handelt andererseits, konnte der jeweilige Einfluss jeder Störung auf die Riffbildung nicht eindeutig identifiziert werden. In der vorliegenden Studie wurde das Untersuchungsgebiet erweitert und versucht, den relativen Effekt von beiden Störungen zu ermitteln. Die Riffentwicklung (Höhe des festen internen Gerüsts) wurde in 15 m Tiefe an 5 verschiedenen Inseln mit unterschiedlicher Distanz zur Schelfkante bestimmt. Verschiedene Umweltvariablen wurden kontinuierlich gemessen, um die beiden Störungen zu charakterisieren und Näherungswerte für deren Einfluss zu ermitteln. In der untersuchten Wassertiefe wurden die Korallen an den Inselwestseiten durch fluktuierende Bedingungen durch LAIW Einfluss (Temperaturanomalien) und erhöhte Sedimentation während des SW Monsuns beeinflusst. Auch herrschten generell stärkere hydrodynamische Bedingungen an den Westseiten (gröberes benthisches Sediment). Die einzelnen Parameter unterschieden sich zwischen den Standorten und konnten gemäß der Intensitäten gereiht werden. Im Gegensatz zu den Westseiten waren die Bedingungen an den Ostseiten weniger variable und es wurde keine erhöhte Sedimentation gemessen. LAIW-Intensitäten sowie die hydrodynamischen Bedingungen korrelierten jeweils mit der Riffentwicklung, wohingegen die Sedimentation keinen Zusammenhang zeigte. Beide Faktoren zusammen (LAIW und hydrodynamische Bedingungen) erklärten 77% der Variabilität in der Riffentwicklung an den untersuchten Standorten. Das deutet daraufhin, dass LAIW und SW Monsun die Riffe in der untersuchten Tiefe beeinflussen. Die Korrelation mit LAIW indiziert zudem, dass diese für das geringe Riffwachstum in 20 m verantwortlich sind und eine Tiefenausbreitung verhindern, da LAIW in der Tiefe an Intensität zunehmen. (→ Manuscript I)

Zudem wurden Korallenskelette von der primär riffbildenden Koralle *Porites lutea* gesammelt und die Wachstumseigenschaften (Längenwachstum, Skelettdichte, Kalzifizierung) im Hinblick auf die unterschiedlichen Umweltbedingungen untersucht. Die Ergebnisse zeigten, dass das Längenwachstum unter und die Dichte über dem weltweiten Durchschnitt liegt. Des Weiteren lassen die Untersuchungen einen Zusammenhang zwischen der LAIW-Intensität und den hydrodynamischen Bedingungen einerseits und der Skelettdichte andererseits erkennen. Allerdings sind weitere Studien notwendig, um diesen Zusammenhang sowohl in der gleichen als auch in größerer Tiefe zu verifizieren. (→ Manuscript III)

Der weltweite Anstieg der Wassertemperatur der Meere und die mit überhöhter Temperatur einhergehenden Korallenbleichen stellen eine enorme Bedrohung für Korallenriffe dar. Korallenbleichen führen zu hohen Mortalitäten und eine Erholung der Riffe kann Jahre bis Jahrzehnte dauern. Das Schicksal der Riffe weltweit hängt stark von der Fähigkeit der Korallen, sich an die steigenden Temperaturen anzupassen, ab. Jedoch weiß man noch zu wenig, ob diese Anpassung möglich ist. Zukunftsprognosen werden erschwert durch die zum Teil sehr heterogenen Reaktionen auf Temperaturstress in unterschiedlichen Regionen und von unterschiedlichen Korallenarten. Verschiedene geographische Standorte wurden als 'Zufluchtsstätten' für Korallen während Temperaturstress hypothetisch identifiziert und es wird vermutet, dass dort Korallen überleben und sich von dort wieder auf geschädigte Bereiche ausbreiten können. Solche Gebiete umfassen Regionen mit Auftrieb von Tiefenwasser (engl. upwelling), Riffe in höheren Breitengraden, Riffe abseits der Küste, wo starke Wasserdurchmischung vorherrscht, sowie Riffe in größeren Tiefen (>30m). LAIW sind im Gegensatz zu 'upwelling' sehr kurzlebig und führen nur zu kurzfristiger Abkühlung. Riffe, die internen Wellen ausgesetzt sind, haben als potentielle 'Zufluchtsstätten' wenig Beachtung bekommen. In der Andamanensee kam es 2010 zu einer starken Korallenbleiche und es wurde untersucht, ob die den LAIW ausgesetzten Inselseiten als sogenannte 'Zufluchtsstätten' dienen können. Die Temperaturdaten zeigten, dass LAIW-induzierte Kaltwasserpulse während der Temperaturstressphase bestehen blieben und für Abkühlung sorgten. Die Abkühlungsintensitäten unterschieden sich zwischen den einzelnen Standorten und waren am stärksten auf den exponierten Westseiten. Unterschiedliche Arten reagieren unterschiedlich empfindlich auf Temperaturstress. Daraus resultierte je nach Artzusammensetzung der Riffe eine unterschiedliche Anfälligkeit für Bleiche. Die Intensität der Korallenbleiche unterschied sich ebenfalls von Standort zu Standort und stellte eine Funktion aus LAIW-Abkühlung und der Riffkorallenartzusammensetzung dar. Der Temperaturstress überstieg die Fähigkeit von empfindlichen Arten, dem Stress standzuhalten, und führte zu deren Absterben an den Ostseiten. Sie überlebten nur an den LAIW exponiertesten Westseiten. Die Studie zeigte, dass LAIW-beeinflusste Riffe Schutz vor starkem Temperaturstress boten und als 'Zufluchtsstätten' fungieren können. (→ Manuscript II)

Korallenskelette bilden jährliche Dichtebänder bestehend aus einem Band aus hoher und einem aus niedriger Dichte, die gerne mit den Jahresringen von Bäumen verglichen werden. Die aus den Jahresringen der Korallen gewonnenen Informationen geben Aufschluss über die Umweltbedingungen während ihres Wachstums. Sogenannte 'Klimaproxies' haben gezeigt, dass z.B. Temperatur, Salzgehalt und Strömungen aus vergangenen Zeiten in Korallenskeletten rekonstruiert werden können. Doch stören mitunter biologische Prozesse die Archivierung von Umweltinformationen. Diese Beeinträchtigung ist bekannt als 'vital effect'. Die Untersuchung von Korallenskeletten, deren Standorte einer hohen natürlichen Schwankung der Umweltbedingungen unterliegen, kann möglicherweise neue Erkenntnisse über die Einschränkungen der Umweltaufzeichnung in Korallen liefern. Es wurden Skelette von zwei gegenüberliegenden Inselseiten (exponiert und nicht exponiert zu LAIW-Kaltwassereinflüssen) gesammelt und ein 'Klimaproxy' für die Temperatur mit einer zeitlichen Auflösung von unter einem Tag analysiert. Die ersten Ergebnisse haben gezeigt, dass die hohen Umweltfluktuationen an der exponierten Inselseite nicht aufgelöst werden können. In Übereinstimmung mit anderen Studien implizieren diese Ergebnisse, dass biologische Prozesse die Kalzifizierung beeinflussen und das Archivierungspotential von Korallen in dieser zeitlichen Auflösung verschleiern. (→ Manuscript IV)

Die Wachtumsraten können einen Effekt auf das Archivierungsverhalten der unterschiedlichen Klimaproxies haben und werden in weiterer Folge untersucht (→ Manuscript IV). Zusätzlich kann auch ein besseres Verständnis der räumlichen Wachstumsabfolgen von Korallenskeletten maßgebend dazu beitragen, die Interpretation von Klimaproxies in höherer zeitlicher Auflösung zu verbessern. Korallenwachstumskonzepte exisitieren auf der Ebene einzelner Wachstumslinien (von ein paar μm

Stärke) im fibrösen Teil des Korallenskelettes (coral fibers) und beschreiben die Abfolge von organischem und mineralischem Material. Andere Wachstumskonzepte beschreiben die räumliche und zeitliche Anordnung von Kalzifizierungszentren und fibrösen Skelettanteil. Diese Konzepte zeigen, dass das Nachverflogen der Wachstumslinien dazu beitragen kann, Klimaproxyanalysen zu verbessern. Die bisherigen Methoden zum Visualisieren dieser Linien erforderten jedoch ein Ätzen der Probenoberfläche, wodurch weitere Analysen nicht mehr an der gleichen Probenoberfläche durchgeführt werden konnten. Die Konfokale Raman Spektroskopie ermöglicht eine Untersuchung von Biomineraloberflächen und konnte zeigen, dass Wachstumslinien sichtbar gemacht werden können. Diese Methode erlaubt ein nachträgliches Analysieren von Klimaproxies an der gleichen Probenoberfläche. Dabei wurden Wachtumsbänder gefunden, die im Gegensatz zu den bisher beschriebenen Bändern einen reduzierten Magnesiumgehalt aufweisen. Die Untersuchungen zeigten, dass Ramananalysen zum besseren Verständnis des Korallenwachstums beitragen können. (→ Manuscript V)

1. INTRODUCTION

1.1 GENERAL INTRODUCTION

1.1.1 Reefs from shallow to deep – environmental constraints and perspectives

M Wall and C Jantzen

published in the YouMaRes (Young Marine Researchers) 3.0 Conference Proceedings – Session VII Review,12.-14. September 2012, Lübeck , Germany

In contrast to mariners who classify reefs as hazardous shoals scientists denote them as permanent hard structure of biological origin distinctly elevated from the substrate. Reefs are built by a variety of organisms such as corals, coralline algae, mussels or sponges. Since Darwin's monography on coral reefs (Darwin, 1842) we usually associate reefs with the tropics, where they are known as "oasis in the sea". Thriving in nutrient-poor waters coral reefs are highly productive featuring a diverse community on various trophic levels. This 'Darwin paradox' can be explained by the close coupling and the comprehensive matter and nutrient fluxes between individuals, functional groups and compartments. Studies on tropical coral reefs started in the early 40ies of the last century with the work of Hans Hass and Thomas F. Goreau and provided first insight into coral reef ecosystem functioning and services.

The distribution of (sub-) tropical coral reefs is mainly limited by temperature and light; further factors controlling reef development may be nutrients, salinity, oxygen concentration and aragonite saturation state (Kleypas *et al.,* 1999). The most vigorous reef growth can be found within the tropic of Capricorn and the tropic of Cancer with minimum mean winter seawater temperature of 18°C (Schuhmacher, 1988) The most divers coral reef communities can be found in the 'coral triangle' the area between the Solomon Islands, Indonesia and the Philippines. At the regional scale physical forces (e.g. waves, currents and storms) and biological factors (e.g. larvae supply, diversity) determine reef morphology and zonation (Kleypas *et al.,* 1999).

Scleractinian corals build reefs with their calcareous skeletons and form the reef framework. Encrusting coralline algae are the reef's cement binding and stabilize the reef structure (Perry *et al.,* 2008). Simultaneously, reef framework structures are subjected to bioerosion by organisms (e.g. boring sponges) and physical forces (e.g. water movement undermining reef formation) (Tribollet & Golubic, 2011). Under optimal conditions construction exceeds destruction and the reef grows. It may develop from a patch reef or fringing reef into a barrier reef (see Box 1 for different reef types). Its hard 3D-structure alters currents and provides a variety of microhabitats (e.g. with respect to light and flow regimes) for numerous organisms (Achituv & Dubinsky, 1990, Riegl & Piller, 2000).

Most tropical corals live in a symbiosis with algae, the so-called zooxanthellae. These autotrophs provide the coral host with sunlight derived assimilates and are a crucial factor for the high growth and productivity rate of coral reefs in shallow areas. A tight coupling of symbionts and host may promote

calcification and therefore reef growth. Nevertheless as definite dependencies and relationships are still elusive, the 'concept of light enhanced calcification' (Goreau & Goreau, 1959) continues to be controversially discussed (Allemand *et al.*, 2011). Hence, the most fundamental process – the creation of the calcareous skeletons – still bears a lot of secrets.

BOX 1: Coral reef types

The classification of the different reef types goes back to Darwin (1842) who provided one of the earliest and comprehensive descriptions for coral reefs. His classifications are still enduring and he basically he distinguished 3 main types: (1) fringing reefs, (2) barrier reefs and (3) atolls. The main criteria for differentiation are the distance to the shore and the association to the non-limestone rock. These first definitions still adequately define the reef systems - however the borders between the 3 types are not always as clear - and resulted in calling them „almost barrier" or „almost atoll" reefs (Kennedy and Woodroffe, 2002). Additionally, terms such as patch reef or bommie are used to describe coral carbonate structures.

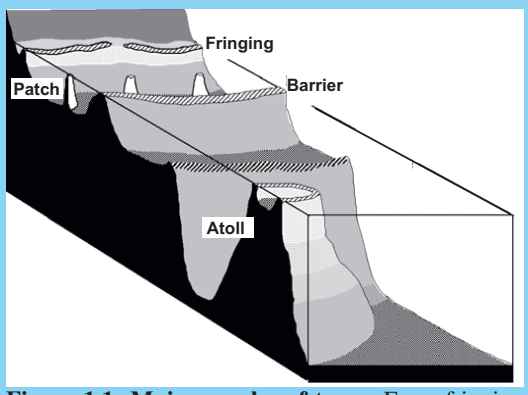

Figure 1.1: Major coral reef types. From fringing reefs, patches and barrier reefs to atolls (modified after http://geology.uprm.edu/)

Main reef types (Fig. 1.1):
Fringing reefs are the morphologically simplest ones close to the shore. *Barrier reefs* are separated from the shoreline by a lagoon. *Atolls* represent ring-like barrier reef surrounding a lagoon.
Patch reefs - are small reefs that crop out like pinnacles. Usually they are located within barrier reefs, but can also occur on the shelf.
All these classifications are based on the corals ability to form a 3-dimensional carbonate framework structure - so called framework building coral communities (Riegl, 2001). However, worldwide coral communities exist that form dense coral carpets without building a rigid framework (Riegl, 2001). Mechanisms keeping them from `framework building´ are described in Box 2.

Tropical coral reefs are often called the rain forests of the sea as they likewise harbor numerous species and are highly productive (Sorokin, 1990, Wood, 2001). They have important commercial relevance by supplying goods and services to people (e.g. tourism, coastal protection, food) (Moberg & Folke, 1999). One third of the world's human population depends – at least to some part - on tropical coral reefs for its livelihood. Today coral reefs are declining as a result of pollution, overfishing, tourism, coral bleaching and diseases (Hughes *et al.*, 2003). The ongoing global climate change and the related alterations in seawater chemistry pose additional threats (Hoegh-Guldberg *et al.*, 2007, Kleypas *et al.*, 2001). The fate of coral reefs, their adaptation potential to cope with rising seawater temperature and ocean acidification cannot be clearly answered with our current knowledge.

Reefs in higher latitudes – subtropical reefs - may face relatively low minimum temperatures (e.g. Iki Island in Japan with minimum temperature values of 13.3 °C, Yamano *et al.*, 2001) or huge annual temperature ranges (e.g. Arabian Gulf with temperature ranges from 14°C to 37°C, Riegl 2003). Borderline conditions and strong environmental gradients can as well be found within the tropics in upwelling regions or close to CO_2 vent system such as the Gulf of Chiriqui or Papua New Guinea, (Glynn, 1993, Fabricius *et al.*, 2011, Manzello, 2010). In these areas coral growth and reef functioning

can be studied beyond optimal conditions (see Box 2 for environmental control of reef framework formation). Adaptation potential and associated costs of living in these extreme environments may give further insight on the fate of coral reefs (Fabricius *et al.*, 2011, Manzello, 2008). High-latitude reefs and reefs in upwelling regions that are exposed to generally lower temperatures are regarded as refuge areas for rising temperature and predicted future recurrence of heating events (Riegl, 2003).

BOX 2: Reef framework formation and non-framework coral communities

Reefs flourish in clear, oligotrophic, warm, tropical water and form complex and extensive 3-dimensional carbonate structures (Perry & Larcombe, 2003). A deviation from optimal conditions results in a reduction of complexity and prevents the formation of true reefs. Globally studied coral communities under different „marginal" conditions range from a slightly depressed framework relief formation to only scattered coral colonies that remain and do not form a carbonate relief at all (Fig. 1.2). The most obvious gradient in environmental conditions is derived from latitudinal differences. Going from the tropics to the subtropics - the high latitudes - the conditions change to environmental settings that do not allow corals to grow towards the sea surface. In these regions corals form communities that follow the rocky bottom (Fig. 1.2C, South Africa - Riegl, 2003). Even within the tropical belt - of, in general, optimal conditions for reef growth - certain environmental settings can prevent framework accretion. Such less developed reefs are often referred to as incipient reefs (van Woesik & Done, 1996). Environmental settings that prevent reef framework formation are for instance high turbidity due to periodic storms (Fig. 1.2B, e.g. Great Barrier Reef - Kleypas, 1996, van Woesik & Done, 1996) or upwelling of diapycnal water into shallow reef areas (Fig. 1.2D, e.g. Oman - Benzoni *et al*., 2003)

Understanding the driving forces of reef formation under marginal conditions can provide a better insight into reef dynamics and how future reefs might look like under changing climatic conditions and associated seawater changes (Perry & Larcombe, 2003).

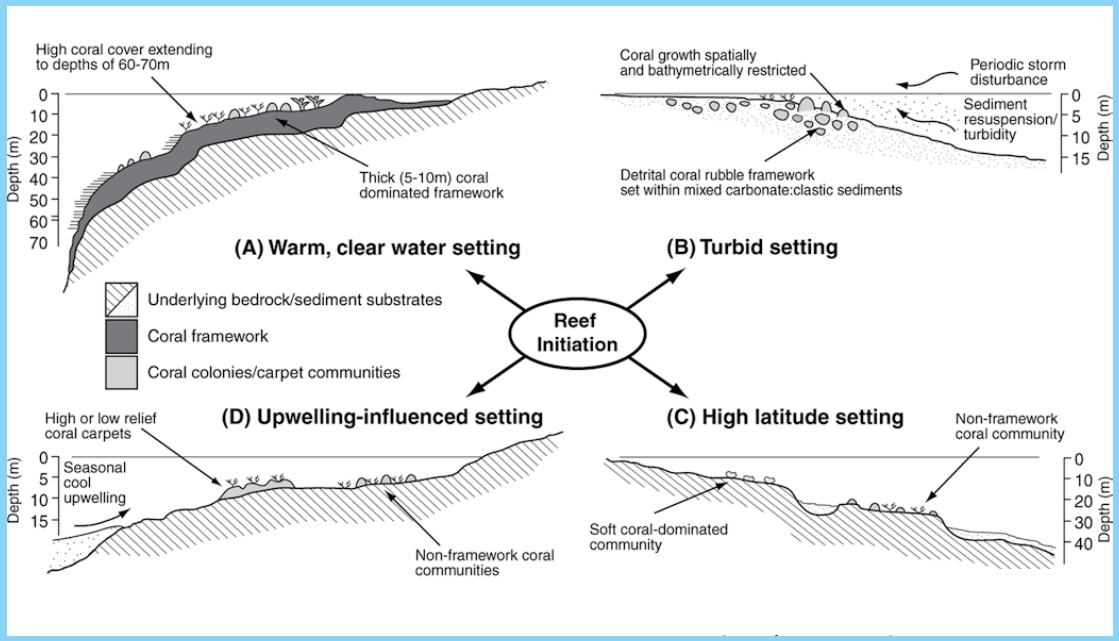

Figure 1.2: Schematic representation of reef formation under different environmental settings (modified after Perry & Larcombe, 2003). Environmental settings: (a) optimal conditions versus different marginal settings (b) high turbidity (c) high latitude and (d) upwelling conditions.

Reefs in deeper regions are recently discussed as a source of larvae that may replenish threatened shallow water reefs. This connectivity may potentially improve shallow reef resilience in a changing

environment (Lesser *et al.*, 2009). The so-called mesophotic reefs extend down to 150 m and comprise symbiont and non-symbiont-bearing corals, macroalgae and reef forming sponge communities.

In the deep sea cold-water corals thrive till depth of over thousands of meters. They face cold and light-less conditions nevertheless forming likewise diverse and productive reefs and providing crucial structures on the otherwise vast sea floor (Roberts *et al.,* 2009). Cold-water corals - and temperate water corals - are not restricted to the abyss. They may be found in shallower water in fjord regions or in the Mediterranean covering a global distribution (Freiwald *et al.*, 2004, Tsounis *et al.*, 2010). Research on cold-water corals is young and due to their mostly deep water occurrence research is often elaborate and expensive. Still, we learned a lot about cold-water corals within the last two decades and therefore they may be still 'out of sight but no longer out of mind' (Freiwald *et al.*, 2004). They may have a great adaptation potential as they could grow close to the oxygen minimum zone (Dodds *et al.*, 2007) and in low aragonite saturation (Maier *et al.*, 2012, McCulloch *et al.*, 2012). Their calcification is regarded as slow, but newer observations indicate an underestimation of their growth potential (Bell & Smith, 1999).

References:

Achituv Y, Dubinsky Z (1990) *Evolution and zoogeography of coral reefs,* In: *Coral Reefs. Ecosystems of the world,* (ed Dubsinky, Z) pp 1-9, Amsterdam, PAYS-BAS, Elsevier.

Allemand D, Tambutté É, Zoccola D, Tambutté S (2011) Coral calcification, cells to reefs. In: *Coral Reefs: An Ecosystem in Transition*. (eds Dubinsky Z & Stambler N) pp 119-150. Springer Netherlands.

Bell N, Smith J (1999) Coral growing on North Sea oil rigs. *Nature*, **402**, 601.

Dodds LA, Roberts JM, Taylor AC, Marubini F (2007) Metabolic tolerance of the cold-water coral *Lophelia pertusa* (Scleractinia) to temperature and dissolved oxygen change. *Journal of Experimental Marine Biology and Ecoloy,* **349**, 205–214.

Fabricius KE, Langdon C, Uthicke S *et al*. (2011) Losers and winners in coral reefs acclimatized to elevated carbon dioxide concentrations. *Nature Climate Change,* **1**, 165-169.

Freiwald AJH, Fosså SJH, Grehan A, Koslow A, Roberts JM (2004) Cold-water coral reefs, Out of sight – no longer out of mind. UNEP-WCMC, Cambridge, p84.

Goreau T, Goreau NI (1959) The physiology of skeleton formation in corals. II. Calcium deposition by hermatypic corals under different conditions. *Biological Bulletin,* **117**, 239-250.

Glynn (1993) Monsoonal upwelling and episodic *Acanthaster* predation as probable controls of coral reef distribution and community structure in Oman, Indian Ocean. *Atoll Research Bulletin*, **379**, 1-66.

Hoegh-Guldberg O, Mumby PJ, Hooten AJ *et al*. (2007) Coral reefs under rapid climate change and ocean acidification. *Science,* **318**, 1737-1742.

Hughes TP, Baird AH, Bellwood DR *et al*. (2003) Climate change, human impacts, and the resilience of coral reefs. *Science,* **301**, 929-933.

Kleypas JA, Buddemeier RW, Gattuso J-P (2001) The future of coral reefs in an age of global change. *International Journal of Earth Science (Geologische Rundschau),* **90**, 426-437.

Kleypas JA, McManus JW, Meñez LAB (1999) Environmental limits to coral reef development: where do we draw the line? *American Zoologist,* **39**, 146-159.

Lesser MP, Slattery M, Leichter JJ (2009) Ecology of mesophotic coral reefs. *Journal of Experimental Marine Biology and Ecology,* **375**, 1-8.

Manzello DP (2008) Reef development and resilience to acute (El Nino warming) and chronic (high-CO_2) disturbances in the eastern tropical Pacific: a real-world climate change model. *Proceedings 11th International Coral Reef Symposium,* **1**, 1299-1303.

Manzello DP (2010) Ocean acidification hot spots: Spatiotemporal dynamics of the seawater CO_2 system of eastern Pacific coral reefs. *Limnology and Oceanography,* **55**, 239-248.

Maier C, Watremez P, Taviani M, *et al*. (2012) Calcification rates and the effect of ocean acidification on Mediterranean cold-water corals. *Proceedings of the Royal Society of London, Series B: Biological Sciences,* **279**, 1716-1723.

McCulloch M, Trotter J, Montagna P, *et al*. (2012) Resilience of cold-water scleractinian corals to ocean acidification: Boron isotopic systematic of pH and saturation state up-regulation. *Geochimica et Cosmochimica Acta*, **87**, 21-34.

Moberg F, Folke C (1999) Ecological goods and services of coral reef ecosystems. *Ecological Economics,* **29**, 215-233.

Perry CT, Spencer T, Kench PS (2008) Carbonate budgets and reef production states: a geomorphic perspective on the ecological phase-shift concept. *Coral Reefs,* **27**, 853-866.

Riegl B (2003) Climate change and coral reefs: different effects in two high-latitude areas (Arabian Gulf, South Africa). *Coral Reefs,* **22**, 433-446.

Riegl B, Piller WE (2000) Reefs and coral carpets in the northern Red Sea as models for organism-environment feedback in coral communities and its reflection in growth fabrics. In: *Carbonate Platform Systems: components and interactions*. (eds Insalaco E, Skelton PW, Palmar TJ) pp 71-88. Geological Society, London.

Roberts J, Wheeler AJ, Freiwald A, Cairns S (2009) *Cold-Water Corals*. Cambridge, UK, Cambridge University Press.

Schuhmacher H (1988) Korallenriffe, München, BLV.

Sorokin Y, I (1990) Aspects of trophic relations, productivity and energy balance in coral-reef ecosystems. In: *Ecosystems of the World 25 Coral Reefs*. (ed Dubinsky Z) pp 401-410. Amsterdam, Elsevier Science Publishers.

Tribollet A, Golubic S (2011) Reef Bioerosion: Agents and Processes. In: *Coral Reefs: An Ecosystem in Transition*. (eds Dubinsky Z & Stambler N) pp 435-449. Springer Netherlands.

Tsounis G, Orejas C, Reynaud S, *et al*. (2010) Prey capture rates in four Mediterranean cold water corals. *Marine Ecology-Progress Series*, **398**, 149-155.

Wood R (2001) Biodiversity and history of reefs. *Geology,* **36**, 251-263.

Yamano HY, Hori KH, Yamauchi MY, *et al*. (2001) Highest-latitude coral reef at Iki Island, Japan. *Coral Reefs,* **20**, 9-12.

1.1.2 Coral reefs in a changing world

Throughout the world, coral reefs are experiencing a decline in live coral cover, abundance and diversity as a result of pollution, overfishing, tourism, coral bleaching and diseases (Hughes *et al.,* 2003). Moreover, the predicted global climate change poses an additional severe threat (Hoegh-Guldberg, 1999, Hoegh-Guldberg *et al.*, 2007, Kleypas *et al.*, 1999a, Kleypas *et al.*, 2001). Specifically, changes in temperature, carbonate chemistry and ocean pH have been predicted to impact marine calcifiers, such as corals, limiting their distribution (see Box 3; Hoegh-Guldberg *et al.*, 2007, Kleypas *et al.*, 2006). Atmospheric CO_2 concentration has been relatively stable for the last 420 000 years (between 180 and 300 ppmv) and a substantial increase has occurred since the industrial revolution (Petit *et al.*, 1999). Anthropogenic combustions of fossil fuels, cement production as well as deforestation account for these rapid changes (Doney & Schimel, 2007). The world's oceans equilibrate with the atmosphere and hence function as a sink for the additional anthropogenically derived CO_2. This abates the heating up of the global climate to some extent (Doney *et al.*, 2009, Kleypas *et al.*, 2006, Orr *et al.*, 2005, Sabine *et al.*, 2004), but acting as a sink causes the other CO_2 problem called ocean acidification – a process that makes the seawater more acidic or, more accurately, less alkaline (Caldeira & Wickett, 2005, Doney *et al.*, 2009, Kleypas *et al.*, 2006, Orr *et al.*, 2005).

Ocean temperature is expected to increase (Fig. 1.3a-c) by 0.2°C per decade (Hoegh-Guldberg & Bruno, 2010) and push corals closer to their upper thermal limit (Hoegh-Guldberg, 1999). As corals are adapted to a narrow temperature window (Kleypas *et al.*, 1999b), ocean temperatures exceeding their upper limit result in coral bleaching. Coral bleaching refers to the disruption of their symbiosis with microscopic algae, consequent symbiont expulsion and thus, loss of coral coloration (Douglas 2003, Baker *et al.*, 2008, and references therein). Bleaching events are often associated with significant loss in live coral cover, and recovery to pre-bleaching states can take years, up to decades, if at all possible (see review Baker *et al.*, 2008). Future predictions expect such events to increase in frequency as well as in intensity by 2050 becoming a biannual or even annual event (Donner *et al.*, 2005) with fatal consequences for coral reef health and distribution.

Carbon dioxide dissolves into the ocean and dissociates by a complex set of chemical equilibrium reactions via carbonic acid (H_2CO_3) to bicarbonate (HCO^{-3}) and carbonate ion (CO_3^{2-}) (Mehrbach *et al.*, 1973):

$$CO_{2(atmos)} \Leftrightarrow CO_{2(aq)} + H_2O \Leftrightarrow H_2CO_3 \Leftrightarrow H^+ + HCO^{-3} \Leftrightarrow 2H^+ + CO_3^{2-}.$$

These reactions are mainly governed by the concentration of the inorganic carbon species and the oceanic charge balance or total alkalinity (Dickson *et al.*, 2007, Kleypas *et al.*, 2006). The increased amount of CO_2 dissolved into the sea shifts the carbonate equilibrium towards HCO^{-3} and diminishes the amount of CO_3^{2-}, thus reducing the calcium carbonate ($CaCO_3$) saturation state (Fig. 1.3d-e). Since pre-industrial times, pH has already dropped by 0.1 pH units (Orr *et al.,* 2005) and the aragonite saturation horizon has shoaled by 200 m towards the ocean surface (Feely et al., 2004). This already represents a

significant change, which constitutes a major threat to polar environments. The projected rise of atmospheric CO_2 in this century will affect a wider range of areas and marine organisms, specifically these building up carbonate structures (Doney *et al.*, 2009, Fabry *et al.*, 2008, Guinotte & Fabry, 2008, Kleypas *et al.*, 2006).

BOX 3: Future changing ocean

Temperature and aragonite saturation state (Fig. 1.3) both are expected to reach levels by the turn of the century that exceed or push calcifiers close to their threshold limits (Doney *et al.*, 2009). Coral reef growth is a complex dynamic of carbonate accretion and erosion (Kleypas *et al.*, 2001). Both will be affected by prospected reduced aragonite saturation state - slowing reef accretion and enhancing their erosion (Langdon *et al.*, 2000). Unfavorable conditions in respect to aragonite saturation state will first affect reefs that already are close to their limit of growth - the higher latitude reefs. Temperature changes, in contrast, will first impact the tropical central regions. Thus, future ocean conditions will further restrict reef distribution.

While it was proposed that corals migrate to higher latitudes to escape heat (Precht & Arosnon, 2004) the decrease in aragonite saturation state is expected to restrict reef framework production to the lower latitudes (Kleypas *et al.*, 2001) limiting suitable habitat for reef existence.

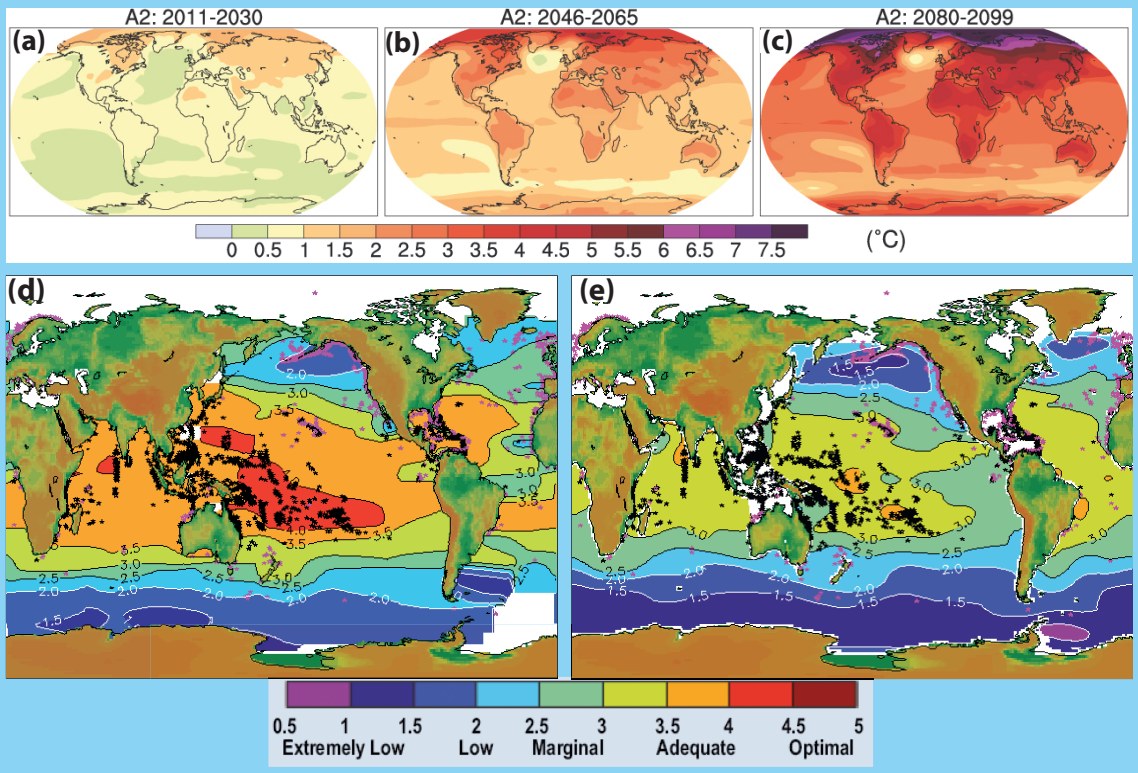

Figure 1.3: Future ocean conditions - warming and acidification. Global temperature projections diplayed as temperature anomaly for (a) 2011-2030, (b) 2046-2065 and (c) 2080-2099 (modified after Meehl *et al.*, 2007, IPCC Report 2007 Fig. 10.8). Aragonite saturation state level of the surface ocean displayed for (d) 1995 and (e) 2040 (modified after Kleypas *et al.*, 2006).

Biomineralization is widespread in organisms and either a biologically-induced or -controlled process (Lowenstam & Weiner 1988). While the environment plays a major role in biologically-induced biomineralization, the latter is strongly controlled by cellular activity (Lowenstam & Weiner 1988). Most experts consider coral calcification to be a highly controlled biologically mediated process, but this is still controversial (see review Tambutte *et al.*, 2011). A detailed understanding of biologically-mediated

biomineralization is missing and appears to bear several mysteries. However, intrinsic control enables organisms to buffer changes in seawater chemistry but on the other hand restricts their adaptability to changing conditions by switching to a more favorable or resistant polymorph of calcium carbonate (Stanley, 2006). Organisms with fast generation time, such as for instance some calcifying planktonic species, potentially adapt via natural selection (Kleypas *et al.*, 2006). With respect to changing seawater properties environmentally-controlled calcification might allow species to react and adapt to these changes. Nevertheless, the predictions are not that simple and environmental changes has differing affects on the calcification process.

Recent investigations showed that coral growth has slowed down within the last two decades. This reduction was attributed different driving forces in different studies – ocean warming (Cantin *et al.*, 2010, Tanzil *et al.*, 2009) or acidification (Cooper *et al.*, 2008, De'ath *et al.*, 2009). However, the ocean is simultaneously warming and acidifying, which makes the identification of the main driving forces difficult. Additionally, different species respond differently to both concomitantly occurring changes (Anthony *et al.*, 2008). Thus, significant gaps still exist in our understanding of reef processes and dynamics as well as their capability to adapt and deal with these changes (Fabry *et al.,* 2009).

1.2 RESEARCH OBJECTIVES & QUESTIONS

1.2.1 Overview Box 4

BOX 4: Schematic overview of the conceptual outline of this thesis

ECOSYSTEM SCALE:

Reef framework development and coral bleaching

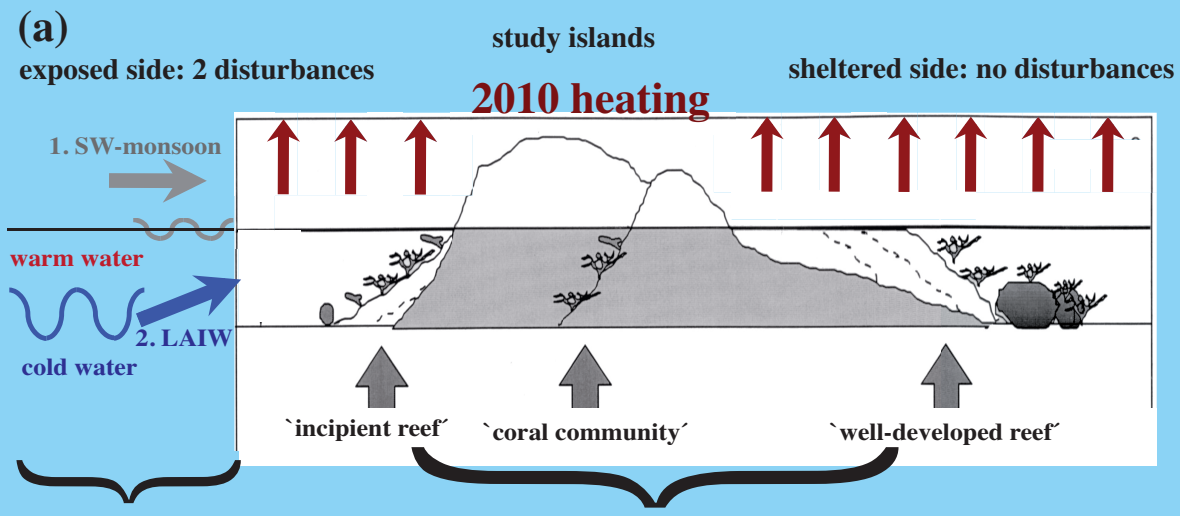

→ LAIW potential cooling during 2010 heating ?
→ Publication II

→ Reef framework development due to SW-monsoon and LAIW forcing ?
→ Publication I

SKELETAL SCALE:

Skeletal density, proxies and growth patterns

Macro scale

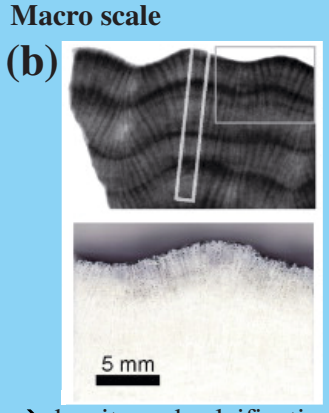

→ density and calcification as a function of LAIW and SW-monsoon forcing ?
→ Publication III

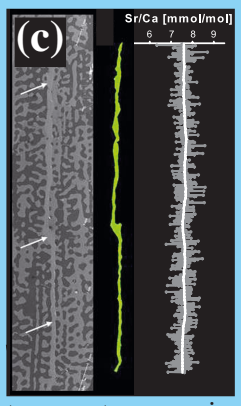

→ temperature proxies record 2010 heating and LAIW-forcing ?
→ Publication IV

Micro scale

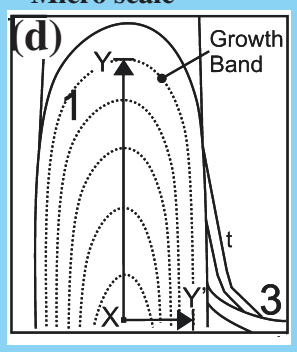

→ can studying growth layers help to understand calcification ?
→ Publication V

Figure 1.4: Schematic overview of the conceptual outline of the thesis. (a) Reef framework development (reef framework scheme modified after van Woesik & Done, 1997) under two kinds of disturbances (large amplitude internal waves (LAIW) and southwest (SW) monsoon), the effect of the 2010 heating on reef community and the potential of LAIW to act as mitigation mechanism. (b) Density banding pattern and growth in *Porites* skeletons (modified after Suzuki *et al*., 2008) - LAIW and SW monsoon effects on skeletal properties. (c) Temperature proxies in *Porites* skeletons (modified after Schmidt *et al*., in prep.) - is the heating and LAIW recorded. (d) Skeletal growth bands at the micrometer scale (modified after Nothdurft & Webb, 2007) - can it provide insight in growth cyclicity.

1.2.2 Environmental variability and disturbances:

In some areas reefs are confronted with high environmental variability due to natural forces (Brown & Howard, 1985, Hughes, 1993, Leichter *et al*., 1996, review Lesser, 2004). These forces result in changing environmental conditions, such as nutrient availability, temperature, turbidity (Leichter *et al*., 2005, Leichter *et al*., 1996, Nielsen *et al*., 2004, Pineda, 1991) and pH (Manzello, 2010, Schmidt *et al*., 2012). Thus, reefs in such areas provide the opportunity to study how these environmental fluctuations affect reefs at the ecosystem scale down to the skeletal level. Moreover, it can be tested whether these reefs are adapted to future environmental conditions and potentially more robust.

1.2.2.1 Environmental disturbances and reef framework:

A common hydrodynamic phenomenon observed in the Andaman Sea (study area) and elsewhere (e.g. Sulu Sea: Apel *et al*., 1985, Scotian Sea: Sandstrom & Elliot, 1984, Indonesian Sea: Susanto *et al*., 2005, Northern South China Sea: Yang *et al*., 2004) is the occurrence of solitons – a special type of internal waves (Osborne & Burch, 1980). Solitons are nonlinear (Russell, 1844) and can occur at the surface or within the water column. Internally, these waves are generated when strong tidal flows interact with topographic features such as the Andaman-Nicobar Island arc or Dreadnought Bank (Alpers & Vlasenko, 2002, Osborne & Burch, 1980). Internal waves are common in all ocean basins (Ewing, 1950) and lakes (Farmer, 1978). They are (tidal) gravity waves that travel along the density gradient in the water column (Leichter *et al*., 1996, Leichter *et al*., 2005, Thorpe, 1975). The stratification of the water body derives from differences in temperature as well as salinity and separates the surface from the deep water, which in general exhibits decreased temperature, higher salinity (Nielsen *et al*., 2004), lower oxygen concentrations (Schmidt *et al*., 2012) and a lowered aragonite saturation state (Feely *et al*., 2004). In the Andaman Sea, solitons show extraordinary large amplitudes of about 60 m (the maximum amplitude is located at the midthermocline depth of approximately 150 m (Kao *et al*., 1985, Osborne & Burch, 1980)) and travel with speeds of ~2 m s^{-1} (Osborne & Burch, 1980). Studies investigating solitons are centered in oceanographic and fluid mechanics research (Ewing, 1950, Helfrich & Melville, 2006, Osborne & Burch, 1980). They deal mainly with the prediction of their occurrence, as they are hazardous to drilling operations (Hyder *et al*., 2005, Osborne & Burch, 1980). Nevertheless, they have also attracted the attention of ecologists who studied their effect on coastal ecosystems and the coupling of pelagic and benthic environments. When internal waves approach areas of lower water depth they can steepen, break and form bores which travel upslope and consequently subthermocline water mixes with surface water (Leichter *et al*., 1996, Pineda, 1994, Wallace & Wilkinson, 1988). In contrast, solitons, according to the mathematical theory, first fission on the continental shelf and develop one or more ranked-ordered solitons (Osborne & Burch, 1980, Wallace & Wilkinson, 1988) before breaking and mixing (Helfrich & Melville, 2006). As a result, coral reefs are confronted with pronounced thermal fluctuations, pH changes and nutrient input (Leichter *et al*., 1996, Pineda, 1991, Schmidt *et al*., 2012, Wolanski & Delesalle,

1995). The Andaman Sea islands of Thailand, where solitons occur at tidal frequency, are suitable sites to study the effect of naturally varying conditions *in situ*, with the possibility of investigating the effect of pH dynamics. Previous studies have shown that pH drops by up to 0.4-0.6 pH units, which represent approximately a 2.5 to 4-fold increase in acidity of the seawater (as pH is logarithmic) and strong fluctuations (Schmidt *et al*., 2012). Simulations of large amplitude internal waves (LAIW) behavior indicated their potential to propagate over the shelf as either secondary wave train or jet, potentially influencing shallow water areas (Helfrich, 1992, Vlasenko & Stashchuk, 2007).

Recent studies on LAIW impact on coral reefs in the Andaman Sea provided a good characterization of exposed and sheltered reef community structure of the Similan Islands by comparing environmental settings, community composition, primary production, coral growth and trophic as well as metabolic adaptations (Jantzen, 2010, Roder *et al*., 2010, Roder *et al*., 2011, Schmidt *et al*., 2012). At the ecosystem level, western (W) reefs show reduced framework at deep and shallow depth (20 m and 7 m, respectively) but a slightly increased framework at intermediate depth of 15 m. The exposed W island sides are additionally subjected to southwest (SW) monsoon surface gravity waves that are expected to cause turbulent mixing and sedimentation. Both disturbances occur in a seasonal pattern with SW monsoon forcing during the wet season (May-November) and LAIW impingement during the dry season (December-May). The limited spatial extent of these investigations, combined with the spatial covariance of the environmental factors, made it difficult to assess the relative contribution of monsoon and LAIW, to the observed biological changes.

Question 1: Is the impact and intensity of large amplitude internal waves on shallow reef areas related to the distance of these areas to the shelf break?

Q: This question follows up a previous investigation (Schmidt *et al*., 2012) by expanding the study area and addressing the extent and characteristics of environmental variability due to LAIW on several islands on the continental shelf. Moreover, the correlation of LAIW intensity to distance to the shelf break will be tested. → **Manuscript I**

Question 2: What are the main driving forces of reef development on LAIW and SW monsoon exposed reefs?

Q: Is LAIW intensity reflected in the reef accretion potential at intermediate depth reefs along an anticipated cross-shelf LAIW gradient or do other processes govern reef development? → **Manuscript I**

1.2.2.2 LAIW cold water pulses as potential cooling agent during heat stress:

Global warming represents a major threat to coral reefs (Greenstein & Pandolfi, 2008, Hoegh-Guldberg, 1999) and future predictions expect that by 2050 bleaching events will occur biannually or even annually (Donner *et al*., 2005). Thermal stress and bleaching response are highly heterogeneous among locations and are due to interactions of local physical, chemical and biological conditions. For instance, water motion moderates water temperatures (West & Salm, 2003) and furthermore, improves the removal of toxic substances (e.g. reactive oxygen species) (Nakamura & Woesik, 2001) that are produced when corals bleach (see references therein Lesser, 2011). It is also known that branching species are in general more susceptible to bleaching than massive species, and even within growth morphologies the response can vary (Marshall & Baird, 2000, McClanahan, 2004, McClanahan *et al*., 2007). This complex set of parameters and variability in community susceptibility complicates future predictions and makes it difficult to identify resilient areas able to recover (Maina *et al*., 2008, McClanahan *et al*., 2011). A better understanding of reef systems response to bleaching is highly valuable because it improves accurate risk assessment and management of coral reefs in a changing climate (Berkelmans, 2009).

Several conceptual environmental settings were hypothesized to help corals withstand thermal stress (Glynn, 1996) including (1) upwelling regions because cold water intrusions are able to abate heating, (2) offshore islands they are expected to have a more vigorous water mixing that moderates heat stress, (3) high-latitude reefs, which, due to their geographic location, are not as close to their upper thermal limit compared to the central tropical regions and (4) deeper reef (> 30 m) areas that are likely protected from heat stress due to their deeper location.

A recent study (Sheppard, 2009) observed large temperature drops at atolls in the Indian Ocean similar to those described for the Andaman Sea coral reefs (Schmidt *et al*., 2012). He argued that internal wave induced temperature plunges coincide with the time period of warmest sea surface temperature (SST) and thus, such areas potentially provide refuge during heating.

Question 3: Can LAIW sites act as refuge areas in the light of increasingly frequent bleaching events? and how do differences in coral community composition affect the bleaching response?

Q: The question is can LAIW cold-water pulses abate heating and mitigate the bleaching response. In 2010 a severe bleaching event occurred in the Andaman Sea and provided an opportunity to monitor the bleaching response and the temperature development at various sites of differential LAIW intensities. Differences in bleaching response might derive from differences in heating and cooling but

also from differences in coral community composition. To account for these confounding effects differences in community bleaching susceptibility are going to be assessed. → **Manuscript II**

1.2.2.3 Skeletal properties and proxies:

Corals build massive calcified structures that form reefs. Studying individual coral's growth rates and skeletons (see Box 5) can give an indication of their vitality and of the environmental conditions corals are confronted with. Different methods have been established to determine coral growth. These methods include repeatedly measuring selected coral heads, applying the buoyant weight method (Dodge *et al.,* 1984) or staining and analyzing coral skeleton increments (Highsmith, 1979).

Coral reefs on offshore islands in the Andaman show a distinct reef formation. The W island sides are exposed to both LAIW and SW-monsoon and feature a reduced reef framework in contrast to the sheltered E island sides (Schmidt *et al.*, 2012). A previous study (Schmidt, 2010) using the buoyant weight method showed that corals grow slower on the exposed W island sides in contrast to the sheltered E of the Similan Islands. The author attributed this difference to the large environmental fluctuations measured on the exposed sites (Schmidt *et al.*, 2012). Furthermore, corals are thought to use different strategies that facilitate them to deal with the environmental conditions they grow in and resist frequent disturbances. One of these strategies opts for constructing massive or dense skeleton structures (Szmant, 1986), whereas another possibility represents morphological adaptation to the environmental settings (Rathburn, 1879, Todd *et al.*, 2004, for review see Todd, 2008) or the ability to regenerate asexually after fragmentation (Highsmith, 1982). Scoffin *et al.* (1992) analyzed coral skeletons of *Porites lutea* from different environmental settings. The authors found a relationship between the hydrodynamic conditions and skeletal density as well as linear extension rate. Skeletal density increased while linear extension decreased along a gradient from protected to exposed sites.

Coral skeleton growth cycles are displayed by skeleton density banding patterns similarly to tree rings. They incorporate environmental information into their skeleton and hence, their analysis opens an exceptional window into the past and provides insight into the marine conditions they have encountered (e.g. Barnes & Lough, 1996, Cohen & McConnaughey, 2003, Goreau, 1977, Smith *et al.*, 1979, Weber, 1973). In particular, the study of coral skeletons has received a lot of attention in paleoclimatology. Skeletal proxies are known to provide useful information of past environmental conditions (e.g. temperature, nutrients, currents) but are subjected to biological processes that potentially blur skeletal recording - the so-called "vital effect" (e.g. Erez, 1978, Lowenstam & Weiner, 1989, Meibom *et al.*, 2008, Weiner & Dove, 2003). Different proxies were analyzed for their potential to record temperature (e.g. Allison & Finch, 2007, Smith *et al.*, 1979). Strontium to calcium (Sr/Ca) ratio has been shown to correlate well with temperature. However, strong differences and high variability were observed at higher spatial resolution (e.g. Allison, 1996, Meibom *et al.*, 2003) and between different skeletal enteties

BOX 5: Coral calcification and growth modes

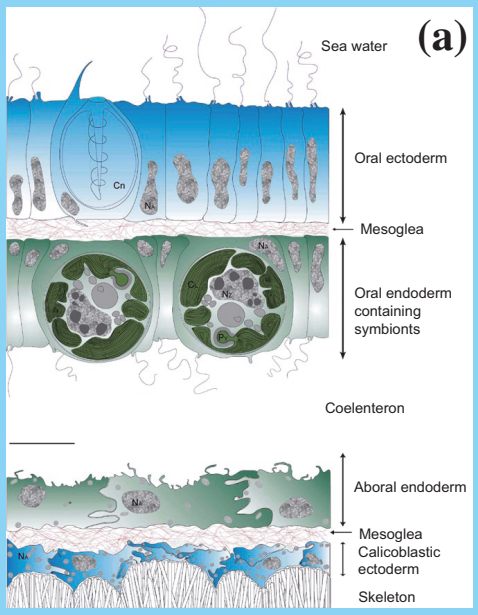

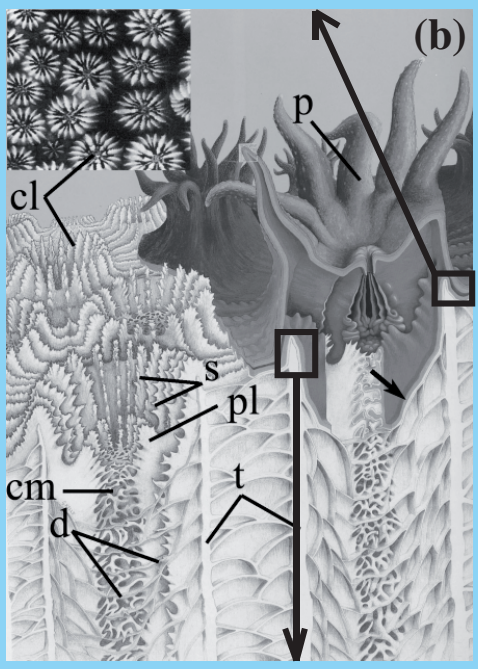

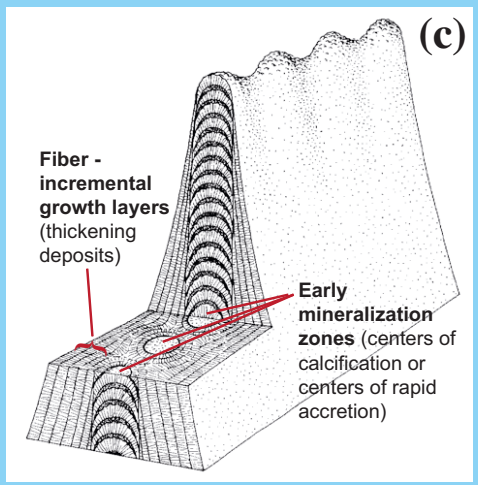

Coral reefs are massive carbonate structures built by a thin layer of numerous coral polyps covering the carbonate structures. A coral polyp consists of two epithelial cell layers - the ecto- and endoderm (Fautin & Mariscal, 1991) separated by the mesoglea (Schmid *et al.,* 1999, Fig. 1.5a). The epithelia layers facing the seawater are called the oral epithelia while the ones attached to the skeleton are named aboral or calicoblastic epithelia (Galloway *et al.*, 2007). Both delimit the coelenteron - the gastral cavity of the corals. The calicoblastic epithelium is thinner than the oral cell layers (Fautin & Mariscal, 1991). The oral layer contains specialized cells (cnidocytes, mucocytes and epithelio-muscular cells) that are not present in the aboral layers and harbor the coral symbionts (Fautin & Mariscal, 1991). Besides calcioblastic cells, desmocytes are present in the aboral tissue and these cells are responsible for the attachment of the tissue to the skeleton (Muscatine *et al.,* 1997). Coral calcification is still controversially discussed. In particular the question of wheter or not there is a space between the calicoblastic cell layer and the skeleton is a matter of debate (Allemand *et al.*, 2011). Contrasting theories exist regarding both the distance between skeleton and tissue and if the space is open to the environment or not.

Coral polyps (Fig. 1.5b) construct several structural elements forming the corallites, in which the polyps reside in. The masses of corallites give the corals their shape and appearance. The morphology of these elements is highly diverse and used for taxonomical purpose to distinguish corals at family, genus and species level. Each single polyp consists of different skeletal elements: a columella (cm) in the center, septa (s) that radiate away from the center, a wall (t - theca and epitheca) and dissepiments (d) bordering the corallite to the lateral and basal end, respectively (Fig. 1.5b). Adjacent corallites either share common walls or, if not, separated corallite walls are connected by skeletal elements forming the coenosteum. A close-up of a corallite i.e. viewing individual macro-morphological skeletal elements, displays micromorphological features such as spines, granules and nodules, which structure walls, septal margins and septal faces (Fig. 1.5b).

Each single skeletal element itself consists of two building blocks - fibers and early mineralization zones (EMZ - also known as centers of calcification or centers of rapid accretion (Cuif *et al.*, 2005a, Stolarski, 2003)). A two step mode of growth was proposed with the EMZ building the skeletal scaffold and the bulk skeleton is then formed by the skeletal fibers. The fibers comprise of cyclic incremental growth layers of mineral and organic phase. This model relies on temporal differences in the formation of both entities (Cuif *et al.,* 2003). Stolarski (2003) proposed the layered model. He emphasized the continuity between skeletal entities that suggests no difference in timing of their formation but a distinction in their growth dynamics. Gaps still remain in understanding growth patterns, however to improve high-resolution proxy sampling such information is highly valuable.

Figure 1.5: Coral calcification from the coral polyp to the skeletal element. (a) Coral polyp histology (reproduced from Allemand *et al.,* 2011) (b) Skeletal elements formed by the coral polyp (scheme reproduced from Cohen & McConnaughey, 2003, p - polyp, cl - coralite, cm - columella, pl - pali, s - septa, d- dissepiment, t -theka). (c) Skeletal elements microstructure (modified after Stolarski, 2003).

(see Box 5 for more detailed information) (e.g. Cohen *et al.*, 2001, Rollion-Bard *et al.*, 2003). This variability cannot be attributed to temperature fluctuations *in situ* but is potentially due to differences in calcification rates and hence, photosynthesis (Cohen *et al.*, 2001) or other biological processes (e.g. reproduction, Meibom *et al.*, 2003).

In order to accurately interpret one of the finest high-resolution environmental archives, more studies are needed to understand the links between environmental conditions, coral physiology and coral carbonate structure to disentangle the factors that influence and drive skeletal growth.

Question 4: Can large amplitude internal wave intensity be recognized at the skeletal level by studying growth characteristics such as skeletal density and linear extension rates?

Q: Is environmental variability due to both LAIW and SW monsoon reflected in skeleton density, linear extension rate and calcification rate? Scoffin *et al.* (1992) described an inshore offshore gradient in skeletal properties in the Andaman Sea – showing a decrease in extension rate and an increase in density with distance to the mainland. The present study tests whether differences in skeletal properties exist between several offshore islands and if such differences are related to environmental conditions monitored at the different sites or simply represent a function of the distance to the shore. → **Manuscript III**

Question 5: Can large amplitude internal wave temperature fluctuations be recognized at the skeletal level by analyzing temperature proxies?

Q: This question addresses whether or not high temperature variability due to LAIW is reflected at the skeletal level when analyzing skeletal proxies. Skeletal thermometry has been applied since the early 20th century and advances in instrumentation allow refined analyses. Knowledge gaps remain concerning the biological effects on trace element inclusions. Studying sites with strong environmental fluctuations can potentially provide new insight into skeletal recording and its constraints. → **Manuscript IV**

1.2.2.4 Skeletal microstructure and growth patterns:

The skeletal elements and crystal arrangements were the focus of coral skeletal studies since the 19th century in particular for taxonomic purpose (Dana, 1846, Pratz, 1882, Vaughan & Wells, 1943). Oglivie (1896) first used the term calcification center for the point fibers radiate away without viewing centers as a specific skeletal entity (as it was recognized later on). First biomineralization concepts for corals were proposed almost a century later resulting in the spherulitic hypothesis pointing out the similarity in the coral skeletal arrangement with abiotic aragonite crystal growth (Bryan & Hill, 1941). Further

investigations revealed a incremental growth of fibers (Cuif & Dauphin, 2005a, Cuif & Dauphin, 2005b) and it was suggested that coral growth requires some sort of control. Within the last 3 decades, novel tools (in particular, Nano-SIMS (Secondary Ion Mass Spectroscopy), synchrotron radiation-based X-ray absorption near edge spectroscopy (XANES) and atomic force microscopy (AFM)) have opened an exceptional possibility for studying skeletal structures at the nanometer-scale and definitively challenged existing concepts (Cuif *et al.*, 2003, Meibom *et al.*, 2004, Stolarski & Mazur, 2005). These studies deepened the understanding of biomineralization concepts and lead to a shift from simple physicochemical to matrix-mediated models of growth highlighting the importance of organic compounds for biomineralization (Cuif & Dauphin, 2005a, Cuif & Dauphin, 2005b). This was supported by biomimetic approach, which provided the first insight on the regulative role of organic compounds (Dey *et al.*, 2010, Mann *et al.*, 1993, Sommerdijk & de With, 2008). Corals were ranked among organisms that have a biologically-controlled extracellular mineralization pathway, which involves a pre-formed matrix that facilitates skeleton formation (Watabe & Kingsley, 1989). Recently, Nothdurft and Webb (2007) have pointed out that understanding patterns and timing of skeletal formation can improve high-resolution proxy sampling. However, knowledge gaps still exist, in particular, of growth processes on a macrosopic scale.

Recently, confocal Raman spectroscopy (see Box 6 for more detail) of high spatial resolution was applied to investigate biomineral structural components (e.g. Hild *et al.*, 2008, Nehrke & Nouet, 2011, Neues *et al.*, 2011). These studies demonstrated the applicability of this method, highlighting, in particular, the simultaneous assessment of mineral and organic phase distribution. In respect to coral growth, the application of confocal Raman mapping can potentially provide further insight into skeletal growth patterns and organic matrix distribution.

Question 6: Can confocal Raman mapping shed light on coral growth patterns and what are the implications for high-resolution proxy studies?

Q: This question addresses if improved (in spectral and spatial resolution) old tools can provide new insight into microstructural growth patterns and cyclicity. A better understanding of coral growth patterns is desirable in order to improve the interpretation of high-resolution proxy data. → **Manuscript V**

BOX 6: Raman spectroscopy

Raman spectroscopy is based on light scattering of excited molecules. Most of the incident light (99.9999 %) is scattered elastically, which means that neither its kinetic energy nor its wavelength are changed, the so-called Rayleigh scattering. However, a very small fraction (1 out of 10^6-10^8) of photons is scattered inelastically and the reemitted light is shifted in frequency. The inelastic scattering is due to excitation or annhilation of a molecular vibration. This results in a shift in energy that is characteristic for the molecule and hence, a fingerprint of the analyzed sample (Smith & Dent, 2005).

Two possilbe energy shifts can be provoked: Stokes scattering: A molecule in basic state absorbs a photon of the incident light, which transfers it to a Raman-active mode. The emitted light consequently is lower in energy. Anti-Stokes scattering: When a photon of the incident light is absorbed by a molecule in Raman-active mode (vibrational state) the excessive energy of the excited molecule is released and by returning to the basic vibrational state the emitted light is of higher energy (Fig. 1.6)(Smith & Dent, 2005).

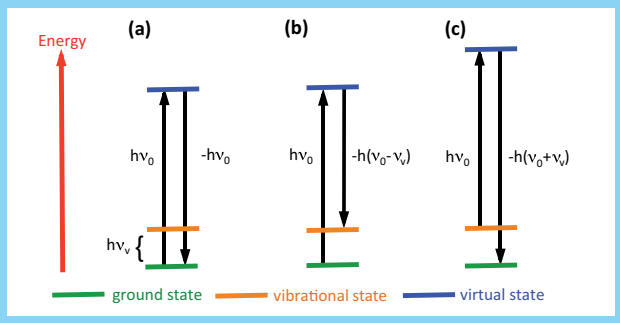

Figure 1.6: Incident light scattering. (a) Rayleigh scattering, (b) Stokes scattering and (c) anti-Stokes scattering.

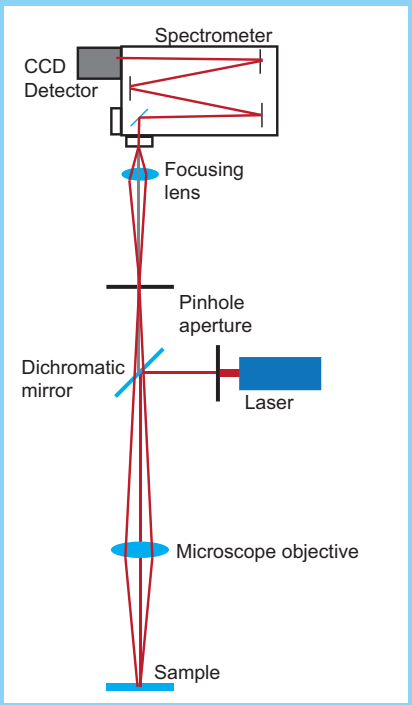

Figure 1.8: Schematic overview of Raman instrumental set-up.

A Raman spectrum contains besides the elastic scattered Rayleigh line additional lines, which are shifted to the excitation light. The spectra are given in wave numbers (1/cm). Anti-stokes and stokes spectra are symmetric (Fig. 1.7). The probability of exciting a molecule in virtual state is small and hence, anti-stokes lines are less intense (Smith & Dent, 2005).

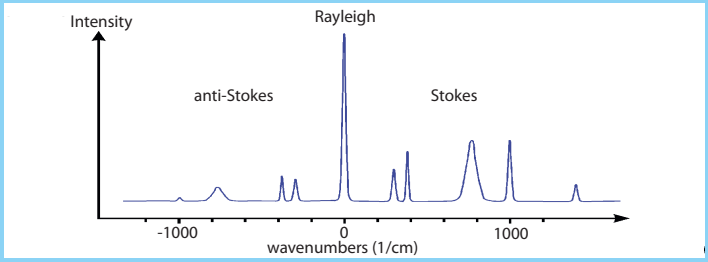

Figure 1.7: Raman spectrum (modified from WITEC Confocal Raman Microscopy Manual).

Raman systems (Fig. 1.8) have an excitation source (laser - UV, VIS or NIR), dichromatic mirror, objectives, wavelength selectors (filter or spectrometer) and a detector. The sample is illuminated with a laser that is focused onto the sample. The emitted light is collected by the same objective and focused through a pinhole ensuring that only light from the focal plane passes to the detector. Often wavelengths close to the Rayleigh line are filtered out (Smith & Dent, 2005).

Raman spectroscopy is used in different disciplines for analyzing solids, liquids, gels, gases. It is most commonly used in chemistry and recently also applied to biological or biomineral samples. The advantage of the method is that it is non-destructive or -invasive and the samples do not need specific preparations. Disadvantageous for Raman spectroscopy are samples that show high fluorescence. Fluorescence in contrast to Raman is the absorption of light and excitation of the molecule to a discrete (not virtual) energy level that overlies Raman lines. Fluorescence often occurs in biological samples and can be reduced by using lasers that do not provoke fluorescence (NIR) (Smith & Dent, 2005).

2. MANUSCRIPTS

MANUSCRIPT OUTLINE

The thesis includes 5 manuscripts – 2 manuscripts in review, 2 in preparation pending submission and one preliminary work with a summary abstract outlining the performed analysis and preliminary data interpretation. The contributions of authors on the study design, data acquisition, analysis and writing of the manuscript are outlined for each manuscript.

MANUSCRIPT I: Differential impact of monsoon and large amplitude internal waves on coral reef development in the Andaman Sea.
M Wall, GM Schmidt, P Janjang, S Khokiattiwong and C Richter
accepted for publication in PLOS One

Contributions: Conceived and designed the study: MW, CR, SK, GMS. Performed the study: MW, JP. Analyzed the data: JP, MW. Contributed reagents/materials/analysis tools: MW, JP, SK, CR. Wrote the paper: MW, CR, GMS.

MANUSCRIPT II: Case study 2010 coral bleaching in the Andaman Sea – internal waves bleaching mitigation and future implications.
M Wall, L Putchim, GM Schmidt, C Jantzen, S Khokkiattiwong and C Richter
in preparation for Global Change Biology

Contributions: Conceived and designed the study: MW, CJ, GMS, CR. Performed the study: MW, LP, CJ, GMS. Analyzed the data: MW, LP. Contributed reagents/materials/analysis tools: SK, CR. Wrote the paper: MW, CJ, GMS, CR.

MANUSCRIPT III: Skeletal properties examined in the light of different degrees of environmental disturbances in the Andaman Sea: Large amplitude internal waves and southwest monsoon.
M Wall, K Bösche, GM Schmidt and C Richter
in preparation as Note for Coral Reefs

Contributions: Conceived and designed the study: MW, CR. Performed the study: MW. Analyzed the data: KB, MW. Contributed reagents/materials/analysis tools: CR. Wrote the paper: MW, KB, CR, GMS.

MANUSCRIPT IV: Strontium/calcium ratios in *Porites lutea* skeletons grown under different temperature conditions.
GM Schmidt, F Ragazzola, M Wall, T Laepple and J Fietzke
in preparation

Contributions: Conceived and designed the study: GMS, MW, FR, JF. Performed the study: MW, FR, GMS. Analyzed the data: GMS, FR, TL, JF. Contributed reagents/materials/analysis tools: JF, Claudio Richter. Wrote the paper: GMS, FR, TL, JF, MW.

MANUSCRIPT V: Identification of two organic bands showing different chemical composition within the skeleton *Porites lutea*: A confocal Raman microscopy study.
M Wall and G Nehrke
submitted to Biogeosciences published as Biogeoscience Discussion 9: 8273-8306
accepted for publication in Biogeosciences

Contributions: Conceived and designed the study: MW, GN. Performed the study: MW, GN. Analyzed the data: MW, GN. Contributed reagents/materials/analysis tools: MW, GN. Wrote the paper: MW, GN.

2.1 MANUSCRIPT I

DIFFERENTIAL IMPACT OF MONSOON AND LARGE AMPLITUDE INTERNAL WAVES ON CORAL REEF DEVELOPMENT IN THE ANDAMAN SEA

M Wall[1], G M Schmidt[1], P Janjang[2], S Khokiattiwong[2] & C Richter[1]

[1]*Alfred Wegener Institute for Polar and Marine Research,*
Am Alten Hafen 26, 27568 Bremerhaven, Germany

[2]*Phuket Marine Biological Center,*
51 Sakdidet Road, 83000 Phuket, Thailand

accepted for publication in PLOS One

Abstract

The Andaman Sea and other macrotidal semi-enclosed tropical seas feature large amplitude internal waves (LAIW). Although these waves induce strong fluctuations i.a. of temperature, pH, and nutrients, their influence on reef development is so far unknown. A better-known source of disturbance is the monsoon affecting corals due to turbulent mixing and sedimentation. Because in the Andaman Sea both, LAIW and monsoon, act from the same westerly direction their relative contribution to reef development is difficult to discern. Here, we explore the framework development in a number of offshore island locations subjected to differential LAIW and SW monsoon impact to address this open question. Cumulative negative temperature anomalies – a proxy for LAIW impact - explained a higher percentage of the variability in coral reef framework height, than sedimentation rates which resulted mainly from the monsoon. Temperature anomalies and sediment grain size provided the best correlation with framework height suggesting that so far neglected subsurface processes (LAIW) play a significant role in shaping coral reefs.

***key words**:* reef formation, large amplitude internal waves, monsoon, Andaman Sea

1. Introduction

Differences in reef community and framework structure have been studied on different temporal and spatial scales and in various regions (e.g. Edmunds & Bruno, 1996, Hughes *et al*., 1999, van Woesik & Done, 1997). These studies highlight the importance of wave action, temperature, sedimentation and other physical factors that shape coral reefs (e.g. Jokiel *et al*., 2004, Kleypas, 1996, Murdoch & Aronson, 1999, Yamano *et al*., 2003). Surface waves are considered a major factor affecting the light-dependent vertical zonation in coral communities (e.g. Dollar, 1982, Yamano *et al*., 2003) but are also described to account for the horizontal differences in coral community composition between windward and leeward reef faces (e.g. Blanchon & Jones, 1995, Gischler, 1995, Stoddart, 1969). Exceptionally strong waves following tropical storms, hurricanes or cyclones can have devastating and long-lasting impacts on reef development (e.g. Grigg, 1998, Massel & Done, 1992, Scoffin, 1993). These episodic events along with the prevalent environmental settings determine reef appearance and growth (e.g. Kleypas, 1996, Perry & Smithers, 2010). Where reef framework development ceases corals grow in scattered colonies or thickets attached to basement rock (Done, 1982, Kleypas, 1996, van Woesik & Done, 1997).

The islands in the Andaman Sea show a distinct reef development. While the ocean facing west (W) fronts of the islands do not harbor true reefs but coral communities lacking a carbonate framework, the shelf facing east (E) sides of the islands display true reefs with a high cover of corals growing on top of a 3-dimensional carbonate framework providing a high topographic relief (Phongsuwan & Changsang, 1992, Schmidt *et al*., 2012, Spalding *et al*., 2001). Although the region is located outside the tropical cyclone area (Subrahmanyam *et al*., 2005), rare storms were shown to affect shallow reef areas

(Phongsuwan 1991). Another episodic disturbance acting on the scale of decades or centuries are tsunamis. Although the latest (2004) tsunami was particularly severe, the subsequent reef surveys revealed only moderate coral reef damage limited to shallow water regions (above 10 m) (Allen & Stone, 2005) with coral recruitment and recovery proceeding rapidly in most places (Sawall *et al*., 2010). Given the long return periods of a disturbance of that magnitude (500 years (Latief *et al*., 2008, Løvholt *et al*., 2006)) and the rareness and shallow impact of tropical storms in the area (Phongsuwan, 1991), the mechanical impact of tsunami and storms can be considered to affect mostly the shallow parts of the reef, where coral growth is most rapid (e.g. Wellington, 1982).

A much more predictable disturbance than the exceptional tropical storm or tsunami is the seasonally recurring monsoon with heavy rains, winds and swell. In the Andaman Sea region winds peak during the SW monsoon (May - October) (Scoffin *et al*., 1992) inducing high surface waves (Hoitink & Hoekstra, 2003). So far most studies emphasized the impact of surface waves on coral community structure (Dollar, 1982, Grigg, 1998, Stoddart, 1969). In shallow water, breaking surface waves cause turbulent mixing and resuspension of sediments resulting in increased turbidity (Piniak & Storlazzi, 2008, Storlazzi *et al*., 2004). Additionally, surface waves generate currents advecting shallow water resuspended sediments down slope (e.g. Lowe *et al*., 2005, Storlazzi *et al*., 2004). As a consequence of induced sedimentation the coral community experiences reduced light intensities (Storlazzi *et al*., 2004), abrasion of soft tissue (Rogers, 1990) and smothering of corals by sediment (Fabricius & Wolanski, 2000, Rogers, 1990).

An underexplored but potentially important source of disturbance in coral reefs is the impact by internal waves (Pomar *et al*., 2012). In contrast to surface waves, internal waves travel along density gradients within the water column and may attain much larger amplitudes (Thorpe, 1975). They are a common hydrodynamic phenomenon in the world oceans (e.g. Apel *et al*., 1985, Leichter *et al*., 2005, Pineda, 1991, Sandstrom & Elliot, 1984, Susanto *et al*., 2005, Wang *et al*., 2007, Wolanski *et al*., 2004, Yang *et al*., 2004). In the Andaman Sea, internal waves show extraordinary large amplitudes of 60 m or higher and travel with speeds of up to 2 m s^{-1} (Jackson, 2004, Osborne & Burch, 1980). In shoaling water, LAIW may steepen, break and form bores, which travel upslope and mix with surface water (Leichter *et al*., 1996, Pineda, 1994, Wallace & Wilkinson, 1988). Coral reefs subjected to LAIW are confronted with rapid and strong fluctuations in temperature, pH, oxygen and nutrients (Leichter *et al*., 1996, Schmidt *et al*., 2012, Wolanski *et al*., 2004, Wolanski & Delesalle, 1995). Since LAIW are very energetic (Moum *et al*., 2007) they can extend into shallow waters (Schmidt *et al*., 2012), affecting the nutritional status of shallow water corals (Roder *et al*., 2010, Roder *et al*., 2011). Previous studies in coral reefs of different regions showed mixed effects of internal waves. Coral calcification was enhanced at depths where the impact of internal waves was stronger in spite of reduced light availability (30 m depth compared to 20 m) (Leichter & Genovese, 2006). *Diploastrea helipora* was found to benefit more from an increased supply of nutrients than *Porites lutea* (Roder *et al*., 2011). On the other hand, the severe temperature

drops (up to 10°C) associated with LAIW are assumed to exert a thermal stress, which could be responsible in part for the observed differences in coral reef development (Wolanski *et al*., 2004).

In the Andaman Sea, LAIW and surface waves both impinge from westerly directions, but vary in intensity between seasons: LAIW peak during the dry season (NE monsoon, November – April) (Brown, 2007, Schmidt *et al*., 2012), when the water is well stratified and the thermocline/pycnocline is shallow (Satapoomin *et al*., 2004). Surface waves are largest during the wet season (SW monsoon May – October) when southwesterly winds are strongest. Pronounced interannual differences in LAIW impact and wave action may occur due to Indian Ocean Dipole (IOD) - related differences in thermocline depth and differences in storminess (Behera *et al*., 2008, Webster *et al*., 1999). Although previous studies in the Andaman Sea highlighted pronounced differences in coral nutritional status, coral community structure and reef framework development between the exposed W and sheltered E faces of the Similan Islands, the limited spatial extent of these investigations, along with the spatial covariance of the environmental factors, made it difficult to assess the relative contribution of monsoon and LAIW to the observed biological changes.

The present study attempts to disentangle the effects of LAIW and SW monsoon on shallow water coral reefs. It also extends the limited spatial scale of previous studies (100s-1000s of m, (Roder *et al*., 2010, Roder *et al*., 2011, Schmidt *et al*., 2012)) to the scale of the continental shelf (10s of km), taking advantage of the geographical setting of the Thai shelf, where a string of islands between the shelf break and Thai mainland was selected for the study. The working hypotheses guiding our study were: (1) LAIW dissipate part of their energy in shoaling water resulting in a cross-shelf decrease in LAIW intensity (Pomar *et al*., 2012) and, hence, temperature variability between islands, and (2) monsoon disturbance is not attenuated across the eastern Andaman Sea shelf, due to the much shorter wave-lengths of surface gravity waves restricting the turbulent dissipation of wave energy to near-shore waters. The two hypotheses combined predict a differential impact of LAIW and monsoon across the shelf, where LAIW intensity varies much more markedly across the shelf than monsoon impact. We take advantage of this natural setting to investigate if and to what extent LAIW and/or monsoon govern the coral reef development in the Andaman Sea.

2. Materials and Methods

2.1 Sites

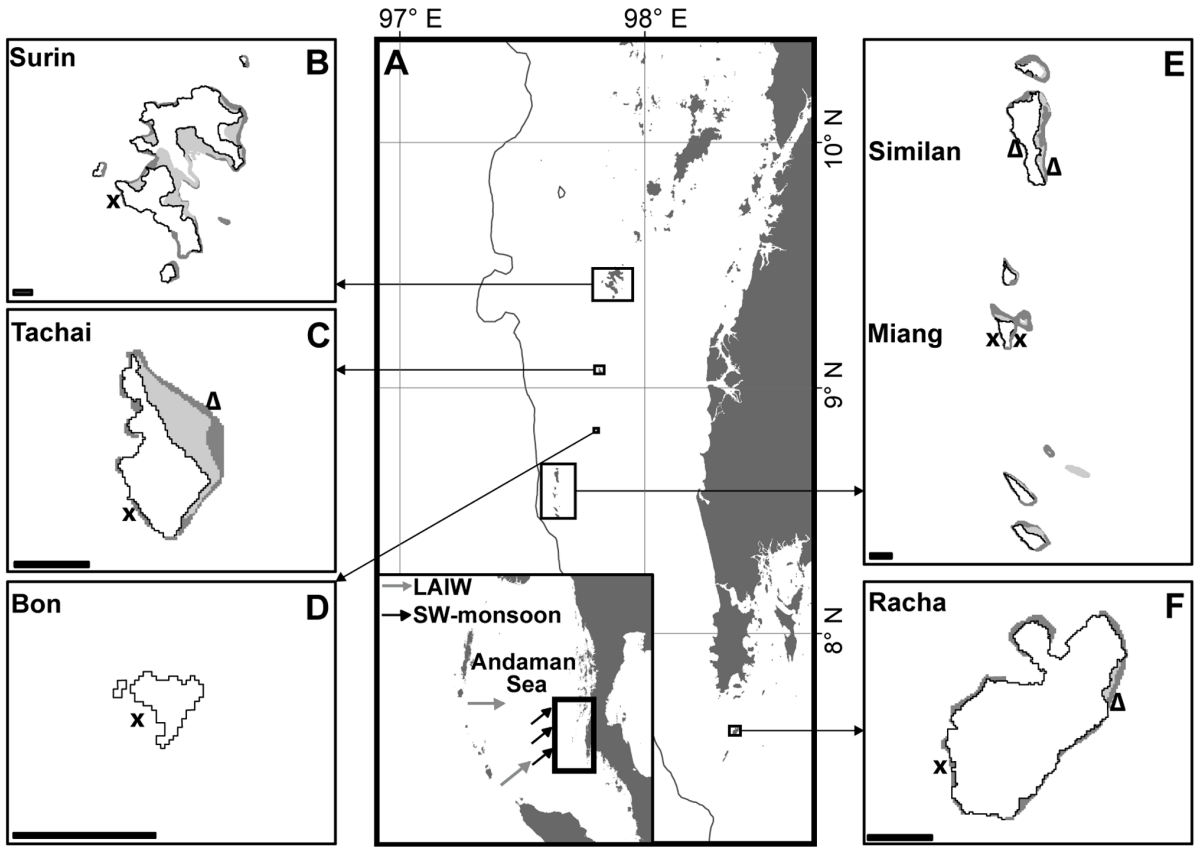

Figure 1: Location of sample sites, Andaman Sea, Thailand. A) Map of the study area in the Andaman Sea offshore the west coast of Thailand with inset showing the Andaman Sea from the Nicobar Islands Arc to the southeast Asian mainland of Burma and Thailand (Mainland: Wessel & Smith, 1996, Bathymetry: Smith & Sandwell, 1997). B-F) Close-up maps of the study islands (Surin, Tachai, Bon, Similan, Miang and Racha) with sampling sites (UNEP Coral Millennium Project). Crosses: core sampling sites with high-resolution temperature monitoring and framework height determination (at Miang W and Surin W additional CTDs were deployed) ; triangles: sites where only framework height was measured (Tachai E and Racha E the present study, Similan E and W framework height derives from (Schmidt *et al.*, 2012)). Scale bar represents 1 km.

Five islands in the Andaman Sea located on the continental shelf off the western Thai coast were chosen for this study. The study covers the area between 9.5°N to 7.5°N and 97.6°E to 98.5°E. From north to south the study islands were: Surin, Tachai, Bon, Similan, Miang and Racha (Fig. 1), which differ in their distance to the shelf break: 62km, 43km, 35km, 22km (Similan and Miang) and 53km, respectively. Thus, the islands are potentially subjected to different degrees of LAIW intensity with the highest LAIW impact expected at Miang W (shortest distance to the shelf-break) and lowest LAIW impact at Surin (longest distance to the shelf break). Six sites were selected for both environmental monitoring and framework measurements with 5 of them facing W, thus being exposed to LAIW and SW monsoon impact and 1 site was chosen as a control site located on the LAIW and SW monsoon sheltered E coast of Miang (Fig. 1; Surin W, Tachai W, Bon W, Miang W, Miang E and Racha W; these sites represent the core sampling sites). Framework height was further determined on 4 additional sites facing

the sheltered E side (Tachai E and Racha E; the present study, Similan E and W derived from Schmidt *et al*. (2012), Fig.1). Sites were selected by snorkeling along the coast of the studied islands. The sites with the most vigorous reef development were chosen to compare the maximum reef development potential between sites. The study was performed within 9 cruises during both, dry and wet seasons from November 2009 through November 2011 with permission for conducting research at the different location provided by the National Research Council Thailand (NRCT) (Table S1, 5.1 Appendix I).

2.2 Reef framework height determination

The lack of a true carbonate framework in the exposed faces of the islands (Schmidt *et al*., 2012) precluded the use of coring to determine the height of the reef framework (e.g. Scoffin & Tissier, 1998). Reef framework height was determined according to Schmidt *et al*. (2012) with a non-destructive method (using scaled images) at a depth of 15 m. Scaled high-resolution (14.7 Mpix) photographs were taken with a digital camera (Canon G10 camera with a 28 mm wide-angle lens in a Canon WP-DC 28 housing), showing the elevation of coral framework above its basement (sediment or rock). A measuring stick with 5 cm tick marks positioned perpendicular to the bottom at the study depth in front of the framework was used as a reference. Up to 45 images were taken along and at both sides of a 50 m transect where corals or carbonate structures were present. The height of the framework was calculated by image analysis with the software ImageJ as the closest distance (in cm) between the top of corals/carbonate structure and the basement. Only corals/carbonate structures in the same plane as the stick were measured (corals/carbonate structures in the front of or behind of the measuring stick would have been over or underestimated in height). This resulted in 1 to 5 measurements per image. A total of 268 framework measurements were carried out (33, 31, 38, 45, 30, 45, 21 and 25 in Surin W, Tachai E, Tachai W, Bon W, Miang E, Miang W, Racha E and Racha W, respectively). Framework height data for Similan E and W derived from Schmidt *et al*. (2012).

2.3 Environmental characterization

Temperature: Temperature was monitored with temperature loggers (3 Onset HOBO Tidbits per site, temperature resolution: ± 0.2°C) deployed in 15 m water depth approx. 30 cm above the bottom fixed on the sediment trap holders. Temperature was recorded at 6 sites (Miang W, Miang E, Bon W, Tachai W, Surin W and Racha W; Fig. 1; temperature data for Similan E and W were set equal to Miang E and W, respectively; justification see Schmidt *et al*. (2012)). The limited storage capacity of the loggers (battery power was not limiting) and limited access to the study area during the monsoon period (May- to October) necessitated the combination of the data of 2 adjacent loggers (sampling interval: 6 minutes, phase lag between loggers: 3 minutes) to 1 time series yielding a composite sampling interval of 3 minutes. During the remainder of the year, where access to the study area was not limited, the loggers were programmed to sample every 3 minutes and exchanged more often. The loggers were intercalibrated

and calibrated in a water bath at room temperature in the lab with a high precision temperature meter (Amarell ama-digit ad3000th, ± 0.01°C, off-sets ranged from 0.33 to -0.24°C).

Conductivity-Temperature-Depth (CTD) - Profilers: In December 2010 and March 2010 2 Seabird CTDs (Seacat SBE 19plus and 19plus V2) were deployed at 2 sites (Miang W and Surin W) to record temperature, conductivity, oxygen and pH (19plus V2 with pH, 19plus with oxygen). Instruments were deployed for approximately 48 hours in December (both sites) and 5 and 14 days in March (Surin W and Miang W, respectively) and the logging interval was set to 5 minutes.

Sedimentation rates: At all core sampling sites (see Fig. 1) 3 sediment traps were deployed in a distance of 12 m to each other. Each of these traps contained 2 glass tubes sealed with a bottom lid (Ø 60x180 mm; 1:3 according to McClanahan and Obura (1997)), which were mounted on a steel rod with concrete base. The bottle openings were placed 50 cm above ground and were fitted with a baffle (grid size 1 cm) to minimize hydrodynamic disturbances in the collector and to prevent the entrance of larger organisms (Bothner *et al*., 2006). The traps were deployed in November/December 2009 and exchanged 6 times during the research period until November 2011 (Table S1, 5.1 Appendix I). From sediment samples macro-invertebrates were removed and the samples dried at 80 °C for 24 h to constant weight. The sedimentation rate was calculated in mg dry mass cm^{-2} day^{-1}.

Grain size distribution: Close to but beyond the hydrodynamic influence of each sediment trap 1 sediment core (in total 3 cores per site, Ø 5cm approximately 5 cm into the sediment) was collected in January, March, May, July, December 2010 and March 2011 (Table S1, 5.1 Appendix I). Each core sample was mixed to assure homogeneity and a subsample of 20 g was mixed with 200 ml distilled water and 8 ml sodium hexametaphosphate and stored over night at room temperature. The soil sample was then poured into a shaker with 63, 125, 250, 500, 1000, and 2000 μm mesh size. Shaking was performed for 5 minutes, the particles of each mesh size washed into pre-weighed aluminum cups and dried over night at 80°C for dry weight determination. Grain size values of each site are expressed as dimensionless mean phi value (Krumbein, 1934) of the 3 sediment cores, and classified according to the Udden-Wentworth (Wenthworth, 1922) size scale into coarse or medium sand (grain size phi: 0-1 coarse sand, 1-2 medium sand and > 2 fine sand).

2.4 Data processing and statistical analysis

Statistical tests were performed with the program R, Sigma Plot v11 was used for plotting the data.

Normality and homoscedasticity of the data was ascertained with the Shapiro-Wilk and Fligner-Killeen test, respectively. Non-parametric tests were applied when data did not comply with the parametric test requirements of normality and homogeneity of variances. Differences between seasons and sites were tested with ANOVA and Tukey HSD post-hoc analysis, Kruskal-Wallis rank sum test and

the Wilcoxon rank sum test, accordingly. Spearman's rank correlation was used to explore the correlations of pH, oxygen and conductivity with temperature.

2.4.1 Environmental variability characterization

To assess the differential impact and the relative contribution of the 2 disturbance regimes, LAIW and monsoon, environmental parameters were calculated characterizing changes in environmental conditions.

Parameter characterizing LAIW

Temperature anomalies: Abrupt and pronounced sea-bed temperature drops are a hallmark of internal wave diapycnal mixing in coastal water, as opposed to the gradual change induced by changing horizontal currents. Surface wave vertical mixing by contrast causes one to two orders of magnitude smaller effects in the opposite direction and can thus be neglected (Thorpe, 2007). The integration of negative temperature deviations from the mean temperature (here we use the modal, i.e. the most common value instead of the arithmetic mean) is thus a good measure of the intensity of environmental fluctuations. The temperature anomalies were calculated as cumulative degree days (DD) for each month according to Schmidt *et al*. (2012) (a modification of Leichter and Genovese (2006) with the only differences that residuals were calculated from the daily running mode instead of mean). Thus the calculated temperature anomalies were comparable to previous investigations in this region (Schmidt *et al*., 2012). Each single temperature record was subtracted from the daily running mode and the negative deviations (°C) first multiplied with the sampling interval (in days) and then summed up for each month. To quantify the yearly LAIW impact (yearly impact) cumulative DD per month were averaged for an entire year (December 2009 to November 2010). Additionally, a measure for the period of maximum temperature variations (maximum impact) was calculated using only the average of the cumulative DD per month of the LAIW-intense dry season (December – to May 2010, as during this time LAIW were strongest).

Parameters describing monsoon

Due to logistical constraints wave measurements during SW monsoon seasons were not feasible and we relied on another measure to quantify the impact of the SW monsoon, in particular, the impact on the hydrodynamic conditions at site (such as wave action, current flow or tidal flow). To quantify the intensity of turbulences due to both LAIW and SW monsoon the amount of sediment collected in the traps (sedimentation rate) as well as bottom sediment characteristics (bottom sediment grain size) were used as proxies.

Sedimentation rate: Sedimentation results from mobilization and resuspension of bottom sediment due to wave action, currents, tidal forcing and internal wave enhanced flow. Because there are no rivers close to the study area run-off and major terrigenous sediment input can be neglected. Hence, the sediment captured by the traps derived from and reflected the hydrodynamic conditions at site, such as (1) currents scouring the sea-bed and enhancing the particle load in the bottom boundary layer (Hoitink & Hoekstra,

2003, Storlazzi *et al*., 2004), (2) oscillating currents due to ocean swell (Porter-Smith *et al*., 2004), (3) LAIW leading to resuspension and subsequent sedimentation of bed-load particles (Pomar *et al*., 2012), and (4) SW-monsoon surface wave impact increasing sediment load (Porter-Smith *et al*., 2004). Sedimentation was thus a composite annual proxy for monsoon and LAIW, where the surface wave impact was captured during the SW monsoon sampling period (May-October), while the internal wave impact is reflected in the dry season samplings (November – April).

Grain size phi: In a previous study (Scoffin *et al*., 1992) in Thailand bottom sediment properties were used as a proxy for reef exposure to rank-order sites. This proxy was adopted in the present study and slightly modified as according to the scale of Scoffin *et al*. (1992) all sites were classified as high hydrodynamic energy reefs (almost mud-free reefs - mud content < 63 μm: 2.40-4.64% weight; Kruskal-Wallis rank sum test: $\chi^2 = 5.68$, df = 5, p-value = 0.338; Table S2, 5.1 Appendix I). Thus, we used the mean grain size phi values to quantify the hydrodynamic energy for each site. Averaging all grain size phi values per sites yielded average yearly hydrodynamic conditions. The maximum impact was anticipated to occur during the wet season when the SW monsoon prevails and hence, values from the July 2010 sampling were used.

These parameters allowed comparison of sites with reference to the reef framework height. General linear models were fitted to the data with reef framework height as dependent and the environmental parameters as independent variables.

3. RESULTS

3.1 Reef framework

LAIW and monsoon exposed (Racha W, Bon W, Surin W, Miang W, Similan W and Tachai W) and LAIW and monsoon sheltered (Tachai E, Similan E, Miang E and Racha E) sites showed significant differences in reef framework height (Welch's t-test: t = 10.66, df = 131, p < 0.001) with highest framework on the protected E faces (Fig 2).

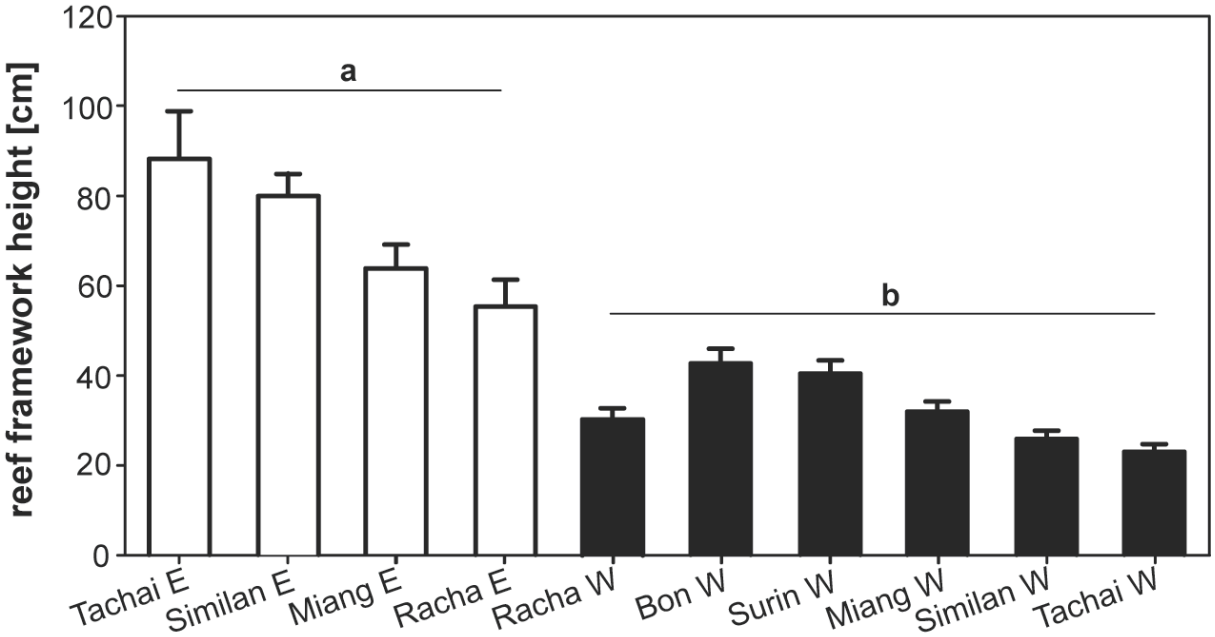

Figure 2: Reef framework height above bottom. Reef framework height (mean ± SE) measured at all study sites. Open bars are E sites (a), black bars W sites (b), showing significant differences (Welch's t-test: $t = 10.66$, $df = 131$, $p < 0.001$). Framework height is arranged from left to right with lowest to strongest LAIW (large amplitude internal waves) intensity (intenstities where estimated for sites were no temperature record were available (Tachai E, Racha E)).

3.2 Temperature variability

The temperature records at the 6 core sampling sites displayed differences in the intensity and frequency of temperature anomalies throughout the year, between sites and years (2010 vs. 2011 dry season, Fig. 3). However, the median temperature values between sites for this region (29 ± 0.69 °C with a maximum of 30.8 °C in 2010 (Fig. 3)) were not different between study sites (Kruskall-Wallis test: $\chi^2 = 6.266$, $df = 5$, $p = 0.281$). On the basis of temperature fluctuations 2 seasons could be distinguished (Fig. 4A) with a higher frequency and intensity of temperature variation during the NE monsoon (November to April) compared to the SW monsoon season (May to October) (t-test: $p < 0.0085$, Table S3, 5.1 Appendix I for p-values per site). Negative temperature anomalies were visible at all sites and these anomalies calculated as monthly cumulative DD differed between sites (ANOVA, $p < 0.001$, Table S4, 5.1 Appendix I) with higher temperature fluctuations on W than on E. Not all W sites showed significantly different temperature variations compared to Miang E suggesting LAIW attenuation, which however did not seem to be related to distance from the shelf break (Spearman rank correlation of yearly mean monthly cumulative DD and distance to the shelf break, $\rho = 0.3$, $S = 14$, $p = 0.683$). Additionally, inter-annual temperature anomaly intensity and frequency differed with stronger LAIW forcing in 2010 compared to 2011 (Fig. 3).

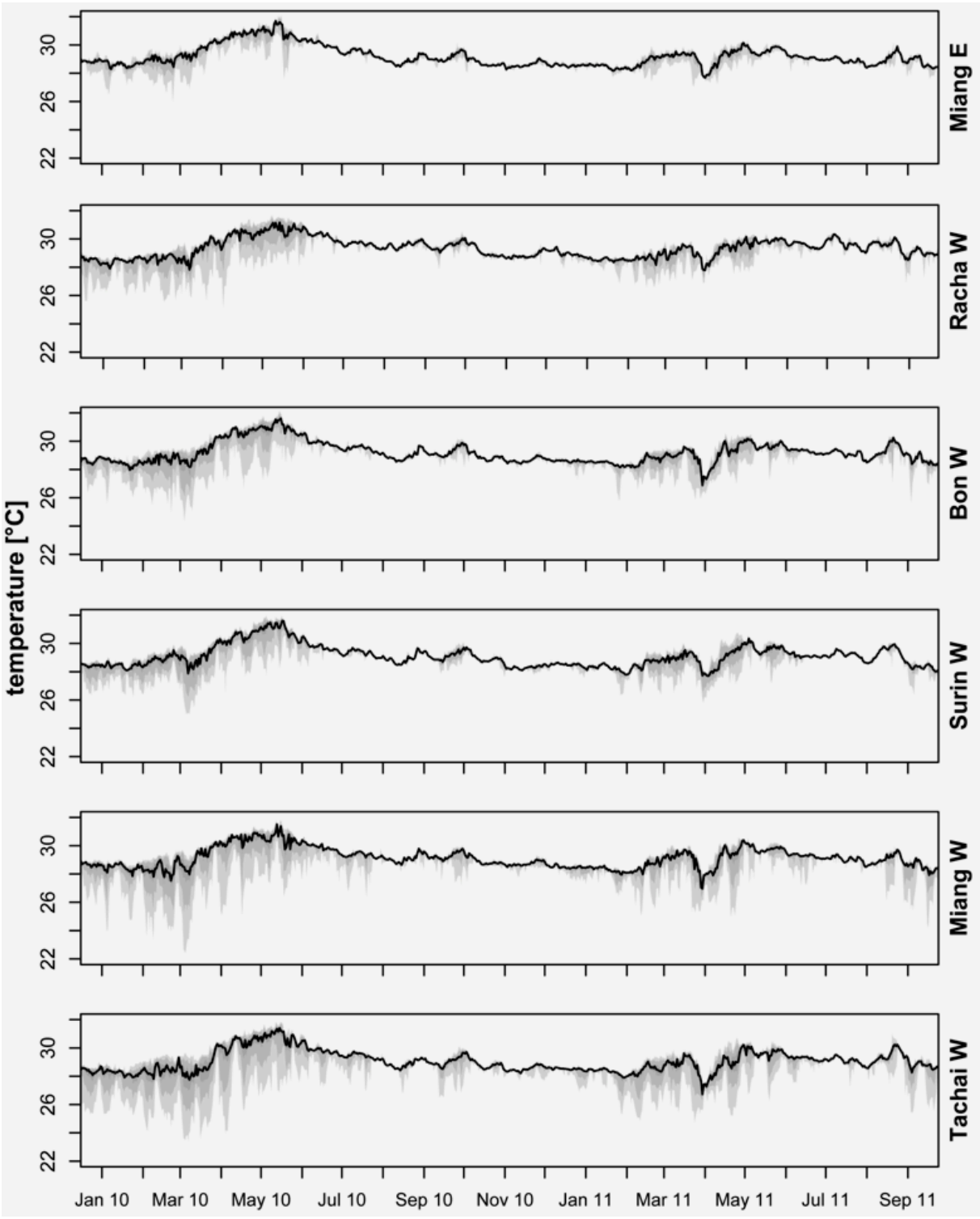

Figure 3: Seabed temperature at 15 m. Temperature record for the 6 core sampling sites (cf. Fig. 1) showing median (black lines) and quantil ranges in shades of grey (light gray: 0-1, intermediate gray: 0.05-0.95 and dark grey: 0.25-0.75). Sites are arranged from top to bottom (Miang E, Racha W, Bon W, Surin W, Miang W and Tachai W) with lowest to strongest LAIW (large amplitude internal waves) intensity.

3.2 Physico-chemical variability with temperature

Changes in chemical water parameters (conductivity, oxygen and pH) were well correlated with temperature fluctuations at the most distant and closest site to the shelf break (Surin W and Miang W, respectively). All correlations were highly significant and showed a decrease in pH, oxygen and an increase in conductivity with decreasing temperature values (Table 1).

Table 1: Correlation of environmental parameters. Spearman's rank correlations analysis of conductivity, pH and oxygen with temperature derived from CTD records at Miang W and Surin W (cf. Fig. 1) during December 2009 and March 2010 deployments. (ρ = correlation coefficient, n = number of measurements, p = probability level, significance levels are: * $p < 0.05$, ** $p < 0.01$, *** $p < 0.001$).

sites	season	correlated parameter		r	p	n
Miang W	December	temperature	conductivity	0.99	***	289
	December	temperature	pH	0.43	***	
	March	temperature	conductivity	0.92	***	4609
	March	temperature	oxygen	0.74	***	
Surin W	December	temperature	conductivity	0.86	***	577
	December	temperature	oxygen	0.65	***	
	March	temperature	conductivity	0.99	***	1008
	March	temperature	pH	0.78	***	

3.3 Sedimentation rates and bottom sediment grain size

Clear seasonal differences in sedimentation rates were measured with largest values at the height of the SW monsoon (Fig. 4B). During the dry season sedimentation rates were low and similar between sites (Kruskall-Wallis test: $\chi^2 = 7.6246$, df = 5, p = 0.1782). Around May rates started to increase only for the island W sites (Fig. 4B; Kruskal-Wallis test: $\chi^2 = 23.8949$, df = 5, $p < 0.001$).

Benthic sediment was composed of coarse to medium sand (Fig. 4C). In the W bottom sediments were coarser than in the E (ANOVA, $p < 0.001$, Table S5, 5.1 Appendix I) with the only exception found for Surin W with less coarse sediment (post-hoc Tukey HSD pairwise comparison Surin W and Miang E: p = 0.891). Racha W showed a strong fluctuation in grain size through out the year with comparable fine sediment in May and the coarsest sediment in July (Fig. 4C).

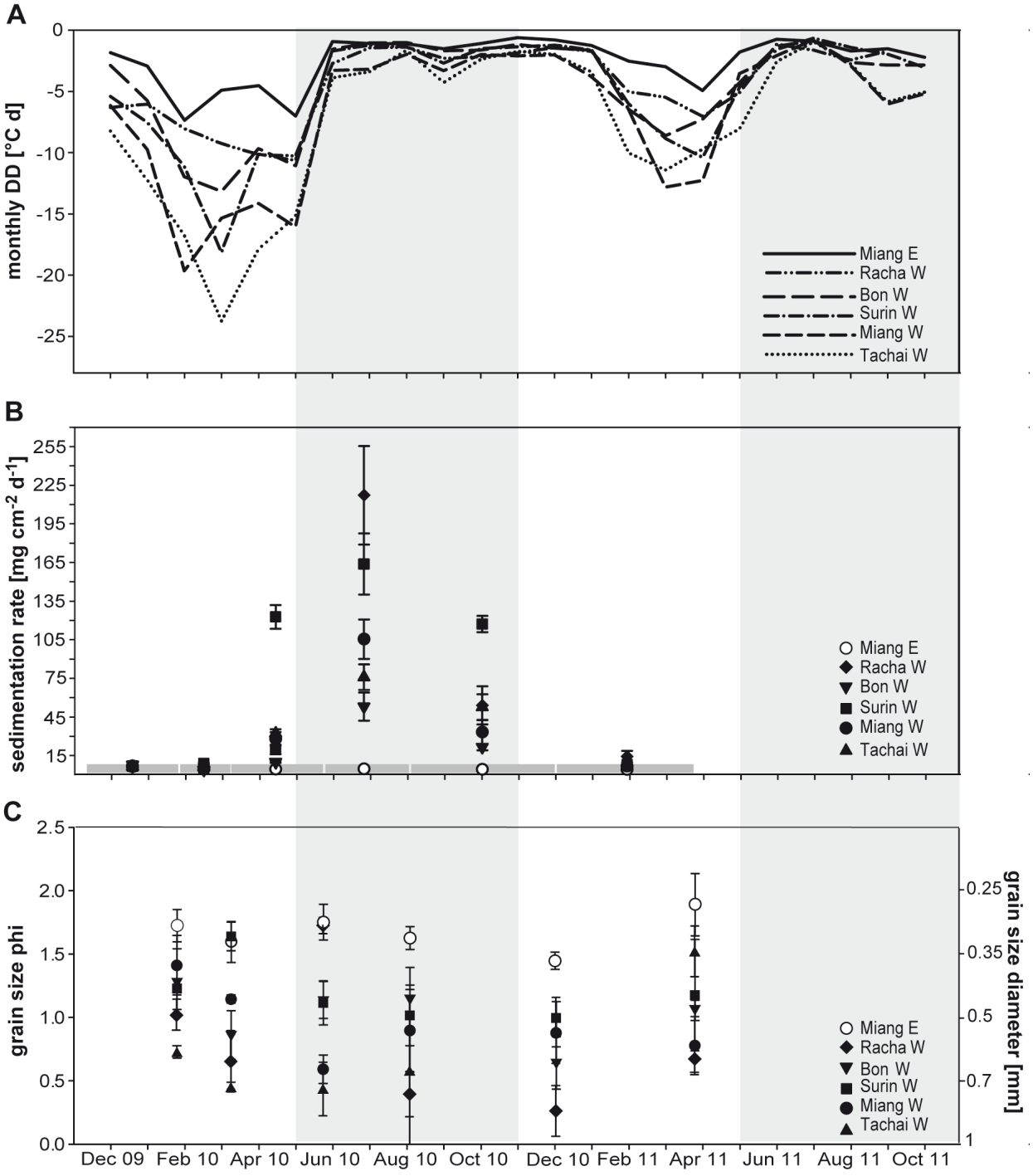

Figure 4: Negative temperature anomaly, sedimentation rate and grain size variation. All parameters are displayed for the study period November 2009 to December 2011 for the core sampling sites (cf. Fig. 1). A) Negative temperature anomalies calculated as cumulative degree days (DD) per month. B) Temporal evolution of sedimentation rates (mean ± SE) as dry sediment mass per cm^2. Deployment periods are indicated by the grey broken line parallel to the time axis. C) Grain size phi (mean ± SE) or diameter (mean ± SE [mm]). Grey shaded area corresponds to the SW-monsoon season May-November.

3.4 Reef framework and environmental indices

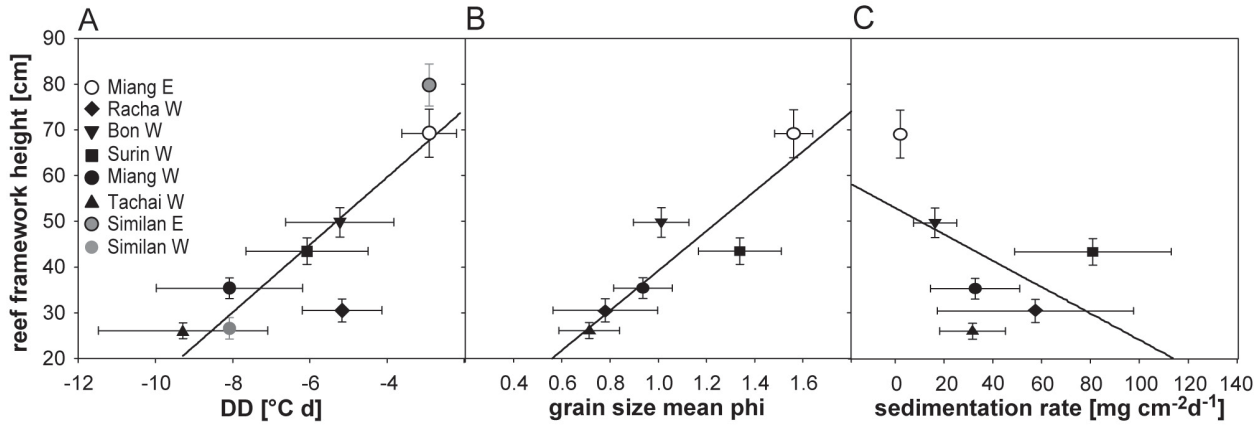

Figure 5: Reef framework height as a function of environmental parameters. Reef framework displayed as a function of A) temperature anomaly (DD = degree days), B) grain size phi and C) sedimentation rate. Environmental parameter represent mean values for an entire year - 12.2009-12.2010 derived for the core sampling sites (cf. Fig. 1): A-C) Miang W, Miang E, Bon W, Tachai W, Surin W, Racha W and for A) additionally from Similan E and W (Schmidt *et al*., 2012). Temperature anomaly values for Similan W and E were set equal to Miang E and W, respectively; justification see Schmidt *et al*., 2012. All values are given as mean ± SE.

Both the environmental parameters and reef framework height displayed differences between sites but these differences were not always statistically resolvable. A general linear model was calculated with reef framework height as dependent variable and the different environmental indices derived for each site as independent variables. The results indicate that both the temperature anomaly and grain size can well explain the reef framework height (core sampling sites: (1) temperature anomaly - yearly mean impact: $n = 6$, $r^2 = 0.68$, $p = 0.045$, max. impact: $n = 6$, $r^2 = 0.64$, $p = 0.055$, and (2) grain size - yearly mean impact: $n = 6$, $r^2 = 0.81$, $p = 0.015$ (Fig. 5B), max. impact: $n = 6$, $r^2 = 0.83$, $p = 0.011$; Table S6, 5.1 Appendix I). Two additional sites from the study Schmidt *et al*. (2012) were included to the model due to the availability of temperature information (see section 2.3) and showed an even stronger relationship between framework height and temperature anomaly (yearly mean impact: $n = 8$, $r^2 = 0.77$, $p = 0.004$ (Fig. 5A), max. impact: $n = 8$, $r^2 = 0.75$, $p = 0.005$ (Fig. 6); Table S6, 5.1 Appendix I). Framework development was inversely related to degree days and grain size. In contrast, the sedimentation rate did not follow the reef framework pattern (yearly mean impact: $n = 6$, $r^2 = 0.27$, $p = 0.286$ (Fig. 5C); max. impact: $n = 6$, $r^2 = 0.28$, $p = 0.278$; Table S6, 5.1 Appendix I) with highest sedimentation rates not corresponding to lowest reef framework height. A multiple linear model best explained the reef framework height (for core sampling sites only: $n = 6$, $r^2 = 0.97$, $p = 0.004$) and resulted in an improvement of the relationship between reef framework height and each single predictor when maximum impact of temperature anomaly and grain size ($p = 0.029$, $p = 0.009$, respectively) were combined. This indicates that the 2 disturbances with anticipated maximum impact during different seasons best explained the reef formation.

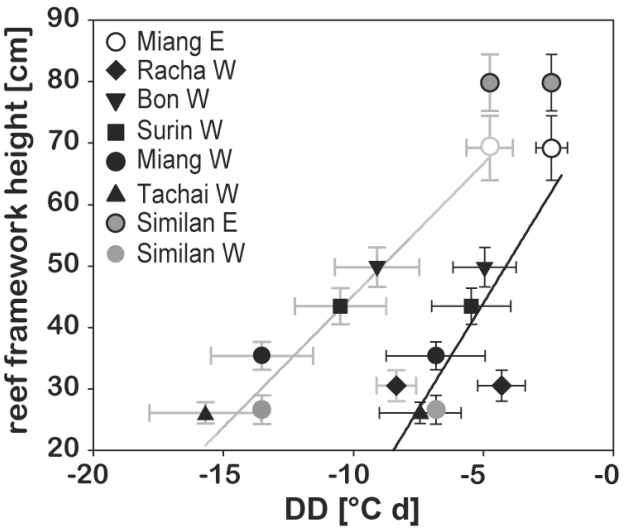

Figure 6: Reef framework height versus 2010 and 2011 dry season negative temperature anomaly. Reef framework height plotted as a function of dry season temperature anomaly (DD = degree days) reflecting the negative temperature anomalies experienced during the peak large amplitude internal waves (LAIW) period for 2010 (grey error bars and regression line) and 2011 (black error bars and regression line) for core sampling sites (cf. Fig. 1) plus Similan E and W (temperature anomaly values were set equal to Miang E and W, respectively; justification see Schmidt *et al*., (2012)). All values given as mean ± SE.

The length of the temperature records (> 2 years) allowed us to resolve the cumulative DD for 2 consecutive dry seasons and relate temperature anomalies for 2011 to reef framework height. The LAIW index for the dry season revealed a consistent ranking of the islands according to the intensity of temperature fluctuations between subsequent years (Fig. 6; period of max impact 2011: $n = 8$, $r^2 = 0.77$, $p = 0.004$; Table S6, 5.1 Appendix I).

4. Discussion

To the best of our knowledge this is the first study to explore the relative roles of internal wave and monsoon exposure on coral reef development. Although a previous study on the coral community composition of the Similan Islands has shown a pronounced difference in reef framework development between the E and W sides of the islands (Schmidt *et al*., 2012), the limited geographical extent and lack of angular resolution between the 2 potential disturbances (both acting from the same westerly direction) did not allow to resolve the relative contributions to the observed patterns. In the present study, the study area has been expanded from the Similan Islands (Schmidt *et al*., 2012) to a total of 6 different islands along the shelf of the Thai coast. Environmental proxy values have been used to determine environmental gradients, which could be attributed to LAIW and/or SW monsoon. We could show that across the entire shelf, temperature variability showed a clear correlation with reef framework height explaining a high percentage of the variability in framework development (77%, $p = 0.004$). These findings suggest that LAIW induced diapycnal mixing may undermine reef development. Similarly, Benzoni *et al*. (2003) found a positive relationship between framework development and distance to upwelling region in the

Gulf of Aden. The reduction in coral cover to single scattered colonies described by Sheppard and Salm (1988) and Glynn (1993) for the Oman reefs is reminiscent of the community structure observed for the Similan islands W sides (Schmidt *et al*., 2012). In spite of the reduced framework development Schmidt *et al*. (2012) found higher species richness on the W sides of the Similan Islands, which they attributed to intermittent and intermediate levels of disturbance (e.g. Glynn, 1993, Riegl, 1996, Riegl, 1999).

The reef framework height was not explained by sedimentation (Fig. 5C) displaying a clear monsoon signal, but by the sediment grain size (Fig. 5B). Temperature anomalies and sediment grain size provided the best correlation with framework height suggesting a combined impact of LAIW and monsoon at the intermediate depth, each having its strongest impact in the deeper and shallower parts of the reef, respectively.

Large amplitude internal waves forcing

Previous findings showed that changes in temperature along the Similan Islands co-varied with pH, oxygen, nutrient and salinity (Schmidt *et al*., 2012). The observed correlation in the present study confirmed these findings even for the most distant site to the shelf break (Surin W). Thus, the temperature anomaly index can be regarded as a good proxy for LAIW induced diapynal mixing involving a diverse set of environmental parameters. Although LAIW have their largest amplitudes in deep offshore waters, observational and modeling work has shown that they may advance onto the continental shelf (Helfrich, 1992, Vlasenko & Huttner, 2002) and propagate shoreward as trapped cores (Klymak & Moum, 2003). Although a physical understanding of LAIW in the study area is beyond the scope of this paper, our observations are consistent with the available models near the Andaman Sea shelf break suggesting that the pronounced temperature anomalies in our study are due to LAIW (Vlasenko & Stashchuk, 2007). Interestingly, the degree of variability observed at our study sites did not relate in all cases to cross-shelf distance from the shelf break. Modeling studies have shown that bottom topography can result in refraction and focusing of LAIW wave energy (Vlasenko & Stashchuk, 2007). Although the fine-scale bathymetry of the Thai shelf and continental slope is largely unknown, underwater features such as mounds or canyons at or near the shelf break (Vlasenko & Stashchuk, 2007) may account for the observed differences in temperature anomaly intensities between our sites.

The available studies on internal waves (the present study, Leichter & Genovese, 2006, Pineda, 1994, Wolanski *et al*., 2004) and coastal upwelling on coral reefs (Glynn, 1993, Jiménez & Cortés, 2003) suggest that diapycnal mixing is a mixed blessing. While the supply of nutrients and plankton are regarded as beneficial (Roder *et al*., 2011, Wolanski & Delesalle, 1995, Wolanski & Pickard, 1983), the cold temperatures (e.g. Al-Horani *et al*., 2005, Coles & Fadlallah, 1991, Jokiel & Coles, 1977, Saxby *et al*., 2003) and low pH (e.g. Feely *et al*., 2008, Kleypas *et al*., 2006, Manzello *et al*., 2008) can be stressful for corals. In particular, nutrient supply and heterotrophic energy supply due to plankton feeding may enhance the energy status of the corals and counterbalance negative effects such as reduced light, low

temperature and pH (Roder *et al*., 2010). In contrast, retraction of polyps during periods of plankton supply potentially off-sets this positive effect (Johannes & Tepley, 1974). On the other hand, it has been shown that for instance reduced light counteracts extreme temperature values both cold and warm (e.g. Jokiel & Coles, 1977) and increased currents favor nutrient uptake (Hearn *et al*., 2001). Positive, negative and synergistic effects are a matter of the intensity of diapycnal mixing due to LAIW or upwelling and potentially species-specific (Leichter & Genovese, 2006, Roder *et al*., 2011). Studies focusing on the ecosystem response showed a relationship between LAIW or upwelling intensity and community composition, reef framework height and cementation (Benzoni *et al*., 2003, Manzello, 2008, Manzello *et al*., 2008, Manzello, 2010, Schmidt *et al*., 2012, Wolanski *et al*., 2004) highlighting the importance of diapycnal mixing for reef development.

SW monsoon forcing – bottom sediment grain size as surrogate for hydrodynamic conditions

The reef framework height was furthermore explained by the grain size composition. Scoffin *et al*. (1992) used a similar value to rank Andaman Sea reefs according to the exposure to hydrodynamic processes. They indicated that hydrodynamic processes represent a main controlling factor of linear extension rate and skeletal density in *Porites lutea* with linear extension rate being inversely correlated to hydrodynamic conditions. However, Scoffin *et al*. (1992) collected coral skeletons close to the low water level and thus surface wave impact is expected as the main driving force. For Hawaiian reefs a relationship between community structure and grain size was observed for reefs in shallow, 3 m and 10 m water depth (Jokiel *et al*., 2004). Both of these studies indicated that grain size distribution serves as a good parameter describing reef hydrodynamic conditions and related them to reef structure and accretion. Grain size distribution combines wave action, current and swell but is also determined by bathymetry (Gagan *et al*., 1988). Both the strength and duration of the underlying processes determine mobilization and deposition (Porter-Smith *et al*., 2004). It has been shown that during the dry season LAIW induced strong currents may account for increased hydrodynamic conditions (Roder *et al*., 2010). Additionally, storm events can result in mobilization and deposition of storm deposits (tempestites). Swell waves can transport sediment towards shallower areas and both storm events and swell can influence bottom sediment composition (Porter-Smith *et al*., 2004). These hydrodynamic phenomena, including tidal currents, can act during both seasons and be responsible for the fact that no strong seasonal pattern could be seen. In general, the grain size properties of the study sites showed that W reefs were subjected to higher current and wave action during both seasons with slightly increased values during the peak SW monsoon season (Fig. 4C). This indicates that the strength of hydrodynamic processes increased resulting in removal of fine sediments but these were not strong enough to mobilize coarser sediment. In Racha strong variation in bottom sediment composition was observed, which could for instance reflect for storm deposits in May (depositing fine sediment) and followed by strong wave action and induced current

conditions reflected by an increased grain size and highest measured sedimentation rate during May through to the end of July.

Grain size gives a good reflection of the differences in hydrodynamic conditions between sites – as shown by several studies (e.g. Gagan *et al*., 1988, Jokiel *et al*., 2004, Porter-Smith *et al*., 2004, Scoffin *et al*., 1992).

SW monsoon forcing – sedimentation rate as surrogate for turbulences

From a climatological point of view, the reversal, onset and extent of the Asian monsoon are well established (Wang & Ho, 2001) but there is a lack of information about the oceanographic conditions (Buranapratheprat *et al*., 2010), in particular of wave height and period. Reversal of monsoon from NE monsoon of low wind conditions to wind-intense SW monsoon sets-in in May and it reaches its full extent during July to September with winds speeds of up to 10 m s^{-1} (Brown, 2007, Scoffin *et al*., 1992). Thus, during this period strongest wave impact can be expected for the monsoon-exposed W sites. Strong wind conditions generally prevailed for several days followed by a period of calm conditions (Wu & Zhang, 1998). Proxy values were used to estimate the turbulences and the hydrodynamic conditions at site. Sedimentation rates clearly displayed a monsoon signal. Peak sedimentation rates were obtained during June through August when the SW monsoon reaches its full extent (Scoffin *et al*., 1992, Wang & Ho, 2001). Comprehensive studies on wave climate exist from other regions linking wave action and reef hydrodynamic processes (Samosorn & Woodroffe, 2008, Storlazzi & Jaffe, 2008, Wolanski *et al*., 2005). These studies indicated a link between shallow water processes where waves break and induce current flow towards the fore reef (Storlazzi & Jaffe, 2008, Storlazzi *et al*., 2004, Woolfe & Larcombe, 1999). Both shallow water and deep-water resuspended sediments are a potential source for sediment settling on coral colonies. Increased hydrodynamic conditions (inferred from grain size data) also suggest a prevention of settlement and the transport of suspended sediment out of the study area (e.g. Bak & Meester, 2000, Larcombe & Woolfe, 1999, Storlazzi *et al*., 2011). Sedimentation on corals is known to be detrimental (Fabricius, 2005, Philipp & Fabricius, 2003, Riegl, 1995, Riegl & Branch, 1995, Weber *et al*., 2006). It definitively affects the coral community during the wet season on the W sites. The degree of damage, however, is species-specific, a matter of duration and of the origin of the sediments with terrigenous silty sediments exerting a stronger impact than carbonate sands (Philipp & Fabricius, 2003, Weber *et al*., 2006). A long-term study on corals subjected to high sedimentation rates inferred that corals suffered from bleaching and necrosis. But sedimentation damage is limited to coral colony grooves and edges resulting in partial mortality but not complete die off (Riegl & Bloomer, 1995). Hence the coral community suffers from increased sediment load (by direct and indirect effects such as light reduction) but the highest impact is limited to a certain time period of strongest monsoon forcing (June through August, and periods of calm wind conditions) and not expected to be continuous over longer time periods following the wind pattern (Wu & Zhang, 1998). Higher survival rates during experimentally excluded

light conditions, higher photosynthetic performance and the increased energy status of W corals suggest that their higher protein and pigment content enables them to cope with harsh peak SW monsoon conditions particularly with the reduced light conditions (Roder *et al*., 2010, Roder *et al*., 2011). Moreover, the fact that sedimentation cannot explain reef framework height agrees with findings of Bak and Meesters (2000) who did not observe a correlation between reef development and sedimentation.

Biological factors influencing reef formation

Biological factors such as larval supply, settlement space, or bioerosion (Kleypas *et al*., 1999) can be responsible for limited reef formation. Settlement space was not limited on either the W of the Similan Islands (Schmidt *et al*., 2012) or the other islands investigated (Phongsuwan pers. communication). This indicates that the availability of suitable substrate for larval settlement limiting reef formation elsewhere (Benzoni *et al*., 2003) does not account for the reduced framework development observed between W and E of the islands across the shelf. Data on larval recruitment rates only exist for the Similan island chain and where shown to be higher in W than in E but survival rates of juvenile corals to adult stage were decreased (Schmidt, 2010). This finding of a lowered survival rate complies with the stressful conditions exerted by LAIW and SW monsoon and the observed reduced framework. Bioerosion counteracts reef accretion and was found to be initially lower in W than in E of the Similan Islands (Schmidt, 2010) indicating a higher grazer abundance at E. The establishment of an internal bioeroder community however combined with a potentially reduced cementation (as described by Manzello *et al*. (2008) stronger upwelling intensity is related to reduced reef cementation) could result in a increased bioerosion at W. The driving force (increased internal bioerosion and decreased cementation) derives from changing environmental conditions and hence, supports the observed relationship between LAIW intensity and reduced framework production.

Differences in community composition were not investigated in the present study but potentially exist. Yet as shown by Benzoni *et al*. (2003) the potential to develop a reef framework is not a matter of community dominance by growth form or genus. Therefore, the observed framework derived from both internal wave, wave and current influence.

In summary

Inhibited framework development was found in several regions resulting form different kinds of disturbances (e.g. wave impact, upwelling, strong temperature fluctuation, turbidity) (e.g. Dollar, 1982, Glynn, 1993, Kleypas, 1996, Riegl, 1996, Riegl, 1999). The impact of episodic extreme events (tsunamis, tropical storms) has been described as a framework development preventative in shallow water areas (<10 m) (Allen & Stone, 2005, Phongsuwan, 1991). However, the coral cover was shown to be reduced and more scattered at greater depths along the W island sides in the present study (15 m, present study; 20 m,

Schmidt *et al*., 2012). This is in contrast to regions such as South Africa where corals evade wave impact and form dense coral communities in deeper areas (Riegl, 2001). Such an escape into deeper areas was not found at the islands W sides. The complex framework development at E 15 m and deeper (Schmidt *et al*., 2012) raised the question why the coral reef community at W does not expand into deeper regions.

Several studies indicated that internal waves impact reef development and represent a source of various disturbances changing inter alia temperature, pH, nutrient concentrations and turbidity (e.g. Pomar *et al*., 2012, Wolanski *et al*., 2004). Here we investigated reef development in intermediate depth (15 m) at reefs subjected to seasonal disturbances by surface waves (SW monsoon) and LAIW (NE monsoon). The Andaman Sea Islands' W faces are impacted by high wave energy indicated by the reduced framework in shallow areas (Schmidt *et al*., 2012). In intermediate depth where reef accretion can potentially take place the would-be reef framework builder are additionally subjected to surface wave induced sedimentation, strong currents and LAIW. In contrast to sedimentation the LAIW intensity and bottom sediment grain size both regressed with the reef framework height. We found a correlation between reef framework height and a combination of grain size and LAIW intensity suggesting a combined impact of LAIW and monsoon affecting the intermediate depth. The W reefs showed a coral community consisting of single isolated coral colonies with reduced framework height in 20 m water depth (Schmidt *et al*., 2012). In contrast, at E 20 m reef framework height equals the intermediate depth. The observed relationship with LAIW intensity supports the decreased framework height in 20 m as LAIW intensity increases with depth (Schmidt *et al*., 2012). Hence, LAIW impact prevents a vertical extension of the framework as well as a lateral expansion of a dense coral community below the storm-accretion limit into deeper areas.

Acknowledgments:

We thank the Director and staff of the Phuket Marine Biological Center (PMBC), in particular Niphon Phongsuwan for helping with site selection as well as the Biological Oceanography group for field assistance and logistical help. The study was funded by the PEOPLE-2007-1-1-ITN Marie Curie Action: CalMarO (Calcification by Marine Organisms). The National Research Council of Thailand (NRCT) provided research permission.

References:

Al-Horani FA, Ferdelman T, Al-Moghrabi SM, De Beer D (2005) Spatial distribution of calcification and photosynthesis in the scleractinian coral *Galaxea fascicularis*. *Coral Reefs,* **24**, 173-180.

Allen GR, Stone GS (2005) Rapid assessment survey of tsunami-affected reefs of Thailand. Final Technical Report. Nov 15, 2005. pp 124.

Apel JR, Holbrook JR, Liu AK, Tsai JJ (1985) The Sulu Sea internal soliton experiment. *Journal of Physical Oceanography,* **15**, 1625-1985.

Bak RPM, Meester EH (2000) Acclimatization/adaptation of coral reefs in a marginal environment. In: *Proc. 9th Int Coral Reef Symp*. pp 265-272. Proc. 9th Int Coral Reef Symp, Bali, Indonesia.

Behera S, Luo J, Yamagata T (2008) Unusual IOD event in 2007. *Geophysical Research Letters,* **35**, doi: 10.1029/2008GL034122.

Benzoni F, Bianchi CN, Morri C (2003) Coral communities of the northwestern Gulf of Aden (Yemen): variation in framework building related to environmental factors and biotic conditions. *Coral Reefs,* **22**, 475-484.

Blanchon P, Jones B (1995) Marine-planation terraces on the shelf around Grand Cayman: a result of stepped Holocene sea-level rise. *Journal of Coastal Research,* **11**.

Bothner MH, Reynolds RL, Casso MA, Storlazzi CD, Field ME (2006) Quantity, composition and source of sediment collected in sediment traps along the fringing coral reef off Molokai, Hawaii. *Marine Pollution Bulletin,* **52**, 1034-1047.

Brown BE (2007) Coral reefs of the Andaman Sea - an integrated perspective. *Oceanography and marine biology: an annual review,* **45**, 173-194.

Buranapratheprat A, Laongmanee P, Sukramongkol N, Prommas R, Promjinda S, Yanagi T (2010) Upwelling induced by meso-scale cyclonic eddies in the Andaman Sea. *Coastal Marine Science,* **34**, 68-73.

Coles SL, Fadlallah YH (1991) Reef coral survival and mortality at low temperatures in the Arabian Gulf: new species-specific lower temperature limits. *Coral Reefs,* **9**, 231-237.

Dollar SJ (1982) Wave stress and coral community structure in Hawaii. *Coral Reefs,* **1**, 71-81.

Done TJ (1982) Patterns in the distribution of coral communities across the central Great Barrier Reef. *Coral Reefs,* **1**, 95-107.

Edmunds PJ, Bruno JF (1996) The importance of sampling scale in ecology: kilometer-wide variation in coral reef communities. *Marine Ecology Progress Series,* **143**, 165-171.

Fabricius KE (2005) Effects of terrestrial runoff on the ecology of corals and coral reefs: review and synthesis. *Marine Pollution Bulletin,* **50**, 125-146.

Fabricius KE, Wolanski E (2000) Rapid smothering of coral reef organisms by muddy marine snow. *Estuarine, Coastal and Shelf Science,* **50**, 120-150.

Feely RA, Sabine CL, Hernandez-Ayon JM, Ianson D, Hales B (2008) Evidence for upwelling of corrosive "acidified" water onto the continental shelf. *Science,* **320**, 1490-1492.

Gagan MK, Chivas AR, Johnson DP (1988) Cyclone-induced shelf sediment transport and the ecology of the Great Barrier Reef. *Proceedings 6th International Coral Reef Symposium,* **2**, 595-600.

Gischler E (1995) Current and wind induced facies patterns in a Devonian atoll; Iberg Reef, Harz Mts., Germany. *Palaios,* **10**, 180-189.

Glynn PW (1993) Monsoonal upwelling and episodic *Acanthaster* predation as probable controls of coral reef distribution and community structure in Oman, Indian Ocean. *Atoll Research Bulletin,* **379**, 1-66.

Grigg RW (1998) Holocene coral reef accretion in Hawaii: a function of wave exposure and sea level history. *Coral Reefs,* **17**, 263-272.

Hearn CJ, Atkinson MJ, Falter JL (2001) A physical derivation of nutrient-uptake rates in coral reefs: effects of roughness and waves. *Coral Reefs,* **20**, 347-356.

Helfrich KR (1992) Internal solitary wave breaking and run-up on a uniform slope. *Journal of Fluid Mechanics,* **243**, 133-154.

Hoitink AJF, Hoekstra P (2003) Hydrodynamic control of the supply of reworked terrigenous sediment to coral reefs in the Bay of Banten (NW Java, Indonesia). *Estuarine, Coastal and Shelf Science,* **58**, 743-755.

Hughes TP, Baird AH, Dinsdale EA, Moltschaniwskij NA, Pratchett MS, Tanner JE, Willis BL (1999) Patterns of recruitment and abundance of corals along the Great Barrier Reef. *Nature,* **397**, 59-63.

Jackson CR (2004) An atlas of internal solitary-like waves and their properties. *2nd Ed. Office of Naval Research, Global Ocean Associates, Alexandria, VA, USA.*

Jiménez C, Cortés J (2003) Growth of seven species of scleractinian corals in an upwelling environment of the eastern Pacific (Golfo de Papagayo, Costa Rica). *Bulletin of Marine Science,* **72**, 187-198.

Johannes RE, Tepley L (1974) Examination of feeding of the coral *Porites lobata in situ* using time lapse photography. *Proceedings 2nd International Coral Reef Symposium,* **1**, 127-131.

Jokiel Pl, Coles Sl (1977) Effects of temperature on the mortality and growth of Hawaiian reef corals. *Marine Biology,* **43**, 201-208.

Jokiel PL, Brown EK, Friedlander A, Rodgers KB, Smith WR (2004) Hawai'i coral reef assessment and monitoring program: spatial patterns and temporal dynamics in reef coral communities. *Pacific Science,* **58**, 159-174.

Kleypas JA (1996) Coral reef development under naturally turbid conditions: fringing reefs near Broad Sound, Australia. *Coral Reefs,* **15**, 153-167.

Kleypas JA, McManus JW, Meñez LAB (1999) Environmental limits to coral reef development: where do we draw the line? *American Zoologist,* **39**, 146-159.

Kleypas JA, Feely RA, Fabry VJ, Langdon C, Sabine CL, Robbins LL (2006) Impacts of oceans acidification on coral reefs and other marine calcifiers: a guide for future research, report of a workshop held 18-20 April 2005. pp 88. St. Petersburg, FL, sponsored by NSF, NOAA, and the U.S. Geological Survey.

Klymak JM, Moum JN (2003) Internal solitary waves of elevation advancing on a shoaling shelf. *Geophysical Research Letters,* **30**, 2045.

Krumbein W (1934) Size frequency distributions of sediments. *Journal of Sedimentary Petrology,* **4**, 65-77.

Larcombe P, Woolfe KJ (1999) Increased sediment supply to the Great Barrier Reef will not increase sediment accumulation at most coral reefs. *Coral Reefs,* **18**, 163-169.

Latief H, Sengara IW, Kusuma SB (2008) Probabilistic seismic and tsunami hazard analysis model for input to tsunami warning and disaster mitigation strategies. *International Conference for Tsunami Warning (ICTW) Bali,* Indonesia.

Leichter JJ, Wing SR, Miller Sl, Denny MW (1996) Pulsed delivery of subthermocline water to Conch Reef (Florida Keys) by internal tidal bores. *Limnology and Oceanography,* **41**, 1490-1501.

Leichter JJ, Deane GB, Stokes MD (2005) Spatial and temporal variability of internal wave forcing on a coral reef. *Journal of Physical Oceanography,* **35**, 1945-1962.

Leichter JJ, Genovese SJ (2006) Intermittent upwelling and subsidized growth of the scleractinian coral *Madracis mirabilis* on the deep fore-reef slope of Discovery Bay, Jamaica. *Marine Ecology Progress Series,* **316**, 95-103.

Løvholt F, Bungum H, Harbitz CB, Glimsdal S, Lindholm CD, Pedersen G (2006) Earthquake related tsunami hazard along the western coast of Thailand. *Natural Hazards and Earth System Science,* **6**, 979-997.

Lowe RJ, Falter JL, Bandet MD, Pawlak G, Atkinson MJ, Monismith SG, Koseff JR (2005) Spectral wave dissipation over a barrier reef. *Journal of Geophysical Research,* **110**, C04001, doi:04010.01029/02004JC002711.

Manzello DP (2008) Reef development and resilience to acute (El Nino warming) and chronic (high-CO_2) disturbances in the eastern tropical Pacific: a real-world climate change model. *Proceedings 11th International Coral Reef Symposium,* **1**, 1299-1303.

Manzello DP (2010) Coral growth with thermal stress and ocean acidification: lessons from the eastern tropical Pacific. *Coral Reefs,* **29**, 749-758.

Manzello DP, Kleypas JA, Budd DA, Eakin CM, Glynn PW, Langdon C (2008) Poorly cemented coral reefs of the eastern tropical Pacific: Possible insights into reef development in a high-CO_2 world. *Proceedings of the National Academy of Sciences,* **105**, 10450-10455.

Massel SR, Done TJ (1992) Effects of cyclone waves on massive coral assemblages on the Great Barrier Reef: meteorology, hydrodynamics and demography. *Coral Reefs,* **12**, 153-166.

McClanahan TR, Obura D (1997) Sedimentation effects on shallow coral communities in Kenya. *Journal of Experimental Marine Biology and Ecology,* **209**, 103-122.

Moum JN, Klymak JM, Nash JD, Perlin A, Smyth WD (2007) Energy transport by nonlinear internal waves. *Journal of Physical Oceanography,* **37**, 1968-1988.

Murdoch TJT, Aronson RB (1999) Scale-dependent spatial variability of coral assemblage along the Florida reef tract. *Coral Reefs,* **18**, 341-351.

Osborne AR, Burch TL (1980) Internal solitons in the Andaman Sea. *Science,* **208**, 451-460.

Perry CT, Smithers SG (2010) Evidence for the episodic "turn on" and "turn off" of turbid-zone coral reefs during the late Holocene sea-level highstand. *Geology,* **38**, 119-122.

Philipp E, Fabricius K (2003) Photophysiological stress in scleractinian corals in response to short-term sedimentation. *Journal of Experimental Marine Biology and Ecology,* **287**, 57-78.

Phongsuwan N (1991) Recolonization of a coral reef damaged by a storm on Phuket island, Thailand. *Phuket Marine Biological Center Research Bulletin,* **56**, 75-83.

Phongsuwan N, Changsang H (1992) Assessment of coral communities in the Andaman Sea (Thailand). *Proceedings 7th International Coral Reef Symposium,* **1**, 114-121.

Pineda J (1991) Predictable upwelling and the shoreward transport of planktonic larvae by internal tidal bores. *Science,* **253**, 548-551.

Pineda J (1994) Internal tidal bores in the nearshore: warm-water fronts, seaward gravity currents and the onshore transport of neustonic larvae. *Journal of Marine Research,* **52**, 427-458.

Piniak GA, Storlazzi CD (2008) Diurnal variability in turbidity and coral fluorescence on a fringing reef flat: Southern Molokai, Hawaii. *Estuarine, Coastal and Shelf Science,* **77**, 56-64.

Pomar L, Morsilli M, Hallock P, Bádenas B (2012) Internal waves, an under-explored source of turbulence events in the sedimentary record. *Earth-Science Reviews,* **111**, 56-81.

Porter-Smith R, Harris PT, Andersen OB, Coleman R, Greenslade D, Jenkins CJ (2004) Classification of the Australian continental shelf based on predicted sediment threshold exceedance from tidal currents and swell waves. *Marine Geology,* **211**, 1-20.

Riegl B (1995) Effects of sand deposition on scleractinian and alcyonacean corals. *Marine Biology,* **121**, 517-526.

Riegl B (1996) Hermatypic coral fauna of subtropical south-east Africa: a checklist. *Pacific Science,* **50**, 404-414.

Riegl B (1999) Corals in a non-reef setting in the southern Arabian Gulf (Dubai, UAE): fauna and community structure in response to recurring mass mortality. *Coral Reefs,* **18**, 63-73.

Riegl B (2001) Inhibition of reef framework by frequent disturbance: examples from the Arabian Gulf, South Africa, and the Cayman Islands. *Palaeogeography, Palaeoclimatology, Palaeoecology,* **175**, 79-101.

Riegl B, Bloomer JP (1995) Tissue damage in scleractinian and alcyonacean corals due to experimental exposure to sedimentation. *Beitr Palaeontol,* **20**, 51-63.

Riegl B, Branch GM (1995) Effects of sediment on the energy budgets of four scleractinian (Bourne 1900) and five alcyonacean (Lamouroux 1816) corals. *Journal of Experimental Marine Biology and Ecology,* **186**, 259-275.

Roder C, Fillinger L, Jantzen C, Schmidt GM, Khokittiawong S, Richter C (2010) Trophic response of corals to large amplitude internal waves. *Marine Ecology Progress Series,* **412**, 113-128.

Roder C, Jantzen C, Schmidt GM, Kattner G, Phongsuwan N, Richter C (2011) Metabolic plasticity of the corals *Porites lutea* and *Diploastrea helipora* exposed to large amplitude internal waves. *Coral Reefs,* **30**, 57-69.

Rogers CS (1990) Response of coral reefs and reef organisms to sedimentation. *Marine Ecology Progress Series,* **62**, 185-202.

Samosorn B, Woodroffe CD (2008) Nearshore wave environments around a sandy cay on a platform reef, Torres Strait, Australia. *Continental Shelf Research,* **28**, 2257-2274.

Sandstrom H, Elliot JA (1984) Internal tide and solitons on the Scotian shelf: a nutrient pump at work. *Journal of Geophysical Research,* **89**, 6415-6426.

Satapoomin S, Nielsen TG, Hansen PJ (2004) Andaman Sea copepods: spatio-temporal variations in biomass and production, and role in the pelagic food web. *Marine Ecology Progress Series,* **274**, 99-122.

Sawall Y, Phongsuwan N, Richter C (2010) Coral recruitment and recovery after the 2004 Tsunami around the Phi Phi Islandas (Krabi Province) and Phuket, Andaman Sea, Thailand. *Helgoland Marine Research,* **64**, 357-365.

Saxby T, Dennison WC, Hoegh-Guldberg O (2003) Photosynthetic response of the coral *Montipora digitata* to cold temperature stress. *Marine Ecology Progress Series,* **248**, 85-97.

Schmidt GM (2010) Corals and waves - calcification and bioerosion in large amplitude internal waves (LAIW) affected coral reefs. PhD Thesis, University of Bremen, Bremen, 199 pp.

Schmidt GM, Phongsuwan N, Jantzen C, Roder C, Khokittiawong S, Richter C (2012) Coral community composition and reef development at large amplitude internal wave affected coral reefs in the Andaman Sea. *Marine Ecology Progress Series,* **456**, 113-126.

Scoffin TP (1993) The geological effects of hurricanes on coral reefs and the interpretation of storm deposits. *Coral Reefs,* **12**, 203-221.

Scoffin TP, Tissier MDAL (1998) Late Holocene sea level and reef-flat progradation, Phuket, South Thailand. *Coral Reefs,* **17**, 273-276.

Scoffin TP, Tudhope AW, Brown BE, Chansang H, Cheeney RF (1992) Patterns and possible environmental controls of skeletogenesis of *Porites lutea*, South Thailand. *Coral Reefs,* **11**, 1-11.

Sheppard C, Salm R (1988) Reef and coral communities of Oman, with a description of new coral species (Order Sclearctinia, Genus *Acanthastrea*). *Journal of Natural History,* **22**, 263-279.

Smith WHF, Sandwell DT (1997) Global seafloor topography from satellite altimetry and ship depth soundings. *Science*, **277**, 1957-1962.

Spalding M, Ravilious C, Green EP (2001) World atlas of coral reefs. *University of California Press, Berkley, California, USA*, pp 424.

Stoddart DR (1969) Ecology and morphology of recent coral reefs. *Biological Reviews,* **44**, 433-498.

Storlazzi CD, Ogston AS, Bothner MH, Field ME, Presto MK (2004) Wave- and tidally-driven flow and sediment flux across a fringing coral reef: Southern Molokai, Hawaii. *Continental Shelf Research,* **24**, 1397-1419.

Storlazzi CD, Jaffe BE (2008) The relative contribution of processes driving variability in flow, shear, and turbidity over a fringing coral reef: West Maui, Hawaii. *Estuarine, Coastal and Shelf Science,* **77**, 549-564.

Storlazzi C, Field M, Bothner M (2011) The use (and misuse) of sediment traps in coral reef environments: theory, observations, and suggested protocols. *Coral Reefs,* **30**, 23-38.

Subrahmanyam B, Murty VSN, Sharp RJ, O'Brien JJ (2005) Air-sea coupling during the tropical cyclones in the Indian Ocean: A case study using satellite observations. *Pure and Applied Geophysics,* **162**, 1643-1672.

Susanto RD, Mitnik L, Zheng Q (2005) Ocean internal waves observed in the Lombok Strait. *Oceanography,* **18**, 81-87.

Thorpe SA (1975) The excitation, dissipation, and interaction of internal waves in the deep ocean. *Journal of Geophysical Research,* **80**, 328-338.

Thorpe SA (2007) *An introduction to ocean turbulence,* Cambridge, Cambridge University Press.

Van Woesik R, Done TJ (1997) Coral communities and reef growth in the southern Great Barrier Reef. *Coral Reefs,* **16**, 103-115.

Vlasenko V, Huttner K (2002) Numerical experiments on the breaking of solitary internal waves over a slope-shelf topography. *Journal of Physical Oceanography,* **32**, 1779-1793.

Vlasenko V, Stashchuk N (2007) Three-dimensional shoaling of large-amplitude internal waves. *Journal of Geophysical Research,* **112**, C11018, 1-15.

Wallace BC, Wilkinson DL (1988) Run-up of internal waves on a gentle slope in a two-layered system. *Journal of Fluid Mechanics,* **191**, 419-442.

Wang B, Ho L (2001) Rainy season of the Asian-Pacific Summer Monsoon. *Journal of Climate,* **15**, 386-398.

Wang Y-H, Dai C-F, Chen Y-Y (2007) Physical and ecological processes of internal waves on an isolated reef ecosystem in the South China Sea. *Geophysical Research Letters,* **34**, L18609.

Weber M, Lott C, Fabricius KE (2006) Sedimentation stress in a scleractinian coral exposed to terrestrial and marine sediments with contrasting physical, organic and geochemical properties. *Journal of Experimental Marine Biology and Ecology,* **336**, 18-32.

Webster P, Moore A, Loschnigg J (1999) Coupled ocean-atmosphere dynamics in the Indian Ocean during 1997-98. *Nature,* **401**, 356-360.

Wellington GM (1982) Depth zonation of corals in the Gulf of Panama: Control and facilitation by resident reef fishes. *Ecological Monographs,* **52**, 224-241.

Wenthworth C (1922) A scale of grade and class terms for clastic sediments. *Journal of Geology,* **30**, 377-392.

Wessel P, Smith WHF (1996) A global self-consistent, hierarchical, high-resolution shoreline database. *Journal of Geophysical Research*, **101**, 8741-8743.

Wolanski E, Pickard GL (1983) Upwelling by internal tides and Kelvin waves at the continental shelf break on the Great Barrier Reef. *Australian Journal of Marine Resarch,* **34**, 65-80.

Wolanski E, Delesalle B (1995) Upwelling by internal waves, Tahiti, French Polynesia. *Continental Shelf Research,* **15**, 357-368.

Wolanski E, Colin P, Naithani J, Deleersnijder E, Golbuu Y (2004) Large amplitude, leaky, island-generated, internal waves around Palau, Micronesia. *Estuarine, Coastal and Shelf Science,* **60**, 705-716.

Wolanski E, Fabricius K, Spagnol S, Brinkman R (2005) Fine sediment budget on an inner-shelf coral-fringed island, Great Barrier Reef of Australia. *Estuarine, Coastal and Shelf Science,* **65**, 153-158.

Woolfe KJ, Larcombe P (1999) Terrigenous sedimentation and coral reef growth: a conceptual framework. *Marine Geology,* **155**, 331-345.

Wu G, Zhang Y (1998) Tibetean plateau forcing and the timing of the monsoon onset over the South Asia and the South China Sea. *American Meterological Society,* **126**, 913-927.

Yamano H, Abe O, Matsumoto E, Kayanne H, Yonekura N, Blachon P (2003) Influence of wave energy on Holocene coral reef development: an example from Ishigaki Island, Ryukyu Islands, Japan. *Sedimentary Geology,* **159**, 27-41.

Yang Y-J, Tang TY, Chang MH, Liu AK, Hsu M-K, Ramp SR (2004) Solitons northeast of Tung-Sha Island during the ASIAEX Pilot studies. *IEEE Journal of Oceanic Engineering,* **29**, 1182-1199.

2.2 MANUSCRIPT II

CASE STUDY 2010 CORAL BLEACHING IN THE ANDAMAN SEA – INTERNAL WAVES BLEACHING MITIGATION AND FUTURE IMPLICATIONS

M Wall[1], L Putchim[1,2], GM Schmidt[1], C Jantzen[1], S Khokiattiwong[2] & C Richter[1]

[1]*Alfred Wegener Institute for Polar and Marine Research,*
Am Alten Hafen 26, 27568 Bremerhaven, Germany

[2]*Phuket Marine Biological Center,*
51 Sakdidet Road, 83000 Phuket, Thailand

in preparation for Global Change Biology

Abstract

Most commonly satellite sea surface temperature data were used to hindcast and predict bleaching events, however, such data do not capture subsurface processes such as internal waves. The Andaman Sea features large amplitude internal waves (LAIW) that induce cold-water intrusions in shallow reef areas. In 2010 the Andaman Sea experienced a severe bleaching event. We monitored the temperature *in situ* at several islands on both west (W) LAIW exposed and east (E) LAIW sheltered island sides. Maximum temperature values reached up to 32.38 °C during the bleaching event. LAIW cold-water pulses prevailed during the heat stress and provided cold showers in particular on the W island sides. During the thermal stress period more bleached and recently dead corals were observed at the sheltered sides in contrast to the exposed island sides. LAIW intensity differed between sites and decreased gradually. This gradual decrease in cooling intensity was reflected in an increase in bleaching response (expressed as bleaching and mortality index - BMI). Southwest monsoon set in at the end of the thermal stress period inducing turbulent mixing and furthermore moderated heating at the exposed sites. Community composition differed between sites and, hence, the susceptibility of the reef community to heat stress. Site-specific community composition and cumulative heat stress together explained 75 % of the observed variability in bleaching response. The heat stress exceeded the stress limits of highly susceptible taxa and they vanished from the E but survived in small numbers on the exposed W sites. It has to be investigated whether the W sites can provide propagules of susceptible species and support their recovery at the sheltered E sites. The exposed island sides of several offshore islands in the Andaman Sea demonstrated that they can provide refuge during times of stress.

***key words**: coral bleaching, large amplitude internal waves, Andaman Sea*

1. Introduction

Global warming represents a major threat to coral reefs (Greenstein & Pandolfi, 2008, Hoegh-Guldberg, 1999) with already reported local extirpations of species (Glynn *et al*., 2001, Loya *et al*., 2001, Riegl, 1999) and decline in coral cover and species diversity (Carpenter *et al*., 2008, Glynn, 1991). In particular, worldwide reported bleaching events – live coral cover turning white due to the loss of their endosymbionts - contribute significantly to coral reef degradation. A continued decline in coral cover after bleaching was often associated with disease, *Acanthaster* outbreaks (Bruno *et al*., 2007, Miller *et al*., 2009, Rogers, 2009) and secondary stressors, such as pollution and intensive fishing activity (West & Salm, 2003).

Thermal stress and bleaching response are highly heterogenous between locations and derive from an interaction with local physical, chemical and biological conditions. Corals that survived such stressful conditions were found to recover from bleaching (e.g. Baker *et al*., 2008, Glynn, 1993, Guzman & Cortés, 2007) but recovery of reefs to pre-stress state conditions is timely and not always possible (Baker

et al., 2008 and references therein). Reefs that are able to return to their pre-stress state are described as resilient (Gunderson, 2000, Nyström & Folke, 2000). The resilience potential depends on environmental settings that abate heating (extrinsic factors) and corals physiological tolerance (intrinsic factors) that promote resistance or tolerance of stress (West & Salm, 2003). These complex set of variables complicates localized predictions and makes identification of resilient areas – so called refuge areas that have some sort of protection from severe heat stress - difficult (Maina *et al*., 2008, McClanahan *et al*., 2011).

Glynn (1996) postulated conceptual refuge areas where extrinsic factors favor coral survival during times of stress. He expected for instance that upwelling of cold water protect coral reefs from severe heat stress. Other environmental refuge settings encompass high latitude reefs, ocean banks, offshore islands exposed to vigorous water mixing and deep reef areas. The ability to alleviate heating response has already been demonstrated for upwelling regions (e.g. Glynn, 1996, Podesta & Glynn, 2001, Riegl & Piller, 2003). Offshore setting, however, not necessarily provide refuge (Riegl & Piller, 2003). Sheppard (2009) observed large temperature plunges at Diego Garcia atoll in the Indian Ocean similar to that described for several Andaman Sea coral reefs (Schmidt *et al*., 2012, Wall *et al*., subm.). He proposed that these internal waves induced temperature plunges coincide with the time period of warmest sea surface temperature (SST) and thus, such areas potentially provide refuge during heating.

The western Thai continental shelf, along the Andaman Sea, is subjected to large amplitude internal waves (LAIW). LAIW are waves that travel along density gradients within the water column (Thorpe, 1975). When they reach the continental shelf these waves break (Helfrich, 1992, Vlasenko & Alpers, 2005, Vlasenko & Stashchuk, 2007) and induce short pulses of deep-water intrusion into shallow reef systems (Leichter *et al*., 2005, Schmidt *et al*., 2012, Sheppard, 2009, Wall *et al*., subm.). These pulses are accompanied by sudden and pronounced temperature changes that can potentially serve as cold showers during heating events. LAIW are strongest during the dry northeast (NE) monsoon season when the pycnocline shoals. They alter not only the physical settings but also the chemical and trophic conditions delivering nutrients and plankton into the reef (Schmidt *et al*., 2012). The SW monsoon sets in after relaxation of the NE monsoon around end of April beginning of May and this transition from NE to SW monsoon correlates with the peak temperature phase (Khokiattiwong & Yu, 2012). Southwesterly winds push water masses towards the coast and start to depress the pycnocline, which results in reducing the intensity of LAIW intrusions. The SW monsoon reaches its full intensity around July/August and at this time cold-water pulses no loger reach shallow areas. The SW monsoon additionally induces turbulent mixing of surface water and resuspension of sediment resulting in increased sedimentation (Wall *et al*., subm.). Both LAIW and SW monsoon act from the same west to southwest directions effecting mainly west (W) island sides.

Recent studies on LAIW impact on coral reefs in the Andaman Sea elaborated a good characterization of exposed W and sheltered east (E) reef community structure of the Similan Islands by comparing

environmental settings, community composition, primary production, coral growth and trophic as well as metabolic adaptations (Jantzen, 2010, Roder *et al*., 2010, Roder *et al*., 2011, Schmidt *et al*., 2012). The coral reef community adapted to both annually recurrent disturbances (LAIW and SW monsoon) with W reef corals exhibiting higher pigment content and containing more energy reserves (Roder *et al*., 2010, Roder *et al*., 2011). The most notable difference constituted the reduced reef framework in W (Schmidt *et al*., 2012, Wall *et al*., subm.).

Compared to previous bleaching events in 1991, 1995 and 2003 (Brown & Phongsuwan, 2012, Kumar & Raghunathan, 2012, Phongsuwan & Changsang, 2012, Yeemin *et al*., 2012) the 2010 bleaching event was the most severe one recorded for the Andaman Sea. Several studies described the effect and consequences of this bleaching event for Thai continental shelf reefs with high losses in live coral cover (Brown & Phongsuwan, 2012, Phongsuwan & Changsang, 2012, Yeemin *et al*., 2012). Yeemin *et al*. (2012) noted that coral community in the W sides of offshore islands showed less mortality in juvenile corals. These authors hypothesized that LAIW may be responsible for the observed pattern.

The natural setting – W exposed to both LAIW cooling and SW monsoon turbulent mixing - provided the possibility to investigate their effect during thermal stress compared to the sheltered E. To test the "upwelling" refugia hypothesis (Glynn, 1996) we focused on an area of differential short-pulsed intrusions of deep water on shallow reef environments due to LAIW - in a broader sense a short-lived form of upwelling. We compared the W and E of several offshore islands with respect to temperature, bleaching response and subsequent mortality as well as recovery of corals from bleaching. Temperature was recorded with *in situ* temperature loggers that allowed a refined analysis of local scale differences in heating as well as cooling intensity. Differences in bleaching response might derive from differences in heating and cooling but also from differences in coral community composition. It is well known that coral species differ in their susceptibility to heat stress (e.g. Marshall & Baird, 2000, McClanahan *et al*., 2004) and this results in differences in bleaching vulnerability of the monitored coral communities. We calculated a site-specific susceptibility index that can be correlated with the observed bleaching response to disentangle confounding effects of community composition and mitigation mechanisms.

We hypothesized that LAIW and SW monsoon exposed sides suffer less during heating events than sheltered sites. Thus, we hypothesize that W reefs can provide refuge during times of stress.

2. Materials and methods

2.1 Sites

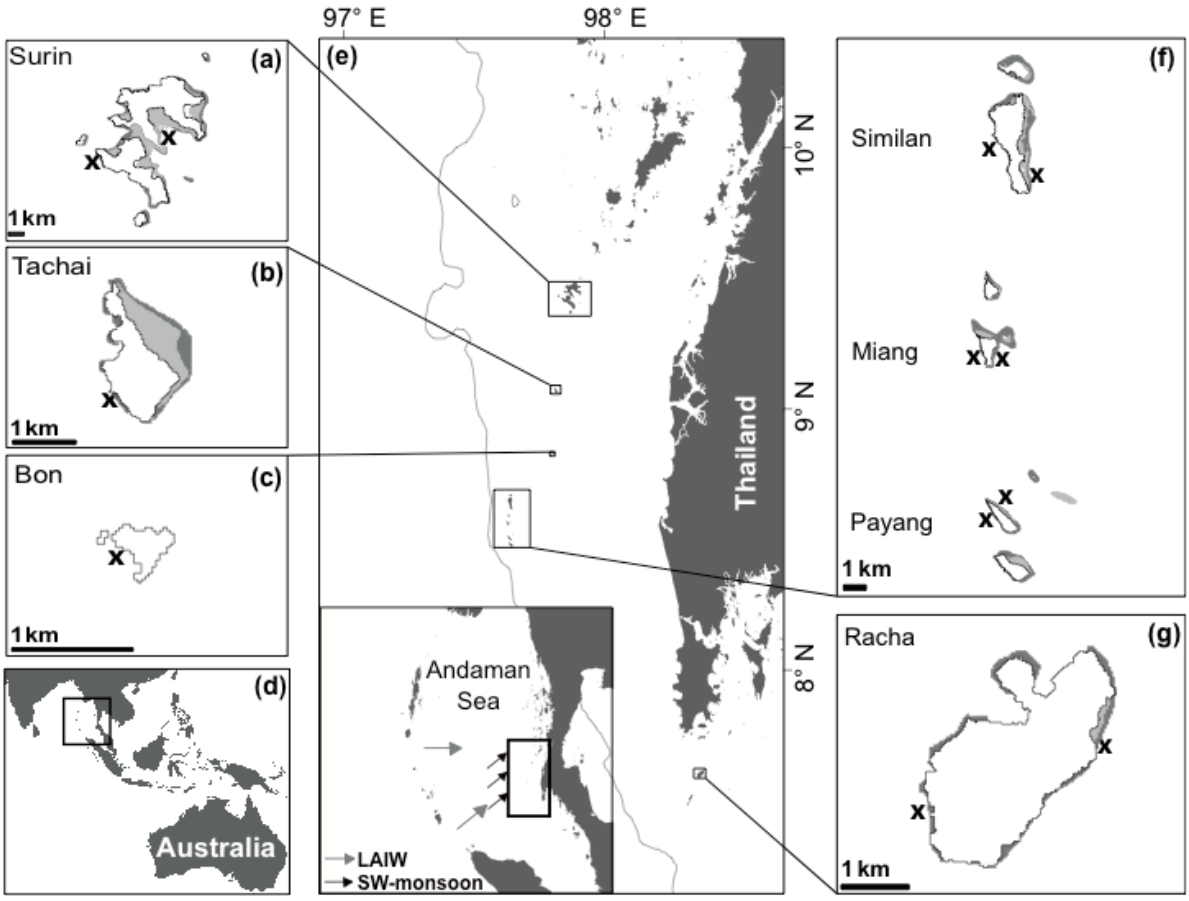

Figure 1: Location of sample sites, Andaman Sea, Thailand. Study area in the Andaman Sea (rectangular in (d) shows insert in (e)) at the west coast of Thailand (e). (e) Contour line indicates 200 m depth. Insert shows the Andaman Sea from the Nicobar Islands Arc to the Southeast Asian mainland of Burma and Thailand. (a-c, f-g) Study islands (Surin (a), Tachai (b), Bon (c), Similan (f), Miang (f), Payang (f) and Racha (g)) are assigned in the map (e) and study sites marked with a cross (a-c, f-g). (source of maps - Mainland: Wessel & Smith, 1996, Bathymetry: Smith & Sandwell, 1997 and study islands: UNEP Coral Millennium Project)

Seven islands in the Andaman Sea were chosen for this study and located on the continental shelf off the western Thai coast. From north to south the study islands were: Racha, Payang, Miang, Similan, Bon, Tachai and Surin (Fig. 1). Twelve sites were selected with seven of the study sites facing W exposed to LAIW and SW monsoon impact and five sites were located on the LAIW and SW monsoon sheltered E.

2.2 Environmental background

The temperature was recorded between March 2010 to the end of December 2011 with temperature loggers (Onset HOBO Tidbits (resolution: ± 0.2°C) per sites) deployed at each site in 15 m water depth at Racha W, Miang E, Miang W, Bon W, Tachai W and Surin W. At these sites temperature was recorded every 3 minutes. At Racha E loggers were deployed at 20 and 10 m in March with a logging interval of

20 minutes and recorded the temperature until the end July (Racha E). To obtain temperature values for the study depth temperature values were interpoloated between the 10 and 20 m logger. For Surin E a temperature record was available from 15 m water depth ranging from March to December 2010 with a logging interval of 20 minutes. Temperature values for E of Payang and Similan, as well as W of Payang and Similan was set equal to the respective island site of Miang (justification see Schmidt *et al*. (2012)). During the May sampling CTD (conductivity, temperature and depth) profiles were performed measuring temperature and salinity. The location of profiles are displayed in the Fig. S1 (5.2 Appendix II).

2.3 Bleaching survey

At each site photoframe images (50 x 50 cm) were taken at a depth of 15 m with a minimum of 29 quadrates during the May sampling and 27 during the recovery phase. Sampling procedure involved placing the frames randomly into the reef following the depth contour line and a photo was taken from above in a right angle to the frame. Photos were taken with a Canon Powershot G12 with underwater housing.

2.4 Analysis

Temperature analysis: Temperature data were analyzed to calculate different indices to characterize heating stress as well as the cooling due to LAIW. In order to receive a measure of the intensity of heating and cooling the temperature anomalies were calculated as cumulative degree days (DD in [°C d]) according to Leichter and Genovese (2006) but slightly modified. Here we considered temperature values as cooling (DDC) if they fell below the bleaching threshold of 30.1°C (Brown *et al*., 1996) and as heating (DDH) if they were above threshold. Each single recorded temperature value was subtracted from the bleaching threshold. The obtained temperature anomalies were multiplied by the sampling interval in days (for instance a sampling interval of 3 minutes equals to 0.0021 interval in days). A site-specific cooling intensity value was obtained by summing up all negative temperature anomalies for the heat stress period (started when diurnal mean exceeded the bleaching threshold and ended when diurnal mean fell below the bleaching threshold). Likewise a site-specific heating value was calculated by summing up all positive temperature anomalies for the same time period.

Other thermal indices were calculated according to Manzello *et al*., (2007), i.e. number of days that daily mean or modal SST was above a critical level, maximum monthly mean.

Photoframes: Photoframes were analysed using coral point count method ((CPCe) of Kohler and Gill (Kohler & Gill, 2006)) to determine the percent live and dead coral cover, coral community composition and coral status. For this purpose the area within the quadrat frame was selected in each image. A uniform grid of 15 x 15 points were laid within this area and the substrate identified. Substrate groups of interest represented live and dead coral (still recognizeable as coral). The status of 'live coral' was scaled ranging from "healthy" (with usual pigmentation), through "pale" (reduced pigmentation) and "bleached"

(complete white tissue) to "recently dead" (corals that just started to become overgrown by algae, but still the underlying white skeleton was still visible) (according to Podesta & Glynn 2001). In the case of live coral, 6 coral groups (*Porites* spp. - additionally distinguished between branching and massive, *Pocillopora* spp. (including *Stylophora* spp. colonies), *Acropora* spp., *Diploastrea heliopora,* other (all remaining taxa)) were distinguished. Additonally, the percentage of sensitive species per site were determined to compare sites and the degree of bleaching in relation to LAIW cooling.

Bleaching and mortality index (BMI) (McClanahan *et al*., 2004) were calculated for each site to receive a site-specific index quantifying the bleaching response of the coral community. This index is based on the field data and calculated as follows:

$$BMI = (0 * c_1 + 1 * c_2 + 2 * c_3 + 3 * c_4) / 3$$

Then the percent of 'live coral' cover of each recorded status-category (c_1 = healthy, c_2 = pale, c_3 = bleached, c_4 = recently dead, all as % cover at each site) was multiplied by a score 0-3, thereby weighing thedifferent status-categories according to their bleaching intensity (with no weight (0) for healthy (no bleaching) and heighest weight (3) for recently dead corals (bleaching lead to mortality)). The sum was normalized to a scale from 0-100 by deviding it by 3.

Community bleaching susceptibility index (CBSI) was derived by ranking the 6 recorded coral groups (see above) according to their reported susceptibility (e.g. Marshall & Baird, 2000, McClanahan, 2004, McClanahan *et al*., 2004, Phongsuwan & Changsang, 2012) into 4 bleaching susceptibility groups (0-3): less susceptible (*Diploastrea helipora* (s_1)), moderate susceptible (*Porites* massive spp. (s_2) and other (s_3)), susceptible (*Acropora* spp. (s_4) and *Porites* branching spp. (s_5)) and highly susceptible (*Pocillopora* incl. *Stylophora* spp. (s_6)). This index was calculated according to the BMI of McClanahan *et al*. (2004) where the s_1 to s_6 are the coral group occurrence (% 'live coral' cover).

$$CBSI = (0 * s_1 + 1 * (s_2 + s_3) + 2 * (s_4 + s_5) + 3 * s_6) / 3$$

Again this value was normalized to a scale form 0-100 by deviding the sum by 3.

The influence of different predictors on the observed BMI was tested. Simple and multiple linear regression models were calculated with R to identify the factors that best explain the observed BMI by using single predictors or combining predictors, i.e. enviornmental indices and the CBSI.

3. Results

3.1 Temperature development

The temperature data for each site are summarized in Table 1. At the end of March beginning of April at all sites the mean temperature values exceeded the bleaching threshold and temperature values stayed

above this level until beginning/mid June. CTD cast revealed that surface water masses showed elevated temperatures of 31°C down to 20 m water depth during the bleaching sampling over the whole continental shelf (Fig. S3, S4, 5.2 Appendix II). Heating was stronger at the E sites with more cumulative days above 30.1°C than at W reefs. In general, opposite island sites experienced pronounced differences in the number of days diurnal mean or mode temperature was above the bleaching threshold (Table 1). For instance, in Miang E and W thermal stress duration differed by 33 days while in Surin E and W 23 days differences were observed. These differences were less extreme when numbers of days above 30.1°C were calculated from the diurnal mode (defined as the most frequent temperature value measured at site and indicated the background normal reef temperature conditions). Between Miang E and W heat stress duration differed by 12 days and between Surin E and W by 17 days. These results indicate a strong effect of the temperature anomalies on the mean temperature values for the most exposed sites.

Table 1: Temperature conditions during the bleaching event in 2010. Temperature conditions summarized for the different sites (Tachai W (TW), Payang W (PW), Miang W (MW), Similan W (SiW), Racha W (RW), Surin W (SuW), Bon W (BW), Racha E (RE), Payang E (PE), Miang E (ME), Similan E (SeE) and Surin E (SuE)) during the bleaching period from March to June 2010. Temperature values are expressed as max. monthly mean SST, mean, min. and max. temperature recorded during this period, temperature anomalies calculated as degree day cooling (DDC) below median values, degree days heating (DDH) above bleaching threshold (30.11°C, cf. Brown et al 1996), the ratio of heating/cooling (DDH/DDC) and the heating rate (HR = DDH/days daily mean > 30.1°C) per site.

sites	days daily mode > 30.1°C	days daily mean > 30.1 °C	max. mean monthly SST [°C]	mean SST [°C]	max SST [°C]	min SST [°C]	DDH >30.1 °C [°C d]	DDC <30.1°C [°C]	ratio DDH/DDC
TW	68	47	30.74	30.34	32.05	22.07	31.46	-16.99	1.85
PW[1)]	73	51	30.34	30.28	31.92	22.05	26.86	-16.37	1.64
MW	73	51	30.34	30.28	31.92	22.05	26.86	-16.37	1.64
SiW[1)]	73	51	30.34	30.28	31.92	22.05	26.86	-16.37	1.64
RW	77	76	30.68	30.30	31.83	24.54	32.98	-12.06	2.74
SuW	62	55	30.82	30.54	32.22	23.87	37.91	-9.69	3.91
BW	71	67	30.83	30.63	32.28	23.39	41.50	-6.88	6.03
RE[2)]	86	86	30.90	30.65	32.29	25.71	50.58	-5.51	9.17
PE[1)]	85	84	30.84	30.62	32.38	26.30	46.36	-3.00	15.47
ME	85	84	30.84	30.62	32.38	26.30	46.36	-3.00	15.47
SiE[1)]	85	84	30.84	30.62	32.38	26.30	46.36	-3.00	15.47
SuE	79	78	31.26	30.81	32.2	27.58	58.49	-1.87	31.35

[1)] Payang E, Similan E, Payang W and Similan W were set equal to Miang West and East. Justifications see Schmidt *et al.* (2012).

[2)] Racha East temperature record was available only for 20 m and 10 m water depth. Values are interpolated to obtain approximated 15 m water depth temperature data.

3.2 Internal wave cooling

Temperature data revealed that during the thermal stress period in 2010 LAIW prevailed and induced cold-water pulses into the shallow reefs (Fig. 2, Fig. S2, 5.2 Appendix II). LAIW intrusion intensity declined at the same time as the temperature fell again below bleaching threshold (Fig. 2, S2 Appendix

II). During bleaching LAIW intensity differed between sites (Table 1, Fig. 2, S2, 5.2 Appendix II). Highest cooling values were recorded in Tachai W and Miang W (16.99 °C d and 16.34 °C d). Comparing heating and cooling values for these sites (Tachai W and Miang W) heating was approximately twice the intensity of the cooling (DDH/DDC of 1.64 and 1.85, respectively; Table 1). Miang E and Racha E showed the longest duration of the thermal stress period (84 and 86 days, respectively) but did not experience the strongest heating. The highest mean SST (30.81 °C) as well as max monthly SST (31.42 °C) was recorded in Surin E with heating values of 58 degree day above 30.1°C followed by Racha E with the second strongest heating (30.65°C, 30.90 °C and 59.42 °C d, respectively; Table 1).

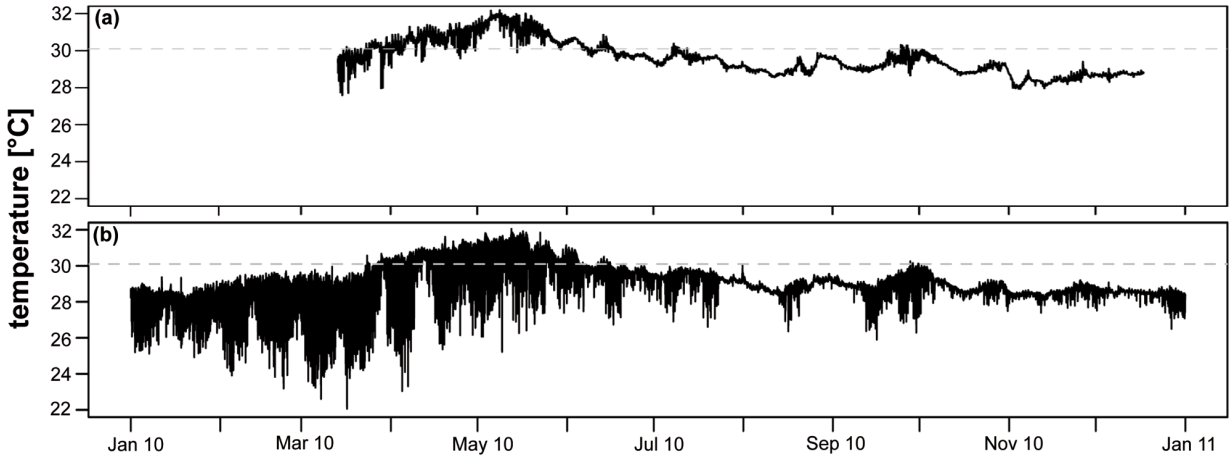

Figure 2: Temperature record during the study period. Example of two temperature profiles recorded during the bleaching year 2010 displaying the difference between protected (a) and exposed (b) sites. Data were measured at 15 m water depth at Surin E (a) and Tachai W (b). Grey line indicates the bleaching threshold temperature for coral reefs in this region (30.1°C, cf. Brown *et al*., 1996).

3.3 Bleaching response

Only a small percentage of corals were healthy in May two months after temperature exceeded the bleaching threshold (Fig. 3a). The coral community conditions differed between sites with a BMI ranging from 39 to 71.4 for Racha W and Miang E, respectively (Table 2). In general, more bleached and recently dead corals were recorded from the E compared to the W. This was particularly apparent when comparing opposite island sites (Fig. 3a, Table 2: e.g. Racha E vs W: 52.6 vs. 39.0, Miang E vs. W: 71.4 vs. 41.8 and Surin E vs. W: 61.2 vs. 45.2).

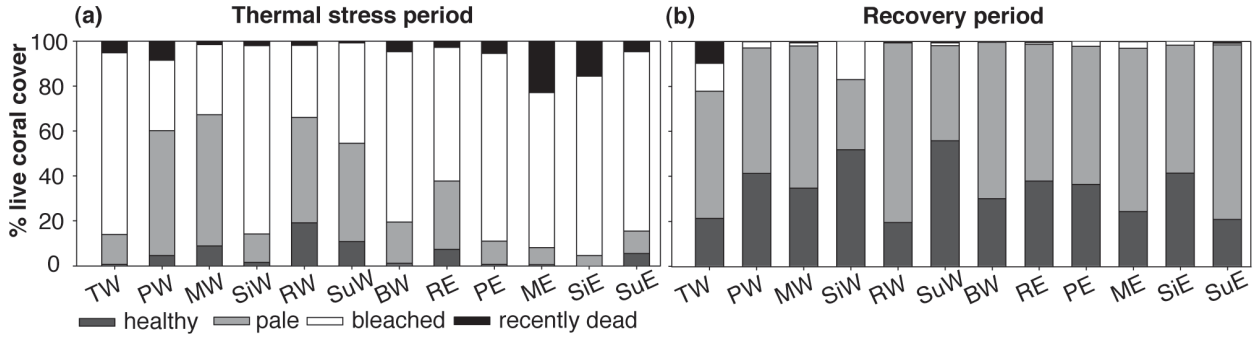

Figure 3: Coral reef community response to the thermal stress. (a,b) Coral status displayed as percentage of live coral cover and scaled as "healthy", "pale", "bleached" or "recently dead" during the bleaching event in May 2010 (a) and recovery phase in December 2010 (b). All data are displayed for all sites (Tachai W (TW), Payang W (PW), Miang W (MW), Similan W (SiW), Racha W (RW), Surin W (SuW), Bon W (BW), Racha E (RE), Payang E (PE), Miang E (ME), Similan E (SeE) and Surin E (SuE)). Sites are arranged according to the degree day cooling values from highest to lowest cooling left to right.

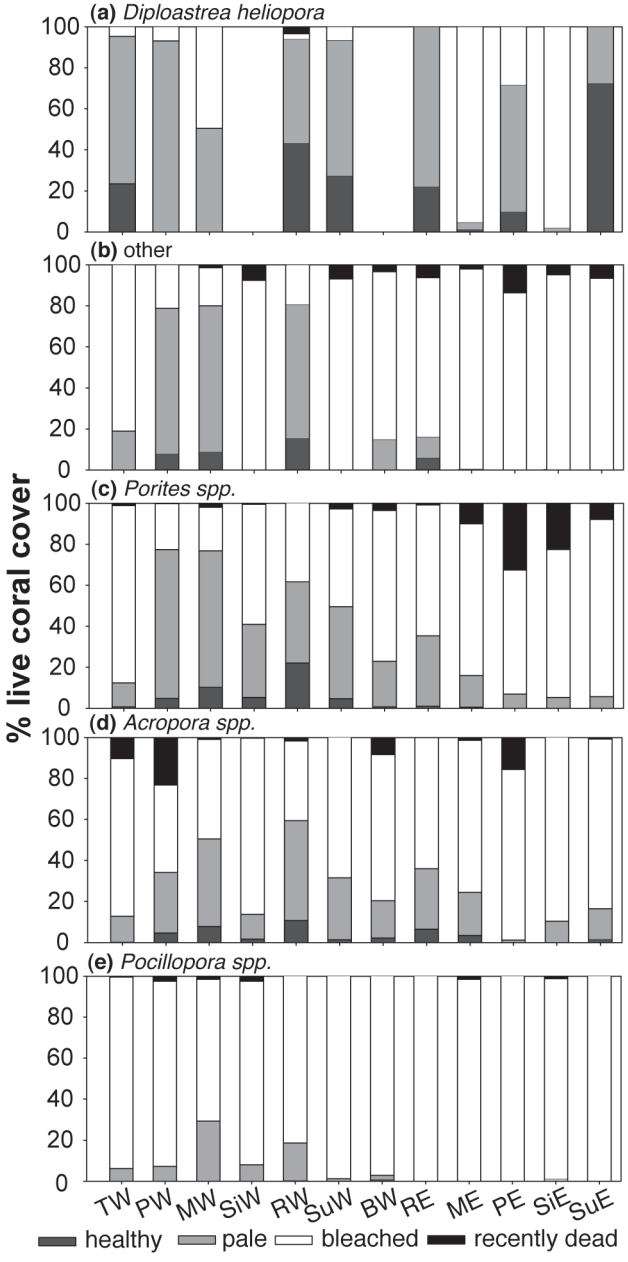

Figure 4: Coral genus status during the bleaching event in May 2010. Coral genus (*Pocillopora* spp. (a), *Acropora* spp. (b), *Porites* spp. (c), other (d), *Diploastrea heliopora* (e)) status as a fraction of live coral cover of each genus during the bleaching event in May 2010 for the sites Tachai W (TW), Payang W (PW), Miang W (MW), Similan W (SiW), Racha W (RW), Surin W (SuW), Bon W (BW), Racha E (RE), Payang E (PE), Miang E (ME), Similan E (SeE) and Surin E (SuE) (sites are arranged according to the degree day cooling with highest to lowest cooling from left to right).

Single coral groups showed strong differences in the extent of bleaching in May (Fig. 4). Least susceptible was *Diploastrea helipora* (Fig. 4a). *Pocillopora* spp. and *Acropora* spp. (Fig. 4d,e) were more vulnerable to the elevated temperature than *Porites* spp. and corals grouped as others (Fig. 4b,c). West reefs showed in average less strong bleaching effect (Fig 4, left to right) and this effect was protracted for different taxa (Fig. 4, bottom to top – susceptible to less susceptible, respectively) according to their bleaching susceptibility (Fig. 4). This confirms our bleaching susceptibility ranking of the monitored coral groups for CBSI.

Table 2: Bleaching and mortality index (BMI) and community bleaching susceptibility index (CBSI). Bleaching and mortality index as well as community bleaching susceptibility index calculated for all sites for May and the recovery phase in December 2010.

	TW	PW	MW	SiW	RW	SuW	BW	RE	PE	ME	SiE	SuE
BMI bleaching	63.5	47.9	41.8	62.1	39	45.2	61.4	52.6	64.6	71.4	70.4	61.2
BMI recovery	36.9	20.6	22.7	21.7	27.1	15.6	23.5	21.2	21.9	26.3	20.1	27.2
CBSI bleaching	44.6	45.3	41.5	46.7	29.7	24.5	43	42.6	47.2	45.5	39.7	35.6
CBSI recovery	34.1	28.6	35.3	34.9	26.7	11.6	33.8	28.4	32.8	29.4	32.7	30.9

3.4 Environmental parameters and community composition

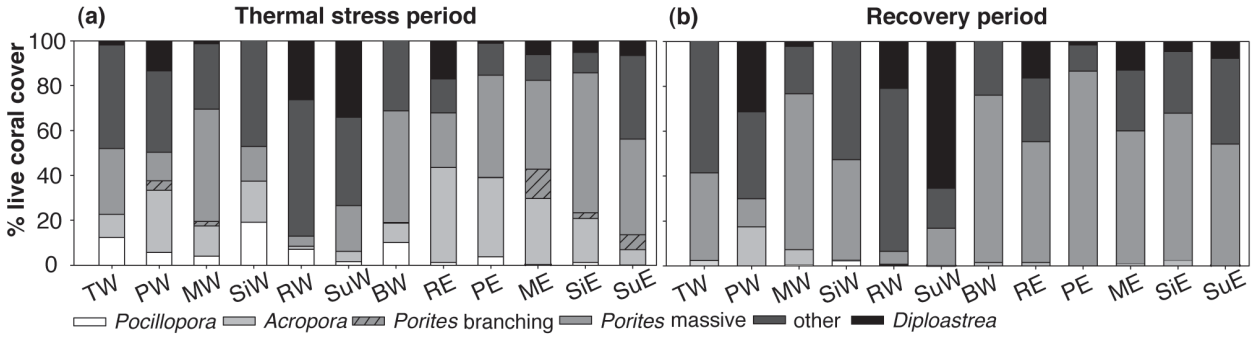

Figure 5: Coral community composition. Coral community composition (*Pocillopora*, *Acropora*, *Porites* branching, *Porites* massive, other and *Diploastrea* arranged from bottom to the top from the most bleaching susceptible to least susceptible taxa) as a fraction of live coral cover during the bleaching event in May (a) and recovery phase in December 2010 (b). All data are displayed for all sites (Tachai W (TW), Payang W (PW), Miang W (MW), Similan W (SiW), Racha W (RW), Surin W (SuW), Bon W (BW), Racha E (RE), Payang E (PE), Miang E (ME), Similan E (SeE) and Surin E (SuE)). Sites are arranged according to the degree day cooling values from highest to lowest cooling left to right.

Coral community composition differed between sites (Fig. 3c). East sites were dominated by *Acropora* spp. and *Porites* spp. massive while at the W none of the recorded groups was clearly dominating the coral community (Fig. 3c). The calculated community bleaching susceptibility index indentified Payang E and W, Miang E, Similan W and Tachai W as the most vulnerable coral communities to thermal stress while Surin E and W sides and Racha W were less susceptible (Table 2).

BMI was explained by the number of days diurnal mean was above 30.7°C but correlated only weakly (Table 3). Similarly BMI correlated weakly with the number of days diurnal mean was above 30.9°C, the CBSI and the DDC, but were marginally non-significant (Table 3). The variability in BMI was better explained (up to 75%) by a multiple linear model combining CBSI with temperature indices, i.e. the number of days the diurnal mean was above 30.7°C, max. monthly mean SST or DDC) as explanatory variables (Table 3).

Table 3: Regression analysis of explanatory variables influencing on bleaching response. Linear and multiple linear regression model for bleaching intensity and mortality index (BMI) as response variable and environmental variables (mean temperature during the bleaching, DDH>30.1°C, DDC<30.1°C, max. monthly mean SST, number of days mean diurnal SST was > bleaching threshold (30.1°C), 30.5°C, 30.7°C and 30.9°C) and community bleaching susceptibility index ($CBSI_{thermal\ stress}$) as explanatory variables.

bleaching response predictors	r^2	F-statistic	df	t-value (slope)	p
mean	0.13	1.469	10	1.21	0.253
DDH >30.1°C	0.22	2.894	10	1.70	0.120
DDC <30.1°C	0.27	3.705	10	1.93	0.083
max. monthly mean SST	0.16	1.84	10	1.36	0.205
days mean >threshold (30.1°C)	0.14	1.638	10	1.28	0.230
days mean >30.3°C	0.20	2.501	10	1.582	0.145
days mean >30.5°C	0.25	3.371	10	1.84	0.096
days mean >30.7°C	0.34	5.257	10	2.29	0.044
days mean >30.9°C	0.33	4.911	10	2.22	0.051
$CBSI_{thermal\ stress}$	0.31	4.422	10	2.10	0.062
	0.47	3.962	9		0.058
mean				1.65	0.123
$CBSI_{thermal\ stress}$				2.40	0.040
	0.59	6.387	9		0.019
DDH				2.47	0.036
$CBSI_{thermal\ stress}$				2.81	0.020
model	0.65	8.301	9		0.009
max. monthly mean SST				2.96	0.016
$CBSI_{thermal\ stress}$				3.55	0.006
	0.62	7.375	9		0.013
DDC <30.1°C				2.73	0.023
$CBSI_{thermal\ stress}$				2.89	0.018
	0.45	3.685	9		0.068
days mean >30.1°C				1.53	0.160
$CBSI_{thermal\ stress}$				2.25	0.051
	0.56	5.782	9		0.024
days mean>30.3°C				2.293	0.048
$CBSI_{thermal\ stress}$				2.729	0.023
	0.66	8.695	9		0.008
days mean>30.5°C				3.05	0.014
$CBSI_{thermal\ stress}$				3.28	0.010
	0.75	13.73	9		0.002
days mean>30.7°C				4.04	0.003
$CBSI_{thermal\ stress}$				3.86	0.004
	0.73	12.13	9		0.003
days mean>30.9°C				3.75	0.005
$CBSI_{thermal\ stress}$				3.65	0.005

3.5 Coral reef recovery

The coral status half a year later revealed that corals surviving the bleaching started to recover but recovery was not completed (Fig. 3b). A high percentage of corals did not regain normal pigmentation and at some sites complete white coral colonies were observed (Fig. 3b). Bleaching and mortality index calculated from the remnant coral community ranged from 20.1-36.9 (Table 2). All sites showed a high loss in live coral cover with slightly reduced mortality rates on the W (Fig. 6). At all E sites over 50 % of live coral cover was (51-76%) lost while on the W sites a mixed response was observed. Some W sites (Tachai W (78%) and Similan W (87%)) featured severe reduction in contrast to other sites (Racha W no loss and Miang W 27%). Opposite island sites showed strong differences in coral mortality with 33, 21, 21, 12 and 5 % more loss on E of Racha, Miang, Surin, Similan and Payang, respectively (Fig. 6).

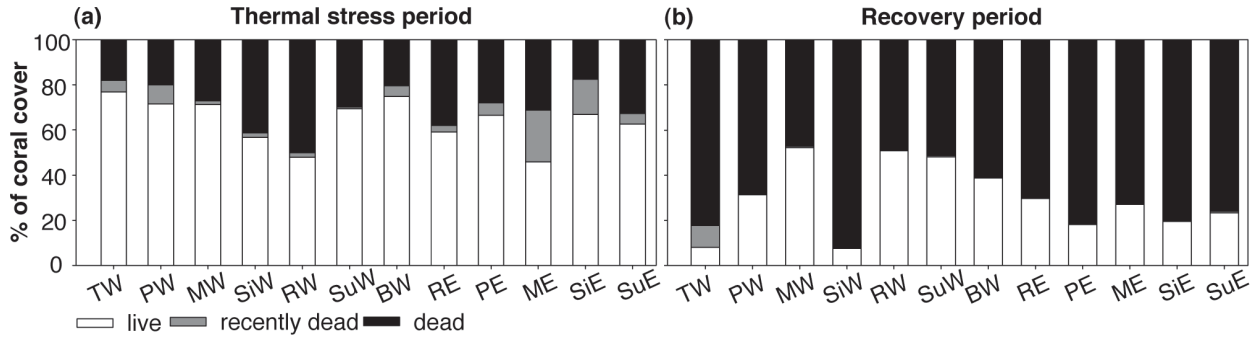

Figure 6: Coral cover as live, recently dead and dead. Fraction of either dead, recently dead and live coral was determined during the bleaching event in May 2010 (a) and during the recovery phase in December 2010 (b). All data are displayed for all sites (Tachai W (TW), Payang W (PW), Miang W (MW), Similan W (SiW), Racha W (RW), Surin W (SuW), Bon W (BW), Racha E (RE), Payang E (PE), Miang E (ME), Similan E (SeE) and Surin E (SuE)). Sites are arranged according to the degree days cooling values from highest to lowest cooling left to right.

After the thermal stress period the coral community changed to a more resilient coral taxa composition at all sites (mean CBSI pooled for all sites during the thermal stress period: 40.79 ± 2.2 and during the recovery phase: 29.94 ± 1.85 (Wilcoxon rank sum test: W = 126, p = 0.002; Table 2)). Highly susceptible and susceptible taxa remained in reduced percentage only on the W island sites (Fig. 5b).

4. Discussion

4.1 LAIW cold water pulses as mitigation mechanisms

The present study is the first of its kind monitoring the persistence of internal wave cooling during heat stress in shallow reef areas. Upwelling regions were already proved to abate heating (Podesta & Glynn, 2001, Riegl & Piller, 2003) and here we continued on the exploration of potential refuge areas under climate change by focusing on LAIW impacted reefs. LAIW cooling constituted periods of relief

during heating with the ability to mitigate bleaching. Short-pulsed delivery of cold-water into the shallow reef system depressed the diurnal mean temperature values (seen in the high differences between the number of days diurnal mean and the number of days diurnal mode was above the bleaching threshold for the exposed sites) during the thermal stress period. This observation confirms a recently hypothesized cooling function of internal waves induced temperature drops recorded at a central Indian Ocean atoll (Sheppard, 2009) and may be of critical importance for other internal wave influenced reef regions in a changing climate (e.g. Apel *et al*., 1985, Susanto *et al*., 2005, Wang *et al*., 2007).

LAIW intensity differed between sites and accordingly the differential cooling intensity determined the degree of mitigation. LAIW impact was shown to exhibit reduced intensities in shallow reef areas (7 m) and increase in strength with depth (Schmidt *et al*., 2012). Therefore, cooling exhibited a depth gradient abating heating stronger in deeper reef regions. The temperature record from the Similan Islands monitored the occurrence of LAIW temperature drops from 2007 to 2011 (Schmidt *et al*., 2012, Wall *et al*., subm.). Both studies revealed that LAIW intensity differed between years. The depth variation of the pycnocline determines both the inter-annual intensity differences and accounts for annual seasonality. Strongest LAIW forcing in shallow reef areas is related to a shallower pycnocline during NE monsoon (Satapoomin *et al*., 2004). During the SW monsoon the temperature drops are diminishing in shallow water areas (Schmidt *et al*., 2012, Wall *et al*., subm.). Highest sea surface temperatures normally occur around April when NE monsoon relaxes and transition to SW monsoon sets in (Khokiattiwong & Yu, 2012). The 2010 bleaching event was described to coincide with intense thermal heating of surface water in the Bay of Bengal that was transported through the Andaman Sea and with a delayed onset of the SW monsoon (Khokiattiwong & Yu, 2012). Ocean circulations are tightly coupled between Bay of Bengal and the Andaman Sea and influenced by the monsoon winds (Tomczak & Godfrey, 1994). Climatic conditions and ocean circulations are assumed to be the main driver of coral bleaching events in the Andaman and it can be expected that LAIW cold-water intrusions to shallow reef areas will prevail during thermal stress period. Hence, LAIW-exposed sites can serve as refuge areas during times of thermal stress.

4.2 Temperature indices and bleaching response

Temperature indices derived from satellite temperature records provide a suitable baseline for a bleaching early warning system on a large spatial scale (Berkelmans, 2009, Manzello *et al*., 2007, Maynard *et al*., 2008). At local scale temperature can be highly variable (Berkelmans *et al*., 2004, Marshall & Baird, 2000) and for an improved understanding of fine-scale bleaching response temperature data information must be refined (Maynard *et al*., 2008). ReefTemp (a remote sensing monitoring system) gathers SST information at high spatial resolution (2 km) and was able to effectively hindcast bleaching events (Maynard *et al*., 2008). Such improved data sets help to identify bleaching temperature thresholds or cumulative temperature exposure curves at the local scale. However, even such high spatial scale

satellite derived SST cannot capture subsurface processes such as pulsed delivery of cold-water due to internal waves. This discrepancy would result in an overestimation of the heat-stress for the W island faces and not explain the heterogeneous bleaching response.

In situ temperature data were used to calculate temperature indices and relate them to the observed bleaching response. These well-established indices provided different information by focusing on different aspects of the thermal stress. While some reflect the short-term acute stress (max. mean monthly sea surface temperature) others incorporate differences in heating, cooling and the duration within one variable (cumulative exposure).

The islands' W sides were described to face both LAIW and SW monsoon forcing and both phenomena entail stronger currents and mixing of water masses (Becerro *et al*., 2006, Roder *et al*., 2010). Increased water motion and turbulent mixing potentially moderated the heating. The mode temperature values are not sensitive to short temperature deviations (such as LAIW intrusions). Thus, differences in days diurnal mode was above bleaching threshold reflect moderation of heat due to improved water exchange and turbulent mixing. In contrast, mean values are rather sensitive to LAIW cooling. The number of days diurnal mean was above the bleaching threshold represented a composite index incorporating both LAIW cooling and moderation of heat due to water mixing. LAIW cooling offsets heating stronger than water mixing for the most exposed sites. Thus, two postulated refuge systems accounted for the observed differences with LAIW cooling mitigating bleaching much stronger than water mixing.

However, the temperature indices alone were only able to explain a third of the observed variability in bleaching response.

4.3 Community composition and bleaching response

We implemented a community bleaching susceptibility index to account for species-specific vulnerability and to calculate a site-specific value. This index alone explained 31% of the observed bleaching response similar to the different temperature indices. Including both environmental indices and community susceptibility into the model the predictability of the observed bleaching response improved markedly (up to 75%). This highlights the importance of including coral community composition to predict bleaching responses (McClanahan *et al*., 2007) with both contributing equally to the observed variability.

The CBSI is similar to that of Manzello *et al*. (2007), who calculated their index based on coral taxa coverage and an assigned bleaching susceptibility value (in their case: 1 = high susceptible, 2 = low susceptible). We scored taxon groups according to their susceptibility obtained from reported susceptibility in the literature that was furthermore supported by the observed taxon-specific bleaching response. In contrast, McClanahan *et al*. (2007) derived their susceptibility index from the taxon-specific

bleaching response recorded for each site (i.e. it requires monitoring surveys *in situ*). The CBSI does not require any prior knowledge of taxon site-specific bleaching response for the studied bleaching event. This allows identification of reefs that are vulnerable to bleaching and modeling coral reef resilience to environmental stress.

We first monitored bleaching response *in situ* almost 2 months after the bleaching threshold was exceeded. McClanahan (1997) showed that recently dead corals can become overgrown very quickly (approx. 20 days) and won't be recognized as recently died colonies. The sampling time in the present study is in general representative for the bleaching event but has potentially exceeded bleaching onset for the most sensitive taxon (*Pocillpora* spp. and *Stylphora* spp.) and underestimated their mortality. Community susceptibility values were similarly derived from the community composition during peak-phase. This potentially led to an underestimation of community bleaching susceptibility in particular at E sites. In general, *Pocillopora* and *Stylophora* did not represent a high fraction of reef coverage (at the Similan island chain (Schmidt *et al*., 2012)) and thus, represent only a minor error. Timing of monitoring constitutes a critical factor and to study the effect of LAIW on different susceptible groups in more detail an additional 'early phase' sampling point (e.g. 1 month earlier) would have been desirable, but was due to logistical constraint not feasible. Nevertheless, the study provided insight into the different timing of bleaching onset as well the effect of differential cooling intensity for different taxa (Fig. 4).

4.4 Other factors influencing bleaching response

Both community susceptibility and temperature indices together predicted up to 75% of the bleaching response but left 25% of the variability unexplained.

One possible explanation derives from the exposure to offshore processes. Turbulent mixing was already described to moderate heating but also affects the boundary layer between corals and the surrounding water. Bleaching of corals is associated with an accumulation of reactive oxygen species leading to oxidative damage (Baird *et al*., 2009 and references therein, Lesser, 2011). Water motion was shown to account for decreasing the boundary layer and supports a faster removal of this harmful reactive oxygen species (Nakamura & Woesik, 2001, West & Salm, 2003) and potentially furthermore alleviated the bleaching response on all exposed sites.

Additionally, solar radiation influences bleaching. Reduced light conditions (e.g. due to turbidity) or prior exposure to elevated light radiation at sites can alleviate the bleaching response (Brown *et al*., 2002). LAIW increase as well turbidity and high sedimentation rate during SW monsoon both reduce light levels at the exposed sites and can account for attenuating the stress.

Corals contain symbiotic algae of the genus *Symbiodinium* that provide energy to their host (Muscatine *et al*., 1981, Muscatine & Porter, 1977) but they will be exposed under thermal stress. Corals can also supply energy by heterotrophic feeding (Houlbreque & Ferrier-Pages, 2009) and even shift to

more heterotrophic energy sources under stress (Grottoli *et al*., 2006). This so called heterotrophic plasticity renders corals less susceptible to heat stress but differs between species (Grottoli *et al*., 2006). Large amplitude internal waves also deliver nutrients and plankton into the reef (Roder *et al*., 2010, Schmidt *et al*., 2012). This additional energy source affectes the coral metabolic and trophic status – with increased protein content and heterotrophic nutrition on W (Roder *et al*., 2010, Roder *et al*., 2011). These adjustments – increasing corals energy status - can also account for bleaching response variability.

The symbionts harbored by corals are highly diverse. The described symbiont clades and sub-clades differ in their bleaching resistance with clade D representing the most resistant to elevated temperatures (e.g. Baker, 2001, Berkelmans & van Oppen, 2006). *Diploastrea helipora* - the most bleaching resistant coral taxa in the study area - was shown to contain solely clade D symbionts (LaJeunesse *et al*., 2010, Phongsuwan & Changsang, 2012). In contrast, *Porites lutea* the most dominant reef building coral in this region harbors only C15 symbionts (LaJeunesse *et al*., 2010), a clade more susceptible to bleaching. Symbiont clade-compositions may partially account for the observed community bleaching response but not for the observed bleaching-pattern of *Porites lutea*.

The host also shows differences in fluorescence pigment and mycosporin-like amino acids (MAA) contents, which demonstrated the potential to scavenge reactive toxic substances and attenuate bleaching (Baird *et al*., 2009).

4.5 Bleaching recovery - additional stressors may counteract mitigation and hamper recovery

No difference was observed between E and W in the pace of recovery of the surviving coral community half a year after the heat stress in December. Southwest monsoon may entail additional stress during recovery by increasing sedimentation rate on the W islands sites in particular during July to August (up to 130 mg cm^{-2} d^{-1}; Wall *et al*., subm.). Sediment settling on corals induces rejection mechanisms such as mucus production, polyp movement and tissue swelling to remove particles from the coral surface (Bak & Elgershuizen, 1976, Riegl & Branch, 1995). Sedimentation is known to reduce coral photosynthetic efficiency and increase respiration (Weber *et al*., 2006) and can lead to bleaching and necrosis (Philipp & Fabricius, 2003, Riegl, 1995). Sediment avoidance mechanisms require energy (Bak & Elgershuizen, 1976). Both reduced energy from photosynthesis and the reallocation of energy for repair potentially hampered the recovery process on the W reefs.

Tachai W showed strong bleaching response and the slowest recovery of the post-heat stress remaining coral community even though this site experienced the strongest cooling. Different factors could be responsible for this offset. This can be partially explained by the high percentage of bleaching susceptible species - *Pocillopora* spp. and *Acropora* spp. - can explain this offset. Another aspect monitored at this reef was the high cover by corallimorpharian that accounted for 40 % benthos coverage

(own unpublished data). Corallimorpharian were described as strong and aggressive space competitors stressing living coral colonies (Kuguru *et al*., 2004 and references therein) – such as shown here for *Porites lutea* (Fig. 7). The settlement of corallimporpharia potentially posed another source of stress to the coral community and potentially exacerbated the stressful conditions.

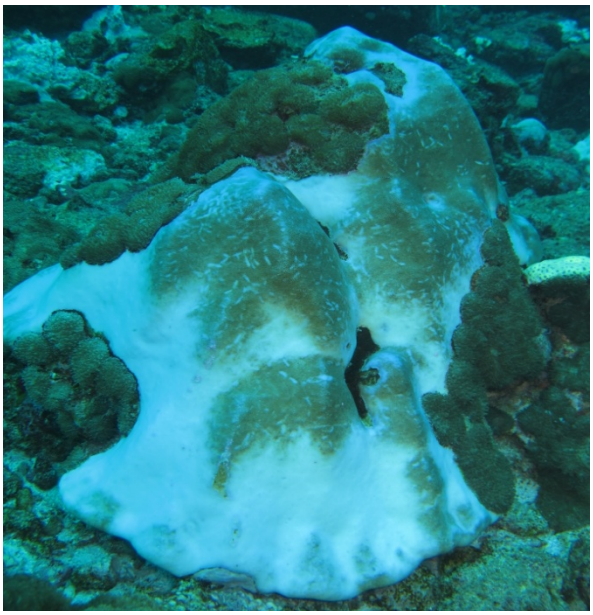

Figure 7: Competition with corallimorpharian. Corallimorpharian space invaders impact the reef in Tachai W covering 40 % of the available substrate.

4.6 Future implications

The putative threshold of 30.1°C for the Andaman Sea (Brown *et al*., 1996) did not correlate with the observed bleaching response. Phongsuwan and Chansang (2012) claimed the threshold for bleaching to lie at 30.34°C, which suggests acclimatization of reefs in the Andaman Sea to higher temperatures. In this study cumulative temperature exposure above 30.5°C or even 30.7°C significantly correlated with the bleaching response. This finding agrees with the proposition of a higher thermal threshold for this region. A shift to a higher heat tolerance would imply some acclimatization gained by the holobiont (Baker *et al*., 2008, Brown & Crossins, 2011, Lesser, 2011). The upper thermal bleaching threshold for corals varies across global scales ranging from 28.3 to almost 35.5°C (e.g. Hoegh-Guldberg, 1999, Riegl, 2002). This huge range suggests that corals are able to adapt to different temperature regimes. It is still unknown how much time (centuries or millennia) such adaptations required and require (Brown & Crossins, 2011). Several studies indicated that water temperatures around Phuket are steadily increasing by a rate of 0.126°C per decade (Brown *et al*., 1996, Tanzil *et al*., 2009). The reefs in this area potentially acclimated to these increasing temperature values and may keep pace with the observed increase in water temperature. However, it is unknown if this potentially acquired acclimation only lies within the temperature tolerance window of the corals or represents a real shift in thermal tolerance.

Besides the bleaching threshold, the duration of heat stress is critical and determines the bleaching response. Coral extirpations were already described for other regions (Riegl, 1999) and yet it needs to be monitored if the susceptible coral taxa (such as *Pocillopra*, branching *Porites* and *Acropora*) can recolonize these reefs. Some of the susceptible species occurred at both sides and survived only at the exposed sites. These species may have a higher chance of recolonization at the sheltered sites, compared to species such as branching *Porites* that vanished completely after the bleaching event and only occurred at the sheltered sites. So far there are no studies investigating the population genetics and the connectivity between island sides as well as between islands and hence, recruitment by adjacent reefs and/or islands is only speculative.

Furthermore, the bleaching event lead to a dominance shift in coral taxa and rendered the coral community structure to one that is more resistant to heat stress. If such coral community shift represents only an alternate state or a long-lasting shift strongly depends on the recurrence period of such severe bleaching events as well as on the occurrence of other stressors such as diseases or *Acanthaster* outbreaks which often following bleaching events (Bruno *et al*., 2007, Miller *et al*., 2009, Rogers, 2009). Future predictions expect that by 2050 bleaching events will occur at an annual or biannual basis (Donner *et al*., 2005) with critical consequences for reef health and distribution (Bruno *et al*., 2009, Greenstein & Pandolfi, 2008). The results presented here indicate a community-shift to a more heat tolerant community composition and to the elimination of sensitive species on sheltered sites under the predicted future bleaching scenarios (Donner *et al*., 2005). These species may survive on the exposed high LAIW intensity sites under the predicted future scenario.

4.7 In conclusion

Internal wave induced cold-water pulses in shallow reef communities have so far not received strong attention as potential cooling agents during bleaching. Such wave phenomena cannot be captured by satellite monitored sea surface temperature data and are short-lived in contrast to upwelling. The bleaching response at coral community level showed strong differences especially between exposed and sheltered sides of the same island. This response was in particular due to LAIW cooling intensity. Additionally, SW monsoon set in during the thermal stress period and induced turbulent water mixing. Thus, two refuge systems accounted for the observed differences in thermal stress, whereby LAIW cooling mitigated bleaching more than vigorous water mixing caused by the SW monsoon. The LAIW cooling intensity varied between sites and this gradual decrease was reflected in a gradual increase in bleaching response. This response was also dependent on the coral community composition. The duration of the heat stress almost exceeded the capability to withstand the thermal stress for highly susceptible species, such as *Pocillopora* and *Stylophora*. These taxa occurred on both sides but only remained, albeit in reduced numbers, at the exposed sites. Additional stressors during and after the bleaching event - corallimorpharian space competitors and increased sedimentation - potentially accounted for a stronger

bleaching response at Tachai and a general reduced recovery at all exposed sites. Hence, the bleaching response represented a complex set of factors (LAIW cooling, species composition) and secondary stressors (sedimentation and space competitors) that may hamper recovery.

The study showed that Andaman Sea offshore island exposed sides provided protection from severe heat stress and that they can serve as refuge areas. Time will tell if the exposed sites are able to replenish the sheltered sites with in particular susceptible species.

Acknowledgments

We thank the Phuket Marine Biological Center (PMBC) for field assistance and logistical help. The study was funded by the PEOPLE-2007-1-1-ITN Marie Curie Action: CalMarO (Calcification by Marine Organisms, 215157) and the German Ministry for Education and Research Project BIOACID (Grant Number 03F0608B, Bioacid 3.2.3, Coral Calcification in marginal reefs). Research permission was provided by the National Research Council of Thailand (NRCT – No. 0002/5675) and additionally from the National Park Authorities.

References

Apel JR, Holbrook JR, Liu AK, Tsai JJ (1985) The Sulu Sea internal soliton experiment. *Journal of Physical Oceanography,* **15**, 1625-1985.

Baird AH, Bhagooli R, Ralph PJ, Takahashi S (2009) Coral bleaching: the role of the host. *Trends in Ecology and Evolution,* **24**, 16-20.

Bak RPM, Elgershuizen JHBW (1976) Patterns of oil-sediment rejection in corals. *Marine Biology,* **37**, 105-113.

Baker AC (2001) Reef corals bleach to survive change. *Nature,* **411**, 765-766.

Baker AC, Glynn PW, Riegl B (2008) Climate change and coral reef bleaching: An ecological assessment of long-term impacts, recovery trends and future outlook. *Estuarine, Coastal and Shelf Science,* **80**, 435-471.

Becerro MA, Bonito V, Paul VJ (2006) Effects of monsoon-driven wave action on coral reefs of Guam and implications for coral recruitment. *Coral Reefs,* **25**, 193-199.

Berkelmans R (2009) Bleaching and mortality thresholds: How much is too much? In: *Coral bleaching - Patterns, processes, causes and consequences*. (eds Oppen MJH, Lough JM) pp 103-119. Heidelberg, Germany, Springer.

Berkelmans R, De'ath G, Kininmonth S, Skirving W (2004) A comparison of the 1998 and 2002 coral bleaching events on the Great Barrier Reef: spatial correlation, patterns, and predictions. *Coral Reefs,* **23**, 74-83.

Berkelmans R, van Oppen MJH (2006) The role of zooxanthellae in the thermal tolerance of corals: a "nuggets of hope" for coral reefs in an era of climate change. *Proceedings of the Royal Society B: Biological Sciences,* **273**, 2305-2312.

Brown BE, Dunne RP, Chansang H (1996) Coral bleaching relative to elevated seawater temperature in the Andaman Sea (Indian Ocean) over the last 50 years. *Coral Reefs,* **15**, 151-152.

Brown BE, Dunne RP, Goodson MS, Douglas AE (2002) Experience shapes the susceptibility of a reef coral to bleaching. *Coral Reefs,* **21**, 119-126.

Brown BE, Crossins A (2011) The potential for temperature acclimatisation of reef corals in the face of climate change. In: *Coral reefs: an ecosystem in transition*. (eds Dubinsky Z, Stambler N) pp 421-434. Heidelberg, Springer.

Brown BE, Phongsuwan N (2012) Delayed mortality in bleached massive corals on the intertidal reef flats around Phuket, Andaman Sea, Thailand. *Phuket Marine Biological Center Research Bulletin,* **71**, 43-48.

Bruno JF, Selig ER, Casey KS *et al*. (2007) Thermal Stress and Coral Cover as Drivers of Coral Disease Outbreaks. *PLoS Biol,* **5**, e124.

Bruno JF, Sweatman H, Precht WF, Selig ER, Schutte VGW (2009) Assessing evidence of phase shifts from coral to macroalgal dominance on coral reefs. *Ecology,* **90**, 1478-1484.

Carpenter KE, Abrar M, Aeby G *et al*. (2008) One-third of reef-building corals face elevated extinction risk from climate change and local impacts. *Science,* **321**, 560-563.

Donner SD, Skirving WJ, Little CM, Oppenheimer M, Hoegh-Guldberg OVE (2005) Global assessment of coral bleaching and required rates of adaptation under climate change. *Global Change Biology,* **11**, 2251-2265.

Glynn PW (1991) Coral reef bleaching in the 1980s and possible connections with global warming. *Trends in Ecology and Evolution,* **6**, 175-179.

Glynn PW (1993) Coral reef bleaching: ecological perspectives. *Coral Reefs,* **12**, 1-17.

Glynn PW (1996) Coral bleaching: facts, hypotheses and implications. *Global Change Biology,* **2**, 495-509.

Glynn PW, Mat LJ, Baker AC, Calder MO (2001) Coral bleaching and mortality in Panama and Ecuador during the 1997-1998 El Niño Southern Oscillation event: spatial/temporal patterns and comparisons with the 1982-1983 event. *Bulletin of Marine Science,* **69**, 79-109.

Greenstein BJ, Pandolfi JM (2008) Escaping the heat: range shifts of reef coral taxa in coastal Western Australia. *Global Change Biology,* **14**, 513-528.

Grottoli AG, Rodrigues LJ, Palardy JE (2006) Heterotrophic plasticity and resilience in bleached corals. *Nature,* **440**, 1186-1189.

Gunderson LH (2000) Ecological resilience: in theory and application. *Annual Review of Ecology and Systematics,* **31**, 425-439.

Guzman H, Cortés J (2007) Reef recovery 20 years after the 1982–1983 El Niño massive mortality. *Marine Biology,* **151**, 401-411.

Helfrich KR (1992) Internal solitary wave breaking and run-up on a uniform slope. *Journal of Fluid Mechanics,* **243**, 133-154.

Hoegh-Guldberg O (1999) Climate change, coral bleaching and the future of the world's coral reefs. *Marine and Freshwater Research,* **8**, 839-866.

Houlbreque F, Ferrier-Pages C (2009) Heterotrophy in tropical scleractinian corals. *Biological Reviews,* **84**, 1-17.

Jantzen C (2010) Primary prodcution in coral reefs - Key players and adaptive strategies to natural environmental variations. PhD Thesis, University of Bremen, Bremen, 184 pp.

Khokittiawong S, Yu W (2012) Note on the occurrence of high sea surface temperatures in the Andaman Sea, in 2010. *Phuket Marine Biological Center Research Bulletin,* **71**, 1-9.

Kohler KE, Gill SM (2006) Coral point count with excel extension (CPCe): a visual basic program for the determination of coral substrate and substrate coverage using random point count methodology. *Computers & Geosciences,* **32**, 1259-1269.

Kuguru BL, Mgaya YD, Öhman MC, Wagner GM (2004) The reef environment and competitive success in the Corallimorpharia. *Marine Biology,* **145**, 875-884.

Kumar JSY, Raghunathan C (2012) Recovery status of scleractinian corals and associated fauna in the Andaman and Nicobar islands. *Phuket Marine Biological Center Research Bulletin,* **71**, 63-70.

LaJeunesse TC, Petty DT, Sampayo EM *et al*. (2010) Long-standing environmental conditions, geographic isolation and host-symbiont specificity influence the relative ecological dominance and genetic diversification of coral endoymbionts in the genus Symbiodinium. *Journal of Biogeography*, doi:10.1111/j.1365-2699.2010.02273.x.

Leichter JJ, Deane GB, Stokes MD (2005) Spatial and temporal variability of internal wave forcing on a coral reef. *Journal of Physical Oceanography,* **35**, 1945-1962.

Leichter JJ, Genovese SJ (2006) Intermittent upwelling and subsidized growth of the scleractinian coral *Madracis mirabilis* on the deep fore-reef slope of Discovery Bay, Jamaica. *Marine Ecology Progress Series,* **316**, 95-103.

Lesser MP (2011) Coral bleaching: causes and mechanisms. In: *Coral reef: an ecosystem in transition*. (eds Dubinsky Z, Stabler N) pp 405-420. Heidelberg, Springer.

Loya Y, Sakai K, Yamazoato K, Nakano Y, Sambali H, van Woesik R (2001) Coral bleaching: the winners and the losers. *Ecology Letters,* **4**, 122-131.

Maina J, Venus V, McClanahan TR, Ateweberhan M (2008) Modelling susceptibility of coral reefs to environmental stress using remote sensing data and GIS models. *Ecological Modelling,* **212**, 180-199.

Manzello DP, Berkelmans R, Hendee JC (2007) Coral bleaching indices and thresholds for the Florida Reef Tract, Bahamas, and St. Croix, US Virgin Islands. *Marine Pollution Bulletin,* **54**, 1923-1931.

Marshall PA, Baird AH (2000) Bleaching of corals on the Great Barrier Reef: differential susceptibilities among taxa. *Coral Reefs,* **19**, 155-163.

Maynard JA, Turner PJ, Kenneth ARN *et al*. (2008) *ReefTemp*: An interactive monitoring system for coral bleaching using high-resolution SST and improved stress predictors. *Geophysical Research Letters,* **35**, doi:10.1029/2007GL032175.

McClanahan TR (1997) Primary succession of coral-reef algae: differing patterns on fished versus unfished reefs. *Journal of Experimental Marine Biology and Ecology,* **218**, 77-102.

McClanahan TR (2004) The relationship between bleaching and mortality of common corals. *Marine Biology,* **144**, 1239-1245.

McClanahan TR, Baird AH, Marshall PA, Toscano MA (2004) Comparing bleaching and mortality responses of hard corals between southern Kenya and the Great Barrier Reef, Australia. *Marine Pollution Bulletin,* **48**, 327-335.

McClanahan T, Ateweberhan M, Ruiz Sebastián C, Graham N, Wilson S, Bruggemann J, Guillaume M (2007) Predictability of coral bleaching from synoptic satellite and in situ temperature observations. *Coral Reefs,* **26**, 695-701.

McClanahan TR, Maina JM, Muthiga NA (2011) Associations between climate stress and coral reef diversity in the western Indian Ocean. *Global Change Biology,* **17**, 2023-2032.

Miller J, Muller E, Rogers C *et al*. (2009) Coral disease following massive bleaching in 2005 causes 60% decline in coral cover on reefs in the US Virgin Islands. *Coral Reefs,* **28**, 925-937.

Muscatine L, Porter JW (1977) Reef corals: mutualistic symbioses adapted to nutrient-poor environments. *Bioscience,* **27**, 454-460.

Muscatine L, McCloskey L, Marian R (1981) Estimating the daily contribution of carbon from zooxanthellae to coral animal respiration. *Limnology and Oceanography,* **26**, 601-611.

Nakamura T, Woesik RV (2001) Water-flow rates and passive diffusion partially explain differential survival of corals during the 1998 bleaching event. *Marine Ecology Progress Series,* **212**, 301-304.

Nyström M, Folke C (2000) Spatial resilience of coral reefs. *Ecosystems,* **4**, 406-417.

Philipp E, Fabricius K (2003) Photophysiological stress in scleractinian corals in response to short-term sedimentation. *Journal of Experimental Marine Biology and Ecology,* **287**, 57-78.

Phongsuwan N, Changsang H (2012) Repeated coral bleaching in the Andaman Sea, Thailand, during the last two decades. *Phuket Marine Biological Center Research Bulletin,* **71**, 19-42.

Podesta GP, Glynn PW (2001) The 1997-98 El Nino event in Panama and Galapagos: an update of thermal stress indices relative to coral bleaching. *Bulletin of Marine Science,* **69**, 43-59.

Riegl B (1995) Effects of sand deposition on scleractinian and alcyonacean corals. *Marine Biology,* **121**, 517-526.

Riegl B (1999) Corals in a non-reef setting in the southern Arabian Gulf (Dubai, UAE): fauna and community structure in response to recurring mass mortality. *Coral Reefs,* **18**, 63-73.

Riegl B (2002) Effect of the 1996 and 1998 positive sea-surface temperature anomalies on corals, coral disease and fish in the Arabian Gulf (Dubai, UAE). *Marine Biology,* **140**, 29-40.

Riegl B, Branch GM (1995) Effects of sediment on the energy budgets of four scleractinian (Bourne 1900) and five alcyonacean (Lamouroux 1816) corals. *Journal of Experimental Marine Biology and Ecology,* **186**, 259-275.

Riegl B, Piller WE (2003) Possible refugia for reefs in times of environmental stress. *International Journal of Earth Sciences,* **92**, 520-531.

Roder C, Fillinger L, Jantzen C, Schmidt GM, Khokittiawong S, Richter C (2010) Trophic response of corals to large amplitude internal waves. *Marine Ecology Progress Series,* **412**, 113-128.

Roder C, Jantzen C, Schmidt GM, Kattner G, Phongsuwan N, Richter C (2011) Metabolic plasticity of the corals *Porites lutea* and *Diploastrea helipora* exposed to large amplitude internal waves. *Coral Reefs,* **30**, 57-69.

Rogers C (2009) Coral bleaching and disease should not be underestimated as causes of Caribbean coral reef decline. *Proceedings of the Royal Society B: Biological Sciences,* **276**, 197-198.

Satapoomin S, Nielsen TG, Hansen PJ (2004) Andaman Sea copepods: spatio-temporal variations in biomass and production, and role in the pelagic food web. *Marine Ecology Progress Series,* **274**, 99-122.

Schmidt GM, Phongsuwan N, Jantzen C, Roder C, Khokittiawong S, Richter C (2012) Coral community composition and reef development at large amplitude internal wave affected coral reefs in the Andaman Sea. *Marine Ecology Progress Series,* **456**, 113-126.

Sheppard C (2009) Large temperature plunges recorded by data loggers at different depths on an Indian Ocean atoll: comparison with satellite data and relevance to coral refuges. *Coral Reefs,* **28**, 399-403.

Smith WHF, Sandwell DT (1997) Global seafloor topography from satellite altimetry and ship depth soundings. *Science*, **277**, 1957-1962.

Susanto RD, Mitnik L, Zheng Q (2005) Ocean internal waves observed in the Lombok Strait. *Oceanography,* **18**, 81-87.

Tanzil JTI, Brown BE, Tudhope AW, Dunne RP (2009) Decline in skeletal growth of the coral *Porites lutea* from the Andaman Sea, South Thailand between 1984 and 2005. *Coral Reefs*, doi:10.1007/s00338-00008-00457-00335.

Thorpe SA (1975) The excitation, dissipation, and interaction of internal waves in the deep ocean. *J. Geophys. Res.,* **80**, 328-338.

Tomczak M, Godfrey JS (1994) *Regional oceanography: An introduction,* Oxford, Pergamon Press.

Vlasenko V, Alpers W (2005) Generation of secondary internal waves by the interaction of an internal solitary wave with an underwater bank. *Journal of Geophysical Research,* **110**, C02019, doi: 02010.01029/02004JC002467.

Vlasenko V, Stashchuk N (2007) Three-dimensional shoaling of large-amplitude internal waves. *Journal of Geophysical Research,* **112**, C11018, 1-15.

Wang Y-H, Dai C-F, Chen Y-Y (2007) Physical and ecological processes of internal waves on an isolated reef ecosystem in the South China Sea. *Geophysical Research Letters,* **34**, L18609.

Weber M, Lott C, Fabricius KE (2006) Sedimentation stress in a scleractinian coral exposed to terrestrial and marine sediments with contrasting physical, organic and geochemical properties. *Journal of Experimental Marine Biology and Ecology,* **336**, 18-32.

Wessel P, Smith WHF (1996) A global self-consistent, hierarchical, high-resolution shoreline database. *Journal of Geophysical Research*, **101**, 8741-8743.

West JM, Salm RV (2003) Resistance and Resilience to Coral Bleaching: Implications for Coral Reef Conservation and Management. *Conservation Biology,* **17**, 956-967.

Yeemin T, Saenghaisuk C, Yucharoen M, Klingthong W, Sutthacheep M (2012) Impact of the 2010 coral bleaching event on survival of juvenile coral colonies in the Similan Islands, on the Andaman Sea coast of Thailand. *Phuket Mar Biol Cent Res Bull,* **70**, 93-102.

2.3 MANUSCRIPT III

SKELETAL PROPERTIES EXAMINED IN THE LIGHT OF DIFFERENT DEGREES OF ENVIRONMENTAL DISTURBANCES IN THE ANDAMAN SEA: LARGE AMPLITUDE INTERNAL WAVES AND SOUTHWEST MONSOON

M Wall[1], K Boesche[1], G M Schmidt[1] & C Richter[1]

[1]*Alfred Wegener Institute for Polar and Marine Research, Am Alten Hafen 26, 27568 Bremerhaven, Germany*

in preparation as Note for Coral Reefs

Abstract

Skeletal properties were studied along a natural gradient of environmental disturbances of large amplitude internal waves (LAIW) and southwest (SW) monsoon forcing. Environmental proxy values (Wall *et al.,* subm.) characterized the different kinds of disturbances and were related to the skeletal properties. Generally the skeletal extension rates (8.92 ± 0.38 mm yr^{-1}) lie well below global average (12.9 mm yr^{-1}) and at the lower confidence interval of an exponential relationship of growth with depth. Skeletal density (1.54 ± 0.03 g cm^{-3}) significantly differed between sites and deviated from global average values (1.28 ± 0.16 g cm^{-3}). The correlations with environmental parameters suggest that hydrodynamic processes, such as increased currents, waves and LAIW, potentially influenced skeletal density at these offshore islands. LAIW intensity increases with depth. Thus, more studies are necessary to reveal whether the relationship between density and LAIW intensity persists with depth.

key words*: Porites,* skeletal density, calcification, monsoon, large amplitude internal waves, Andaman Sea

1. Introduction

Coral skeletons are well known for their potential to record prevailing environmental settings at the time of growth and used to identify past climate conditions (e.g. Druffel, 1997, Moore & Krishnaswami, 1974). Environmental conditions affect skeletal trace element and isotopic composition and growth properties (i.e. skeletal density, extension rate and calcification rate) (e.g. Barnes, 1972, Druffel, 1997, Felis *et al*., 2003, Smith *et al*., 1979). Many factors have been described which influence coral growth properties. Environmental influence on growth derives for instance from differences in light conditions (Buddemeier *et al*., 1974, Knutson *et al*., 1972), temperature (Carricart-Ganivet, 2004, Hudson *et al*., 1976, Lough & Barnes, 1997, Lough & Barnes, 2000), hydraulic energy/hydrodynamic conditions (Scoffin *et al*., 1992), rainfall, river run-off or anthropogenic perturbations are also relevant factors (Barnes & Lough, 1999, Dodge *et al*., 1984, Lough & Barnes, 1990). Studying different growth properties and the prevailing environmental conditions can help to identify main drivers for coral growth at site (Lough & Barnes, 2000). Such information can help to predict how future changes effect coral growth and reef development.

The present study was conducted on several offshore islands in the Andman Sea, Thailand. The Andaman Sea is dominated by a monsoon climate with strong rain, winds and waves during the southwest (SW) monsoon wet season (May-October). The northeast (NE) monsoon ranges from November to April and is calm and dry. The Andaman Sea features large amplitude internal waves (LAIW) that are generated in the Andaman Sea basin (Osborne & Burch, 1980). These waves travel within the water column towards the continental shelf and when they break cold water travels up-slope (Vlasenko & Stashchuk, 2007). During the NE monsoon cold-water intrusions were observed in shallow reef areas (Schmidt *et al.,* 2012, Wall *et*

al., subm.). This corresponds to the time the pycnocline shoals (Satapoomin *et al*., 2004) before it is depressed during the SW monsoon and LAIW induced cooling dimishes.

Previous studies already indicated that reef development and calcification rates differ between SW monsoon and LAIW exposed west (W) and protected east (E) island sites. Most prominent difference were the reduced reefs framework in W compared to E (Schmidt *et al*., 2012, Wall *et al*., subm.). This agrees with the observed reduced growth rate in W of the dominant reef forming species *Porites lutea* (Schmidt, 2010). The author suggested that the reduced growth rates in W deep resulted from LAIW forcing. The strongest LAIW impact is in W deep reefs and corals need to cope with these sudden changes in environemntal settings. The SW monsoon also changes environmental parameters that are known to affect skeletal characteristics e.g. increasing sedimentation rate on the exposed sites (Wall *et al*., subm.). The aim of this study is to investigate whether these environmental changes are reflected at the skeletal level of the species *P. lutea* in terms of changing skeletal density, linear extension rate and calcification rate.

2. Materials and methods

2.1 Sites

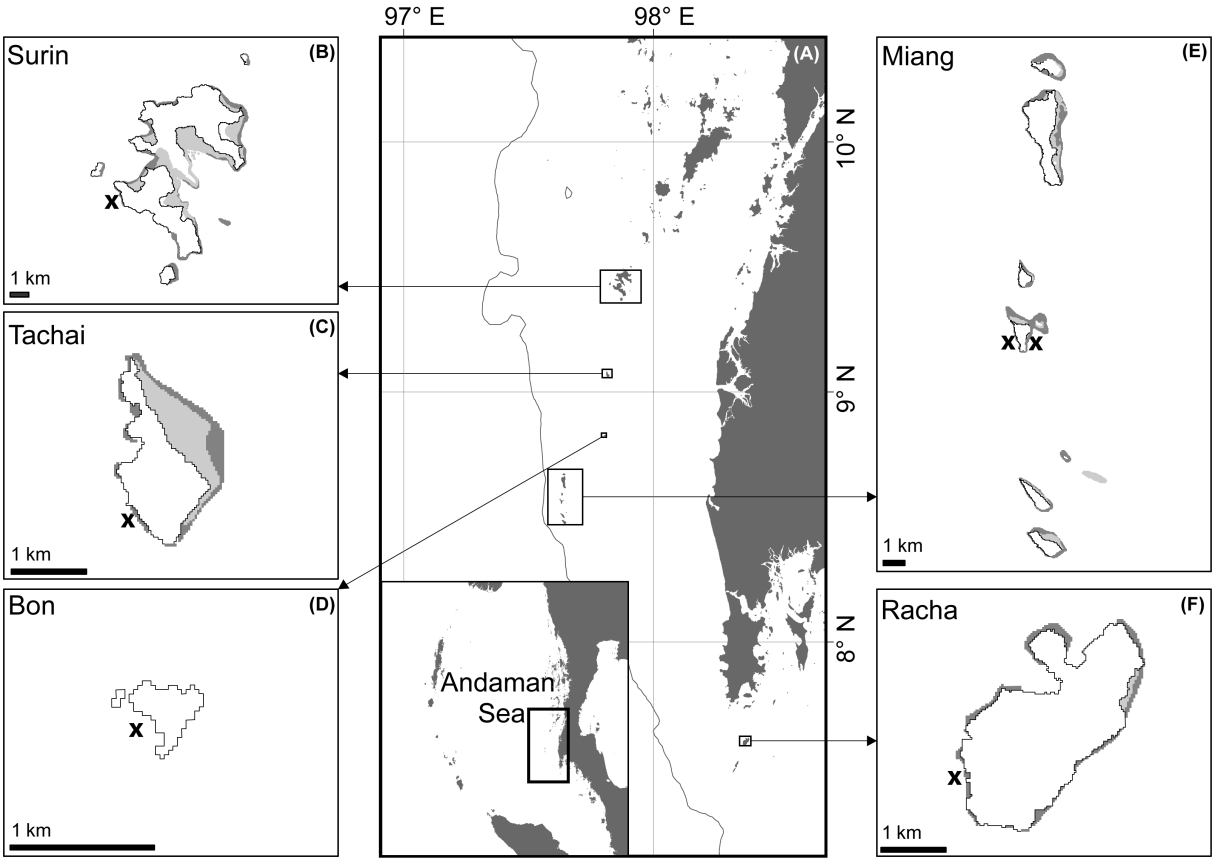

Figure 1: Location of sample sites, Andaman Sea, Thailand. A) Map displays the study area in the Andaman Sea offshore the west coast of Thailand and insert shows the Andaman Sea from the Nicobar Islands Arc to the Southeast Asian mainland of Burma and Thailand (Mainland: Wessel & Smith, 1996, Bathymetry: Smith & Sandwell, 1997). B-F) Study islands (Surin, Tachai, Bon, Miang and Racha) are magnified and displayed and sample sites marked (UNEP Coral Millennium Project). Cross marks the sites marks the sites for coral sampling.

Five islands were chosen for this study located in the Andaman Sea on the continental shelf off the western Thai coast (north to south: Surin, Tachai, Bon, Miang and Racha). Six sites were selected for environmental monitoring and coral collection. Five of them facing W exposed to LAIW and SW monsoon impact (Surin W, Tachai W, Bon W, Miang W and Racha W) and one site was located on the sheltered E side (Miang E).

2.2 Environmental settings

Different environmental parameters were monitored – temperature, sedimentation rate, bottom grain size, pH, salinity, oxygen – at the different study sites. The environmental conditions at the different sites were presented in detail elsewhere (Wall *et al.,* subm). The environmental proxies derived by Wall *et al.*, (subm.) were adopted in the present study. These proxies were used to relate them to the skeletal characteristics and identify drivers for variations in skeletal properties.

2.3 Collection of corals

At each site 5 *Porites lutea* (Milne Edwards & Haime, 1860) colonies were collected at 15 m water depth in March 2011. A coral lobe at the apex of the colony was collected with a diameter of approx. 20 cm. Corals were bleached (5% concentration) for 24 hours, rinsed with distilled water and dried at 60°C for 24 hours. Coral skeletons were then cut along their major growth direction into approx. 5 mm slabs. Slabs were rinsed with distilled water and ultrasonically cleaned after cutting for 30 minutes.

2.4 Skeletal growth variables

Linear extension rate: Coral slabs were X-rayed to determine chronology and density banding patterns. X-ray images were taken from each slab by placing them on an Agfa (Agfa Structurix, D4 FW) and with exposure to 300 seconds at 3.5 mA and 42 kV. Afterwards X-ray films were scanned with a ScanMaker 9800XL scanner at 600dpi resolution and the images inverted to obtain positives. Linear extension rates were measured by following three individual polyps along the major growth axis. One year of growth is equivalent to the distance of a high and a low-density band. Images were scaled and measurement performed with the program imageJ.

Skeletal density: Coral slabs were cut along the major growth axis into similar sized skeletal blocks of approx. 5 by 10 mm. Skeletal reference density standards were produced from the remaining fragments. A precision rock saw with (FKS/E Proxxon stand saw) diamond blade was used to cut fragments into small pieces (approx. 5 x 5 mm). Care was taken to use different amounts of high or low-density band to obtained a variety of different bulk density values. Standard pieces (n = 14) were accurately measured using a caliper (± 0.1 mm) and weighed using an analytical balance to calculate bulk density of these blocks. Standards and coral skeletons were scanned with a spiral CT (AWI-ICE CT; Freitag, pers. comm.) at an X-ray voltage of 140 kV and a target current of 200 µA. X-ray images had a resolution of

100 µm per pixel and were stacked one image every 100 µm. Standard pieces density and CT-image grey values showed a linear relationship (r^2 = 0. 91, $p < 0.001$, y = 0.00143*x+0.1186) allowing conversion of coral slice's grey values into density values.

Calcification rate: Calcification rates were calculated by multiplying skeletal density with linear extension rate.

2.5 Data analysis

Data processing was performed with the programms R and Sigma Plot v11 for statistical tests and graphical plotting, respectively.

All data were tested for the assumption of normality and homoscedadicity with the Shapiro-Wilk and Fligner-Killeen test, respectively. Differences between skeletal properties and sites were tested with ANOVA and Tukey HSD post-hoc analysis. General linear models were fitted to the data with skeletal properties as dependent and the environmental indices as independent variables.

2.6 Environmental conditions

Large amplitude internal wave intensity differed between sites as reflected by temperature anomaly plots (Fig. S1, 5.3 Appendix III). Cold-water intrusions due to LAIW concomitantly change other parameters such as pH, oxygen, nutrients, which correlate with temperature changes (Schmidt *et al*., 2012). Hence, degree days cooling represent a composite proxy of a set of changed environmental parameters and clearly display differences in LAIW-forcing between sites. Scoffin *et al*. (1992) used grain size as a surrogate for hydraulic conditions. This proxy was adopted and slightly modified by Wall *et al*. (subm.). Bottom sediment grain size provided an indication of the exposure of the reefs to currents and waves. SW-monsoon induced turbulent mixing and resuspension of sediment. Both the hydraulic conditions and sedimentation rate peaked during SW monsoon for the exposed sites but not for the sheltered site (Wall *et al*., subm.). Differences in hydraulic conditions for the exposed sites between seasons were not as clear as for sedimentation rate. These observed differences in environmental conditions constituted the basis for analyzing variations in skeletal properties.

3. Results and discussion

3.1 Coral growth properties

All skeletal properties varied between sites (Table 1), however, linear extension rate and calcification rate were not significantly different between sites (one-way ANOVA, $p = 0.205$ for linear extension rate and $p = 0.478$ for calcification rate). Density was significantly different between sites (one-way ANOVA, $n = 30$, $F = 7.41$, $p < 0.001$) with a higher density for the exposed sites. The most exposed sites Tachai W differed significantly from the protected E side of Miang (TukeyHSD, $p < 0.05$). Differences between

Miang W and E – the opposite island sites - were marginally non-significant (TukeyHSD, $p = 0.073$) with higher density in W than in E.

Table 1: Skeletal growth properties. Skeletal growth properties (linear extension rate, skeletal density and calcification rate) displayed for the different study sites (mean ± SE).

	Miang E	Racha W	Bon W	Surin W	Miang W	Tachai W
Linear extension rate [mm yr^{-1}]	10.04 (±0.09)	7.66 (±0.10)	10.34 (±0.08)	8.41 (±0.06)	7.94 (±0.11)	9.15 (±0.08)
Skeletal density [g cm^{-3}]	1.45 (±0.03)	1.50 (±0.06)	1.33 (±0.04)	1.59 (±0.06)	1.66 (±0.05)	1.69 (±0.05)
Calcification rate [g cm^{-2} yr-1]	1.45 (±0.11)	1.15 (±0.17)	1.38 (±0.12)	1.34 (±0.12)	1.30 (±0.16)	1.53 (±0.11)

The skeletal growth properties deviated (density 1.54 ± 0.03 g cm^{-3}, linear extension rate 8.92 ± 0.38 mm yr^{-1} and calcification rate 1.36 ± 0.05 g cm^{-2} yr^{-1}) from global values (1.28 ± 0.16 g cm^{-3} density, 12.9 ± 3.4 mm yr^{-1} linear extension rate and calcification rate 1.63 ± 0.38 g cm^{-2} yr^{-1} Lough & Barnes 2000). Linear extension rate was in the lower range of worldwide-observed values and skeletal density in the upper range.

Linear extension and calcification rates were shown to have high variability (coefficient of variance of 23.2 % and 22 %, respectively) and depend on differences in turbidity (Carricart-Ganivet & Merino 2001, Lough & Barnes 2000) as well as on temperature (Lough & Barnes 2000, Carricart-Ganivet 2004). Both environmental conditions can vary between years (Schmidt *et al.,* 2012) and can account for the high variability (Lough & Barnes 1997). Schmidt (2010) studied calcification by buoyant weight method. She observed also a high variability in growth. Due to higher number of studied individuals she could prove a significant difference in growth between exposed and sheltered island sites. In contrast to linear extension and calcification skeletal density is less variable with a coefficient of variance of 10.4 %. These differences in variability are in agreement with global data (Lough & Barnes 2000, Carricart-Ganivet *et al*., 2007). Thus, skeletal density represents a better discriminator between sites.

Comparing the differences in density between exposed and protected sites of Miang and Schmidt's (2010) results for the same island suggests that Schmidt's observed differences in calcification rates corresponds to an even stronger reduced extension of the reef. This result supports the observed reduced reef framework (Schmidt *et al*., 2012, Wall *et al*., subm.) that mainly is built by *Porites*.

3.2 Growth properties inter-correlations

Variation in calcification rate was more closely linked to linear extension rate (Fig. 2b, $r^2 = 0.80$, $n = 30$, $p < 0.001$) than with density (Fig. 2a), which is in line with global findings (Carricart-Ganivet & Merino, 2001, Lough & Barnes, 2000, Scoffin *et al*., 1992). This suggests that *Porites lutea* in the Andaman Sea follows global growth strategies (Lough & Barnes 2000, Carricart-Ganivet *et al.,* 2007), which are investment in extension rather than density. This strategy was thought to allow *Porites* to

occupy space rapidly (Carricart-Ganivet & Merino 2001). This is in contrast to the growth strategy for instance in *Montastrea annularis* which favors density over extension rate.

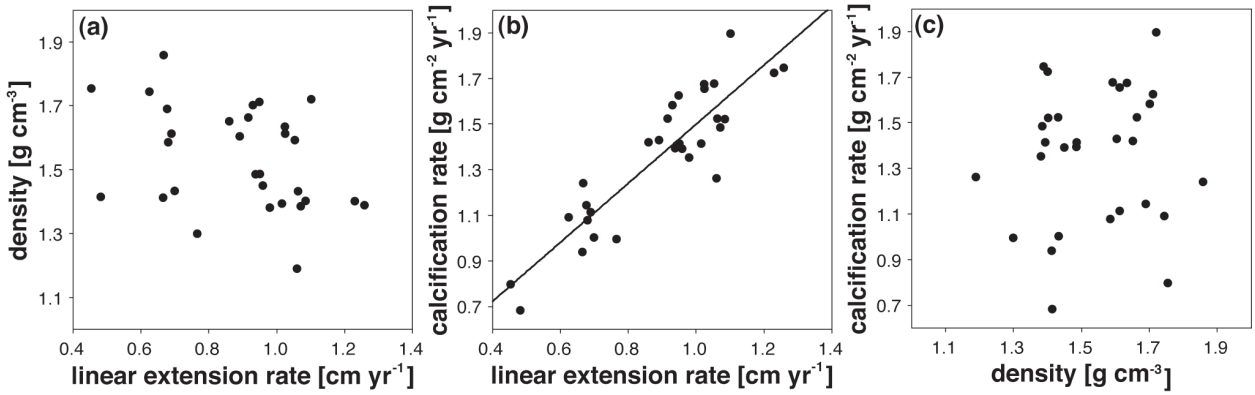

Figure 2: Relationship between growth properties in *Porites lutea.* a) density vs. extension rate. b) calcification rate vs. extension rate and c) density vs. calcification rate. Regression line is shown were it is significant.

3.3 Environmental influence on growth properties

Several studies observed a decrease in extension rate with increasing distance from the shore (Scoffin *et al*., 1992, Lough & Barnes 1997, 2000, Carricart-Ganivet & Merino 2001). An inverse relationship was found in other studies for density with distance to the shore (Risk & Sammarco 1991, Lough & Barnes 1992, Scoffin *et al*., 1992). Scoffin *et al*. (1992) attributed this change to an increase in hydraulic energy, Lough and Barnes (2000) related it to decreased temperature values offshore and Risk and Sammarco (1991) to reduced terrigenous influence. Plotting skeletal growth properties as a function of several environmental parameters (Fig. 3, LAIW cooling intensity expressed as degree days cooling, hydrodynamic conditions expressed as bottom grain size and sedimentation rate) showed no obvious trends except for density and LAIW-cooling ($r^2 = 0.57$, $n = 6$, $p = 0.08$) and hydrodynamic conditions ($r^2 = 0.50$, $n = 6$, $p = 0.1$) although both were not statistically significant.

Similar to extension rate density did not vary with distance to the shore in the present study. In contrast to Scoffin *et al*. (1992), who observed the general trend with shore distance. While in shallow reef areas surface gravity waves are expected to provide the main hydraulic impact (Scoffin *et al*., 1992, corals derived from 1m depth), the corals at our study depth were subjected to two different disturbances that affect the hydrodynamic conditions. LAIW changes temperature and as well currents, pH, oxygen and nutrients (Roder *et al*., 2010, Schmidt *et al*., 2012). Additionally, SW monsoon increases water movement and potentially induces stronger currents at the study depth. All the aforementioned parameters affect coral growth as well as skeletal properties and potentially drive skeletal density changes.

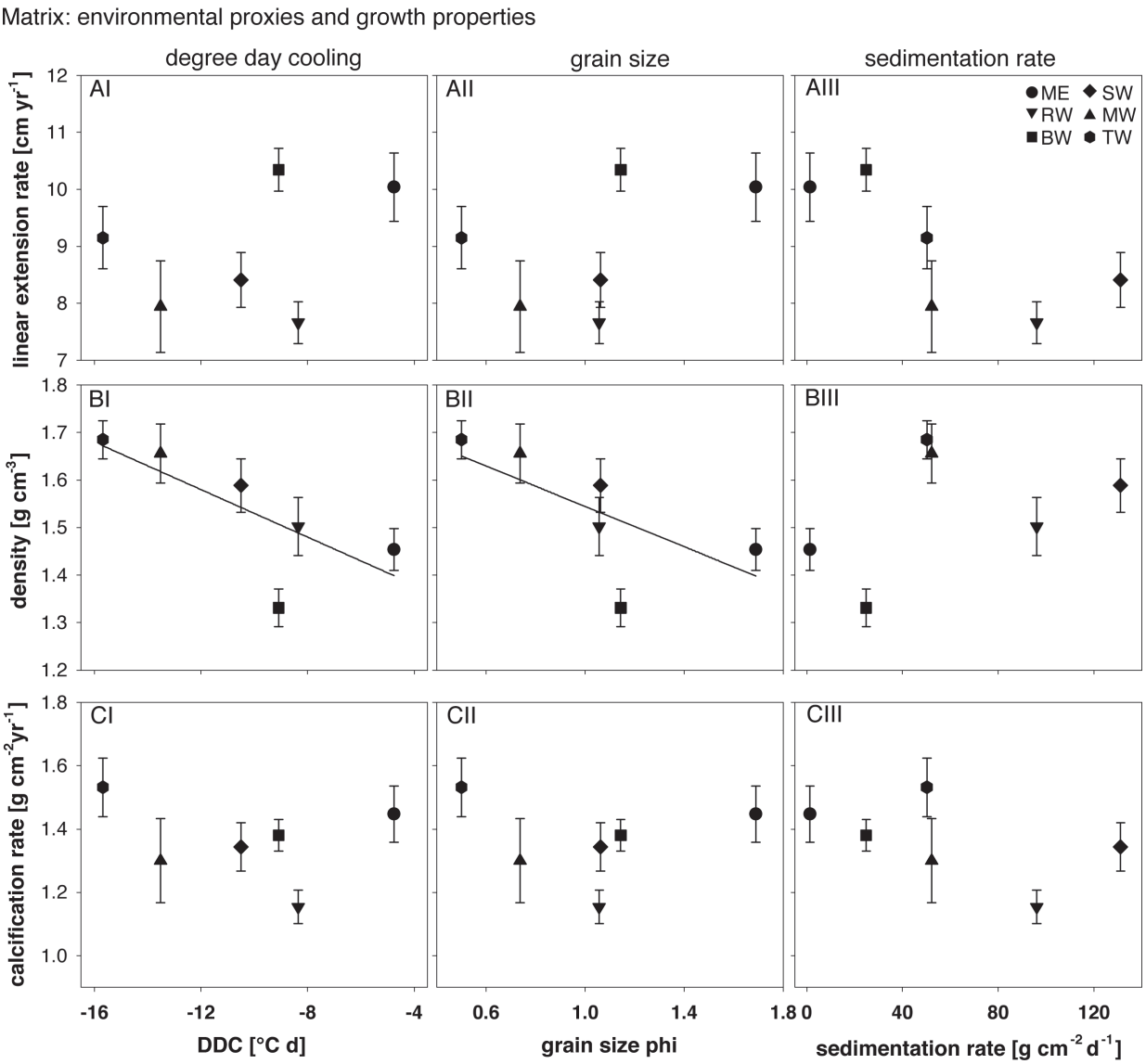

Figure 3: Skeletal properties of *Porites lutea* as a function of environmental proxies. Linear extension rate (A), skeletal density (B) and calcification rate (C) are displayed as a function of site-specific environmental proxy values: degree days cooling (I), grain size (II) and sedimentation rate (III) for the different study sites (Miang E, Racha W, Bon W, Surin W, Miang W and Tachai W).

3.6 Variation of growth with depth

Depth related changes in extension rate were obtained from the literature and coral growth values derived from different regions (Buddemeier *et al*., 1974, Felis *et al*., 2003, Grigg 2006, Scoffin *et al*., 1992, Rixen *et al*., 2011 from Eniwetok, Red Sea, Hawaii and Andaman Sea, Nicobar island, respectively). The average growth rate observed in the present study fell on the lower 95% confidence interval line of the established exponential relationship (Grigg, 2006) between growth and depth (Fig. 4). In contrast, *Porites* from Great Barrier Reef did not show a variation with depth at least until 20 m (Carricart-Ganivet *et al*., 2007) and had on average higher values than observed in the present study. Our growth rate values agree well with the depth relationship observed in Buddemeier *et al*. (1974). Buddemeier *et al*. (1974) studied growth in Eniweok a region that shows similar annual monthly mean

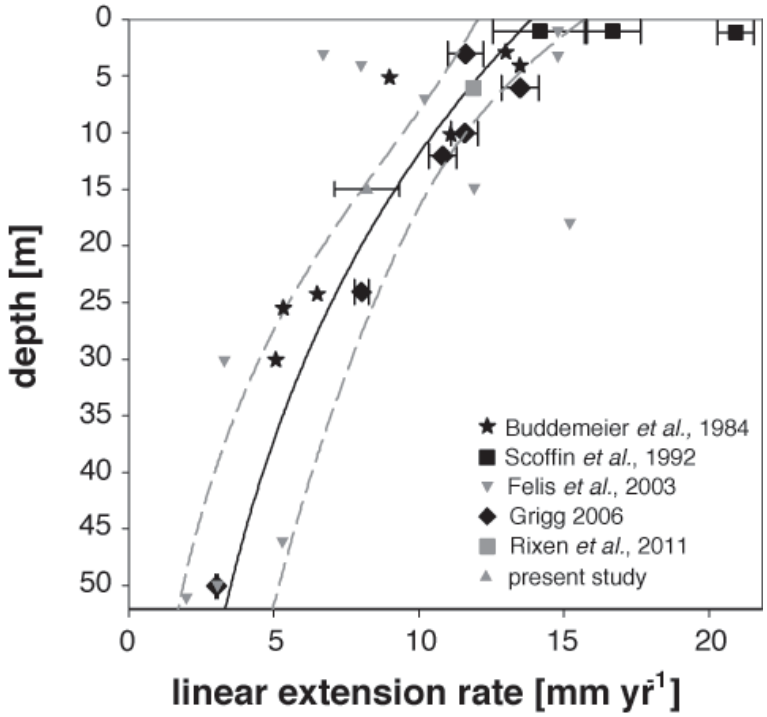

Figure 4: Depth variation of linear extension rate. Linear extension rate displayed as a function of depth. Data derived from Eniwetok (Buddemeier *et al*., 1974), Andaman Sea (Scoffin *et al*., 1992) Red Sea (Felis et al., 2003), Hawaii (Grigg 2006) and Andaman Island (Rixen *et al*., 2011). Exponential regression with 95%-confidence interval (CI) was fitted to the data. Data from the present study fell at the lower range of the regression 95%- CI.

temperature range as the Andaman Sea. However, growth rates measured in shallow areas in the Andaman Sea were much higher compared to Eniwetok in particular for reefs close to the Thai mainland (Scoffin *et al*., 1992). Scoffin *et al*. (1992) showed a huge range in extension rates for the same yearly SST values. Carricart-Ganivet and Merion (2001) described a "stretching modulation" of growth in *Montastrea*. In turbid areas corals tend to favor extension by sacrificing density. This could potentially account for some nearshore reefs in the Andaman Sea that are known for their high turbidity and explain the observed high extension rates (up to 31 mm yr^{-1}; Scoffin *et al*., 1992).

Lough and Barnes (1997, p 35) stated that: "a considerable amount of work is needed before we can begin to understand and, hopefully, predict, which growth characteristic of which species is likely to respond to a given environmental change in a particular location." Since then several studies (Carricart-Ganivet *et al*., 2007, Grigg 2006) investigated environmental influence on skeletal growth properties with sometimes contrasting results. Variation of skeletal properties with depth (Baker & Weber 1975, Buddemeier *et al*., 1974, Grigg 2006) - in particular density (Carricart-Ganivet *et al*., 2007) - are not so thoroughly studied. The latter study suggests that density and linear extension rate did not vary with depth. Here we observed a trend that density increases with increasing LAIW cooling intensity. Considering that that LAIW intensity increases with depth (Schmidt *et al*., 2012) potentially lead to increased density in depth. However, further studies are required to test if the density increase persists in depth and hence, LAIW impact represent a major driving force of skeletal density.

Acknowledgments:

We thank the Phuket Marine Biological Center (PMBC) for field assistance and logistical help. The study was funded by the PEOPLE-2007-1-1-ITN Marie Curie Action: CalMarO (Calcification by Marine Organisms, 215157). Research permission was provided by the National Research Council of Thailand (NRCT – No. 0002/5675) and additionally from the National Park Authorities. Permissions for collecting and transporting coral skeletons were provided by the National Research Council of Thailand, the Fisheries Department, Thailand and the Bundestamt für Naturschutz, Germany – CITES documents: AC.0510.2/5007.

References:

Baker PA, Weber JN (1975) Coral growth rate: Variation with depth. *Physics of the Earth and Planetary Interiors,* **10**, 135-139.

Barnes DJ (1972) The Structure and Formation of Growth-Ridges in Scleractinian Coral Skeletons. *Proceedings of the Royal Society of London. Series B: Biological Sciences,* **182**, 331-350.

Barnes DJ, Lough JM (1999) *Porites* growth characteristics in a changed environment: Misima Island, Papua New Guinea. *Coral Reefs,* **18**, 213-218.

Buddemeier RW, Maragos JE, Knutson DW (1974) Radiographic studies of reef coral exoskeletons: Rates and patterns of coral growth. *Journal of Experimental Marine Biology and Ecology,* **14**, 179-199.

Carricart-Ganivet JP, Merino M (2001) Growth responses of the reef-building coral *Montastraea annularis* along a gradient of continental influence in the southern Gulf of Mexico. *Bulletin of Marine Science,* **68**, 133-146.

Carricart-Ganivet JP (2004) Sea surface temperature and the growth of the West Atlantic reef-building coral Montastraea annularis. *Journal of Experimental Marine Biology and Ecology,* **302**, 249-260.

Carricart-Ganivet JP, Lough JM, Barnes DJ (2007) Growth and luminescence characteristics in skeletons of massive *Porites* from a depth gradient in the central Great Barrier Reef. *Journal of Experimental Marine Biology and Ecology,* **351**, 27-36.

Dodge RE, Wyers SC, Frith HR, Knap AH, Smith SR, Cook CB, Sleeter TD (1984) Coral calcification rates by the buoyant weight technique: effects of Alizarin staining. *Journal of Experimental Marine Biology and Ecology,* **75**, 217-232.

Druffel ERM (1997) Geochemistry of corals: Proxies of past ocean chemistry, ocean circulation, and climate. *Proceeding of the National Academic Science of the United States of America,* **94**, 8354-8361.

Felis T, Pätzold J, Loya Y (2003) Mean oxygen-isotope signatures in *Porites* spp. corals: inter-colony variability and correction for extension-rate effects. *Coral Reefs,* **22**, 328-336.

Grigg R (2006) Depth limit for reef building corals in the Au'au Channel, S.E. Hawaii. *Coral Reefs,* **25**, 77-84.

Hudson JH, Shinn EA, Halley RB, Lidz B (1976) Sclerochronology: A tool for interpreting past environments. *Geology,* **4**, 361-364.

Knutson DW, Buddemeier RW, Smith SV (1972) Coral chronometers: seasonal growth bands in reef corals. *Science,* **177**, 270-272.

Lough JM, Barnes DJ (1990) Intra-annual timing of density band formation of *Porites* coral from the central Great Barrier Reef. *Journal of Experimental Marine Biology and Ecology,* **135**, 35-57.

Lough JM, Barnes DJ (1992) Comparisons of skeletal density variations in *Porites* from the central Great Barrier Reef. *Journal of Experimental Marine Biology and Ecology,* **155**, 1-25.

Lough JM, Barnes DJ (1997) Several centuries of variation in skeletal extension, density and calcification in massive *Porites* colonies from the Great Barrier Reef: A proxy for seawater temperature and a background of variability against which to identify unnatural change. *Journal of Experimental Marine Biology and Ecology,* **211**, 29-67.

Lough JM, Barnes DJ (2000) Environmental controls on growth of the massive coral *Porites*. *Journal of Experimental Marine Biology and Ecology,* **245**, 225-243.

Moore W, Krishnaswami S (1974) Correlation of X-radigraphy revealed banding in corals with radiometric growth rates. In: *2nd International Coral Reef Symposium*. pp 269-276. Great Barrier Reef Committee, Brisbane, December, 1974.

Nielsen TG, Bjornsen PK, Boonruang P *et al*. (2004) Hydrography, bacteria and protist communites across the continental shelf and shelf slope of the Andaman Sea (NE Indian Ocean). *Marine Ecology Progress Series,* **274**, 69-86.

Osborne AR, Burch TL (1980) Internal solitons in the Andaman Sea. *Science,* **208**, 451-460.

Risk MJ, Sammarco PW (1991) Cross-shelf trends in skeletal density of the massive coral *Porites lobata* from the Great Barrier Reef. *Marine Ecology Progress Series,* **69**, 195-200.

Rixen T, Ramachandran P, Lehnhoff L *et al*. (2011) Impact of monsoon-driven surface ocean processes on a coral off Port Blair on the Andaman Islands and their link to North Atlantic climate variations. *Global and Planetary Change,* **75**, 1-13.

Roder C, Fillinger L, Jantzen C, Schmidt GM, Khokittiawong S, Richter C (2010) Trophic response of corals to large amplitude internal waves. *Marine Ecology Progress Series,* **412**, 113-128.

Satapoomin S, Nielsen TG, Hansen PJ (2004) Andaman Sea copepods: spatio-temporal variations in biomass and production, and role in the pelagic food web. *Marine Ecology Progress Series,* **274**, 99-122.

Schmidt GM (2010) Corals and waves - calcification and bioerosion in large amplitude internal waves (LAIW) affected coral reefs. PhD Thesis, University of Bremen, Bremen, 199 pp.

Schmidt GM, Phongsuwan N, Jantzen C, Roder C, Khokittiawong S, Richter C (2012) Coral community composition and reef development at large amplitude internal wave affected coral reefs in the Andaman Sea. *Marine Ecology Progress Series,* **456**, 113-126.

Scoffin TP, Tudhope AW, Brown BE, Chansang H, Cheeney RF (1992) Patterns and possible environmental controls of skeletogenesis of *Porites lutea*, South Thailand. *Coral Reefs,* **11**, 1-11.

Smith SV, Buddemeier RW, Redalje RC, Houck JE (1979) Strontium-calcium thermometry in coral skeletons. *Science,* **204**, 404-407.

Smith WHF, Sandwell DT (1997) Global seafloor topography from satellite altimetry and ship depth soundings. *Science*, **277**, 1957-1962.

Vlasenko V, Stashchuk N (2007) Three-dimensional shoaling of large-amplitude internal waves. *Journal of Geophysical Research,* **112**, C11018, 1-15.

Wessel P, Smith WHF (1996) A global self-consistent, hierarchical, high-resolution shoreline database. *Journal of Geophysical Research*, **101**, 8741-8743.

2.4 MANUSCRIPT IV

STRONTIUM/CALCIUM RATIOS IN *PORITES LUTEA* SKELETONS GROWN UNDER DIFFERENT TEMPERATURE CONDITIONS

GM Schmidt[1], F Ragazolla[2] , M Wall[1], T Laepple[1] & J Fietzke[3]

[1]*Alfred Wegener Institute for Polar and Marine Research,*
Am Alten Hafen 26, 27568 Bremerhaven, Germany

[2]*University of Bristol, Department of Earth Sciences*
Queen's Road, Bristol, United Kingdom

[3]*GEOMAR, Marine Geosystems*
Wischhofstraße 1-3, 24148 Kiel, Germany

in preparation

Summary abstract

The Similan Island chain off the Thai coast in the Andaman Sea is exposed to strong environmental fluctuations along its western (W) reef sides while the eastern (E) sides, which are only some hundred meters away, offer virtually sheltered conditions. The fluctuations are characterized by frequent, sub-daily (several events per hour) and abrupt (within minutes) drops in temperature accompanied by concomitant decreases in pH and oxygen concentration, and increases in nutrient loads due to the entrainment of deep subpycnocline waters into the shallow reef areas (Schmidt *et al*., 2012). The deep-water influxes exhibit seasonal peaks and occur mainly during the dry season (January through April). The coral reef distribution along the island chain with a complex carbonate framework constricted to the shelf oriented E and the lack of a coral framework in the ocean facing W has been related to the difference in environmental stress conditions between the island sides (Schmidt *et al*., 2012). The massive coral *Porites lutea* (Milne Edwards & Haime 1851) is one of the dominating species along both W and E sides of the Similans (Schmidt *et al*., 2012). It has been shown to exhibit high metabolic plasticity with respect to the prevailing environmental conditions. *Porites lutea* in W exhibits elevated pigment concentrations compared to those from the sheltered E (Jantzen, 2010). It further contains higher protein content and biomass under the influence of increased nutrient concentrations (Roder *et al*., 2011). For this study *P. lutea* was chosen to determine if the temperature and consequently environmental differences between W and E are documented in the elemental composition of the calcium carbonate skeleton. Elemental ratios in coral skeleton such as strontium to calcium (Sr/Ca, Weber 1973, Beck *et al*., 1997, Alibert & McCulloch 1997) allow reconstruction of seawater temperature conditions. However the reliability of proxies has been found to be impaired by the influence of 'vital' effects on the incorporation of strontium (Weber 1973, de Villiers *et al*., 1995; Cohen *et al*., 2001; 2002, Meibom *et al*., 2003) especially at the scale of short skeletal lengths equivalent to only a few days of growth or even less (Meibom *et al*., 2003; Cohen & Sohn 2004, Sinclair 2005, Sinclair *et al*., 2006, Meibom *et al*., 2006, 2008). Nevertheless even at short skeletal distances representing short periods of skeletal growth (several days), accordance between elemental ratios and temperature has been documented (Cohen *et al*., 2001, Cohen & Sohn 2004). It was therefore expected that the distinct seasonal difference between high and low temperature variances along the W in contrast to the E Similans could be recorded in the elemental ratios of the *P. lutea* skeletons.

Here an electron microprobe study (JEOL JXA 8200 electron superprobe) is presented of trace element variations deriving from a total of 5 corals. The corals were grown in 15 m water depth at the exposed W (3 corals) and sheltered E (2 corals) of the central Similan island Ko Miang (cf. Schmidt *et al*., 2012). The temperature was recorded *in situ* with temperature loggers at a maximum of 10 m distance to the individual coral colonies. An alizarin red S staining line (Fig. 1a) in each of the corals served to calculate an average daily growth rate (of 18.7 and 18.4 μm d^{-1} for the E corals, and of 25.4, 21.9, and 18.7 μm d^{-1} for the W corals, respectively), which was about 15.6 % higher in the W than in the E corals. For each sample one long, straight skeletal element ranging between 6.5 and 12.4 mm in length orientated

parallel to the growth axis was chosen for the analysis. The elemental distributions of Sr and Ca were mapped with a beam diameter of 10 μm over the width of the whole skeletal element (Fig. 1b, c) taking into account that Sr/Ca ratios are not homogeneously distributed but vary across the width of a skeletal element, from the calcification center to the tips of the skeletal fibers (Cohen & McConnaughey 2003, Meibom *et al*., 2007). This resulted in a sampling resolution of 0.39 to 0.54 days with a total time period documented of 107 to 318 days (between January 2010 and March 2011) depending on the coral sample.

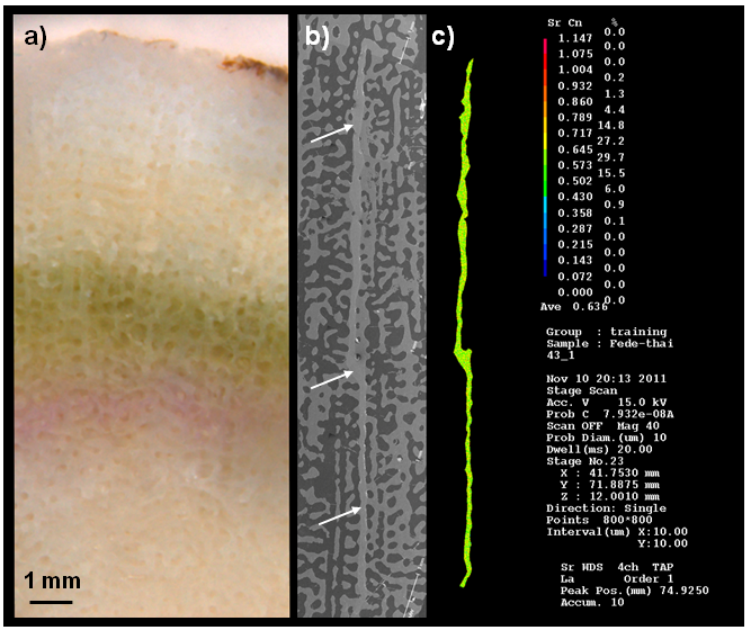

Figure 1: Skeletal sample analysis. a) Subsample of a coral slab (10 mm wide by 20 mm long) cut from the fastest growth axis, epoxy-mounted and polished; alizarin red S staining visible as pink coloration underneath the greenish band comprised by endolithic algae; b) SEM picture of a carbon-coated sample with one long, straight corallite wall segment oriented parallel to the growth axis visible in the center (indicated by arrows) chosen for the analysis; c) example for elemental distribution of Strontium mapped over the width of the whole segment (shown in b)) with a JEOL JXA 8200 electron superprobe (acceleration voltage 15.0 kV, beam current 50 nA, dwell time 20 ms, accumulation time 10); elements were mapped with beam diameter of 10 μm and calibrated against known standards (strontianite for strontium and calcite for calcium)

The study period comprised a thermal anomaly occurring in the transition period between dry northeast (NE) monsoon (November to April) and wet southwest (SW) monsoon season (May to October) with monthly mean temperatures exceeding the proposed bleaching threshold (30.1 °C, Brown *et al*., 1996) of the area over a period of 4 months (March to June 2010, Dunne 2012). Nevertheless the maximum ranges of monthly mean temperatures for the whole study period (maximum May 2010 minus minimum January 2011) were unexpectedly small with >2.4 °C in E and >2.1 °C in W. This was in contrast to the maximum daily mean temperature ranges caused by the frequent sub-daily temperature plunges during January through March of up to 5 °C in W and 2.4 °C in E (Fig. 2).

The Sr/Ca ratios of both E (between 6.08±0.03 and 8.65±0.23 mmol mol^{-1}) and W samples (between 6.43±0.13 and 8.82±0.24 mmol mol^{-1}) were lower than might have been expected from other studies with similar monthly temperature ranges (Allison 1996, Meibom *et al*., 2003, Cohen & Sohn 2004) and insignificantly higher in W compared to E despite the significantly lower monthly mean temperatures

especially during the NE monsoon periods (January through March). The preliminary results on the Sr/Ca ratios indicate a high variability with so far no detectable (a) similarities within skeletal records of the same island sides and (b) differences according to the temperature records between E and W samples. An inclusion of the different growth rates of the single samples into the analysis might help to detect possible accordances within or differences between island sides. A seasonal temperature signal has so far been detected only in one of the E samples. The sub-daily temperature plunges were not found to be resolved in the Sr/Ca data of the W samples despite the high measurement resolution. Thus, the seasonally occurring highly fluctuating temperature conditions at W do not seem to be described in the Sr/Ca ratios. Biological processes interfering with the incorporation process of Sr into the skeleton potentially mask the temperature fluctuations, which is especially eminent at these scales of short skeletal lengths (Weber 1973; de Villiers *et al*., 1995; Meibom *et al*., 2003).

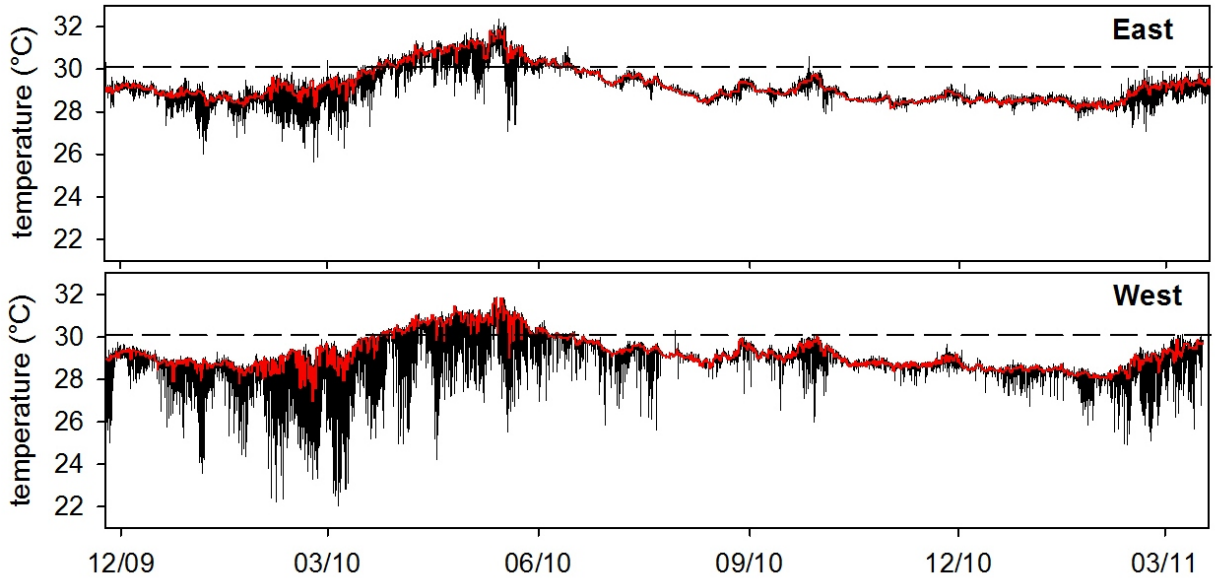

Figure 2: Temperature record at opposite island sides at the central Similan Island Miang. Temperature record (logging interval 3 minutes) at east and west side of central Similan island Ko Miang in 15 m water depth from November 24th 2009 until March 31st 2011 (black: raw data record, red: daily running mode, dashed line: 30.1 °C bleaching threshold (Brown *et al*., 1996))

***key words**: Porites,* Sr/Ca, electron microprobe, large amplitude internal waves, Andaman Sea

Acknowledgments:

Funding for this study was provided by the National Research Council of Thailand (NRCT) and the German Federal Ministry of Education and Research (BMBF, Grant number 03F0608B, BIOACID 3.2.3 Coral calcification in marginal reefs). The authors would like to thank the Phuket Marine Biological Center (PMBC) and the Similan Island National Park staff for the very kind field assistance and support in logistical issues.

References

Alibert C, McCulloch MT (1997) Strontium/calcium ratios in modern *Porites* corals from the Great Barrier Reef as a proxy for sea surface temperature: calibration of the thermometer and monitoring the ENSO. *Paleoceanography*, **12**, 345-363.

Allison N (1996) Comparative determinations of trace and minor elements in coral aragonite by ion microprobe analysis, with preliminary results from Phuket, southern Thailand. *Geochimica Cosmochimica Acta*, **60**, 3457-3470.

Beck JW, Récy J, Tylor F, Edwards RL, Cabloch G (1997) Abrupt changes in early Holocene tropical sea surface temperature derived from coral records. *Nature*, **385,** 705-707.

Brown BE, Dunne RP, Chansang H (1996) Coral bleaching relative to elevated seawater temperature in the Andaman Sea (Indian Ocean) over the last 50 years. *Coral Reefs,* **15**, 151-152.

Cohen AL (2002) The effect of algal symbionts on the accuracy of Sr/Ca paleotemperatures from coral. *Science*, **296**, 331-333.

Cohen AL, Layne GD, Hart SR (2001) Kinetic control of skeletal Sr/Ca in a symbiotic coral: Implications for the paleotemperature proxy. *Paleooceanography*, **16**, 20-26.

Cohen AL, McConnaughey T (2003) Geochemical perspectives on coral mineralization. In: *Biomineralization*. (eds Dove PM, Weiner S, De Yoreo JJ). Reviews in Mineralogy and Geochemistry, Mineralogical Society of America.

Cohen AL, Sohn RA (2004) Tidal modulation of Sr/Ca ratios in a Pacific reef coral. *Geophysical Research Letters,* **31**, L16310.

de Villiers S, Nelson BK, Chivas AR (1995) Biological controls on coral Sr/Ca and δ18O reconstructions of sea surface temperatures. *Science*, **269**, 1247-1249.

Dunne RP (2012) The record of sea temperature during the 2010 coral bleaching at Phuket, Thailand – different datasets, different perspectives – unexplained errors in HADISST 1.1. *Phuket Marine Biological Center Research Bulletin*, **71**, 11-18.

Jantzen C (2010) Primary prodcution in coral reefs - Key players and adaptive strategies to natural environmental variations. Doctoral PhD Thesis, University of Bremen, Bremen, 184 pp.

Meibom A, Stage M, Wooden J *et al*. (2003) Monthly Strontium/Calcium oscillations in symbiotic coral aragonite: Biological effects limiting the precision of the paleotemperature proxy. *Geophysical Research Letters,* **30**, 1418.

Meibom A, Yurimoto H, Cuif JP, *et al*. (2006) Vital effects in coral skeletal composition display strict three-dimensional control. *Geophysical Research Letters,* **33**, L11608, doi:10.1029/2006GL025968.

Meibom A, Mostefaoui S, Cuif J-P, Dauphin Y, Houlbreque F, Dunbar R, Constantz B (2007) Biological forcing controls the chemistry of reef-building coral skeleton. *Geophysical Research Letters,* **34**, 1-5.

Meibom A, Cuif J-P, Houlbreque F, Mostefaoui S, Dauphin Y, Meibom KL and Dunbar R (2008) Compositional variations at ultra-structure length scales in coral skeleton, *Geochimica Cosmochimica Acta*, **72**, 1555-1569, 2008.

Roder C, Jantzen C, Schmidt GM, Kattner G, Phongsuwan N, Richter C (2011) Metabolic plasticity of the corals *Porites lutea* and *Diploastrea heliopora* exposed to large amplitude internal waves. *Coral Reefs*, **30**, 57-69.

Schmidt GM, Phongsuwan N, Jantzen C, Roder C, Khokiattiwong S, Richter C (2012) Coral community composition and reef development in response to strong environmental variations. *Marine Ecology Progress Series*, **456**, 113-126.

Sinclair DJ (2005) Correlated trace element "vital effects" in tropical corals: a new geochemical tool for probing biomineralization. *Geochimica Cosmochimica Acta*, **69**, 3265-3284.

Sinclair DJ, Williams B, Risk M (2006) A biological origin for climate signals in corals – trace element "vital effects" are ubiquitous in scleractinian coral skeletons. *Geophysical Research Letters*, **33**, L17707, doi:10.1029/2006GL02718£3.

Weber JN (1973) Incorporation of strontium into reef coral skeletal carbonate. *Geochimica Cosmochimica Acta*, **37**, 2173-2190.

2.5 MANUSCRIPT V

IDENTIFICATION OF TWO ORGANIC BANDS SHOWING DIFFERENT CHEMICAL COMPOSITION WITHIN THE SKELETON OF *PORITES LUTEA*: A CONFOCAL RAMAN MICROSCOPY STUDY

M Wall[1] and G Nehrke[1]

[1]*Alfred Wegener Institute for Polar and Marine Research, Am Alten Hafen 26, 27568 Bremerhaven, Germany*

submitted to Biogeosciences published as Biogeoscience Discussion 9: 8273-8306
accepted for publication in Biogeosciences

Abstract

Confocal Raman microscopy mapping was used to investigate the organic matrix distribution within the skeleton of the coral *Porites lutea*. Two types of growth lines could be identified: one corresponds to the well-known incremental growth layers, whereas the second type of growth lines showed an elemental composition that differed from the incremental growth layers. The position and shape of the latter growth lines resemble either denticle finger-like structures (most likely traces of former spines) or former skeletal surfaces. We hypothesize that these lines are involved in the three-dimensional arrangement of skeletal elements and represent the outer skeletal surface before another growth cycle of elongation, infilling and thickening of skeletal components continues. We show that high spatial resolution mapping can significantly improve our understanding of skeletal growth patterns in coral skeletons.

key words: confocal raman microscopy, coral calcification, growth lines, growth patterns

1. Introduction

Scleractinian corals are marine organisms that thrive most vigorously in clear tropical oceans, forming one of the most important marine ecosystems – coral reefs. A thin layer of coral polyps secrete an aragonitic skeleton beneath their basal ectoderm forming an intricate and complex exoskeleton, which represents a chronological layered archive (e.g. Cohen & McConnaughey, 2003, Lough & Barnes, 2000, Knutson *et al.,* 1972). The fact that environmental information is recorded within these layered structures makes corals an important archive for paleo climate research. Even though coral reefs have been studied since Darwin's monography (Darwin, 1842) and successfully employed to learn about the past, the fundamental biomineralization processes behind their formation is still not fully understood.

The morphology of skeletal structures of corals represents the foundation of this investigation and will be explained in the following part, followed by a summary of the different biomineralization concepts that have been developed to explain their formation.

Each single polyp consists of different skeletal elements: a columella in the center, septa that radiate away from the center, a wall (theca and epitheca) and dissepiment bordering the corallite to the lateral and basal end, respectively (Sorauf, 1972; Fig. 1). Adjacent corallites either share common walls or, if not, separated corallite walls are connected by skeletal elements forming the coenosteum. All of these macro-morphological elements can be more or less well developed depending on the coral genus (Nothdurft & Webb, 2007, Veron, 2000). A close-up of a corallite i.e. viewing individual macro-morphological skeletal elements (such as septa and columella), displays micromorphological features such as spines, granules and nodules, which structure walls, septal margins and septal faces (Sorauf, 1972; Fig. 1). The skeletons of the species studied in this investigation, *Porites lutea*, are relatively porous and less differentiated into marcromorphological elements (Fig. 1) than other species (Barnes & Devereux, 1988, Nothdurft & Webb, 2007, Sorauf, 1972). The skeleton is formed of vertical rods (trabecluae) that are interconnected

horizontally by bars called synapticulae or radi and each vertical rod terminates in pali or denticle (Fig. 1 A, E) with several spines (Fig. 1 C). Both macro- and micro-morphological elements – are composed of two building blocks (microstructural elements) first described by Ogilvie (1896): the centers of calcification (COC) and fibers. The COC – later described as early mineralization zone (EMZ) (Cuif et al., 2004) - build the scaffold for the coral skeleton ultimately responsible for the colony shape, while fibers represent the bulk of the skeleton (e.g. Cohen & McConnaughey, 2003, Nothdurft & Webb, 2007). These different skeletal morphological levels reflect the complex arrangement of coral skeletal elements and it is astonishing how precisely they are repeated.

Even though early descriptive studies of coral skeletons focused on the classification of species they also led to the development of biomineralization concepts, of which the first date back to the end of the 19th century (e.g. Cuif & Dauphin, 2005b, Pratz, 1882, Stolarski, 2003). The first biomineralization concepts emphasize the resemblence of microstructural elements as purely inorganic crystals. These growth concepts are based on a simple physico-chemical precipitation process, where centers act as "germs" and facilitate and direct the growth of aragonite crystals (Barnes, 1970, Bryan & Hill, 1941). Goreau (1959) observed a layer of organic compounds that he interpreted as a template for growth. Young (1971) was one of the first showing that proteins are part of the skeleton. Later scanning electron microscopy (SEM) revealed the incremental growth of coral fibers (Cuif & Dauphin, 1998, Sorauf & Jell, 1977). This insight, together with information from UV-fluorescence examinations, clearly demonstrated microstructural and chemical differences between fibers and centers of calcification (e.g. Cuif & Dauphin, 1998; Cuif et al., 1999). Since then the number of studies that addressed the distribution (Cuif & Dauphin, 1998, Gautret *et al*., 2000), composition (e.g. Dauphin & Cuif, 1997, Gautret *et al*., 1997, Puverel *et al*., 2005) and origin (Clode & Marshall, 2002, Puverel *et al*., 2005, Tambutte *et al*., 2007) of organic components within skeletal structures increased rapidly. The incremental growth of coral fibers is expressed in the alternation of organic-rich and organic-depleted growth lines and a layered distribution of trace elements (Meibom *et al*., 2004, Meibom *et al*., 2007) and of sulphated polysaccharides. To explain the formation of these layered structures Cuif and Dauphin (2005b) proposed a two-step mode of growth by introducing a sequential process acting at micrometer scale emphasizing an ectodermal control of biomineralization. The ecotoderm secretes an organic framework (where sulphated polysaccharides potentially play a major role) on which minerals grow. The high fluctuation of Mg within fibers (Meibom *et al*., 2004) suggests that Mg might be incorporated to suppress crystal growth and end the growth cylce (Cuif & Dauphin, 2005b). Stolarski (2003) supported the alternating nature of growth in corals but challenged the proposition of differing temporal formation of EMZ and fibers.

In summary all these observations led to the perception that the formation of a coral skeleton involves the regulative control of dedicated cells / organic molecules during the different stages of growth, rather than "simple inorganic" precipitation of a mineral from a liquid. (Cuif & Dauphin, 2005a, Cuif & Dauphin, 2005b). However, "simple" bioinorganic models still prevail pointing out the morphological

and compositional similarity of abiotic precipitated aragonite under cyclically varying saturation state and pH with skeletal fiber growth of coral microstructural elements (Holcomb *et al.,* 2009). This analogy corresponds to the idea of a liquid filled space between epithelium and skeleton, where supersaturation is maintained to induce crystallization (Adkins *et al*., 2003, Furla *et al*., 2000). A critical review of the shortcomings associated with the latter perception can be found in Cuif *et al*. (2012).

The recent biomineralization concepts explain processes on the micrometer length scale e.g. growth of fibers around the EMZ. However, they do not provide a linkage to macroscopic structures such as synapticulae joining skeletal elements in regular intervals (Fig. 1) or to temporal differences in formation of different skeletal elements and areas, such as secondary thickening of septa and the formation of dissepiments at the base of the polyp (Nothdurft & Webb, 2007). In coral skeletons, the distribution of the organic matrix – a term encompassing all organic compounds within coral skeletons (Tambutté *et al.,* 2011) – with respect to crystal arrangement has been thoroughly described and attributed a function in calcification (Cuif & Dauphin, 2005b). This skeletal organic matrix was shown to be tightly associated with the mineral phase down to submicrometer scale delineating nano-crystals (Cuif & Dauphin, 2005a, Stolarski & Mazur, 2005) and to act as a pre-oriented organic framework that potentially directs the self-assembly of the nano-crystals to form crystal fibers (Cuif & Dauphin, 2005a). Several studies described the different functions for organic compounds extracted from the organic matrix of biominerals. These functions involve mechanisms such as the binding of calcium (Endo *et al*., 2004, Watanabe *et al*., 2003), stabilization of amorphous calcium carbonate (Addadi *et al.,* 2003) or inhibition of growth (Marin *et al*., 1996, Wheeler & Sikes, 1984). According to Cuif *et al*. (2011, p177) „present knowledge of the distribution of organic compounds at the submicrometer scale completely refutes any (…) accidental inclusion of organic compounds within skeletons“. However, the exact function on site within the skeleton and the role in the formation of different structural elements (and potentially the three-dimensional arrangement of macromorphological skeletal elements) is still elusive.

The high spatial resolution (sub-micrometer scale) of Confocal Raman Microscopy (CRM), has been demonstrated to be ideal to describe the structural relation between organic and inorganic phases in biogenic materials (e.g. Hild *et al*., 2008, Nehrke & Nouet, 2011, Nehrke *et al*., 2012, Neues *et al*., 2011). Recently, one study (Zhang *et al.,* 2011) used CRM to map the skeleton of a blue coral (*Helipora coerulea*, Octocorallia). They mapped a small region providing a preliminary insight into the ability of CRM to relate the distribution of organic compounds to the mineral phase in coral skeletons. In this study we applied CRM in combination with Polarized Light Microscopy (PLM), SEM and Electron Micro Probe mapping (EMP) to the scleractinian coral species *Porites lutea* (Milne Edwards & Haime, 1860. The main focus was the organic matrix distribution in relation to the mineral phase, in particular the organic-rich (ORGL) and organic-depleted (ODGL) growth lines (as first described in Cuif & Dauphin 1998) that form a growth layer (the so-called environment recording unit as described by e.g. Cuif & Dauphin 2005a) and how they correlate with the distribution of the elements Sr, Mg, and S. Furthermore

we also investigated how the information obtained by CRM can be compared to the information obtained by long established methods like PLM and SEM.

2. Material and methods

2.1 Coral sample

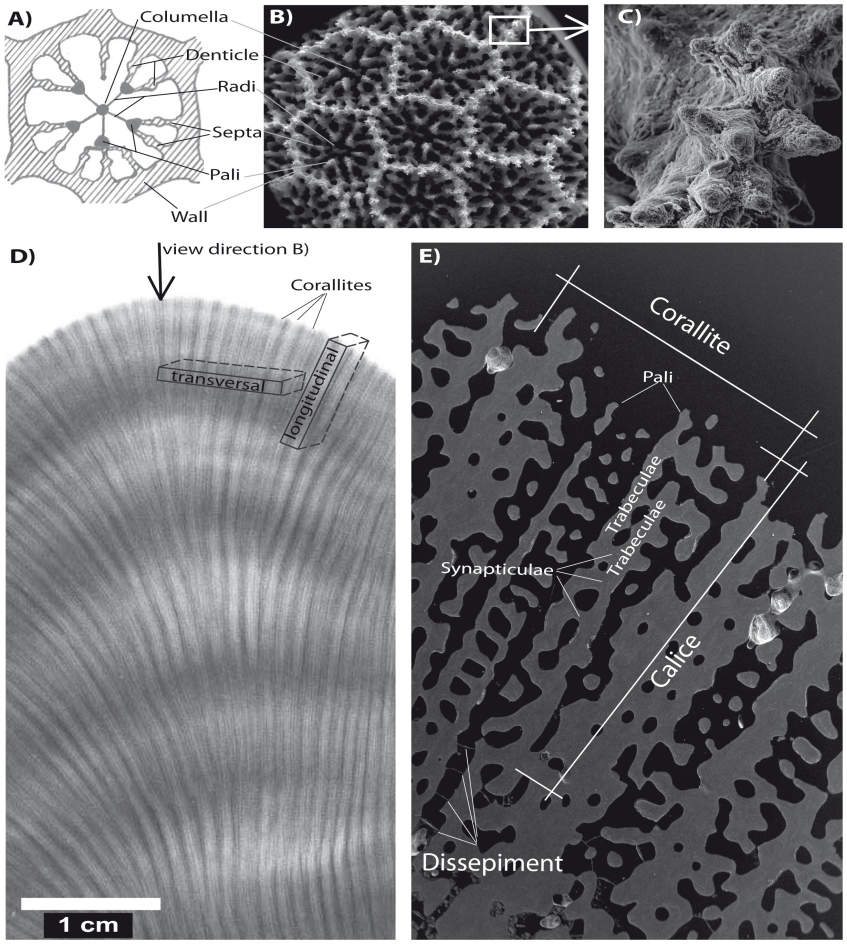

Figure 1: **Scanning electron microscopic (SEM) images and X-radiograph positive of *Porites lutea* (Milne Edwards & Haime, 1860).** A) Schematic representation of a *Porites* corallite indicating the macromorphological elements. B) Distal view of ceroid corallites. C) Detail showing the spines structuring septal walls. D) X-radiograph of the coral skeleton displaying yearly density banding pattern. Arrow indicates view direction in B and rectangles show how skeletal blocks were cut out of the skeleton to obtain transversal and longitudinal samples. E) Scanning electron microscopic (SEM) image of a longitudinal section displaying skeletal elements forming the corallite.

The scleractinian coral *Porites lutea* (Milne Edwards & Haime, 1860) was collected by SCUBA divers from an offshore island in the Andaman Sea, Thailand in March 2011. Coral tissue was removed by submerging the specimen in a 5% sodium hypochlorite solution for 24 hours, and subsequently rinsing with de-ionised water and drying at 60°C for 24 hours.

The flow chart in Fig. 2 provides an overview of samples (with sample ID) derived from this specimen and gives an outline of the preparation and measurements applied. After tissue removal, three longitudinal and one transversal block (Fig. 1) were cut out of the skeleton and all but one of the longitudinal skeletal

blocks were embedded in an epoxy resin (Araldite 2020, Huntsmann). All samples were ground using HERMES water grinding papers (in the order P1200, P2400, and P4000) and polished with a Struers diamond suspension of 3 μm and finished with a 0.3 μm aluminum oxide suspension. The sample was rinsed with de-ionised water and shortly cleaned in an ultrasonic bath after each grinding and polishing step. To determine how the observed structures continue into deeper levels of the skeleton, a vertical skeletal rod (trabeculae) of one sample was mapped by CRM in three different levels. This was done by re-grinding and polishing after each mapping to remove ~10 μm of the sample.

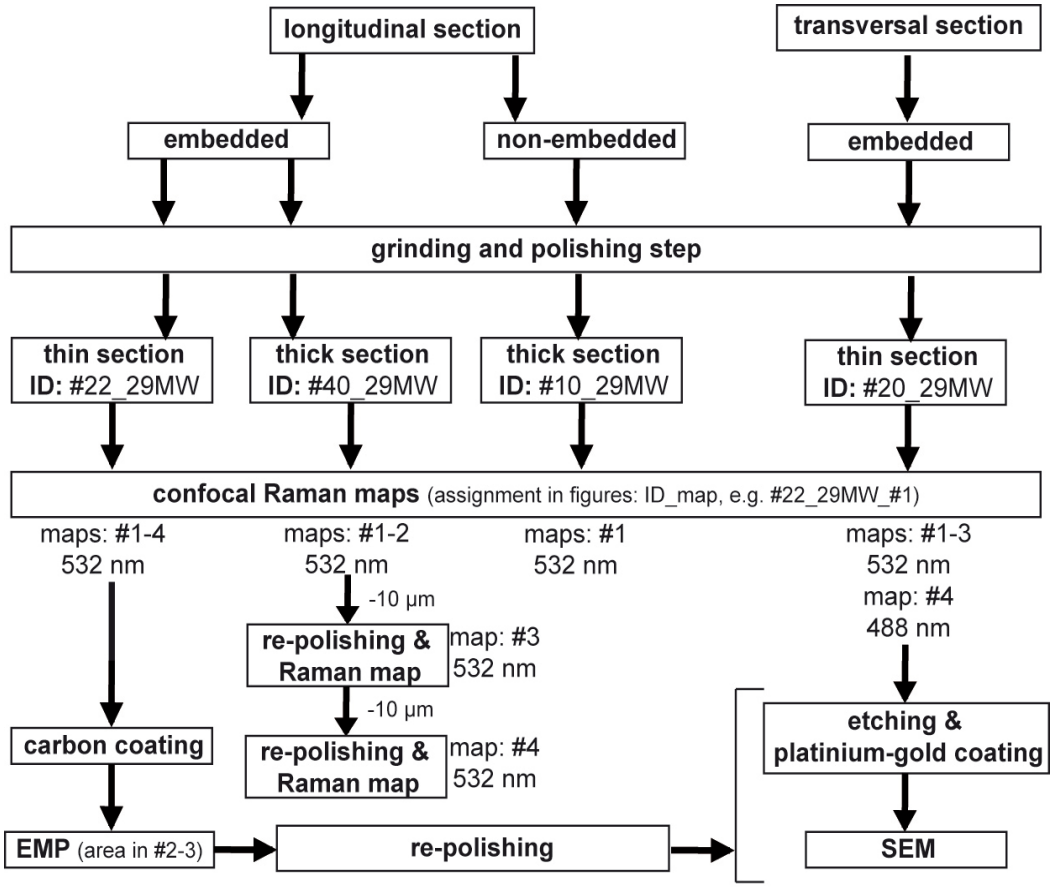

Figure 2: Sample overview and preparation. Flow chart displays the chronology of preparation and measure-ment steps for individual samples (ID). For confocal Raman measurements, the number of maps and laser wavelength used for each map are also given. (Within subsequent figures Raman maps are denoted by: ID_map, e.g. #22_29MW_#1).

2.2 Confocal Raman microscopy

Raman mapping was done using a WITec alpha 300 R (WITec GmbH, Germany) CRM. Scans with a high spatial resolution were performed using a piezoelectric scanner table having a maximum scan range of 200 μm x 200 μm and a minimum step size of 4 nm lateral and 0.5 nm vertical. An ultra high throughput spectrometer (UHTS 300, WITec, Germany) equipped with en EMCCD camera was used with a grating of 600 grooves mm^{-1}, blazed at 500 nm. This set-up allows for a very short integration time (down to a few ms) and a spectral range from 0-3600 cm^{-1} or 0-4000 cm^{-1} depending on the wavelength used (532 nm or 488 nm, respectively). The Raman instrument could also be operated as a normal light

microscope using transmitted and reflected light and was equipped with a polarizing filter (one before the sample - the polarizer and one after the sample - the analyzer). The analyzer can be used in the range from 500 to 800 nm allowing on the one hand the operation of the microscope for PLM and on the other hand for polarized Raman microscopy (at 532 nm). All Raman maps were obtained using a Nikon 100x (NA = 0.9) objective, with the polarizer set to 0° and the analyzer to 90°. The spectra during mapping were recorded with a step size of 0.5 μm and an integration time of 50 ms or 10 ms for 532 or 488 nm, respectively. Raman measurements of biogenic materials are often hindered by strong fluorescence, which overlay distinct Raman lines. However, as shown for the shell of the snail *Nerita undata* by e.g. Nehrke and Nouet (2011), fluorescence intensity distribution of a region can be used as a proxy to map organic matrix distribution within biogenic minerals. Thus, we used the spectral range between 2400 - 2700 cm^{-1} to map the fluorescence intensity distribution across the sample. The spectral analysis and image processing was performed using the WITecProject software (verion 2.04, WITec GmbH, Germany).

2.3 Scanning electron microscopy

Prior to SEM analysis the samples were etched using 0.1% formic acid and 3% glutaraldehyde solution for 50 seconds to make microstructural features visible (Waite and Andersen, 1980; Cuif and Dauphin, 1998; Stolarski, 2003). After etching the sample was air dried, put on aluminum stabs, and sputter-coated using a plantinum-gold target. Scanning electron microscopic images were acquired at 10kV or 15kV and 1.7 μA filament current using a Philipps XL 30 Environmental Scanning Electron Microscope (ESEM).

2.4 Electron microprobe mapping

Electron Micro-Probe mapping (EMP: JXA- 8200 JEOL, Geomar) was used to study minor and trace element distribution in relation to the structures determined by CRM. The EMP maps were obtained by wavelength dispersive spectrometry (WDS) mode measuring simultaneously Mg (Ka, TAP), Sr (La, TAP) and S (Ka, PETH). The electron beam was focused to a spot size of 1 μm, accelerating voltage set to 15 kV and beam current to 20 nA. A step size of 1 μm as well as an accumulation time of 20 ms was used and the map was repeated to gather 10 accumulations of the selected area. Standards (Vulcanicglass – VG-2) were measured before mapping the sample to calculate concentrations of the trace elements.

2.5 Linear extension rate and growth layer thickness

The coral colony was stained *in situ* using alizarin red (15 mg l^{-1}, approx. 16 h) three months before collection. Daily growth rates can be calculated from this staining experiment by measuring the distance from the staining line (visible in longitudinal sections cut along the major growth direction of corallites) to the colony outer surface with a caliper and dividing this distance by the number of days between

staining and collection. *Porites* skeletons consist of vertical rods (trabeculae) that are built of EMZ and fibers (Fig. 3). The fibers are deposited to both sides of the EMZ and composed of incremental growth layers (Cuif and Dauphin, 2005a). The growth layer thickness was measured perpendicular to the outer coral mineralizing epithelium and comprises a pair of an ORGL and ODGL (see Fig. 3). The vertical growth rate (determined from the staining experiment) was compared to growth layer thickness (determined using CRM fluorescence mapping). Differences in vertical and lateral extension rates result from the oblique arrangement of the growth layers with respect to the vertical line of EMZ. Both growth layer thickness and the angle between growth layers were measured in all Raman maps that displayed the alternation of a ORGL and ODGL using the computer program imageJ.

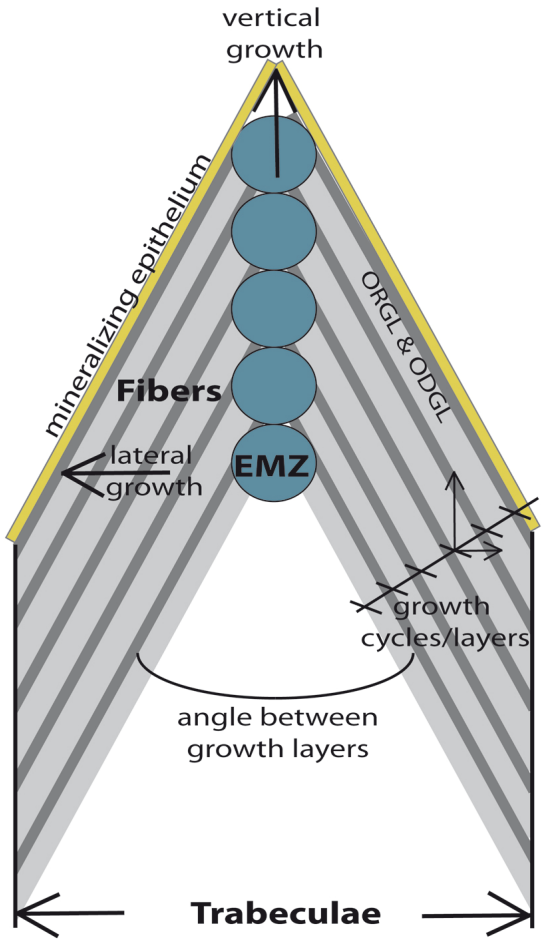

Figure 3: Schematic representation of coral skeletal growth of a trabeculae (modified after Cuif & Dauphin, 2005a). Stepping growth mode of fibers results in growth layers of organic-rich (ORGL, dark grey) and organic-depleted growth lines (ODGL, light grey) to both sides of the early mineralization zone (EMZ). The growth layers are oblique and encompass an angel resulting in differences in vertical and lateral extension per growth cycle.

3. Results and discussion

3.1 Structural sample characterization

The spectroscopic datasets obtained during the different Raman mappings where first analyzed for the characteristic Raman peaks of aragonite (Fig. 4) – namely translational mode (155 cm^{-1}), librational mode

(208 cm^{-1}), in-plane bend (710 cm^{-1}) and symmetric stretch (1085 cm^{-1}) (Fig. 4; Bischoff *et al.*, 1985, Urmos *et al.*, 1991). The differences in crystallographic orientation of aragonite (Fig. 4) were visualized by using the relative peak intensity changes as shown by Nehrke and Nouet (2011) for the orientation of aragonite prisms in a gastropod shell. The images show the typical fan like fibers described by Cuif and Dauphin (2005b) for scleractinian coral skeletons using PLM (Fig. 4 B-C).

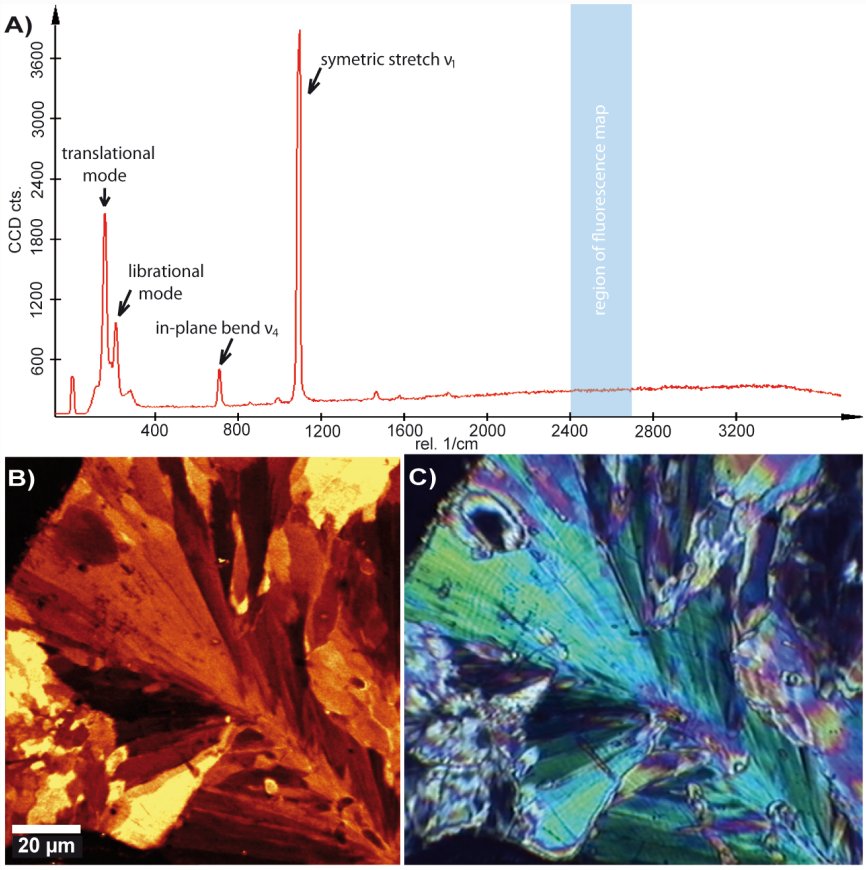

Figure 4: Raman lines and Raman map that assemble crystal arrangement. A) Raman spectra of *Porites lutea* skeleton sample showing the characteristic peaks for aragonite (translational mode at 155 cm^{-1}, librational mode at 208 cm^{-1}, in-plane band at 710 cm^{-1} and symmetric stretch at 1085 cm^{-1}). Highlighted in blue is the spectral region used to derive the fluorescence maps. B) Crystallographic orientation derived from symmetric stretch resembles the fiber orientation in polarized light microscopy (C). (#22_29MW_#1, integration time of 0.5 sec and 10 accumulations, 100x Nikon Objective)

The intensity distribution of the major aragonite peak can be used to visualize changes in crystal orientations. The visualization of these orientations was possible in embedded as well as non-embedded polished samples (Fig. 5). Hence, structural information of the mineral phase and relative orientation can be derived without preparation of thin section, as required for PLM. This allowed determination of the distribution of organic compounds in relation to different structural elements as will be shown below.

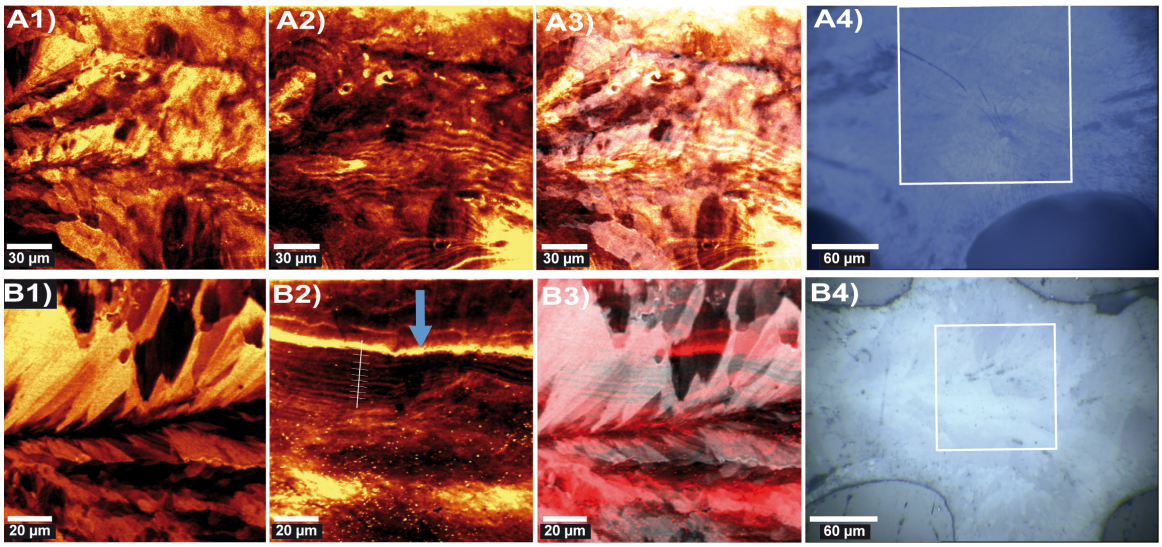

Figure 5: Raman maps of longitudinal skeletal surfaces. Raman maps of longitudinal non-embedded (A; #10_29MW_#1) and embedded (B: #40_29MW_#1) thick sections of *Porites lutea* (Milne Edwards and Haime, 1860). A4-B4) Reflected light images with insert showing the location of the Raman maps. The number of each Raman map (from sample A and B) indicates the spectral region used for mapping: 1) represents the intensity distribution of the symmetric stretch of aragonite (1085cm^{-1}), 2) the fluorescence intensity distribution within the area and 3) shows the superposition of map 1) and 2). Blue arrows indicate repeated features of organic-rich growth lines (ORGL 2) of increased fluorescence detected within fluorescence maps. The scale bar within fluorescence maps displays the skeletal extension for each growth cycle comprised of one high and one low fluorescence growth line. (Superimposed images derive from WITecProject software)

Fluorescence intensity maps allow visualization of the distribution and arrangement of the organic matrix within coral skeletons, as revealed by means of acridine orange staining (Cuif & Dauphin, 1998, Cuif *et al.,* 1999, Gautret *et al*., 2000, Stolarski, 2003). Both the distribution of incremental ORGL and the EMZ (e.g. Cuif & Dauphin, 1998) could be visualized using CRM (Fig. 6). The mapped organic matrix distribution was confirmed by a direct comparison with SEM micrographs after etching (Fig. 7). The superimposed maps of crystal orientation and fluorescence (Fig. 5-6) confirmed the synchronism in formation of growth layers between adjacent fibers (Cuif *et al*., 2004). Therefore, Raman mapping can simultaneously determine differences in crystallographic orientation, the distribution of incremental growth layers, and the location of the EMZ within corals without alteration by staining. This improves the interpretation of data while reducing the number of different sample preparation steps and therewith the possibility of sample alteration.

3.2 Determination of growth rates and daily growth cycles

Based on the previously described results, fluorescence images can be used to derive information on growth layer thickness. As described in the section 2.5 a growth layer comprise of an ORGL and a ODGL here reflected by a high and a low fluorescence line. These two together illustrate the stepping growth mode of coral fibers (e.g. Cuif & Dauphin, 2005b).

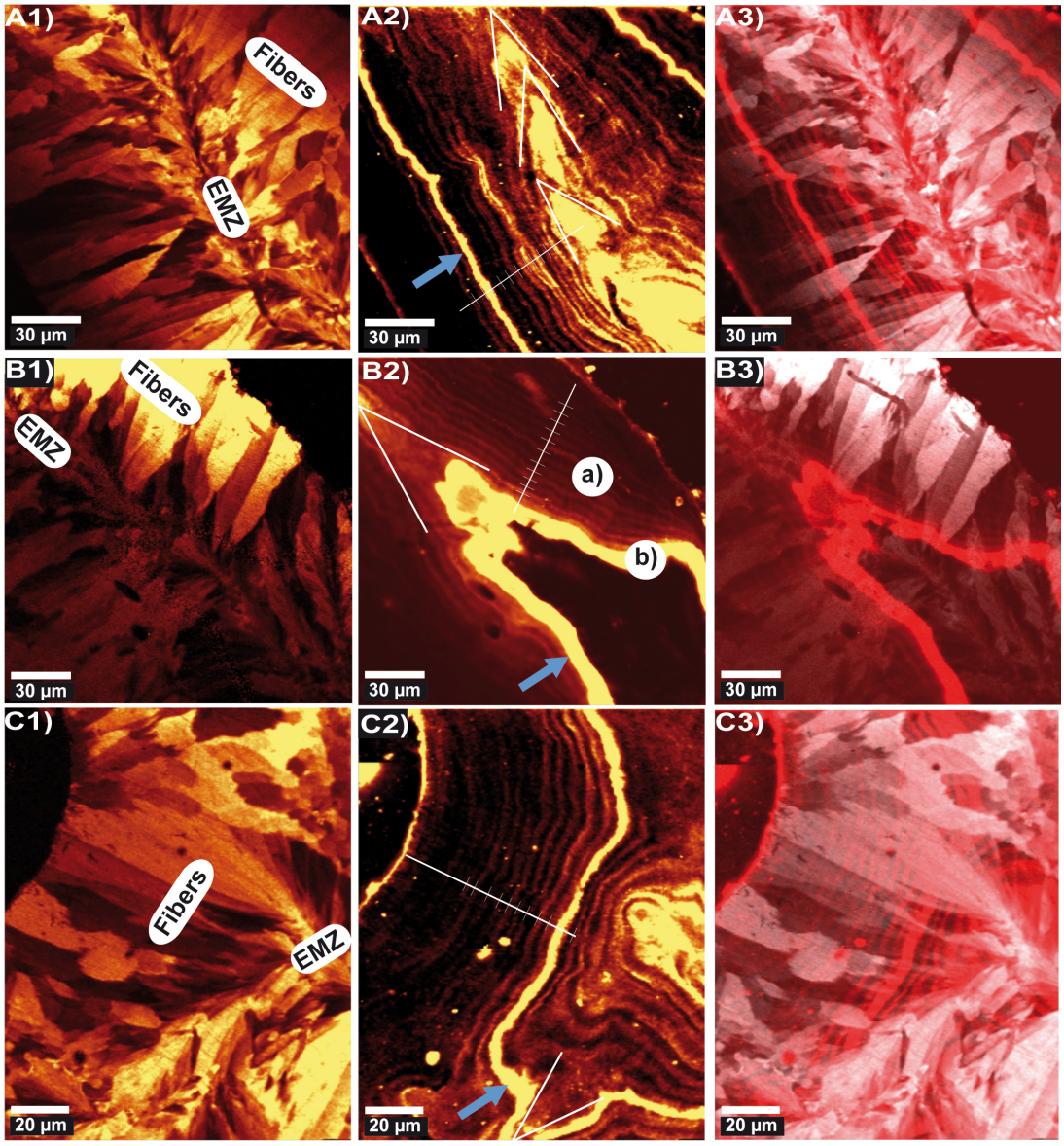

Figure 6: Raman maps of thin sections. A-C) Raman maps of *Porites lutea* (Milne Edwards and Haime, 1860) skeleton elements in longitudinal thin section (#22_29MW_#2-4). Numbers indicate the spectra region used for the maps: 1) represents the intensity distribution of the symmetric stretch of aragonite (1085 cm^{-1}), 2) the fluorescence intensity distribution and 3) shows the superposition of map 1) and 2). Blue arrows indicate repeated features of organic-rich growth lines (ORGL 2) of increased fluorescence detected within fluorescence maps. White arrow heads represent the oblique traces of the position of mineralizing epithelium forming layered growth increments with a high and a low fluorescence growth line comprising one growth cycle. The scale bar within fluorescence maps displays the skeletal extension for each growth cycle. The two types of growth lines within fluorescence map are indicated in B2 with a) representing the incremental growth layers (organic-rich and organic-depleted growth lines) and b) the high fluorescence growth lines (ORGL 2). (Superimposed images derive from WITecProject software)

The distances of growth layers were measured perpendicular to the growth lines as explained in section 2.5 (indicated by the position of the scale bar within fluorescence maps, e.g. Fig. 6A2) and corresponds to a distance of 3.9 ± 0.2 μm (mean ± SE; n = 18). These layers encompass on average an angle of 36 ± 2° (mean ± SE; n = 16) and hence, a growth layer results in a mean vertical extension of 12 μm (see Fig. 3; calculation: growth layer thickness/sin (angle between growth layers/2)). This vertical extension (often referred to as linear extension) was compared to the mean daily growth rate (in vertical

direction) of this specimen of approx. 30 μm day^{-1}. These data suggest that 2-3 growth cycles per day occur. Meibom *et al*. (2007) compared average linear extension rates to distances between high Mg bands determined by means of nanoSIMS measurements (on *Porites* sp.) and suggested that within a day up to five growth cycles could be deposited. In his measurements, one growth layer was between 2-5 μm wide, thus, both – cyclicity and growth layer thickness correspond to the values obtained in this study. Cuif *et al*. (2011) obtained 10-15 cycles per week (~2 cycles per day) for *Galaxea fascicularis* from a consecutive calcein staining experiment. Thus, this study and the study by Meibom *et al*. (2007) observed a slightly higher number of cycles per day for *Porites* spp. than Cuif *et al*. (2011) for *Galaxea fascicularis*. Nothdurft and Webb (2007) observed that a vertical extension of 384 μm corresponds to 36 μm in lateral growth by tracking growth lines in a skeletal rod of *Porites lobata*. This vertical distance was deposited within 12 days (derived from mean growth rates for this species; see Nothdurft & Webb 2007) and equals a lateral growth of 3 μm per day. Based on the growth rates determined in this study and the study by Meibom *et al*. (2007), 3 μm lateral growth corresponds to approximately one growth cycle per day.

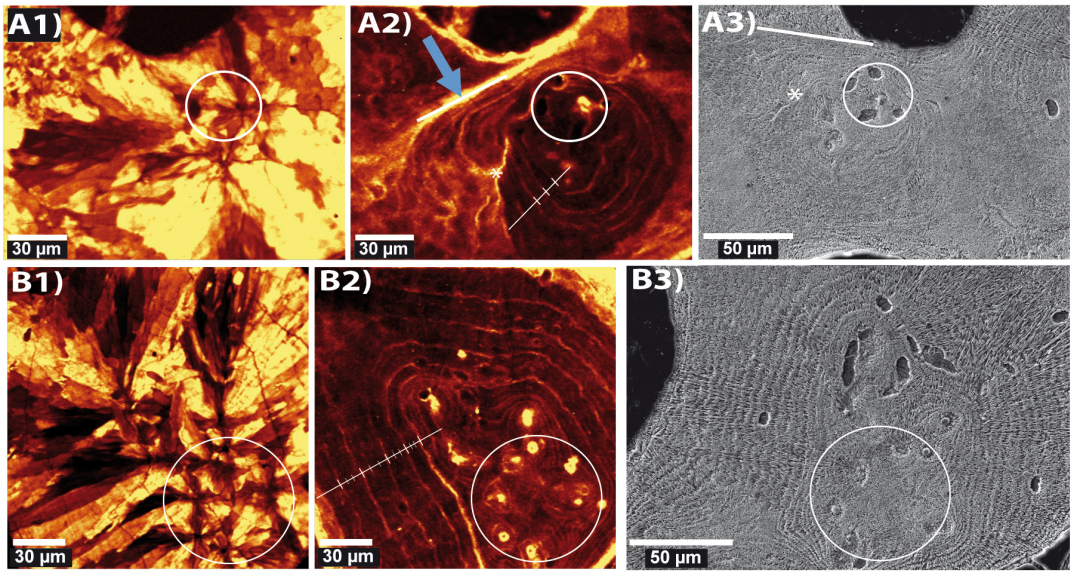

Figure 7: Raman maps of transversal skeletal surfaces. Raman maps of transversal thin section represent the intensity distribution of the symmetric stretch of aragonite (1085 cm^{-1}, A1, B1) and the fluorescence intensity distribution (A2, B2). A3, B3) Scanning electron microscopic images were obtained after Raman mapping and etching of sample (A: #20_29MW_#1, B: #20_29MW_#2). Circle in the images illustrates same areas within the different maps for each row. Blue arrows indicate repeated features of organic-rich growth lines (ORGL 2) of increased fluorescence detected within fluorescence maps. The scale bar within fluorescence maps displays the skeletal extension for each growth cycle comprised of one high and one low fluorescence growth lines. Asterisk indicates same regions within the same row of maps.

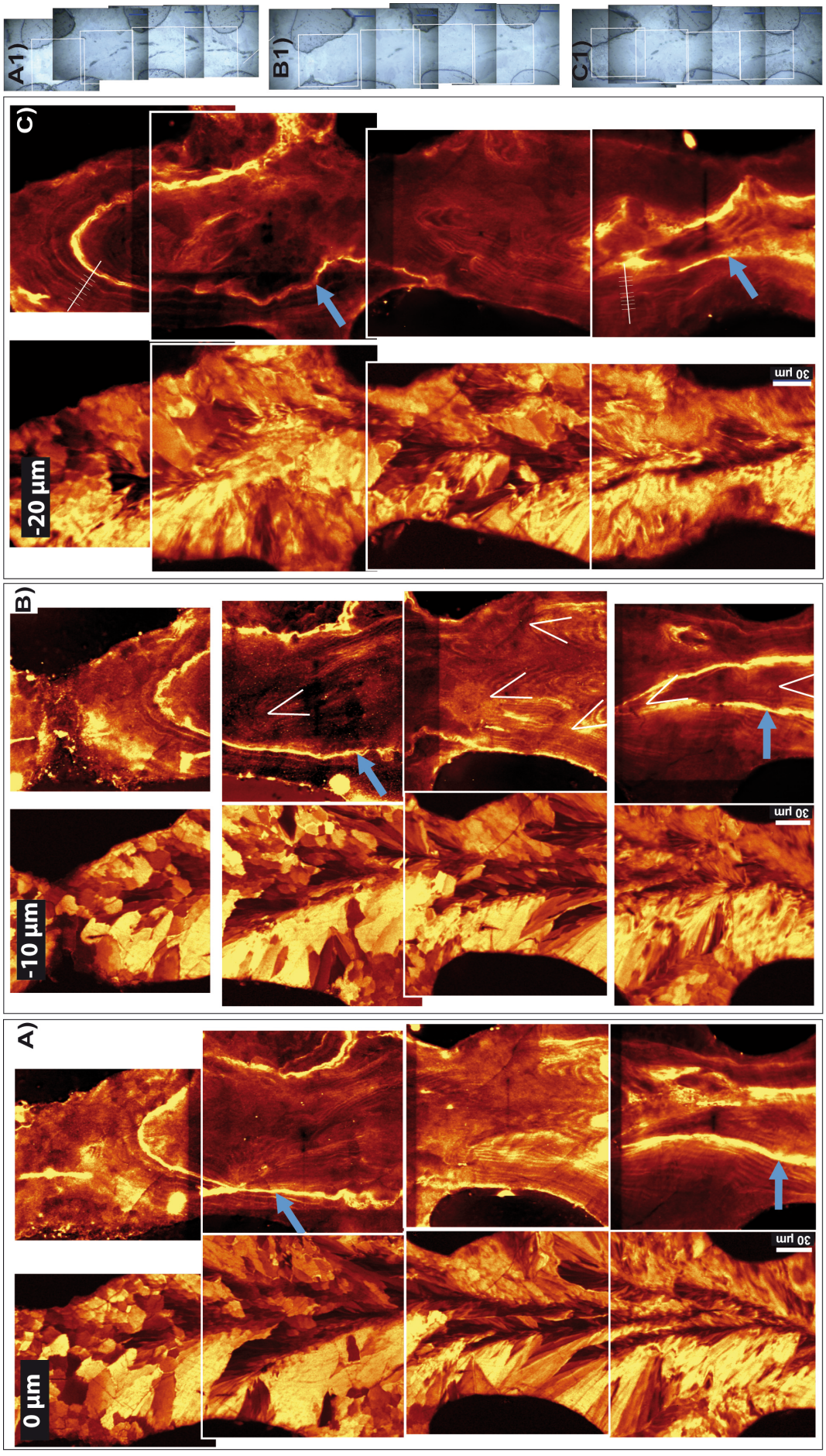

Figure 8: Raman maps in 3 dimensions. A-C) Raman maps per depth level (A: 0 μm, B: -10 μm and C: -20 μm; #40_29MW_#2-4) of intensity distribution of the symetric stretch of aragonite and of fluorescence are plotted on the left and right, respectively. Reflected light images are displayed on the right for each mapped depth layer (A1: 0 μm, B1: -10 μm, C1: -20 μm). Blue arrows indicate repeated features of organic-rich growth lines (ORGL 2) of increased fluorescence detected within fluorescence maps. White arrow heads represent the oblique traces of the position of mineralizing epithelium forming layered growth increments with a high and a low fluorescence growth line comprising one growth cycle. The scale bar within fluorescence maps dispays the skeletal extension for each growth cycle.

The differences in growth cycles per day summarized here could be of various nature: (1) the coral was stressed from the staining process (Houlbreque *et al*., 2009, Thebault *et al*., 2006), (2) effect of the nutritional status (Cuif *et al*., 2011), (3) daily growth cycles are species-specific (Cuif *et al*., 2011), and/or (4) growth rates could differ depending on the location within the skeleton for which they are determined. However, a nonlinear growth rate in lateral and longitudinal direction and/or different growth rates depending on the distance from the EMZ could explain the observed decrease in number of growth cycles when tracing growth lines over larger areas.

This study detected two types of ORGL, which differ in thickness and intensity. From here on the wide growth lines showing increased fluorescence (indicated by a blue arrow within Raman fluorescence maps; Fig. 5-7) are referred to as ORGL 2 (Fig. 6B2 (b)) whereas the thinner incremental growth lines are referred to as ORGL 1 (Fig. 6 B2 (a)). It could be shown that the ORGL 2 continue in deeper skeletal layers of a vertical rod (Fig. 8 A-C). Moreover, these lines resemble the corals outer surface forming a three-dimensional organic envelope. Within a skeletal rod the location of this growth line changes slightly (Fig. 8), in particular in regions where other skeletal elements, such as radi or synapticulae arise. Early mineralization zones are known to build the central skeletal framework directing growth. The organic envelopes described here indicate former outer surfaces and could potentially play a role as initiation points for interconnecting skeletal elements where new EMZ are formed.

3.3 Correlation between organic matrices and elemental composition

EMP mapping showed that Sr is slightly variable within the sample without a distinct pattern (Fig. 9). On the other hand, the Mg distribution displayed a banding pattern, which correlates with the fluorescence bands determined by CRM (Fig. 9). Mapping of S showed elevated concentrations in the areas representing the EMZ (Fig. 9). These findings qualitatively agree with previous studies (Cuif *et al*., 2003, Meibom *et al*., 2004, Meibom *et al*., 2007, Meibom *et al*., 2008), even though the resolution of EMP is not comparable with high-resolution techniques such as XANES or nanoSIMS (Cuif *et al*., 2003, Meibom *et al*., 2004). Therefore, a cyclic variation of S within fibers could not be resolved in this study.

As described above, two different types of ORGL were identified by CRM (named type 1 and type 2). The ORGL 1 show elevated Mg concentrations whereas the ORGL 2 are depleted in Mg. In general it is assumed that in corals Mg is associated with organic compounds (Finch & Allison, 2008), which often also show increased S concentrations (Cuif *et al*., 2012). However, the ORGL 2 do not follow this pattern but show decreased Mg concentration and no pattern in S (Fig. 9). The low Mg ORGL 2 most likely correspond to the distinct low Mg lines described by Meibom *et al*. (2004, their Fig. 2 - *Pavona clavus*, 2007, their Fig. 2 - *Porites* sp.). Therefore, they would represent a structural feature not restricted to the skeleton of *P. lutea*. Cuif and Dauphin (2005b) proposed that Mg incorporation in incremental growth lines (type one) functions to repress growth before another layer is added. The ORGL 2 identified in this study, however, is characterized by a decreased Mg concentration and a potentially different function.

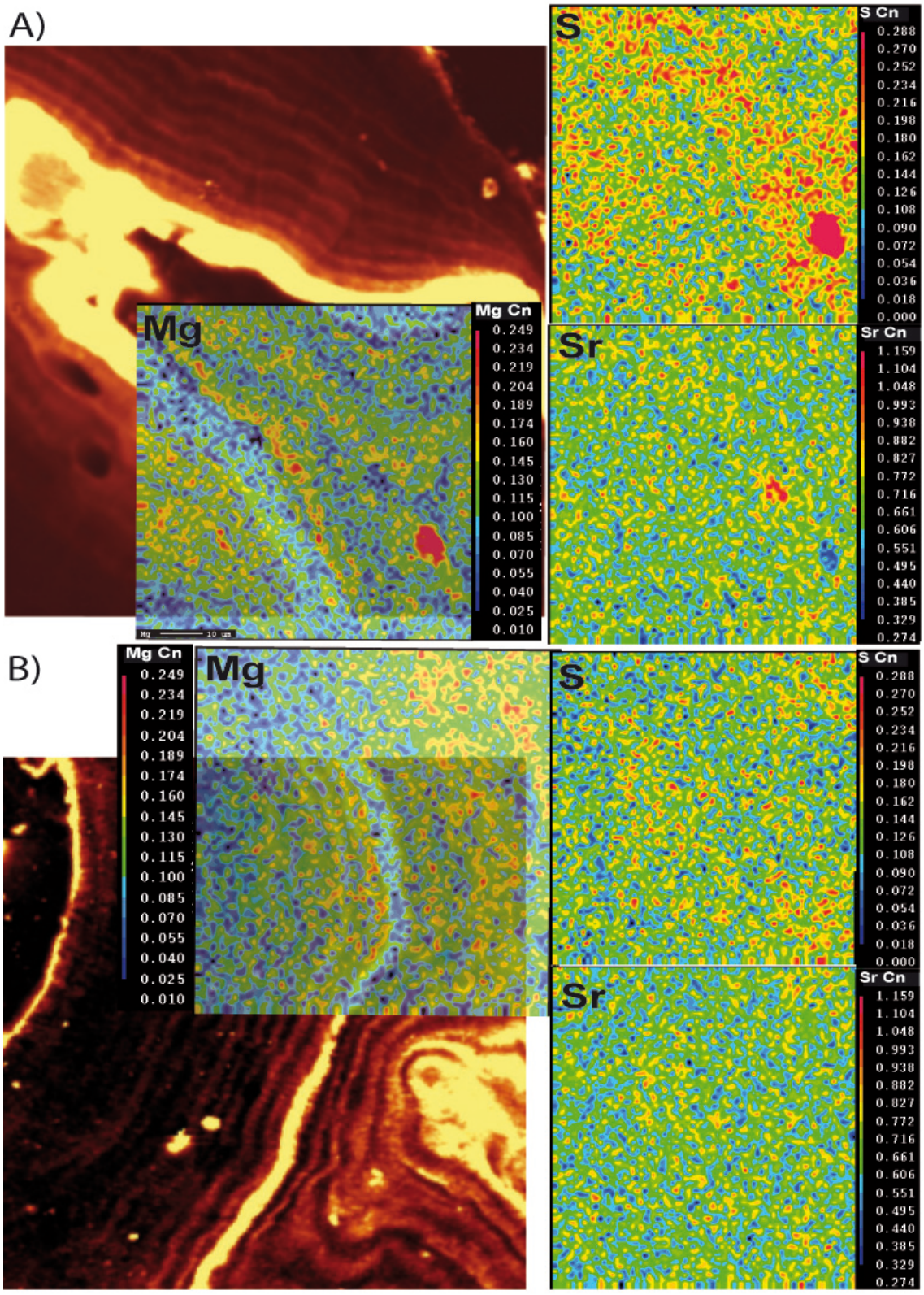

Figure 9: Trace element maps. Trace element concentrations (Mg, S, Sr) were mapped with electron microprobe. Mg distribution of the mapped area was superimposed on the respective fluorescence intensity distribution map derived from Raman mapping (A: Fig. 3 B2, #22_29MW_#3, B: Fig. 3 C2, #22_29MW_#4). The trace element maps of S and Sr are displayed on the right side of the superimposed images (Adobe Photoshop CS4).

3.4 Growth patterns and cyclicity

Nothdurft and Webb (2007) pointed out that adjoining structural elements such as dissepiments and septa are formed at different times. This temporal heterogeneity is not taken into account in existing growth models and therefore requires their adaptation above the microstructural level. The temporal heterogeneity in skeletal formation also becomes obvious when trying to track spines along the calice into deeper parts of the skeleton, where it appears that they are not present. Hence, different regulative processes must act to produce the spine-rich distal end of the corallites, the skeletal layer covering spines above dissepiments before the skeleton is cut off from the polyp as well as the formation of synapticulae at a regular interval. Position and shape of the ORGL 2 resemble either denticle finger-like structures, traces of former spines or previous skeletal surfaces. Hence, the ORGL 2 which differ in elemental composition and location compared to previously described ORGL 1 arrangements, could be involved in regulating three-dimensional growth patterns of micro- and macroarchitectural elements. We hypothesize that these ORGL 2 act as an "envelope" representing the outer surface at a certain time of deposition (Fig. 10 C), before it becomes overgrown and covered by the following growth cycle. The temporal units 1-3 in Fig. 10 C represent different growth cycles with 1 being the oldest and 3 the youngest deposited skeleton. Each growth cycle lasts about two weeks and ends with an ORGL 2 (Fig. 10 C). Infilling between spine tips and thickening of macromorphological elements takes place within this biweekly cycle elongation (Fig. 10 D). This periodicity in growth agrees with the growth model proposed by Nothdurft and Webb (2007). They traced a growth band in their study (Nothdurft & Webb 2007; their Fig. 16 C & 17 B) that resembles the ORGL 2 described in this study (Fig. 10 B) with a similar longitudinal extension spanning approx. 12 days of growth. This observation supports the proposed mechanism of a three-dimensional structural regulation by ORGL 2 in *Porites* skeletal growth that follows a biweekly periodicity.

Cyclicity represents a ubiquitous characteristic of coral skeletal formation. The described cycles range from the cm-level displayed by seasonal density bands (e.g. Lough & Barnes, 2000; Fig. 1D) down to the μm-level of daily/sub-daily formation of incremental growth layers (e.g. Meibom *et al.,* 2007). High-resolution proxy studies detected a cyclicity of measured proxy values in the range of weekly to monthly periods (Meibom *et al.,* 2003, Rollion-Bard *et al.*, 2003, Cohen & Sohn, 2004, Allison *et al.,* 2010, Allison *et al.,* 2011). In these studies the proxy relation (e.g. Sr/Ca) did not only depend on the target parameter (e.g. Temperature) but was potentially influenced by other parameters including: (1) metabolic changes involving spawning and larval release at a lunar periodicity (Meibom *et al.,* 2003), (2) weekly tidal forcing overlying temperature forcing (Cohen & Sohn, 2004) and (3) a strong bi-weekly periodicity that was hypothesized to result from increased calcification required for the formation of synapticulae (Cohen & Sohn, 2004). The latter corresponds to the biweekly growth bands (ORGL2) described in this study.

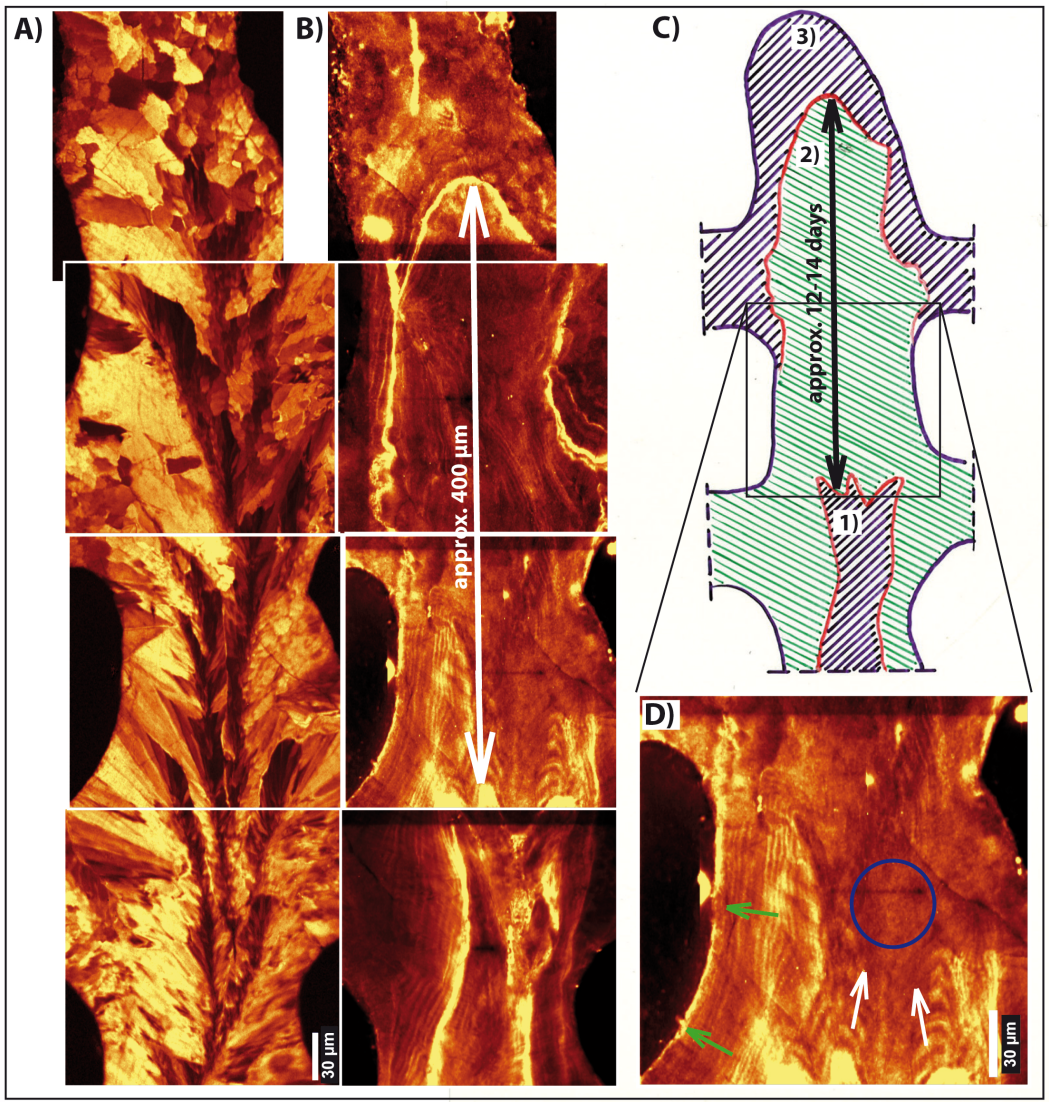

Figure 10: Model of skeletal growth patterns. Schematic representation of growth patterns mapped with confocal Raman microscopy. A-B) Raman map of the intensity distribution of the symmetric stretch of aragonite (1085cm^{-1}, A) and the fluorescence intensity distribution of the same area (B) from Fig. 8A (#40_29MW_#2) in a longitudinal sections of *Porites lutea*. C) Schematic image of cyclicity in growth representing three cycles each ending with a high fluorescence growth line (red line), which equals approx. 12-14 day periodicity (daily growth rate of this specimen of ~ 30 μm d^{-1}). D) During each cycle different growth modes are suggested to be responsible for the three-dimensional appearance of the skeletal vertical rod. Vertical extension in the direction of the spines reflects thicker growth layers (white arrows) than in lateral growth. Lateral growth represents thickening of skeletal element (green arrows) and both lateral and vertical growth potentially is associated with different growth rates. Blue circle marks an area of no clearly visible banding pattern where the skeleton was potentially sectioned parallel to the position of the growth layers.

3.5 Chemical characterization of organic compounds

So far we have used the fluorescence intensity determined by CRM as a "black box" for organic molecules. This concept is sufficient since the scope of this investigation is on structural information of coral skeletons in relation to three-dimensional growth patterns and not the characterization of organic compounds. Emphasis was made on obtaining Raman maps of high spatial resolution (requiring a hundred thousand spectra per scan) hence it was not possible to obtain spectra with high spectral resolution at the same time. However, it should be pointed out that CRM is much more powerful and can deliver more detailed information for the chemical characterization. Most studies that applied CRM on coral skeletons derived single spectra. Their aim was to check for different carbonate polymorphs (with a spectra range up to 1300 cm^{-1}; (e.g. Cuif & Dauphin, 1998, Clode *et al.,* 2011)) and only a few studies focused on organic spectral lines (Perrin & Smith, 2007, Zhang *et al*., 2011). To demonstrate what kind of chemical information can be obtained, we analyzed the spectra of some areas showing increased fluorescence in more detail and compared the spectra to other studies using Raman spectroscopy on biominerals. Spectral lines not attributed to aragonite were detected (Fig. 11) corresponding to asymmetric SO_4^{2-} bend (646 cm-1, Jolivet *et al*., 2008, Zhang *et al*., 2011), Amid III (1190-1310 cm^{-1}, (Jolivet *et al*., 2008, Zhang *et al*., 2011)), CH bands (2850-3080 cm^{-1}, (Jolivet *et al*., 2008, Perrin & Smith, 2007) and OH group (3200-3400 cm^{-1}, (Jolivet *et al.,* 2008). However, there are some difficulties associated with Raman spectral studies of biominerals that need to be considered. In biominerals the mineral phase is generally dominating the spectra and long integration times are necessary to obtain the very weak organic bands. Additionally, such samples often show high fluorescence that can lead to oversaturation of detectors when long integration times are used (which sometimes can be avoided by decreasing the intensity of the laser, which on the other hand also increases the integration time). Contaminations of the sample during sample preparation such as embedding in epoxy resins need to be considered and accounted for. We used non-embedded samples to reproduce banding pattern of skeletal fibers to exclude the possibility that during grinding and polishing abraded material accumulates predominately at the organic layers. Recent studies used Raman spectroscopy to characterize organic matrix in biominerals (Jolivet *et al*., 2008, Kaczorowska *et al*., 2003, Nehrke & Nouet, 2011, Perrin & Smith, 2007, Zhang *et al*., 2008, Zhang *et al*., 2011), but coral Raman spectroscopic analyses covering a spectral region between 100-3200 cm^{-1} are quite rare. However, organic compound bands were detected by all studies (Kaczorowska *et al*., 2003, Perrin & Smith, 2007, Zhang *et al*., 2011, this study), although, Kaczorowska *et al*. (2003) compared the Raman spectra of scleractinian corals to pure aragonite and only detected organic bands for precious corals. In contrast, Perrin and Smith (2007, *Lobophyllia corymbosa* and *Leptastrea purpurea*) and this study (*Porites lutea*) both detected organic compounds within scleractinian coral skeletons. The ability of Raman spectroscopy to observe both differences in quantity (not absolut but relative Fig. 5-7,) as well as quality (spatial distribution, Fig. 11 A1, B1, as well Perrin & Smith, 2007) was demonstrated. These observations have also been derived for other biominerals (Jolivet

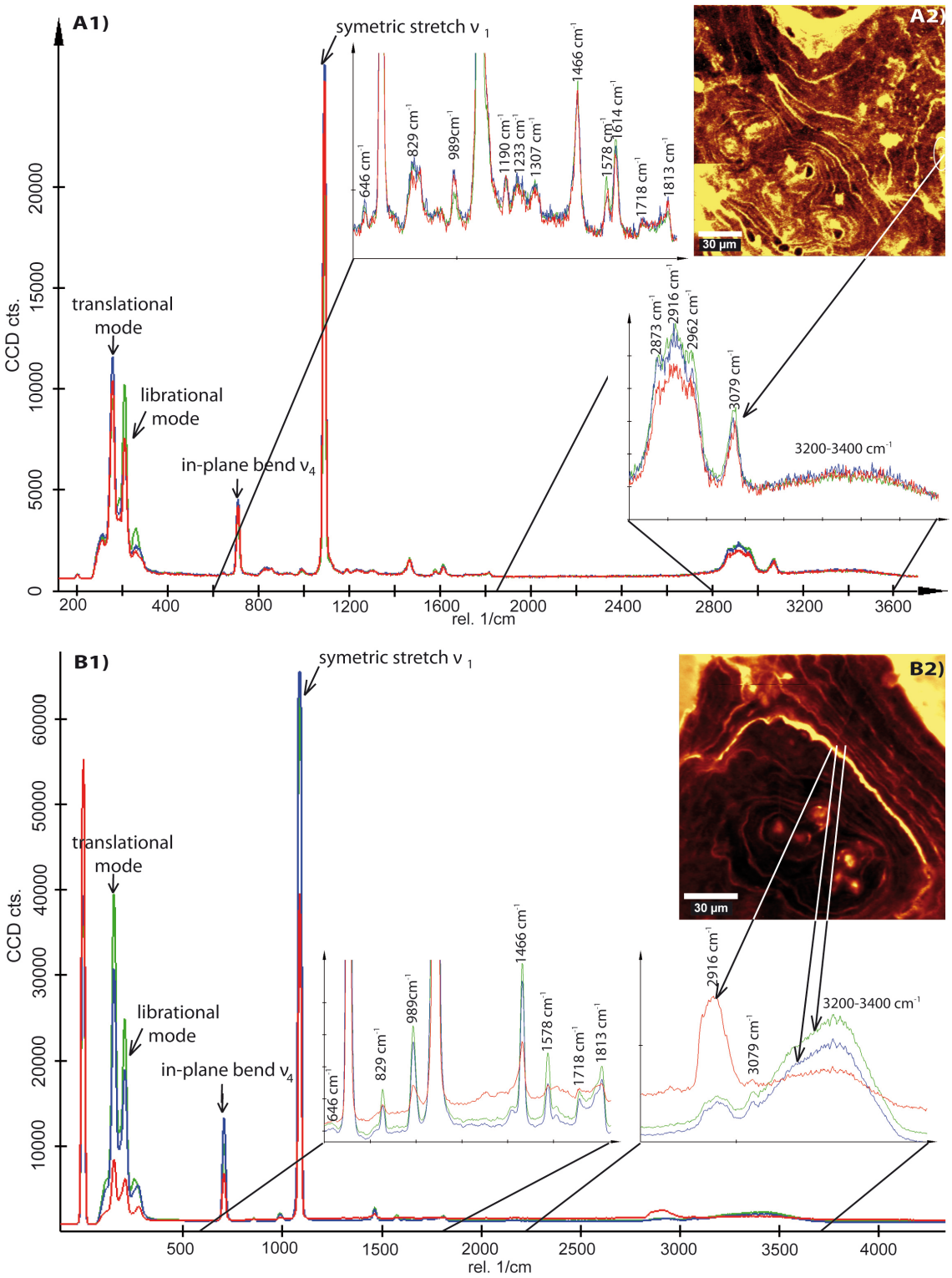

Figure 11: Raman spectral lines. Raman spectra of *Porites lutea* (Milne Edwards and Haime, 1860) skeleton sample (A: #20_29MW_#3, B: #20_29MW_#4) showing the characteristic peaks for aragonite (translational mode at 155 cm^{-1}, librational mode at 208 cm^{-1}, in-plane band at 710 cm^{-1} and symmetric stretch at 1085 cm^{-1}). Regions of minor peaks are zoomed out: 600-1850 cm^{-1} and 2800-3600 cm^{-1}. Raman spectra were obtained after mapping the region marked in the fluorescence map in A2 & B2 with following settings for A1: 532 nm laser wavelength, centered at 2000 cm^{-1}, integration time of 0.5 sec and 10 accumulations, 100x Nikon Objective, Analyzator set 90° to laser wavelength and B1: 488 nm laser wavelength, centered at 2400 cm^{-1}, integration time of 6 sec and 10 accumulations, 100x Nikon Objective. (Raman spectra were derived in different points and displayed by different colors).

et al., 2008, for otholiths; Nehrke & Nouet 2011, for gastropods). Zhang *et al*. (2011) even discussed the potential to retrieve diurnal environmental variability of phosphorus by mapping the intensity distribution of the symmetric P-O stretch. Corals are well known for recording environmental parameters, however, high-resolution analysis revealed some constraints associated with the skeletal structural complexity (e.g. Cuif & Dauphin, 2005b, Juillet-Leclerc *et al*., 2009, Meibom *et al*., 2004, Rollion-Bard *et al*., 2010). Thus, the full capability of CRM to acquire environmental information needs to be further investigated.

4. Conclusions

In the present study we used CRM on *P. lutea* skeleton samples to demonstrated:
(1) that two different types of organic-rich growth lines are present. One of these growth lines corresponds to the well-known incremental growth lines. In contrast, the second type of organic-rich growth lines showed an elemental composition that differs from the incremental growth lines (low Mg concentration).
(2) that mapping by CRM can be used to visualize the differences in crystal orientation, without the necessity to prepare thin sections.
(3) that the layered distribution of organic matrices could be shown and simultaneously related to the orientation of fibers.
(4) that CRM mapping can provide information on skeletal growth patterns by tracking growth lines within a skeletal rod (in the polished plane as well as in depth). Position and shape of the second type of organic-rich growth line (within the text referred to as ORGL 2) resemble either denticle finger-like structure, traces of former spines or previous skeletal surfaces. Thus, we hypothesize that these growth lines are involved in the three-dimensional arrangement of skeletal macro- to micromorphological elements and represent the outer skeletal surface before another cycle of elongation, infilling and thickening of skeletal components continues.
and
(5) that Raman spectra of organic compounds can be measured. The latter represents a powerful possibility in the chemical characterization of organic compounds within coral skeletons.

Hence, high spatial resolution CRM mapping enables the tracking of growth lines over large skeletal areas and relates skeletal entities (EMZ and incremental growth layer) as well as the organic to the mineral phase. This simultaneously obtained information can definitively deepen our understanding of growth patterns in coral skeletons and improve growth concepts above micrometer scale. Organic compounds are hypothesized to play a crucial role in coral biomineralization. Here we detected an organic-rich growth line that potentially regulates coral growth. EMP maps provided a first indication of how to complement CRM studies and added new information. Instruments of high spatial resolution (e.g.

nanoSIMS, or XANES) are crucial in the investigation of biogenic materials but are restricted by the small area that can be mapped. Thus, a combination of these methods with CRM is highly valuable. CRM allows identification of the area of interest prior to measurements by other methods, which are often difficult to access and are cost intensive.

Acknowledgement:

The authors thank Jan Fietzke (Geomar) for the assistance with the EMP measurements. This work was supported by the European Commission through grant 211384 (EU FP7 "EPOCA"), the German Federal Ministry of Education and Research (BMBF, FKZ 03F0608, "BIOACID"), and has received funding from the European Community's Seventh Framework Programme under grant agreement 265103 (Project MedSeA) and the FP7-PEOPLE-2007-1-1-ITN Marie Curie Action: CalMarO (Calcification by Marine Organisms, Grant number: 215157).

References:

Addadi L, Raz S, Weiner S (2003) Taking advantage of disorder: Amorphous calcium carbonate and its roles in biomineralization. *Advanced Materials,* **15**, 959-970.

Adkins JF, Boyle EA, Curry WB, Lutringer A (2003) Stable isotopes in deep-sea corals and a new mechanism for "vital effcts". *Geochimica et Cosmochimica Acta,* **67**, 1129-1143.

Allison N, Finch AA, and Eimf (2010) Δ^{11}B, Sr, Mg and B in a modern *Porites* coral: The relationship between calcification site pH and skeletal chemistry, *Geochimica Cosmochimica Acta*, **74**, 1790-1800.

Allison N, Cohen I, Finch AA, Erez J, and Emif (2011) Controls on Sr/Ca and Mg/Ca in scleractinian corals: The effects of Ca-ATPase and transcellular Ca channels on skeletal chemistry, *Geochimica Cosmochimica Acta*, **75**, 6350-6360.

Barnes DJ (1970) Coral skeletons: an explanation of their growth and structure. *Science,* **170**, 1305-1308.

Barnes DJ, Devereux MJ (1988) Variations in skeletal architecture associated with density banding in the hard coral *Porites*. *Journal of Experimental Marine Biology and Ecology,* **121**, 37-54.

Bischoff WD, Sharma SK, Mackenzie FT (1985) Carbonate ion disorder in synthetic and biogenic magnesian calcites: a Raman spectral study. *American Mineralogist,* **70**, 581-589.

Bryan W, Hill D (1941) Spherulitic crystallization as a mechanism of skeletal growth in the hexacorals. *Proceedings of the Royal Society of Queensland,* **52**, 78-91.

Clode PL, Marshall AT (2002) Low temperature FESEM of the calcifying interface of a scleractinian coral. *Tissue & Cell,* **34**, 187-198.

Cohen AL, McConnaughey T (2003) Geochemical perspectives on coral mineralization. In: *Biomineralization*. (eds Dove PM, Weiner S, De Yoreo JJ) pp 151-187. Reviews in Mineralogy and Geochemistry, Mineralogical Society of America.

Cohen AL, Sohn RA (2004) Tidal modulation of Sr/Ca ratios in a Pacific reef coral. *Geophysical Research Letters,* **31**, L16310.

Cuif J-P, Dauphin Y (1998) Microstructural and physico-chemical characterization of 'centers of calcification' in septa of some recent scleractinian corals. *Paläontologische Zeitschrift,* **72**, 257-270.

Cuif J-P, Dauphin Y and Gautret P (1999) Compositional diversity of soluble mineralizing matrices in some recent coral skeletons compared to fine-scale growth structures of fibres: Discussion of consequences for biomineralization and diagenesis, *International Journal of Earth Sciecne*., **88**, 582-592.

Cuif J-P, Dauphin Y, Doucet J, Salomé M, Susini J (2003) XANES mapping of organic sulfate in three scleractinian coral skeletons. *Geochimica et Cosmochimica Acta,* **67**, 75-83.

Cuif J-P, Dauphin Y, Berthet P, Jegoudez J (2004) Associated water and organic compounds in coral skeletons: quantitative thermogravimetry coupled to infrared absorption spectrometry. *Geochemistry, Geophysics and Geosystems,* **5**, doi:10.1029/2004GC000783.

Cuif J-P, Dauphin Y (2005a) The environment recording unit in coral skeletons - a synthesis of structural and chemical evidences of a biochemically driven stepping-growth process in coral fibres. *Biogeosciences,* **2**, 61-73.

Cuif J-P, Dauphin Y (2005b) The two-step mode of growth in the scleractinian coral skeletons from the micrometer to the overall scale. *Journal of Structural Biology,* **150**, 319-331.

Cuif J-P, Dauphin Y, Sorauf J (2011) *Biominerals and fossils through time,* Cambridge, Cambridge University Press, 490 pp.

Cuif J-P, Dauphin Y, Nehrke G, Nouet J, Perez-Huerta A (2012) Layered growth and crystallization in calcareous biominerals: Impact of structural and chemical evidences on two major concepts in invertebrate biomineralization studies. *Minerals,* **2**, 11-39.

Darwin C (1842) *The structure and distribution of coral reesf,* London, UK, University of California Press.

Dauphin Y, and Cuif J-P (1997) Isoelectric properties of the soluble matrices in relation to the chemical composition of some scleractinian skeletons, *Electrophoresis*, **18**, 1180-1183.

Endo H, Takagi Y, Ozaki N, Kogure T, Watanabe T (2004) A crustacean Ca^{2+}-binding protein with a glutamate-rich sequence promotes $CaCO_3$ crystallization. *Biochemical Journal,* **384**, 159-167.

Finch AA, Allison N (2008) Mg structural state in coral aragonite and implications for the paleoenvironmental proxy. *Geophysical Research Letters,* **35**, L08704, 1-5.

Furla P, Galgani I, Durand I, Allemand D (2000) Sources and mechanisms of inorganic carbon transport for coral calcification and photosynthesis. *The Journal of Experimental Biology,* **203**, 3445-3457.

Gautret P, Cuif J-P and Freiwald A (1997) Composition of soluble mineralizing matrices in zooxanthellate and non-zooxanthellate scleractinian corals: Biochemical assessment of photosynthetic metabolism through the study of a skeletal feature, *Facies*, **36**, 189-194.

Gautret P, Cuif J-P, Stolarski J (2000) Organic components of the skeleton of scleractinian corals - evidence from *in situ* acridine orange staining. *Acta Palaeontologica Polonica,* **45**, 107-118.

Goreau TF (1959) The physiology of skeleton formation in corals. I. A method for measuring the rate of calcium deposition by corals under different conditions. *Biological Bulletin,* **116**, 59-75.

Hild S, Marti O, Ziegler A (2008) Spatial distribution of calcite and amorphous calcium carbonate in the cuticle of the terrestrial crustaceans *Porcellio scaber* and *Armadillidium vulgare*. *Journal of Structural Biology,* **163**, 100-108.

Holcomb M, Cohen AL, Gabitov RI, Hutter JL (2009) Compositional and morphological features of aragonite precipitated experimentally from seawater and biogenically by corals. *Geochimica et Cosmochimica Acta,* **73**, 4166-4179.

Houlbreque F, Meibom A, Cuif J-P *et al*. (2009) Strontium-86 labeling experiments show spatially heterogeneous skeletal formation in the scleractinian coral *Porites porites*. *Geophysical Research Letters,* **36**, L04604, 1-5.

Jolivet A, Bardeau JF, Fablet R, Paulet YM, DE Pontual H (2008) Understanding otolith biomineralization processes: new insights into microscale spatial distribution of organic and mineral fractions from Raman microspectrometry. *Analytical and Bioanalytical Chemistry,* **392**, 551-560.

Juillet-Leclerc A, Reynaud S, Rollion-Bard C *et al*. (2009) Oxygen isotopic signature of the skeletal microstructures in cultured corals: Identification of vital effects. *Geochimica et Cosmochimica Acta,* **73**, 5320-5332.

Kaczorowska B, Hacura A, Kupka T, Wrzalik R, Talik E, Pasterny G, Matuszewska A (2003) Spectroscopic characterization of natural corals. *Analytical and Bioanalytical Chemistry,* **377**, 1032-1037.

Knutson DW, Buddemeier RW, Smith SV (1972) Coral chronometers: seasonal growth bands in reef corals. *Science,* **177**, 270-272.

Lough JM, Barnes DJ (2000) Environmental controls on growth of the masisve coral *Porites*. *Journal of Experimental Marine Biology and Ecology,* **245**, 225-243.

Marin F, Smith M, Isa Y, Muyzer G, Westbroek P (1996) Skeletal matrices, muci, and the origin of invertebrate calcification. *Proceedings of the National Academy of Sciences of the United States of America,* **93**, 1554-1559.

Meibom A, Stage M, Wooden J *et al*. (2003) Monthly Strontium/Calcium oscillations in symbiotic coral aragonite: Biological effects limiting the precision of the paleotemperature proxy. *Geophysical Research Letters,* **30**, 1418.

Meibom A, Cuif J-P, Hillion FO *et al*. (2004) Distribution of magnesium in coral skeleton. *Geophysical Research Letters,* **31**.

Meibom A, Mostefaoui S, Cuif J-P, Dauphin Y, Houlbreque F, Dunbar R, Constantz B (2007) Biological forcing controls the chemistry of reef-building coral skeleton. *Geophysical Research Letters,* **34**, 1-5.

Meibom A, Cuif J-P, Houlbreque F, Mostefaoui S, Dauphin Y, Meibom KL, Dunbar R (2008) Compositional variations at ultra-structure length scales in coral skeleton, *Geochimica Cosmochimica Acta*, **72**, 1555-1569, 2008.

Nehrke G, Nouet J (2011) Confocal Raman microscope mapping as a tool to describe different mineral and organic phases at high spatial resolution within marine biogenic carbonates: case study on *Nerita undata* (Gastropoda, Neritopsina). *Biogeosciences,* **8**, 3761-3769.

Nehrke G, Poigner H, Wilhelms-Dick D, Brey T, Abele D (2012) Coexistence of three calcium carbonate polymorphs in the shell of the Antarctic clam *Laternula elliptica*. *Geochemistry Geophysics Geosystems,* **13**, Q05014.

Neues F, Hild S, Epple M, Marti O, Ziegler A (2011) Amorphous and crystalline calcium carbonate distribution in the tergite cuticle of moulting *Porcellio scaber* (Isopoda, Crustacea). *Journal of Structural Biology,* **175**, 10-20.

Nothdurft LD, Webb GE (2007) Microstructure of common reef-building coral genera *Acropora*, *Pocillopora*, *Goniastrea* and *Porites*: constraints on spatial resolution in geochemical sampling. *Facies,* **53**, 1-26.

Ogilvie M (1896) Microscopic and systematic study of Madreporarian types of corals. *Philosophical Transactions of the Royal Society of London,* **187**, 83-187.

Perrin C, Smith DC (2007) Earliest steps of diagenesis in living scleractinian corals: evidence from ultrastructural pattern and Raman spectroscopy. *Journal of Sedimentary Research,* **77**, 495-507.

Pratz E (1882) Über die verwandtschaftlichen Beziehungen einiger Korallengattungen mit hauptsächlicher Berücksichtigung ihrer Septalstruktur. *Palaeontographica,* **29**, 81-122.

Puverel S, Tambutte E, Zoccola D *et al*. (2005) Antibodies against the organic matrix in scleractinians: a new tool to study coral biomineralization. *Coral Reefs,* **24**, 149-156.

Rollion-Bard C, Chaussidon M, France-Lanord C (2003) pH control on oxygen isotopic composition of symbiotic corals. *Earth and Planetary Science Letters,* **215**, 275-288.

Rollion-Bard C, Blamart D, Cuif J-P, Dauphin Y (2010) *In situ* measurements of oxygen isotopic composition in deep-sea coral, *Lophelia pertusa*: Re-examination of the current geochemical models of biomineralization. *Geochimica et Cosmochimica Acta,* **74**, 1338-1349.

Sorauf J (1972) Skeletal microstructure and microarchitecture in scleractinian (Coelenterata). *Palaeontology,* **15**, 88-107.

Sorauf J, Jell JS (1977) Structure and incremental growth in the ahermatypic coral *Desmophyllum cristagalli* from the north Atlantic. *Palaeontology,* **20**, 1-19.

Stolarski J (2003) Three-dimensional micro- and nanostructural characteristics of scleractinian coral skeleton: A biocalcification proxy. *Acta Palaeontologica Polonica,* **48**, 497-530.

Stolarski J, Mazur M (2005) Nanostructure of biogenic versus abiogenic calcium carbonate crystals. *Acta Palaeontologica Polonica,* **50**, 847-865.

Tambutte E, Allemand D, Zoccola D, Meibom A, Lotto S, Caminiti N, Tambutte S (2007) Observations of the tissue-skeleton interface in the scleractinian coral *Stylophora pistillata*. *Coral Reefs,* **26**, 517-529.

Tambutté S, Holcomb M, Ferrier-Pagès C, Reynaud S, Tambutté E, Zoccola D, Allemand D (2011) Coral biomineralization: From the gene to the environment. *Journal of Experimental Marine Biology and Ecology*, doi:10.10166/j.jembe.12011.10107.10026.

Thebault J, Chauvaud L, Clavier J, Fichez R, Morize E (2006) Evidence of a 2-day periodicity of striae formation in the tropical scallop *Comptopallium radula* using calcein marking. *Marine Biology,* **149**, 257-267.

Urmos J, Sharma SK, Mackenzie FT (1991) Characterization of some biogenic carbonates with Raman-spectroscopy. *American Mineralogist,* **76**, 641-646.

Veron JEN (2000) *Corals of the World*. *Volume 1,* Townsville, Australian Institute of Marine Science.

Watanabe T, Fukuda I, China K, Isa Y (2003) Molecular analyses of protein components of the organic matrix in the exoskeleton of two scleractinian coral species. *Comparative Biochemistry and Physiology B-Biochemistry & Molecular Biology,* **136**, 767-774.

Waite J, Andersen O (1980) 3,4-dihydroxyphenylalanine (DOPA) and sclerotization of periostracum in *Mytilus edulis* L. *Biological Bulletin,* **158**, 164-173.

Wheeler AP, Sikes CS (1984) Regulation of carbonate calcification by organic matrix. *American Zoologist,* **24**, 933-944.

Young S (1971) Organic material from scleractinian coral skeletons -I. variation in composition between several species. *Comparative Biochemistry and Physiology, Part B: Biochemistry and Molecular Biology,* **40**, 113-120.

Zhang F, Cai W, Sun Z, Zhang J (2008) R egular variations in organic matrix composition of small yellow croaker (*Pseudociaena polyactis*) otoliths: an *in situ* Raman microspectroscopy and mapping study. *Analytical and Bioanalytical Chemistry,* **390**, 777-782.

Zhang FF, Cai WY, Zhu JC, Sun ZR, Zhang J (2011) *In situ* Raman spectral mapping study on the microscale fibers in Blue Coral (*Heliopora coerulea*) skeletons. *Analytical Chemistry,* **83**, 7870-7875.

3. SYNTHESIS

Question 1:

Is the impact and intensity of large amplitude internal waves on shallow reef areas related to the distance of these areas to the shelf break?

Q: This question follows up a previous investigation (Schmidt *et al*., 2012) by expanding the study area and addressing the extent and characteristics of environmental variability due to LAIW on several islands on the continental shelf. Moreover, the correlation of LAIW intensity to distance to the shelf break will be tested. → **2.1 Manuscript I**

A: NO: LAIW impact shallow reef areas at different locations on the shelf, however, LAIW intensity does not represent a function of the distance to the shelf break. Temperature drops correlate with concomitantly measured changes in salinity, pH and oxygen at both the most distant and closest sites to the shelf break. This suggests that temperature plunges originate from diapycnal mixing.

The temperature record revealed that LAIW induced cold-water pulses occurred at all west-facing islands sites but differed in their intensity. The concomitant changes of salinity, oxygen and pH with temperature showed a strong correlation indicating the origin of the cold-water masses from diapycnal mixing. Observational and modeling work had shown that LAIW might advance onto the continental shelf (Helfrich, 1992, Vlasenko & Huttner, 2002, Vlasenko & Stashchuk 2007) and propagate shoreward as trapped cores (Klymak & Moum, 2003). Interestingly, the degree of variability observed at our study sites did not relate to cross-shelf distance from the shelf break. Modeling studies have shown that bottom topography can result in refraction and focusing of LAIW wave energy (Vlasenko & Stashchuk, 2007). Although, the fine-scale bathymetry of the Thai shelf and continental slope is largely unknown, underwater features such as mounds or canyons at or near the shelf break (Vlasenko & Stashchuk, 2007) may account for the observed differences in temperature anomaly intensities between our sites.

The observations are consistent with available models near the Andaman Sea shelf break suggesting that the pronounced temperature anomalies in the study area are due to LAIW (Vlasenko & Stashchuk, 2007).

Question 2:

What are the main driving force of reef development on LAIW and southwest (SW) monsoon exposed reefs?

Q: Is LAIW intensity reflected in the reef accretion potential at intermediate depth reefs along an anticipated cross-shelf LAIW gradient or do other processes govern reef development? → **2.1 Manuscript I**

A: Yes, LAIW intensity partially accounts for the observed reef framework height at the study depth but SW monsoon induced currents and changes in hydrodynamic conditions also act at this depth and the combined effect of LAIW and SW monsoon water motion best explained the reef framework height at the study depth (97 %).

A previous study on the coral community composition of the Similan Islands has shown a pronounced difference in reef framework development between the LAIW and SW monsoon sheltered east (E) and the LAIW and SW monsoon exposed west (W) sides of the islands (Schmidt *et al*., 2012). However, the limited geographical extent and lack of angular resolution between the 2 potential disturbances (both acting from the same westerly direction) did not resolve the relative contributions of monsoon and LAIW to the observed patterns. Differences in reef framework height were determined from scaled images (Fig. 3.1) and revealed differences between exposed W and sheltered E island sites.

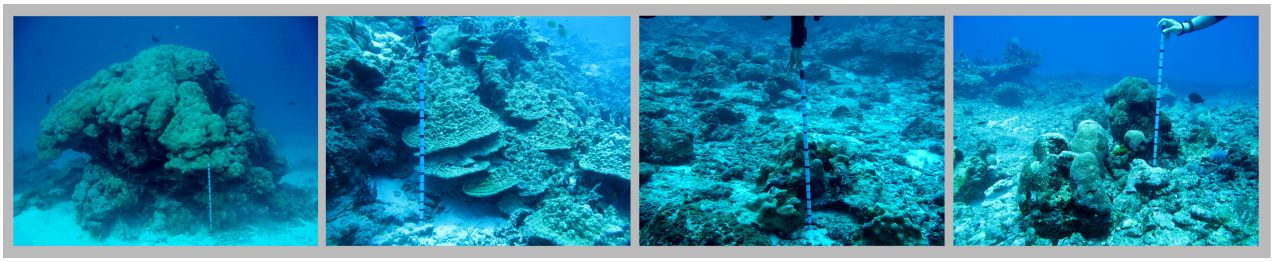

Figure 3.1: Reef framework development potential at different sites. From left to right reef framework height decreased with increasing LAIW intensity (Tachai east, Similan east, Miang west and Similan west).

Environmental proxy values were used to disentangle confounding effects and relate them to reef framework height. The results indicate that both LAIW intensity and grain size distribution (a proxy for hydrodynamic conditions at site) best explained the reef framework height. Sedimentation rate that clearly showed a monsoon signal did not correlate with reef framework height. Temperature variability showed a clear correlation with reef framework height explaining a high percentage of the variability in framework development (77 %, $p = 0.004$). These findings suggest that LAIW-induced diapycnal mixing undermines reef development. Similarly, Benzoni *et al.* (2003) found a positive relationship between framework development and distance to upwelling region in the Gulf of Aden. The reduction in coral cover to single scattered colonies described by Sheppard and Salm (1988) and Glynn (1993) for the Oman reefs is similar to the community structure observed for the Similan Islands W sides (Schmidt *et al.*, 2012). Temperature anomalies and sediment grain size correlations suggest a combined impact of LAIW and monsoon at the intermediate depth. LAIW intensity increased and SW monsoon decreased with depth, resulting in their strongest impact in the deeper and shallower parts of the reef, respectively. The W reefs of the Similan Islands showed a coral community consisting of single isolated coral colonies with reduced framework height in 20 m water depth (Schmidt *et al.*, 2012). In contrast, at E 20 m reef framework height equaled the intermediate depth. The observed relationship with LAIW intensity

supports the decreased framework height in 20 m as LAIW intensity increases with depth (Schmidt *et al.*, 2012). Hence, LAIW impact prevents a vertical extension of the framework as well as a lateral expansion of a dense coral community below the storm-accretion limit into deeper areas while SW monsoon forcing can explain the reduced reef framework in shallower zones.

Question 3:

Can LAIW sites act as refuge areas in the light of increasingly frequent bleaching events? and how do differences in coral community composition affect the bleaching response?

Q: The question is can LAIW cold-water pulses abate heating and mitigate the bleaching response. In 2010 a severe bleaching event occurred in the Andaman Sea and provided an opportunity to monitor the bleaching response and the temperature development at various sites of differential LAIW intensities. Differences in bleaching response might derive from differences in heating and cooling but also from differences in coral community composition. To account for these confounding effects differences in community bleaching susceptibility are going to be assessed. → **2.2 Manuscript II**

A: YES, LAIW induced cold-water pulses were able to abate heating and mitigate the bleaching response. The study sites differed in the intensity of cooling and the observed bleaching response was a function of the cooling intensity. Thus, W sites can serve as refuge area from thermal stress. A multiple linear model best explained the bleaching response with site-specific coral community bleaching susceptibility and cumulative temperature exposure time as explanatory variables.

Here we confirmed the hypothesis proposed by Sheppard (2009) who monitored large temperature drops at the Diego Garcia Atoll in the Indian Ocean and hypothesized a potential cooling function during heat stress. The bleaching investigation in the Andaman Sea was the first of its kind where internal wave cooling during heat stress was monitored. The study showed the potential to abate heating and mitigate bleaching. Internal waves are ubiquitous in the world oceans and, hence, this cooling function can be of relevance to other coral reef ecosystems.

The temperature record revealed that LAIW induced cold-water pulses prevailed during the heat stress. LAIW intensity differed between sites and was reflected in a gradual increase in bleaching response (expressed as bleaching and mortality index) with decreased cooling intensity. Differences in bleaching response were most apparent when comparing opposite island sides of the most exposed reefs with stronger bleaching in E than in W (Fig. 3.2). Additionally, turbulent mixing due to SW monsoon winds and waves moderated heating at the exposed sites.

Community composition determined a site-specific bleaching susceptibility. Together with cumulative heat stress it explained 75 % of the observed bleaching response. The heat stress exceeded the stress limit

of highly susceptible taxa and they only survived in small numbers at the LAIW exposed western sites. Hence, the duration of the bleaching event was most critical for these taxa. The recovery of remnant living corals was not completed half a year later after the heat anomaly and was not faster at the exposed western sites. Sedimentation stress due to the SW monsoon for only the exposed sites potentially accounted for this pattern. The community composition shifted to more heat tolerant species whereas susceptible species almost vanished at the sheltered islands sides. Further monitoring is needed into whether the exposed western island sites can provide propagules of susceptible species for the sheltered sites and support their recovery and/or resettlement.

Figure 3.2: Bleaching response at opposite islands sites of Miang. Left image indicated the strong bleaching response with complete white coral colonies in Miang East while at Miang W (right image) coral showed normal or pale pigmentation during the same sampling time and at the same depth.

Under a climate change scenario with bleaching events increasing in frequency and intensity (Donner *et al*., 2005) these results would suggest a phase-shift to a more heat tolerant community composition and the elimination of sensitive species at LAIW-sheltered sites. The survival of sensitive species on the west sides was limited to the most LAIW-exposed sites and critically depends on the their ability to regenerate and recover to the prior coverage numbers after such events before another bleaching event occurs.

Question 4:

Can large amplitude internal wave intensity be recognized at the skeletal level by studying growth characteristics such as skeletal density and linear extension rates?

Q: Is environmental variability due to both LAIW and SW monsoon reflected in skeleton density, linear extension rate and calcification rate? Scoffin *et al.* (1992) described an inshore offshore gradient in skeletal properties in the Andaman Sea – showing a decrease in extension rate and an increase in density with distance to the mainland. The present study tested whether differences in

skeletal properties exist between several offshore islands and if such differences were related to environmental conditions monitored at the different sites or simply represent a function of the distance to the shore. → **2.3 Manuscript III**

A: This question cannot be clearly answered. Skeletal density differed between the protected E site and all other sites. Difference in density between Miang E and W was marginally non-significant. A trend was observed that density varied with LAIW intensity but no relationship was observed with distance to the shore.

An inverse relationship was found for density with distance to the shore (Risk & Sammarco 1991, Lough & Barnes 1992, Scoffin *et al*., 1992). Scoffin *et al*. (1992) attributed this change to an increase in hydraulic energy. Density similar to extension rate did not vary with distance to the shore in the present study but a trend emerged of an increase in density with increasing LAIW cooling. In contrast to Scoffin *et al*. (1992) the corals in the present study derived from deeper depth (15 m instead of 1 m). While in shallow areas surface gravity waves are expected to provide the main hydraulic impact the corals in our study corals are subjected to LAIW impact that potentially was responsible for the observed trend.

However, further studies are required to confirm this trend of a positive relationship of density with LAIW cooling intensity. LAIW impact was shown to increase with depth (Schmidt *et al*., 2012). Hence, future studies should emphasize a refined sampling along the natural environmental gradient and in different depth zones.

Question 5:

Can large amplitude internal wave temperature fluctuations be recognized at the skeletal level by analyzing temperature proxies?

Q: This question addressed whether or not high temperature variability due to LAIW is reflected at the skeletal level when analyzing skeletal proxies. Skeletal thermometry has been applied since the early 20th century and advances in instrumentation allow refined analyses. Knowledge gaps remain concerning the biological effects of trace element inclusions. Studying sites with strong environmental fluctuations can potentially provide new insight into skeletal recording and its constraints. → **2.4 Manuscript IV**

A: NO. Preliminary results suggest that skeletal proxies do not resolve the high variability in the LAIW-exposed west site. Only one east coral proxy data reflected the seasonal temperature variation. An inclusion of growth rate into the analysis potentially helps to identify seasonal differences.

The Sr/Ca ratios of both E and W samples were lower than might have been expected from other studies with similar monthly temperature ranges (Allison 1996, Meibom *et al*., 2003, Cohen & Sohn

2004) and insignificantly higher in W compared to E despite the significantly lower monthly mean temperatures especially during the NE monsoon periods (January through March). The preliminary results on the Sr/Ca ratios indicate a high variability with no detectable (a) similarities within skeletal records of the same island sides and (b) differences according to the temperature records between E and W samples. An inclusion of the different growth rates of the single samples into the analyses might help to detect possible accordances within or differences between island sides. A seasonal temperature signal has so far only been detected in one of the E samples. The sub-daily temperature plunges were not found to be resolved in the Sr/Ca data of the W samples despite the high measurement resolution.

In accordance with other studies (Weber 1973, de Villiers *et al.,* 1995, Meibom *et al.,* 2003) the preliminary results suggest that biological processes that influence the calcification process mask the recording potential of corals at daily to sub-daily scales.

Question 6:

Can confocal Raman mapping shed light on coral growth patterns and what are the implications for high-resolution proxy studies?

Q: This question addressed if improved (in spectral and spatial resolution) old tools can provide new insight into microstructural growth patterns and cyclicity. A better understanding of coral growth patterns is desirable in order to improve the interpretation of high-resolution proxy data. → **2.5 Manuscript V**

A: YES, coral skeleton analyses with Raman spectroscopy definitively improve the understanding of growth patterns in corals. Raman mapping can be applied (1) to trace growth lines that reflect skeleton that was accreted at the same time and (2) to identify specific areas for high-resolution proxy analyses that help to disentangle biological and environmental forcing on trace element inclusion.

Taylor *et al*. (1995) stated: "Recent increase in the number of reports on the inclusive records relative to the total number of reports on coral banding suggests that attemps to extract palaeoclimatic records from corals is being undertaken at the expense of developing the necessary understanding of skeletal growth mechanisms." Several growth models have been developed since then (Cuif & Dauphin, 1998, Cuif & Dauphin, 2005a, Meibom *et al*., 2008) but they still lack a full understanding of growth patterns at micrometer scale even though proxy sampling are and can be perfomed at this scale and even higher (Allison, 1996, Meibom *et al*., 2007). Nothdurft and Webb (2007) concentrated on microstructural arrangments of skeletal fibers and crystals to illustrate the high diversity between genera. The authors highlighted the temporal differences in formation of skeletal regions that differ between genus. By tracing growth lines (Figure 3.3C) and fiber arrangment Nothdurft and Webb (2007) could show that following

such lines helps to improve proxy sampling. However, the usual sample treatment - to make growth lines visible - involves etching of sample surface at the expense of that follow up trace element or istope analyses not be possible on the same sample surface. Here we continued their study by applying Raman mapping on a coral genus most commonly used in palaeo-studies. We could show that Raman spectroscopy is a powerful tool that allows tracing of growth lines and identifying growth limits without special prior sample treatment. Confocal Raman mapping enables use of the same sample surface for other high-resolution analyses such as SIMS, XANES or NanoSIMS.

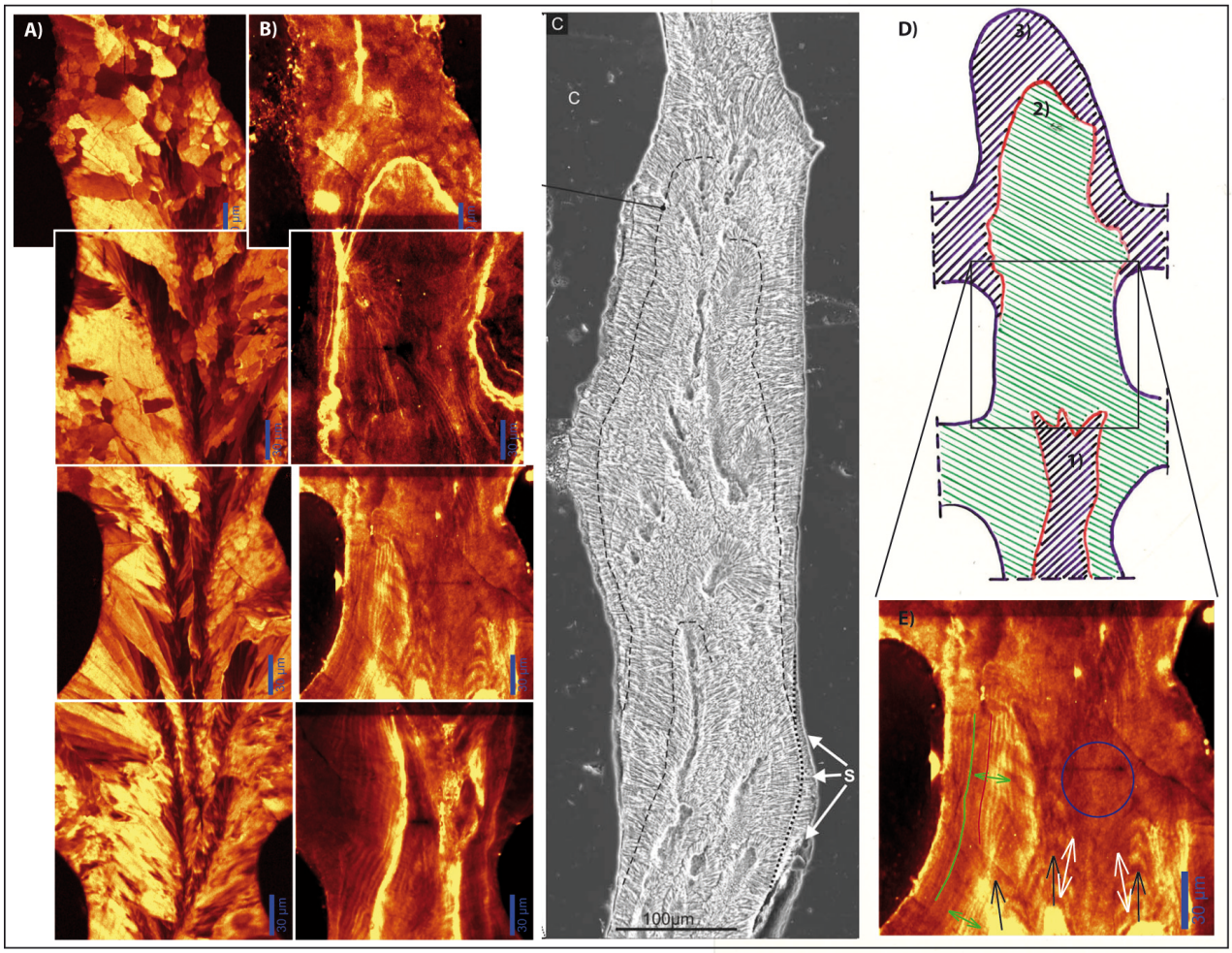

Figure 3.3: Comparison of Raman maps with an etched SEM image of a longitudinal skeletal surface and model of skeletal growth. A-B) Raman map of fiber orientation (A) and the fluorescence intensity distribution of the same area (B) in *Porites lutea*. C) The high fluorescence lines in B assemble the growth lines traced in *Porites lobata* by Nothdurft and Webb (modified after Nothdurft & Webb 2007) D) Schematic image of cyclicity in growth representing three cycles each ending with a high fluorescence growth line (red line), which corresponds to an approx. 12-14 day periodicity. E) During each cycle different growth modes are suggested: vertical extension (black and white arrows), thickening of skeletal element (green arrows) and both vertical extension and thickening are potentially associated with different growth rates. Blue circle marks an area of no clearly visible banding pattern where the skeleton was potentially sectioned parallel to the position of the growth layer.

The growth lines visualized by fluorescence mapping (Fig. 3.3B) clearly reflect that calcification is not a continous and regular process. However, the periodic repeated appearance of the high fluorescence growth lines (Figure 3.3B) suggests some kind of cyclicity. Cyclicity represents a ubiquitous characteristic of coral skeletal formation. The described cycles range from the cm-level displayed by

seasonal density bands (e.g. Knutson *et al.,* 1972) down to the µm-level of daily/sub-daily formation of incremental growth layers (e.g. Meibom *et al.,* 2007). The temporal units 1-3 in Fig. 3.3D represent different growth cycles with 1 being the oldest and 3 the youngest deposited skeleton. Each growth cycle lasts about two weeks and ends with a high fluorescence line. Within this biweekly cycle elongation, infilling between spine tips and thickening of macromorphological elements takes place (Fig. 3.3E). This periodicity in growth agrees with the growth model proposed by Nothdurft and Webb (2007). They traced a growth band in their study (Nothdurft & Webb 2007; their Fig. 16 C & 17 B) that resembles the high fluorescence growth lines described in Manuscript V with a similar longitudinal extension spanning approx. 12 days of growth.

Confocal Raman mapping is a highly valuable diagnostic tool, which enables tracing of growth lines over large skeletal areas and a relation of skeletal entities (EMZ and incremental growth layer) to both the organic and the mineral phases. This simultaneously obtained information definitively deepens our understanding of growth patterns in coral skeletons and improves growth concepts above micrometer scale.

BOX 7: Key findings

- A relationship was found between large amplitude internal waves (LAIW) intensity and reef framework height development in the Andaman Sea, Thailand. This observation suggests that LAIW entail negative effects that inhibit reef formation. LAIW intensity increases with depth and thus, prevents reef extension in deeper regions. This agrees with findings in upwelling regions were coral reefs are reduced to single scattered colonies the closer they are to upwelling regions.

- The bleaching response to the 2010 thermal stress differed markedly between sites and in particular between opposite island sides. The LAIW and SW monsoon exposed western island sites showed reduced bleaching intensity in contrast to the sheltered east island sites. The variability in bleaching response was explained by differences in cooling and coral community bleaching susceptibility. These findings suggest that LAIW exposed sites provided protection from heat stress and mitigated bleaching. Therefore, LAIW exposed sites can potentially serve as refuge areas during times of heat stress.

- Skeletal properties examined at several offshore islands showed that skeletal density differed between sites and was higher at the investigated offshore islands than the global average. In contrast, the extension rate were not statistically different between sites but lower than the global average values. Preliminary results indicated that density increases with increasing LAIW intensity.

- Preliminary results suggest that skeletal proxies do not resolve the high variability in LAIW exposed west sites. An inclusion of growth rate into the analysis potentially helps to identify seasonal differences and probably differences between LAIW-intense and LAIW-weak seasons. Nevertheless, the preliminary findings imply that biological processes that influence the calcification process mask the recording potential of corals at daily to sub-daily scales.

- High-resolution proxy analyses emphasized the need for a better understanding of spatial variability in skeletal growth to improve proxy sampling. Raman spectroscopy provided new insights into coral growth patterns by tracing individual growth lines. It enables visualization of growth lines without chemically altering the sample surface. This allows follow up analyses such as trace element mapping. Linking growth lines and skeletal entities - centers of calcification and fibers - with trace element concentration can deepen our understanding of skeletal formation and help to shed light on the relative influences of the environment and ‘vital effects‘.

4. BIBLIOGRAPHY

Achituv Y, Dubinsky Z (1990) *Evolution and zoogeography of coral reefs,* In: *Coral Reefs. Ecosystems of the world,* (ed Dubsinky, Z) pp 1-9, Amsterdam, PAYS-BAS, Elsevier.

Addadi L, Raz S, Weiner S (2003) Taking advantage of disorder: Amorphous calcium carbonate and its roles in biomineralization. *Advanced Materials,* **15**, 959-970.

Adkins JF, Boyle EA, Curry WB, Lutringer A (2003) Stable isotopes in deep-sea corals and a new mechanism for "vital effcts". *Geochimica et Cosmochimica Acta,* **67**, 1129-1143.

Al-Horani FA, Ferdelman T, Al-Moghrabi SM, De Beer D (2005) Spatial distribution of calcification and photosynthesis in the scleractinian coral *Galaxea fascicularis*. *Coral Reefs,* **24**, 173-180.

Alibert C, McCulloch MT (1997) Strontium/calcium ratios in modern *Porites* corals from the Great Barrier Reef as a proxy for sea surface temperature: calibration of the thermometer and monitoring the ENSO. *Paleoceanography*, **12**, 345-363.

Allemand D, Tambutté É, Zoccola D, Tambutté S (2011) Coral Calcification, Cells to Reefs. In: *Coral Reefs: An Ecosystem in Transition*. (eds Dubinsky Z, Stambler N) pp 119-150. Springer Netherlands.

Allen GR, Stone GS (2005) Rapid assessment survey of tsunami-affected reefs of Thailand. Final Technical Report. Nov 15, 2005. pp 124.

Allison N (1996) Comparative determinations of trace and minor elements in coral aragonite by ion microprobe analysis, with preliminary results from Phuket, southern Thailand. *Geochimica et Cosmochimica Acta,* **60**, 3457-3470.

Allison N, Finch AA (2007) High temporal resolution Mg/Ca and Ba/Ca records in modern Porites lobata corals. *Geochemistry, Geophysics and Geosystems,* **8**, Q05001, doi:05010.01029/02006GC001477.

Allison N, Finch AA, and Eimf (2010) Δ^{11}b, sr, mg and b in a modern *porites* coral: The relationship between calcification site ph and skeletal chemistry, *Geochimica Cosmochimica Acta*, **74**, 1790-1800.

Allison N, Cohen I, Finch AA, Erez J, and Emif (2011) Controls on Sr/Ca and Mg/Ca in scleractinian corals: The effects of Ca-ATPase and transcellular ca channels on skeletal chemistry, *Geochimica Cosmochimica Acta*, **75**, 6350-6360.

Alpers W, Vlasenko V (2002) Study of secondary internal wave generation by the interaction of an internal solitary wave with an underwater bank by using ERS SAR imagery and a numerical model.

Anthony KRN, Kline DI, Diaz-Pulido G, Dove S, Hoegh-Guldberg O (2008) Ocean acidification causes bleaching and productivity loss in coral reef builders. *Proceeding of the National Academic Science of the United States of America,* **105**, 17442-17446.

Apel JR, Holbrook JR, Liu AK, Tsai JJ (1985) The Sulu Sea internal soliton experiment. *Journal of Physical Oceanography,* **15**, 1625-1985.

Baird AH, Bhagooli R, Ralph PJ, Takahashi S (2009) Coral bleaching: the role of the host. *Trends in Ecology and Evolution,* **24**, 16-20.

Bak RPM, Meester EH (2000) Acclimatization/adaptation of coral reefs in a marginal environment. In: *Proc. 9th Int Coral Reef Symp*. pp 265-272. Proc. 9th Int Coral Reef Symp, Bali, Indonesia.

Baker PA, Weber JN (1975) Coral growth rate: Variation with depth. *Physics of the Earth and Planetary Interiors,* **10**, 135-139.

Baker AC (2001) Reef corals bleach to survive change. *Nature,* **411**, 765-766.

Baker AC, Glynn PW, Riegl B (2008) Climate change cand coral reef bleaching: An ecological assessment of long-term impacts, recovery trends and future outlook. *Estuarine, Coastal and Shelf Science,* **80**, 435-471.

Barnes DJ (1970) Coral skeletons: an explanation of their growth and structure. *Science,* **170**, 1305-1308.

Barnes DJ (1972) The Structure and Formation of Growth-Ridges in Scleractinian Coral Skeletons. *Proceedings of the Royal Society of London. Series B: Biological Sciences,* **182**, 331-350.

Barnes DJ, Devereux MJ (1988) Variations in skeletal architecture associated with density banding in the hard coral *Porites*. *Journal of Experimental Marine Biology and Ecology,* **121**, 37-54.

Barnes DJ, Lough JM (1996) Coral skeletons: storage and recovery of environmental information. *Global Change Biology,* **2**, 569-582.

Barnes DJ, Lough JM (1999) Porites growth characteristics in a changed environment: Misima Island, Papua New Guinea. *Coral Reefs,* **18**, 213-218.

Becerro MA, Bonito V, Paul VJ (2006) Effects of monsoon-driven wave action on coral reefs of Guam and implications fro coral recruitment. *Coral Reefs,* **25**, 193-199.

Beck JW, Récy J, Tylor F, Edwards RL, Cabloch G (1997) Abrupt changes in early Holocene tropical sea surface temperature derived from coral records. *Nature*, **385**, 705-707.

Behera S, Luo J, Yamagata T (2008) Unusual IOD event in 2007. *Geophysical Research Letters,* **35**, doi: 10.1029/2008GL034122.

Bell N, Smith J (1999) Coral growing on the North Sea oil rigs. *Nature,* **402**, 601.

Benzoni F, Bianchi CN, Morri C (2003) Coral communities of the northwestern Gulf of Aden (Yemen): variation in framework building related to environmental factors and biotic conditions. *Coral Reefs,* **22**, 475-484.

Berkelmans R (2009) Bleaching and mortality thresholds: How much is too much? In: *Coral bleaching - Patterns, processes, causes and consequences*. (eds van Oppen MJH, Lough JM) pp 103-119. Heidelberg, Germany, Springer.

Berkelmans R, De'ath G, Kininmonth S, Skirving W (2004) A comparison of the 1998 and 2002 coral bleaching events on the Great Barrier Reef: spatial correlation, patterns, and predictions. *Coral Reefs,* **23**, 74-83.

Berkelmans R, van Oppen MJH (2006) The role of zooxanthellae in the thermal tolerance of corals: a "nuggest of hope" for coral reefs in an era of climate change. *Proceedings of the Royal Society B: Biological Sciences,* **273**, 2305-2312.

Blanchon P, Jones B (1995) Marine-planation terraces on the shelf around Grand Cayman: a result of stepped Holocene sea-level rise. *Journal of Coastal Research,* **11**.

Bothner MH, Reynolds RL, Casso MA, Storlazzi CD, Field ME (2006) Quantity, composition and source of sediment collected in sediment traps along the fringing coral reef off Molokai, Hawaii. *Marine Pollution Bulletin,* **52**, 1034-1047.

Brown BE (2007) Coral reefs of the Andaman Sea - an integrated perspective. *Oceanography and marine biology: an annual review,* **45**, 173-194.

Brown BE, Howard LS (1985) Assessing the effects of "stress" on reef corals. In: *Advances in Marine Biology*. (eds Blaxter Jhs, Russell Fs, Yonge M) pp 1-63. London, Academic Press Inc. Ltd.

Brown BE, Dunne RP, Chansang H (1996) Coral bleaching relative to elevated sewater temperature in the Andaman Sea (Indian Ocean) over the last 50 years. *Coral Reefs,* **15**, 151-152.

Brown BE, Dunne RP, Goodson MS, Douglas AE (2002) Experience shapes the susceptibility of a reef coral to bleaching. *Coral Reefs,* **21**, 119-126.

Brown BE, Crossins A (2011) The potential for temperature acclimatisation of reef corals in the face of climate change. In: *Coral reefs: an ecosystem in transition*. (eds Dubinsky Z, Stambler N) pp 421-434. Heidelberg, Springer.

Brown BE, Phongsuwan N (2012) Delayed mortality in bleaced massive corals on the intertidal reef flats around Phuket, Andaman Sea, Thailand. *Phuket Marine Biological Center Research Bulletin,* **71**, 43-48.

Bruno JF, Selig ER, Casey KS *et al*. (2007) Thermal Stress and Coral Cover as Drivers of Coral Disease Outbreaks. *PLoS Biol,* **5**, e124.

Bruno JF, Sweatman H, Precht WF, Selig ER, Schutte VGW (2009) Assessing evidence of phase shifts from coral to macroalgal dominance on coral reefs. *Ecology,* **90**, 1478-1484.

Bryan W, Hill D (1941) Spherulitic crystallization as a mechanism of skeletal growth in the hexacorals. *Proceedings of the Royal Society of Queensland,* **52**, 78-91.

Buddemeier RW, Maragos JE, Knutson DW (1974) Radiographic studies of reef coral exoskeletons: Rates and patterns of coral growth. *Journal of Experimental Marine Biology and Ecology,* **14**, 179-199.

Buranapratheprat A, Laongmanee P, Sukramongkol N, Prommas R, Promjinda S, Yanagi T (2010) Upwelling induced by meso-scale cyclonic eddies in the Andaman Sea. *Coastal Marine Science,* **34**, 68-73.

Caldeira K, Wickett ME (2005) Ocean models predictions of chemistry changes from carbon dioxide emission to the atmosphere and ocean. *Journal of Geophysical Research,* **110:C09S04**.

Cantin N, Cohen AL, Karnauskas KB, Trarrant AM, McCorkle DC (2010) Ocean warming slows coral growth in the central Red Sea. *Science,* **329**, 322-325.

Carpenter KE, Abrar M, Aeby G *et al*. (2008) One-third of reef-building corals face eleated extinction risk from climate change and local impacts. *Science,* **321**, 560-563.

Carricart-Ganivet JP, Merino M (2001) Growth responses of the reef-building coral Montastraea annularis along a gradient of continental influence in the southern Gulf of Mexico. *Bulletin of Marine Science,* **68**, 133-146.

Carricart-Ganivet JP (2004) Sea surface temperature and the growth of the West Atlantic reef-building coral Montastraea annularis. *Journal of Experimental Marine Biology and Ecology,* **302**, 249-260.

Carricart-Ganivet JP, Lough JM, Barnes DJ (2007) Growth and luminescence characteristics in skeletons of massive Porites from a depth gradient in the central Great Barrier Reef. *Journal of Experimental Marine Biology and Ecology,* **351**, 27-36.

Clode PL, Marshall AT (2002) Low temperature FESEM of the calcifying interface of a scleractinian coral. *Tissue & Cell,* **34**, 187-198.

Cohen AL (2002) The effect of algal symbionts on the accuracy of Sr/Ca paleotemperatures from coral. *Science*, **296**, 331-333.

Cohen AL, Layne GD, Hart SR (2001) Kinetic control of skeletal Sr/Ca in a symbiotic coral: implications for the paleaotemperature proxy. *Paleoceanography,* **16**, 20-26.

Cohen AL, McConnaughey T (2003) Geochemical perspectives on coral mineralization. In: *Biomineralization*. (eds Dove PM, Weiner S, de Yoreo JJ) pp 151-187, Reviews in Mineralogy and Geochemistry, Mineralogical Society of America.

Cohen AL, Sohn RA (2004) Tidal modulation of Sr/Ca ratios in a Pacific reef coral. *Geophysical Research Letters,* **31**, L16310.

Coles SL, Fadlallah YH (1991) Reef coral survival and mortality at low temperatures in the Arabian Gulf: new species-specific lower temperature limits. *Coral Reefs,* **9**, 231-237.

Cooper TF, De'ath G, Fabricius KE, Lough JM (2008) Declining coral calcification in massive *Porites* in two nearshore regions of the northern Great Barrier Reef. *Global Change Biology,* **14**, 529-538.

Cuif J-P, Dauphin Y (1998) Microstructural and physico-chemical characterization of 'centers of calcification' in septa of some recent scleractinian corals. *Paläontologische Zeitschrift,* **72**, 257-270.

Cuif J-P, Dauphin Y and Gautret P (1999) Compositional diversity of soluble mineralizing matrices in some recent coral skeletons compared to fine-scale growth structures of fibres: Discussion of consequences for biomineralization and diagenesis, *International Journal of Earth Sciecne*., **88**, 582-592.

Cuif J-P, Dauphin Y, Doucet J, Salomé M, Susini J (2003) XANES mapping of organic sulfate in three scleractinian coral skeletons. *Geochimica et Cosmochimica Acta,* **67**, 75-83.

Cuif J-P, Dauphin Y, Berthet P, Jegoudez J (2004) Associated water and organic compounds in coral skeletons: quantitative thermogravimetry coupled to infrared absorption spectrometry. *Geochemistry, Geophysics and Geosystems,* **5**, doi:10.1029/2004GC000783.

Cuif J-P, Dauphin Y (2005a) The environment recording unit in coral skeletons - a synthesis of structural and chemical evidences of a biochemically driven stepping-growth process in coral fibres. *Biogeosciences,* **2**, 61-73.

Cuif J-P, Dauphin Y (2005b) The two-step mode of growth in the scleractinian coral skeletons from the micrometer to the overall scale. *Journal of Structural Biology,* **150**, 319-331.

Cuif J-P, Dauphin Y, Sorauf J (2011) *Biominerals and fossils through time,* Cambridge, Cambridge University Press, 490 pp.

Cuif J-P, Dauphin Y, Nehrke G, Nouet J, Perez-Huerta A (2012) Layered growth and crystallization in calcareous biominerals: Impact of structural and chemical evidences on two major concepts in invertebrate biomineralization studies. *Minerals,* **2**, 11-39.

Dana JD (1846) Sturcture and classification of zoophytes. United States exploring expedition during the years 1838, 1839, 1840, 1841, 1842, under the command of Charles Wilkes. *U.S. N.,* **7**, 1-740.

Darwin C (1842) *The structure and distribution of coral reesf,* London, UK, University of California Press.

Dauphin Y, and Cuif J-P (1997) Isoelectric properties of the soluble matrices in relation to the chemical composition of some scleractinian skeletons, *Electrophoresis*, **18**, 1180-1183.

de Villiers S, Nelson BK, Chivas AR (1995) Biological controls on coral Sr/Ca and δ18O reconstructions of sea surface temperatures. *Science*, **269**, 1247-1249.

De'ath G, Lough JM, Fabricius KE (2009) Declining coral calcification on the Great Barrier Reef. *Science,* **323**, 116-118.

Dey A, de With G, Sommerdijk NAJM (2010) In situ techniques in biomimetic mineralization studies of calcium carbonate. *Chemical Society Reviews,* **39**, 397-409.

Dickson AG, Sabine CL, Christian JR (2007) *Guide to best practices for ocean CO_2 measurements*, PICES Special Publication.

Dodds LA, Roberts JM, Taylor AC, Marubini F (2007) Metabolic tolerance of the cold-water coral Lophelia pertusa (Scleractinia) to temperature and dissolved oxygene change. *Journal of Experimental Marine Biology and Ecology,* **349**, 205-214.

Dodge RE, Wyers SC, Frith HR, Knap AH, Smith SR, Cook CB, Sleeter TD (1984) Coral calcification rates by the buoyant weight technique: effects of Alizarin staining. *Journal of Experimental Marine Biology and Ecology,* **75**, 217-232.

Dodge RE, Wyers SC, Frith HR, Knap AH, Smith SR, Cook CB, Sleeter TD (1984) Coral calcification rates by the buoyant weight technique: effects of Alizarin staining. *Journal of Experimental Marine Biology and Ecology,* **75**, 217-232.

Dollar SJ (1982) Wave stress and coral community structure in Hawaii. *Coral Reefs,* **1**, 71-81.

Done TJ (1982) Patterns in the distribution of coral communities across the central Great Barrier Reef. *Coral Reefs,* **1**, 95-107.

Doney SC, Schimel DS (2007) Carbon and climate system coupling on timescales from the Precambrian to the Anthroocene. *Annual Review of Environmental Resources,* **32**, 31-66.

Doney SC, Fabry VJ, Feely RA, Kleypas JA (2009) Ocean acidification: the other CO_2 problem. *Annual Review of Marine Science,* **1**, 169-192.

Donner SD, Skirving WJ, Little CM, Oppenheimer M, Hoegh-Guldberg OVE (2005) Global assessment of coral bleaching and required rates of adaptation under climate change. *Global Change Biology,* **11**, 2251-2265.

Douglas AE (2003) Coral bleaching - how and why? *Marine Pollution Bulletin*, **46**, 385-392.

Druffel ERM (1997) Geochemistry of corals: Proxies of past ocean chemistry, ocean circulation, and climate. *Proceeding of the National Academic Science of the United States of America,* **94**, 8354-8361.

Dunne RP (2012) The record of sea temperature during the 2010 coral bleaching at Phuket, Thailand – different datasets, different perspectives – unexplained errors in HADISST 1.1. *Phuket Marine Biological Center Research Bulletin*, **71**, 11-18.

Edmunds PJ, Bruno JF (1996) The importance of sampling scale in ecology: kilometer-wide variation in coral reef communities. *Marine Ecology Progress Series,* **143**, 165-171.

Endo H, Takagi Y, Ozaki N, Kogure T, Watanabe T (2004) A crustacean Ca^{2+}-binding protein with a glutamate-rich sequence promotes $CaCO_3$ crystallization. *Biochemical Journal,* **384**, 159-167.

Erez J (1978) Vital effect on stable-isotope composition seen in foraminifera and coral skeletons. *Nature,* **273**, 199-202.

Ewing GC (1950) Relation between band slicks at the surface and internal waves in the sea. *Science,* **111**, 91-94.

Fabricius KE, Wolanski E (2000) Rapid smothering of coral reef organisms by muddy marine snow. *Estuarine, Coastal and Shelf Science,* **50**, 120-150.

Fabricius KE (2005) Effects of terrestrial runoff on the ecology of corals and coral reefs: review and synthesis. *Marine Pollution Bulletin,* **50**, 125-146.

Fabricius KE, Langdon C, Uthicke S *et al*. (2011) Losers and winners in coral reefs acclimatized to elevated carbon dioxide concentrations. *Nature Clim. Change,* **1**, 165-169.

Fabry VJ, Langdon C, Balch WM *et al*. (2009) Present and future impacts of ocean acidification on marine ecosystems and biogeochemical cycles. In: *Report of the Ocean Carbon and Biogeochemistry Scoping*

Workshop on Ocean Acidificaiton Research. pp 64. La Jolla, CA, UCSD, Scripps Institution of Oceanography; 9-11 October 2007.

Fabry VJ, Seibel BA, Feely RA, Orr JC (2008) Impact of ocean acidification on marine fauna and ecosystem processes. *Journal of Marine Science,* **65**, 414-432.

Farmer DM (1978) Observation of long nonlinear internal waves in a lake. *Journal of Physical Oceanography,* **8**, 63-73.

Fautin D, Mariscal R (1991) Cnidaria: Anthozoa. In: *Placozoa, Porifera, Cnidaria, and Ctenophora*. (eds Harrison F, Westfall J). New York, USA, Wiley-Liss.

Feely RA, Sabine CL, Lee K, Berelson W, Kleypas JA (2004) Impact of anthropogenic CO2 on the CaCO3 system in the oceans. *Science,* **305**, 362-366.

Felis T, Pätzold J, Loya Y (2003) Mean oxygen-isotope signatures in <i>Porites</i> spp. corals: inter-colony variability and correction for extension-rate effects. *Coral Reefs,* **22**, 328-336.

Finch AA, Allison N (2008) Mg structural state in coral aragonite and implications for the paleoenvironmental proxy. *Geophysical Research Letters,* **35**, L08704, 1-5.

Freiwald A, Fosså S, Grehan A, Koslow A, Roberts JM (2004) Cold-water coral reefs, out of sight - no loger out of mind. Cambridge, UNEP-WCMC, p84.

Furla P, Galgani I, Durand I, Allemand D (2000) Sources and mechanisms of inorganic carbon transport for coral calcification and photosynthesis. *The Journal of Experimental Biology,* **203**, 3445-3457.

Gagan MK, Chivas AR, Johnson DP (1988) Cyclone-induced shelf sediment transport and the ecology of the Great Barrier Reef. *Proceedings 6th International Coral Reef Symposium,* **2**, 595-600.

Galloway S, Work T, Bochsler V *et al*. (2007) Coral disease and health workshop: coral histopathology workshop II. *National Oceanoic and Atmospheric Administration*, Silver Spring.

Gautret P, Cuif J-P and Frewald A (1997) Composition of soluble mineralizing matrices in zooxanthellate and non-zooxanthellate scleractinian corals: Biochemical assessment of photosynthetic metabolism through the study of a skeletal feature, *Facies*, **36**, 189-194.

Gautret P, Cuif J-P, Stolarski J (2000) Organic components of the skeleton of scleractinian corals - evidence from *in situ* acridine orange staining. *Acta Palaeontologica Polonica,* **45**, 107-118.

Gischler E (1995) Current and wind induced facies patterns in a Devonian atoll; Iberg Reef, Harz Mts., Germany. *Palaios,* **10**, 180-189.

Glynn PW (1991) Coral reef bleaching in the 1980s and possible connections with global warming. *Trends in Ecology and Evolution,* **6**, 175-179.

Glynn PW (1993) Coral reef bleaching: ecological perspectives. *Coral Reefs,* **12**, 1-17.

Glynn PW (1993) Monsoonal upwelling and episodic *Acanthaster* predation as probable controls of coral reef distribution and community structure in Oman, Indian Ocean. *Atoll Research Bulletin,* **379**, 1-66.

Glynn PW (1996) Coral bleaching: facts, hypotheses and implications. *Global Change Biology,* **2**, 495-509.

Glynn PW, Mat LJ, Baker AC, Calder MO (2001) Coral bleaching and mortality in Panama and Ecuador during the 1997-1998 El Niño Southern Oscillation event: spatial/temporal patterns and comparisons with the 1982-1983 event. *Bulletin of Marine Science,* **69**, 79-109.

Goreau TF (1959) The physiology of skeleton formation in corals. I. A method for measuring the rate of calcium deposition by corals under different conditions. *Biological Bulletin,* **116**, 59-75.

Goreau T, Goreau NI (1959) The physiology of skeleton formation in corals. II. Calcium deposition by hermatypic corals under different conditions. *Biological Bulletin,* **117**, 239-250.

Goreau TJ (1977) Coral Skeletal Chemistry: Physiological and Environmental Regulation of Stable Isotopes and Trace Metals in Montastrea annularis. *Proceedings of the Royal Society of London. Series B. Biological Sciences,* **196**, 291-315.

Greenstein BJ, Pandolfi JM (2008) Escaping the heat: range shifts of reef coral taxa in coastal Western Australia. *Global Change Biology,* **14**, 513-528.

Grigg RW (1998) Holocene coral reef accretion in Hawaii: a function of wave exposure and sea level history. *Coral Reefs,* **17**, 263-272.

Grigg R (2006) Depth limit for reef building corals in the Au'au Channel, S.E. Hawaii. *Coral Reefs,* **25**, 77-84.

Grottoli AG, Rodrigues LJ, Palardy JE (2006) Heterotrophic plasticity and resilience in bleached corals. *Nature,* **440**, 1186-1189.

Guinotte JM, Fabry VJ (2008) Ocean acidification and its potential effects on marine ecosystems. *Annals of New York Academy of Sciences,* **1134**, 320-342.

Gunderson LH (2000) Ecological resilience: in theory and application. *Annual Review of Ecology and Systematics,* **31**, 425-439.

Guzman H, Cortés J (2007) Reef recovery 20 years after the 1982–1983 El Niño massive mortality. *Marine Biology,* **151**, 401-411.

Hearn CJ, Atkinson MJ, Falter JL (2001) A physical derivation of nutrient-uptake rates in coral reefs: effects of roughness and waves. *Coral Reefs,* **20**, 347-356.

Helfrich KR (1992) Internal solitary wave breaking and run-up on a uniform slope. *Journal of Fluid Mechanics,* **243**, 133-154.

Helfrich KR, Melville WK (2006) Long nonlinear internal waves. *Annual Review of Fluid Mechanics,* **38**, 395-425.

Highsmith RC (1979) Coral growth rates and environmental control of density banding. *Journal of Experimental Marine Biology and Ecology,* **37**, 105-125.

Highsmith RC (1982) Reproduction by fragmentation in corals. *Marine Ecology Progress Series,* **7**, 207-226.

Hild S, Marti O, Ziegler A (2008) Spatial distribution of calcite and amorphous calcium carbonate in the cuticle of the terrestrial crustaceans *Porcellio scaber* and *Armadillidium vulgare*. *Journal of Structural Biology,* **163**, 100-108.

Hoegh-Guldberg O (1999) Climate change, coral bleaching and the future of the world's coral reefs. *Marine and Freshwater Research,* **8**, 839-866.

Hoegh-Guldberg O, Mumby PJ, Hooten AJ *et al*. (2007) Coral reefs under rapid climate change and ocean acidification. *Science,* **318**, 1737-1742.

Hoegh-Guldberg O, Bruno JF (2010) The Impact of Climate Change on the World's Marine Ecosystems. *Science,* **328**, 1523-1528.

Hoitink AJF, Hoekstra P (2003) Hydrodynamic control of the supply of reworked terrigenous sediment to coral reefs in the Bay of Banten (NW Java, Indonesia). *Estuarine, Coastal and Shelf Science,* **58**, 743-755.

Holcomb M, Cohen AL, Gabitov RI, Hutter JL (2009) Compositional and morphological features of aragonite precipitated experimentally from seawater and biogenically by corals. *Geochimica et Cosmochimica Acta,* **73**, 4166-4179.

Houlbreque F, Ferrier-Pages C (2009) Heterotrophy in tropical scleractinian corals. *Biological Reviews,* **84**, 1-17.

Houlbreque F, Meibom A, Cuif J-P *et al*. (2009) Strontium-86 labeling experiments show spatially heterogeneous skeletal formation in the scleractinian coral *Porites porites*. *Geophysical Research Letters,* **36**, L04604, 1-5.

Hudson JH, Shinn EA, Halley RB, Lidz B (1976) Sclerochronology: A tool for interpreting past environments. *Geology,* **4**, 361-364.

Hughes TP (1993) Disturbances: effects on coral reef dynamics. In: *Coral Reefs*. (ed Hughes Tp) pp 115-234.

Hughes TP, Baird AH, Dinsdale EA, Moltschaniwskij NA, Pratchett MS, Tanner JE, Willis BL (1999) Patterns of recruitment and abundance of corals along the Great Barrier Reef. *Nature,* **397**, 59-63.

Hughes TP, Baird AH, Bellwood DR *et al*. (2003) Climate change, human impacts, and the resilience of coral reefs. *Science,* **301**, 929-933.

Hyder P, Jeans DRG, Cauquil E, Nerzic R (2005) Observations and predictability of internal solitons in the northern Andaman Sea. *Applied Ocean Research,* **27**, 1-11.

Jackson CR (2004) An atlas of internal solitary-like waves and their properties. *2nd Ed. Office of Naval Research, Global Ocean Associates, Alexandria, VA, USA*.

Jantzen C (2010) Primary prodcution in coral reefs - Key players and adaptive strategies to natural environmental variations. PhD Thesis, University of Bremen, Bremen, 184 pp.

Jiménez C, Cortés J (2003) Growth of seven species of scleractinian corals in an upwelling environment of the eastern Pacific (Golfo de Papagayo, Costa Rica). *Bulletin of Marine Science,* **72**, 187-198.

Johannes RE, Tepley L (1974) Examination of feeding of the coral *Porites lobata in situ* using time lapse photography. *Proceedings 2nd International Coral Reef Symposium,* **1**, 127-131.

Jokiel PL, Coles SL (1977) Effects of temperature on the mortality and growth of Hawaiian reef corals. *Marine Biology,* **43**, 201-208.

Jokiel PL, Brown EK, Friedlander A, Rodgers KB, Smith WR (2004) Hawai'i coral reef assessment and monitoring program: spatial patterns and temporal dynamics in reef coral communities. *Pacific Science,* **58**, 159-174.

Jolivet A, Bardeau JF, Fablet R, Paulet YM, DE Pontual H (2008) Understanding otolith biomineralization processes: new insights into microscale spatial distribution of organic and mineral fractions from Raman microspectrometry. *Analytical and Bioanalytical Chemistry,* **392**, 551-560.

Juillet-Leclerc A, Reynaud S, Rollion-Bard C *et al*. (2009) Oxygen isotopic signature of the skeletal microstructures in cultured corals: Identification of vital effects. *Geochimica et Cosmochimica Acta,* **73**, 5320-5332.

Kaczorowska B, Hacura A, Kupka T, Wrzalik R, Talik E, Pasterny G, Matuszewska A (2003) Spectroscopic characterization of natural corals. *Analytical and Bioanalytical Chemistry,* **377**, 1032-1037.

Kao TW, Pan F-S, Renourad D (1985) Internal solitons on the pycnocline: generation, propagation, and shoaling and breaking over a slope. *Journal of Fluid Mechanics,* **159**, 19-53.

Kennedy D, Woodroffe C (2002) Fringing reef growth and morphology: a review. *Earth-Science Reviews,* **57**, 255-277.

Khokittiawong S, Yu W (2012) Note on the occurrence of high sea surface temperatures in the Andaman Sea, in 2010. *Phuket Marine Biological Center Research Bulletin,* **71**, 1-9.

Kleypas JA (1996) Coral reef development under naturally turbid conditions: fringing reefs near Broad Sound, Australia. *Coral Reefs,* **15**, 153-167.

Kleypas JA, Buddemeier RW, Archer D, Gattuso J-P, Langdon C, Opdyke BN (1999a) Geochemical consequences of increased atmospheric carbon dioxide on coral reefs. *Science,* **284**, 118-120.

Kleypas JA, McManus JW, Meñez LAB (1999b) Environmental limits to coral reef development: where do we draw the line? *American Zoologist,* **39**, 146-159.

Kleypas JA, Buddemeier RW, Gattuso J-P (2001) The future of coral reefs in an age of global change. *International Journal of Earth Science (Geologische Rundschau),* **90**, 426-437.

Kleypas JA, Feely RA, Fabry VJ, Langdon C, Sabine CL, Robbins LL (2006) Impacts of ocean acidification on coral reefs and other marine calcifiers: a guide for future research, report of a workshop held 18-20 April 2005. pp 88. St. Petersburg, FL, sponsored by NSF, NOAA, and the U.S. Geological Survey.

Klymak JM, Moum JN (2003) Internal solitary waves of elevation advancing on a shoaling shelf. *Geophysical Research Letters,* **30**, 2045.

Knutson DW, Buddemeier RW, Smith SV (1972) Coral chronometers: seasonal growth bands in reef corals. *Science,* **177**, 270-272.

Kohler KE, Gill SM (2006) Coral point count with excel extension (CPCe): a visual basic program for the determination of coral substrate and substrate coverage using random point count methodology. *Computers & Geosciences,* **32**, 1259-1269.

Krumbein W (1934) Size frequency distributions of sediments. *Journal of Sedimentary Petrology,* **4**, 65-77.

Kuguru BL, Mgaya YD, Öhman MC, Wagner GM (2004) The reef environment and competitive success in the Corallimorpharia. *Marine Biology,* **145**, 875-884.

Kumar JSY, Raghunathan C (2012) Recovery status of scleractinian coras and associated fauna in the Andman and Nicobar islands. *Phuket Marine Biological Center Research Bulletin,* **71**, 63-70.

LaJeunesse TC, Petty DT, Sampayo EM *et al*. (2010) Long-standing environmental conditions, geowgraphic isolgation and host-symbiont specificity influence the relative ecologcial dominance and genetic diversitfication of coral endoymbionts in the genus Symbiodinium. *Journal of Biogeography*, doi:10.1111/j.1365-2699.2010.02273.x.

Langdon C, Takaheshi T, Sweeney C *et al*. (2000) Effect of calcium carbonate saturation state on calcification rate of an experimental coral reef. *Global Biogeochemical Cycles,* **14**, 639-654.

Larcombe P, Woolfe KJ (1999) Increased sediment supply to the Great Barrier Reef will not increase sediment accumulation at most coral reefs. *Coral Reefs,* **18**, 163-169.

Latief H, Sengara IW, Kusuma SB (2008) Probabilistic seismic and tsunami hazard analysis model for input to tsunami warning and disaster mitigation strategies. In: *International Conference for Tsunami Warning (ICTW) Bali,* Indonesia.

Leichter JJ, Wing SR, Miller SL, Denny MW (1996) Pulsed delivery of subthermocline water to Conch Reef (Florida Keys) by internal tidal bores. *Limnology and Oceanography,* **41**, 1490-1501.

Leichter JJ, Deane GB, Stokes MD (2005) Spatial and temporal variability of internal wave forcing on a coral reef. *Journal of Physical Oceanography,* **35**, 1945-1962.

Leichter JJ, Genovese SJ (2006) Intermittent upwelling and subsidized growth of the scleractinian coral *Madracis mirabilis* on the deep fore-reef slope of Discovery Bay, Jamaica. *Marine Ecology Progress Series,* **316**, 95-103.

Lesser MP (2004) Experimental biology of coral reef ecosystems. *Journal of Experimental Marine Biology and Ecology,* **300**, 217-252.

Lesser MP (2011) Coral bleaching: causes and mechanisms. In: *Coral reef: an ecosystem in transition*. (eds Dubinsky Z, Stabler N) pp 405-420. Heidelberg, Springer.

Lesser MP, Slattery M, Leichter JJ (2009) Ecology of mesophotic coral reefs. *Journal of Experimental Marine Biology and Ecology,* **375**, 1-8.

Lough JM, Barnes DJ (1990) Intra-annual timing of density band formation of Porites coral from the central Great Barrier Reef. *Journal of Experimental Marine Biology and Ecology,* **135**, 35-57.

Lough JM, Barnes DJ (1992) Comparisons of skeletal density variations in *Porites* from the central Great Barrier Reef. *Journal of Experimental Marine Biology and Ecology,* **155**, 1-25.

Lough JM, Barnes DJ (1997) Several centuries of variation in skeletal extension, density and calcification in massive Porites colonies from the Great Barrier Reef: A proxy for seawater temperature and a background of variability against which to identify unnatural change. *Journal of Experimental Marine Biology and Ecology,* **211**, 29-67.

Lough JM, Barnes DJ (2000) Environmental controls on growth of the masisve coral *Porites*. *Journal of Experimental Marine Biology and Ecology,* **245**, 225-243.

Løvholt F, Bungum H, Harbitz CB, Glimsdal S, Lindholm CD, Pedersen G (2006) Earthquake related tsunami hazard along the western coast of Thailand. *Natural Hazards and Earth System Science,* **6**, 979-997.

Lowe RJ, Falter JL, Bandet MD, Pawlak G, Atkinson MJ, Monismith SG, Koseff JR (2005) Spectral wave dissipation over a barrier reef. *Journal of Geophysical Research,* **110**, C04001, doi:04010.01029/02004JC002711.

Lowenstam HA, Weiner S (1989) *On Biomineralization,* New York, Oxford University Press.

Maier C, Watremez P, Taviani M, Weinbauer MG, Gattuso J-P (2012) Calcification rates and the effect of ocean acidification on Mediterranean cold-water corals. *Proceedings of the Royal Society B: Biological Sciences,* **279**, 1716-1723.

Maina J, Venus V, McClanahan TR, Ateweberhan M (2008) Modelling susceptibility of coral reefs to environmental stress using remote sensing data and GIS models. *Ecological Modelling,* **212**, 180-199.

Mann S, Archibald DD, Didymus JM, Douglas T, Heywood BR, Meldrum FC, Reeves NJ (1993) Crystallization at inorganic-organic interfaces: biominerals and biomimetic synthesis. *Science,* **261**, 1286-1292.

Manzello DP (2008) Reef development and resilience to acute (El Nino warming) and chronic (high-CO_2) disturbances in the eastern tropical Pacific: a real-world climate change model. *Proceedings 11th International Coral Reef Symposium,* **1**, 1299-1303.

Manzello DP (2010) Ocean acidification hot spots: Spatiotemporal dynamics of the seawater CO_2 system of eastern Pacific coral reefs. *Limnology and Oceanography,* **55**, 239-248.

Manzello DP, Berkelmans R, Hendee JC (2007) Coral bleaching indices and thresholds for the Florida Reef Tract, Bahamas, and St. Croix, US Virgin Islands. *Marine Pollution Bulletin,* **54**, 1923-1931.

Manzello DP, Kleypas JA, Budd DA, Eakin CM, Glynn PW, Langdon C (2008) Poorly cemented coral reefs of the eastern tropical Pacific: Possible insights into reef development in a high-CO_2 world. *Proceedings of the National Academy of Sciences,* **105**, 10450-10455.

Marin F, Smith M, Isa Y, Muyzer G, Westbroek P (1996) Skeletal matrices, muci, and the origin of invertebrate calcification. *Proceedings of the National Academy of Sciences of the United States of America,* **93**, 1554-1559.

Marshall PA, Baird AH (2000) Bleaching of corals on the Great Barrier Reef: differential susceptibilities among taxa. *Coral Reefs,* **19**, 155-163.

Massel SR, Done TJ (1992) Effects of cyclone waves on massive coral assemblages on the Great Barrier Reef: meteorology, hydrodynamics and demography. *Coral Reefs,* **12**, 153-166.

Maynard JA, Turner PJ, Kenneth ARN *et al*. (2008) *ReefTemp*: An interactive monitoring system for coral bleaching using high-resolution SST and improved stress predictors. *Geophysical Research Letters,* **35**, doi:10.1029/2007GL032175.

McClanahan TR (1997) Primary succession of coral-reef algae: differing patterns on fished versus unfished reefs. *Journal of Experimental Marine Biology and Ecology,* **218**, 77-102.

McClanahan TR (2004) The relationship between bleaching and mortality of common corals. *Marine Biology,* **144**, 1239-1245.

McClanahan TR, Obura D (1997) Sedimentation effects on shallow coral communities in Kenya. *Journal of Experimental Marine Biology and Ecology,* **209**, 103-122.

McClanahan TR, Baird AH, Marshall PA, Toscano MA (2004) Comparing bleaching and mortality responses of hard corals between southern Kenya and the Great Barrier Reef, Australia. *Marine Pollution Bulletin,* **48**, 327-335.

McClanahan TR, Ateweberhan M, Graham NAJ, Wilson SK, Sebastian CR, Guillaume MMM, Bruggemann JH (2007) Western Indian Ocean coral communities: bleaching responses and susceptibility to extinction. *Marine Ecology-Progress Series,* **337**, 1-13.

McClanahan TR, Maina JM, Muthiga NA (2011) Associations between climate stress and coral reef diversity in the western Indian Ocean. *Global Change Biology,* **17**, 2023-2032.

McCulloch M, Trotter J, Montagna P *et al*. (2012) Resilience of Cold-Water Scleractinian Corals to Ocean Acidification: Boron Isotopic Systematics of pH and Saturation State Up-Regulation. *Geochimica et Cosmochimica Acta,* **87**, 21-34.

Meehl G, Stocker T, Collins W *et al*. (2007) Global Climate Projections. In: *Climate change 2007: The physical science basis. Contributions of working group I to the fourth assessment report of the Intergovernmental Panel on Climate Change*. (eds Solomon S, Qin D, Manning M, Chen Z, Marquis M, Averyt K, Tignor M, Miller H). Cambridge, United Kingdom and New York, NY, USA, Cambridge University Press.

Mehrbach C, Culberson CH, Hawley JE, Pytkowicz RM (1973) Measurement of the apparent dissociation constants of carbonic acid in seawater at atmospheric pressure. *Limnology and Oceanography,* **18**, 897-907.

Meibom A, Stage M, Wooden J *et al*. (2003) Monthly Strontium/Calcium oscillations in symbiotic coral aragonite: Biological effects limiting the precision of the paleotemperature proxy. *Geophysical Research Letters,* **30**, 1418.

Meibom A, Cuif JP, Hillion FO *et al*. (2004) Distribution of magnesium in coral skeleton. *Geophysical Research Letters,* **31**.

Meibom A, Yurimoto H, Cuif J-P, *et al*. (2006) Vital effects in coral skeletal composition display strict three-dimensional control. *Geophysical Research Letters,* **33**, L11608, doi:10.1029/2006GL025968.

Meibom A, Mostefaoui S, Cuif J-P, Dauphin Y, Houlbreque F, Dunbar R, Constantz B (2007) Biological forcing controls the chemistry of reef-building coral skeleton. *Geophysical Research Letters,* **34**, 1-5.

Meibom A, Cuif J-P, Houlbreque F, Mostefaoui S, Dauphin Y, Meibom KL, Dunbar R (2008) Compositional variations at ultra-structure length scales in coral skeleton. *Geochimica et Cosmochimica Acta,* **72**, 1555-1569.

Miller J, Muller E, Rogers C *et al*. (2009) Coral disease following massive bleaching in 2005 causes 60% decline in coral cover on reefs in the US Virgin Islands. *Coral Reefs,* **28**, 925-937.

Milne Edwards H (1857) Histoire naturelle des Coralliaires ou polypes proprement dits. Librairie Encycloédique de Roret, Paris. 326 pp.

Moberg F, Folke C (1999) Ecological goods and services of coral reef ecosystems. *Ecological Economics,* **29**, 215-233.

Moore W, Krishnaswami S (1974) Correlation of X-radigraphy revealed banding in corals with radiometric growth rates. In: *2nd International Coral Reef Symposium*. pp 269-276. Great Barrier Reef Committee, Brisbane, December, 1974.

Moum JN, Klymak JM, Nash JD, Perlin A, Smyth WD (2007) Energy transport by nonlinear internal waves. *Journal of Physical Oceanography,* **37**, 1968-1988.

Murdoch TJT, Aronson RB (1999) Scale-dependent spatial variability of coral assemblage along the Florida reef tract. *Coral Reefs,* **18**, 341-351.

Muscatine L, Porter JW (1977) Reef corals: mutualistic symbioses adapted to nutrient-poor environments. *Bioscience,* **27**, 454-460.

Muscatine L, McCloskey L, Marian R (1981) Estimating the daily contribution of carbon from zooxanthellae to coral animal respiration. *Limnology and Oceanography,* **26**, 601-611.

Muscatine L, Tambutté E, Allemand D (1997) Morphology or coral desmocytes, cells that anchor the calicoblastic epithelium to the skeleton. *Coral Reefs,* **16**, 205-213.

Nakamura T, Woesik Rv (2001) Water-flow rates and passive diffusion partially explain differential survival of corals during the 1998 bleaching event. *Marine Ecology Progress Series,* **212**, 301-304.

Nehrke G, Nouet J (2011) Confocal Raman microscope mapping as a tool to describe different mineral and organic phases at high spatial resolution within marine biogenic carbonates: case study on *Nerita undata* (Gastropoda, Neritopsina). *Biogeosciences,* **8**, 3761-3769.

Nehrke G, Poigner H, Wilhelms-Dick D, Brey T, Abele D (2012) Coexistence of three calcium carbonate polymorphs in the shell of the Antarctic clam Laternula elliptica. *Geochem. Geophys. Geosyst.,* **13**, Q05014.

Neues F, Hild S, Epple M, Marti O, Ziegler A (2011) Amorphous and crystalline calcium carbonate distribution in the tergite cuticle of moulting *Porcellio scaber* (Isopoda, Crustacea). *Journal of Structural Biology,* **175**, 10-20.

Nielsen TG, Bjornsen PK, Boonruang P *et al*. (2004) Hydrography, bacteria and protist communites across the continental shelf and shelf slope of the Andaman Sea (NE Indian Ocean). *Marine Ecology Progress Series,* **274**, 69-86.

Nothdurft LD, Webb GE (2007) Microstructure of common reef-building coral genera *Acropora*, *Pocillopora*, *Goniastrea* and *Porites*: constraints on spatial resolution in geochemical sampling. *Facies,* **53**, 1-26.

Nystörm M, Folke C (2000) Spatial resilience of coral reefs. *Ecosystems,* **4**, 406-417.

Ogilvie M (1896) Microscopic and systematic study of Madreporarian types of corals. *Philosophical Transactions of the Royal Society of London,* **187**, 83-187.

Orr JC, Fabry VJ, Aumont O *et al*. (2005) Anthropogenic ocean acidification over the twenty-first century and its impact on calcifying organisms. *Nature,* **437**, 681-686.

Osborne AR, Burch TL (1980) Internal solitons in the Andaman Sea. *Science,* **208**, 451-460.

Perrin C, Smith DC (2007) Earliest steps of diagenesis in living scleractinian corals: evidence from ultrastructural pattern and Raman spectroscopy. *Journal of Sedimentary Research,* **77**, 495-507.

Perry CT, Larcombe P (2003) Marginal and non-reef-building coral environments. *Coral Reefs,* **22**, 427-432.

Perry CT, Spencer T, Kench PS (2008) Carbonate budgets and reef production states: a geomorphic perspective on the ecological phase-shift concept. *Coral Reefs,* **27**, 853-866.

Perry CT, Smithers SG (2010) Evidence for the episodic "turn on" and "turn off" of turbid-zone coral reefs during the late Holocene sea-level highstand. *Geology,* **38**, 119-122.

Petit JR, Jouzel J, Raynaud D *et al*. (1999) Climate and atmospheric history of the past 420,000 years from the Vostok ice core, Antartica. *Nature,* **399**, 429-436.

Philipp E, Fabricius K (2003) Photophysiological stress in scleractinian corals in response to short-term sedimentation. *Journal of Experimental Marine Biology and Ecology,* **287**, 57-78.

Phongsuwan N (1991) Recolonization of a coral reef damaged by a storm on Phuket island, Thailand. *Phuket Marine Biological Center Research Bulletin,* **56**, 75-83.

Phongsuwan N, Changsang H (1992) Assessment of coral communities in the Andaman Sea (Thailand). *Proeedingsc 7th International Coral Reef Symposium,* **1**, 114-121.

Phongsuwan N, Changsang H (2012) Repeated coral bleaching in the Andaman Sea, Thailand, during the last two decades. *Phuket Marine Biological Center Research Bulletin,* **71**, 19-42.

Pineda J (1991) Predictable upwelling and the shoreward transport of planktonic larvae by internal tidal bores. *Science,* **253**, 548-551.

Pineda J (1994) Internal tidal bores in the nearshore: warm-water fronts, seaward gravity currents and the onshore transport of neustonic larvae. *Journal of Marine Research,* **52**, 427-458.

Piniak GA, Storlazzi CD (2008) Diurnal variability in turbidity and coral fluorescence on a fringing reef flat: Southern Molokai, Hawaii. *Estuarine, Coastal and Shelf Science,* **77**, 56-64.

Podesta GP, Glynn PW (2001) The 1997-98 El Nino event in Panama and Galapagos: an update of thermal stress indices relative to coral bleaching. *Bulletin of Marine Science,* **69**, 43-59.

Pomar L, Morsilli M, Hallock P, Bádenas B (2012) Internal waves, an under-explored source of turbulence events in the sedimentary record. *Earth-Science Reviews,* **111**, 56-81.

Porter-Smith R, Harris PT, Andersen OB, Coleman R, Greenslade D, Jenkins CJ (2004) Classification of the Australian continental shelf based on predicted sediment threshold exceedance from tidal currents and swell waves. *Marine Geology,* **211**, 1-20.

Precht WF, Aronson RB (2004) Climate flickers and range shifts of reef corals. *Frontiers in Ecology and the Environment,* **2**, 307-314.

Pratz E (1882) Über die verwandtschaftlichen Beziehungen einiger Korallengattungen mit hauptsächlicher Berücksichtigung ihrer Septalstruktur. *Palaeontographica,* **29**, 81-122.

Puverel S, Tambutte E, Zoccola D *et al*. (2005) Antibodies against the organic matrix in scleractinians: a new tool to study coral biomineralization. *Coral Reefs,* **24**, 149-156.

Rathburn R (1879) Brazilian corals and coral reefs. *The American Naturalist,* **13**, 539-551.

Riegl B (1995) Effects of sand deposition on scleractinian and alcyonacean corals. *Marine Biology,* **121**, 517-526.

Riegl B (1996) Hermatypic coral fauna of subtropical south-east Africa: a checklist. *Pacific Science,* **50**, 404-414.

Riegl B (1999) Corals in a non-reef setting in the southern Arabian Gulf (Dubai, UAE): fauna and community structure in response to recurring mass mortality. *Coral Reefs,* **18**, 63-73.

Riegl B (2001) Inhibition of reef framework by frequent disturbance: examples from the Arabian Gulf, South Africa, and the Cayman Islands. *Palaeogeography, Palaeoclimatology, Palaeoecology,* **175**, 79-101.

Riegl B (2002) Effect of the 1996 and 1998 positive sea-surface temperature anomalies on corals, coral disease and fish in the Arabian Gulf (Dubai, UAE). *Marine Biology,* **140**, 29-40.

Riegl B (2003) Climate change and coral reefs: different effects in two high-latitude areas (Arabian Gulf, South Africa). *Coral Reefs,* **22**, 433-446.

Riegl B, Bloomer JP (1995) Tissue damage in scleractinian and alconycean corals due to experimental exposure to sedimentation. *Beitr Palaeontol,* **20**, 51-63.

Riegl B, Branch GM (1995) Effects of sediment on the energy budgets of four scleractinian (Bourne 1900) and five alcyonacean (Lamouroux 1816) corals. *Journal of Experimental Marine Biology and Ecology,* **186**, 259-275.

Riegl B, Piller WE (2000) Reefs and coral carpets in the northern Red Sea as models for organism-environment feedback in coral communities and its reflection in growth fabrics. In: *Carbonate Platform Systems: components and interactions*. (eds Insalaco E, Skelton PW, Palmar TJ) pp 71-88. Geological Society, London.

Risk MJ, Sammarco PW (1991) Cross-shelf trends in skeletal density of the massive coral Porites lobata from the Great Barrier Reef. *Marine Ecology Progress Series,* **69**, 195-200.

Rixen T, Ramachandran P, Lehnhoff L *et al*. (2011) Impact of monsoon-driven surface ocean processes on a coral off Port Blair on the Andaman Islands and their link to North Atlantic climate variations. *Global and Planetary Change,* **75**, 1-13.

Roberts J, Wheeler A, Freiwald A, Cairns S (2009) *Cold-water corals,* Cambridge, UK, Cambridge Universtiy Press.

Roder C, Fillinger L, Jantzen C, Schmidt GM, Khokittiawong S, Richter C (2010) Trophic response of corals to large amplitude internal waves. *Marine Ecology Progress Series,* **412**, 113-128.

Roder C, Jantzen C, Schmidt GM, Kattner G, Phongsuwan N, Richter C (2011) Metabolic plasticity of the corals *Porites lutea* and *Diploastrea helipora* exposed to large amplitude internal waves. *Coral Reefs,* **30**, 57-69.

Rogers CS (1990) Response of coral reefs and reef organisms to sedimentation. *Marine Ecology Progress Series,* **62**, 185-202.

Rogers C (2009) Coral bleaching and disease should not be underestimated as causes of Caribbean coral reef decline. *Proceedings of the Royal Society B: Biological Sciences,* **276**, 197-198.

Rollion-Bard C, Chaussidon M, France-Lanord C (2003) pH control on oxygen isotopic composition of symbiotic corals. *Earth and Planetary Science Letters,* **215**, 275-288.

Rollion-Bard C, Blamart D, Cuif J-P, Dauphin Y (2010) *In situ* measurements of oxygen isotopic composition in deep-sea coral, *Lophelia pertusa*: Re-examination of the current geochemical models of biomineralization. *Geochimica et Cosmochimica Acta,* **74**, 1338-1349.

Russell JS (1844) Report on waves. *Brit. Ass. Rep.,* **14**, 311-389.

Sabine CL, Feely RA, Gruber N *et al*. (2004) The oceanic sink for anthropogenic CO_2. *Science,* **305**, 367-371.

Samosorn B, Woodroffe CD (2008) Nearshore wave environments around a sandy cay on a platform reef, Torres Strait, Australia. *Continental Shelf Research,* **28**, 2257-2274.

Sandstrom H, Elliot JA (1984) Internal tide and solitons on the Scotian shelf: a nutrient pump at work. *Journal of Geophysical Research,* **89**, 6415-6426.

Satapoomin S, Nielsen TG, Hansen PJ (2004) Andaman Sea copepods: spatio-temporal variations in biomass and production, and role in the pelagic food web. *Marine Ecology Progress Series,* **274**, 99-122.

Sawall Y, Phongsuwan N, Richter C (2010) Coral recruitment and recovery after the 2004 Tsunami around the Phi Phi Islandas (Krabi Province) and Phuket, Andaman Sea, Thailand. *Helgoland Marine Research,* **64**, 357-365.

Saxby T, Dennison WC, Hoegh-Guldberg O (2003) Photosynthetic response of the coral *Montipora digitata* to cold temperature stress. *Marine Ecology Progress Series,* **248**, 85-97.

Schmid V, Ono S, Reber-Muller S (1999) Cell-substrate interactions in cnidaria. *Microscopy Research and Technique,* **44**, 254-268.

Schmidt GM (2010) Corals and waves - calcification and bioerosion in large amplitude internal waves (LAIW) affected coral reefs. PhD Thesis, University of Bremen, Bremen, 199 pp.

Schmidt GM, Phongsuwan N, Jantzen C, Roder C, Khokittiawong S, Richter C (2012) Coral community composition and reef development at large amplitude internal wave affected coral reefs in the Andaman Sea. *Marine Ecology Progress Series,* **456**, 113-126.

Schuhmacher H (1988) *Korallenriffe,* München, BLV.

Scoffin TP (1993) The geological effects of hurricanes on coral reefs and the interpretation of storm deposits. *Coral Reefs,* **12**, 203-221.

Scoffin TP, Tudhope AW, Brown BE, Chansang H, Cheeney RF (1992) Patterns and possible environmental controls of skeletogenesis of *Porites lutea*, South Thailand. *Coral Reefs,* **11**, 1-11.

Scoffin TP, Tissier MDAL (1998) Late Holocene sea level and reef-flat progradation, Phuket, South Thailand. *Coral Reefs,* **17**, 273-276.

Sinclair DJ (2005) Correlated trace element "vital effects" in tropical corals: a new geochemical tool for probing biomineralization. *Geochimica Cosmochimica Acta*, **69**, 3265-3284.

Sinclair DJ, Williams B, Risk M (2006) A biological origin for climate signals in corals – trace element "vital effects" are ubiquitous in scleractinian coral skeletons. *Geophysical Research Letters*, **33**, L17707, doi:10.1029/2006GL02718£3.

Sheppard C (2009) Large temperature plunges recorded by data loggers at different depths on an Indian Ocean atoll: comparison with satellite data and relevance to coral refuges. *Coral Reefs,* **28**, 399-403.

Sheppard C, Salm R (1988) Reef and coral communities of Oman, with a description of new coral species (Order Sclearctinia, Genus *Acanthastrea*). *Journal of Natural History,* **22**, 263-279.

Smith SV, Buddemeier RW, Redalje RC, Houck JE (1979) Strontium-Calcium thermometry in coral skeletons. *Science,* **204**, 404-407.

Smith WHF, Sandwell DT (1997) Global seafloor topography from satellite altimetry and ship depth soundings. *Science*, **277**, 1957-1962.

Smith E, Dent G (2005) *Modern Raman spectroscopy - a practical approach,* West Sussex, UK, John Wiley & Sons Ltd., 210pp.

Sommerdijk NAJM, de With G (2008) Biomimetic $CaCO_3$ mineralization using designer molecules and interfaces. *Chemical Reviews,* **108**, 4499-4550.

Sorauf J (1972) Skeletal microstructure and microarchitecture in scleractinian (Coelenterata). *Palaeontology,* **15**, 88-107.

Sorauf J, Jell JS (1977) Strucutre and incremental growth in the ahermatypic coral *Desmophyllum cristagalli* from the north Atlantic. *Palaeontology,* **20**, 1-19.

Sorokin Y, I (1990) Aspects of trophic relations, productivity and energy balance in coral-reef ecosystems. In: *Ecosystems of the World 25 Coral Reefs*. (ed Dubinsky Z) pp 401-410. Amsterdam, Elsevier Science Publishers.

Spalding M, Ravilious C, Green Ep (2001) World atlas of coral reefs. *University of California Press, Berkley, California, USA,* p 424.

Stanley SM (2006) Influence of seawater chemistry on biomineralization throughout phanerozoic time: Paleontological and experimental evidence. *Palaeogeography, Palaeoclimatology, Palaeoecology,* **232**, 214-236.

Stoddart DR (1969) Ecology and morphology of recent coral reefs. *Biological Reviews,* **44**, 433-498.

Stolarski J (2003) Three-dimensional micro- and nanostructural characteristics of scleractinian coral skeleton: A biocalcification proxy. *Acta Palaeontologica Polonica,* **48**, 497-530.

Stolarski J, Mazur M (2005) Nanostructure of biogenic versus abiogenic calcium carbonate crystals. *Acta Palaeontologica Polonica,* **50**, 847-865.

Storlazzi CD, Ogston AS, Bothner MH, Field ME, Presto MK (2004) Wave- and tidally-driven flow and sediment flux across a fringing coral reef: Southern Molokai, Hawaii. *Continental Shelf Research,* **24**, 1397-1419.

Storlazzi CD, Jaffe BE (2008) The relative contribution of processes driving variability in flow, shear, and turbidity over a fringing coral reef: West Maui, Hawaii. *Estuarine, Coastal and Shelf Science,* **77**, 549-564.

Storlazzi C, Field M, Bothner M (2011) The use (and misuse) of sediment traps in coral reef environments: theory, observations, and suggested protocols. *Coral Reefs,* **30**, 23-38.

Subrahmanyam B, Murty VSN, Sharp RJ, O'Brien JJ (2005) Air-sea coupling during the tropical cyclones in the Indian Ocean: A case study using satellite observations. *Pure and Applied Geophysics,* **162**, 1643-1672.

Susanto RD, Mitnik L, Zheng Q (2005) Ocean internal waves observed in the Lombok Strait. *Oceanography,* **18**, 81-87.

Suzuki A, Yokoyama Y, Kan H, Minoshima K, Matsuzaki H, Hamanaka N, Kawahata H (2008) Identification of 1771 Meiwa Tsunami deposits using a combination of radiocarbon dating and oxygen isotope microprofiling of emerged massive Porites boulders. *Quaternary Geochronology,* **3**, 226-234.

Szmant AM (1986) Reproductive ecology of Caribbean reef corals. *Coral Reefs,* **5**, 43-54.

Tanzil JTI, Brown BE, Tudhope AW, Dunne RP (2009) Decline in skeletal growth of the coral *Porites lutea* from the Andaman Sea, South Thailand between 1984 and 2005. *Coral Reefs*, **28,** 519-528.

Tambutte E, Allemand D, Zoccola D, Meibom A, Lotto S, Caminiti N, Tambutte S (2007) Observations of the tissue-skeleton interface in the scleractinian coral *Stylophora pistillata*. *Coral Reefs,* **26**, 517-529.

Tambutté S, Holcomb M, Ferrier-Pagès C, Reynaud S, Tambutté E, Zoccola D, Allemand D (2011) Coral biomineralization: From the gene to the environment. *Journal of Experimental Marine Biology and Ecology*, doi:10.10166/j.jembe.12011.10107.10026.

Taylor RB, Barnes DJ, Lough JM (1995) On the inclusion of trace materials into massive coral skeletons. 1. Materials occuring in the environment in short pulses. *Journal of Experimental Marine Biology and Ecology,* **185**, 255-278.

Thebault J, Chauvaud L, Clavier J, Fichez R, Morize E (2006) Evidence of a 2-day periodicity of striae formation in the tropical scallop *Comptopallium radula* using calcein marking. *Marine Biology,* **149**, 257-267.

Thorpe SA (1975) The excitation, dissipation, and interaction of internal waves in the deep ocean. *J. Geophys. Res.,* **80**, 328-338.

Thorpe SA (2007) *An introduction to ocean turbulence,* Cambridge, Cambridge University Press.

Todd PA (2008) Morphological plasticity in scleractinian corals. *Biological Reviews,* **83**, 315-337.

Tomczak M, Godfrey JS (1994) *Regional oceanography: An introduction,* Oxford, Pergamon Press.

Tribollet A, Golubic S (2011) Reef Bioerosion: Agents and Processes. In: *Coral Reefs: An Ecosystem in Transition*. (eds Dubinsky Z, Stambler N) pp 435-449. Springer Netherlands.

Tsounis G, Orejas C, Reynaud S, Gili J, Allemand D, Ferrier-Pagès C (2010) Preycapture rates in four Mediterranean cold water corals. *Marine Ecology Progress Series,* **398**, 149-155.

Urmos J, Sharma SK, Mackenzie FT (1991) Characterization of some biogenic carbonates with Raman-spectroscopy. *American Mineralogist,* **76**, 641-646.

van Woesik R, Done TJ (1997) Coral communities and reef growth in the southern Great Barrier Reef. *Coral Reefs,* **16**, 103-115.

Veron JEN (2000) *Corals of the World. Volume 1,* Townsville, Australian Institute of Marine Science.

Vlasenko V, Huttner K (2002) Numerical experiments on the breaking of solitary internal waves over a slope-shelf topography. *Journal of Physical Oceanography,* **32**, 1779-1793.

Vlasenko V, Alpers W (2005) Generation of secondary internal waves by the interaction of an internal solitary wave with an underwater bank. *Journal of Geophysical Research,* **110**, C02019, 1-16.

Vlasenko V, Stashchuk N (2007) Three-dimensional shoaling of large-amplitude internal waves. *Journal of Geophysical Research,* **112**, C11018, 1-15.

Waite J, Andersen O (1980) 3,4-dihydroxyphenylalanine (DOPA) and sclerotization of periostracum in *Mytilus edulis* L. *Biological Bulletin,* **158**, 164-173.

Wallace BC, Wilkinson DL (1988) Run-up of internal waves on a gentle slope in a two-layered system. *Journal of Fluid Mechanics,* **191**, 419-442.

Wang B, Ho L (2001) Rainy season of the Asian-Pacific Summer Monsoon. *Journal of Climate,* **15**, 386-398.

Wang Y-H, Dai C-F, Chen Y-Y (2007) Physical and ecological processes of internal waves on an isolated reef ecosystem in the South China Sea. *Geophysical Research Letters,* **34**, L18609.

Watabe N, Kingsley RJ (1989) Extra-, inter- and intracellular mineralization in invertebrates and algae. In: *Origin, evolution, and modern aspects of biomieralization in plants and animals*. (ed Crick Re) pp 209-223. New York, Plenum.

Watanabe T, Fukuda I, China K, Isa Y (2003) Molecular analyses of protein components of the organic matrix in the exoskeleton of two scleractinian coral species. *Comparative Biochemistry and Physiology B-Biochemistry & Molecular Biology,* **136**, 767-774.

Weber J (1973) Incorporation of strontium into reef coral skeletal carbonate. *Geochimica et Cosmochimica Acta,* **37**, 2173-2190.

Weber M, Lott C, Fabricius KE (2006) Sedimentation stress in a scleractinian coral exposed to terrestrial and marine sediments with contrasting physical, organic and geochemical properties. *Journal of Experimental Marine Biology and Ecology,* **336**, 18-32.

Webster P, Moore A, Loschnigg J (1999) Coupled ocean-atmosphere dynamics in the Indian Ocean during 1997-98. *Nature,* **401**, 356-360.

Weiner S, Dove PM (2003) An Overview of Biomineralization Processes and the Problem of the Vital Effect. *Reviews in Mineralogy and Geochemistry,* **54**, 1-29.

Wellington GM (1982) Depth zonation of corals in the Gulf of Panama: Control and facilitation by resident reef fishes. *Ecological Monographs,* **52**, 224-241.

Wenthworth C (1922) A scale of grade and class terms for clastic sediments. *Journal of Geology,* **30**, 377-392.

Wessel P, Smith WHF (1996) A global self-consistent, hierarchical, high-resolution shoreline database. *Journal of Geophysical Research*, **101**, 8741-8743.

West JM, Salm RV (2003) Resistance and Resilience to Coral Bleaching: Implications for Coral Reef Conservation and Management. *Conservation Biology,* **17**, 956-967.

Wheeler AP, Sikes CS (1984) Regulation of carbonate calcification by organic matrix. *American Zoologist,* **24**, 933-944.

Wolanski E, Pickard Gl (1983) Upwelling by internal tides and Kelvin waves at the continental shelf break on the Great Barrier Reef. *Australian Journal of Marine Resarch,* **34**, 65-80.

Wolanski E, Delesalle B (1995) Upwelling by internal waves, Tahiti, French Polynesia. *Continental Shelf Research,* **15**, 357-368.

Wolanski E, Colin P, Naithani J, Deleersnijder E, Golbuu Y (2004) Large amplitude, leaky, island-generated, internal waves around Palau, Micronesia. *Estuarine, Coastal and Shelf Science,* **60**, 705-716.

Wolanski E, Fabricius K, Spagnol S, Brinkman R (2005) Fine sediment budget on an inner-shelf coral-fringed island, Great Barrier Reef of Australia. *Estuarine, Coastal and Shelf Science,* **65**, 153-158.

Wood R (2001) Biodiversity and history of reefs. *Geology,* **36**, 251-263.

Woolfe Kj, Larcombe P (1999) Terrigenous sedimentation and coral reef growth: a conceptual framework. *Marine Geology,* **155**, 331-345.

Wu G, Zhang Y (1998) Tibetean plateau forcing and the timing of the monsoon onset over the South Asia and the South China Sea. *American Meterological Society,* **126**, 913-927.

Yamano HY, Hori KH, Yamauchi MY, Yamagawa OY, Ohmura AO (2001) Highest-latitude coral reef at Iki Island, Japan. *Coral Reefs,* **20**, 9-12.

Yamano H, Abe O, Matsumoto E, Kayanne H, Yonekura N, Blachon P (2003) Influence of wave energy on Holocene coral reef development: an example from Ishigaki Island, Ryukyu Islands, Japan. *Sedimentary Geology,* **159**, 27-41.

Yang Y-J, Tang TY, Chang MH, Liu AK, Hsu M-K, Ramp SR (2004) Solitons northeast of Tung-Sha Island during the ASIAEX Pilot studies. *IEEE Journal of Oceanic Engineering,* **29**, 1182-1199.

Yeemin T, Saenghaisuk C, Yucharoen M, Klingthong W, Sutthacheep M (2012) Impact of the 2010 coral bleaching event on survival of juvenile coral colonies in the Similan Islands, on the Andaman Sea coast of Thailand. *Phuket Mar Biol Cent Res Bull,* **70**, 93-102.

Young S (1971) Organic material from scleractinian coral skeletons -I. variation in composition between several species. *Comparative Biochemistry and Physiology, Part B: Biochemistry and Molecular Biology,* **40**, 113-120.

Zhang F, Cai W, Sun Z, Zhang J (2008) Regular variations in organic matrix composition of small yellow croaker (*Pseudociaena polyactis*) otoliths: an *in situ* Raman microspectroscopy and mapping study. *Analytical and Bioanalytical Chemistry,* **390**, 777-782.

Zhang FF, Cai WY, Zhu JC, Sun ZR, Zhang J (2011) *In situ* Raman spectral mapping study on the microscale fibers in Blue Coral (*Heliopora coerulea*) skeletons. *Analytical Chemistry,* **83**, 7870-7875.

5. APPENDIX

5.1 APPENDIX I:

Supplemental tables - 2.1 Publication I:

Table S1: Cruise schedules and tasks. Timetable for temperature logger, sediment trap and CTD deployments/exchanges at the core sampling sites (cf. Fig. 1).

cruis	date	temperature logger exchange	sediment trap exchange	sediment cores	CTD
Nov/Dec 2009	18.11-15.12	start	start		x
Jan 2010	15.-25.01	x	x	x	
Feb/Mar 2010	26.02-20.03	x	x	x	x
May 2010	19.-26.05.	x	x	x	
Jul/Aug 2010	26.07-01.08	x	x	x	
Nov/Dec 2010	30.11-12.12	x	x	x	
Mar 2011	17.-27.03.	x	x	x	
Aug 2011	23.-28.08	x			
Dec/Nov 2011	27.11-01.12	x			

Table S2: Bottom sediment mud content. Comparison of mud content (%) of bottom sediment samples (mean ± SE) between core sampling sites. Non-parametric test (Kruskal-Wallis One Way Analysis of Variance on Ranks) was performed with no differences between sites ($H = 5.682$, $df = 5$, $p = 0.338$).

sites	% weight mud
Miang E	4.64 ± 1.18
Miang W	3.65 ± 0.62
Bon W	2.75 ± 0.59
Tachai W	2.40 ± 0.44
Surin W	2.93 ± 0.57
Racha W	3.99 ± 1.14

Table S3: Comparison of temperature anomalies between seasons. Comparison of temperature anomalies (calculated as cummulative degree days) between seasons for each core sampling site (cf. Fig. 1). Non-parametric test (Wilcoxon rank test) was performed and test statistics are given (df = degrees of freedom, t = test-statistic and p = probability level, significance levels are: * $p < 0.05$, ** $p < 0.01$, *** $p < 0.001$).

sites	df	W	p
Miang E	10	0	***
Miang W	10	0	***
Bon W	10	0	***
Tachai W	10	0	***
Surin W	10	0	***
Racha W	10	0	***

Table S4: Comparison of temperature anomalies between sites during dry season. Analysis of Variance (ANOVA) for temperature anomalies (calculated as cumulative degree days) during the dry season between core sampling sites (cf. Fig. 1). Posthoc pair wise comparisons were performed via TukeyHSD-tests. (df = degrees of freedom; MS = means square; F = F-value; p = probability level, significance levels are: * p < 0.05, ** p < 0.01, *** p < 0.001).

Response	**df**	**MS**	**F**	**p**
Sites	5	90.51	5.796	***
Residuals	30	15.62		
TukeyHSD	Pairwise comparison			p
Miang E	>	Tachai W		***
Miang E	>	Miang W		**

Table S5: Comparison of bottom sediment grain size. Analysis of Variance (ANOVA) for bottom sediment grain size mean phi value between core sampling sites (cf. Fig. 1). Posthoc pair wise comparisons were performed via TukeyHSD-tests. (df = degrees of freedom; MS = means square; F = F-value; p = probability level, significance levels are: * p < 0.05, ** p < 0.01, *** p < 0.001).

Response	**df**	**MS**	**F**	**p**
Sites	5	1.321	5.91	***
Residuals	99	0.223		
TukeyHSD	Pairwise comparison			p
Miang E	>	Racha W		***
Miang E	>	Tachai W		**
Miang E	>	Miang W, Bon W		*
Surin W	>	Tachai W, Racha W		*

Table S6: Regression analysis of explanatory variables influencing reef framework height. General linear models conducted for reef framework height as dependent variable with environmental parameters (temperature anomaly, grain size, sedimentation rate) as independent variables. a) Framework height and environmental parameters derived from 6 core sampling sites and 2 additional sites (cf. Fig. 1). Parameters were quantified as: mean annual impact (Y) and maximum impact (max). Temperature anomaly maximum impact was calculated during the dry season in 2010 and 2011. (n = number of sites, r^2 = regression coefficient, p = probability level, significance levels are: * p < 0.05, ** p < 0.01, *** p < 0.001).

General linear model (Fig. 5 & 6):						
Frame~Environmental parameters of annual mean impact (Y) or max impact (max)						
Environmental parameters	df	F-statistic	t-value (slope)	n	r^2	p
Temperature anomaly (Y)	4	8.353	2.89	6	0.68	0.045
Temperature anomaly (max)	4	7.249	2.7	6	0.64	0.055
Temperature anomaly (Y)*)	6	20.27	4.502	8	0.77	0.004
Temperature anomaly (max 2010) *)	6	18.48	4.298	8	0.75	0.005
Grain size (Y)	4	16.56	4.069	6	0.81	0.015
Grain size (max)	4	20	4.472	6	0.83	0.011
Sedimentation (Y)	4	1.512	-1.229	6	0.27	0.286
Sedimentation (max)	4	1.572	-1.254	6	0.28	0.278
Temperature anomaly (max 2011) *)	6	20.57	4.536	8	0.77	0.004
Temperature anomaly (max) + Sedimentation (max):	3	4.715		6	0.76	0.119
Temperature anomaly (max)			2.434			0.093
Sedimentation max			-1.191			0.319
Grain size max + Sedimentation max:	3	12.21		6	0.89	0.036
Grain size max			4.085			0.027

Sedimentation max			-1.254			0.299
Temperature anomaly (max) + Grain size (max)	3	54.84		6	0.97	0.004
Temperature anomaly (max)			-3.973			0.029
Grain size (max)			6.088			0.009

*) including core sampling sites plus additional sites from Schmidt *et al*. (2012).

5.2 APPENDIX II

Supplemental figures - 2.2 Publication II:

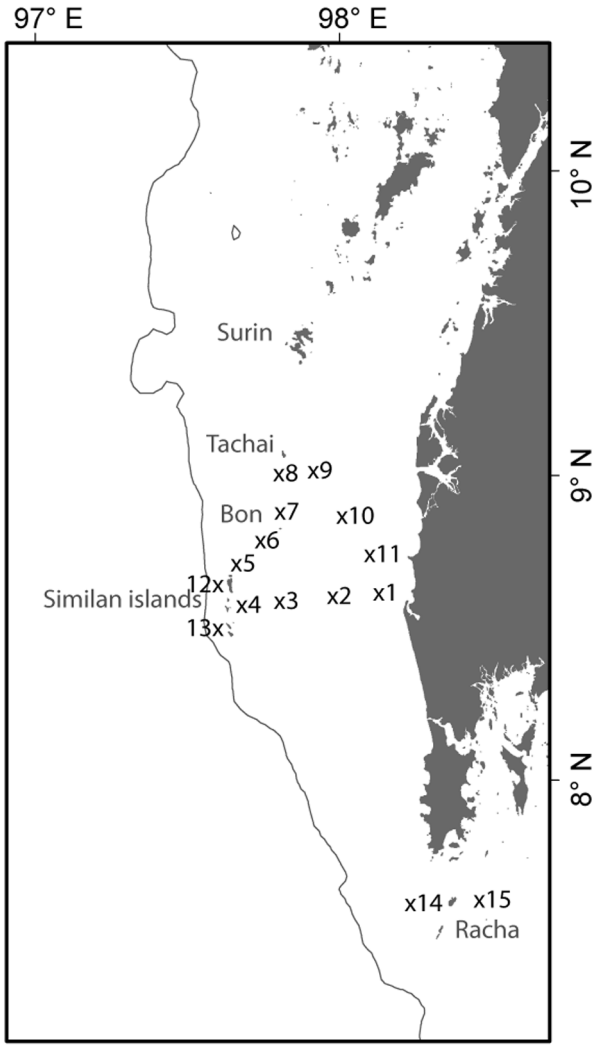

Figure S1: Location of CTD profile measured within the study area, Andaman Sea, Thailand. Locations are marked with x and the number indicates the CTD profile displayed in Figure S3,S4. Contour line indicates 200 m depth.

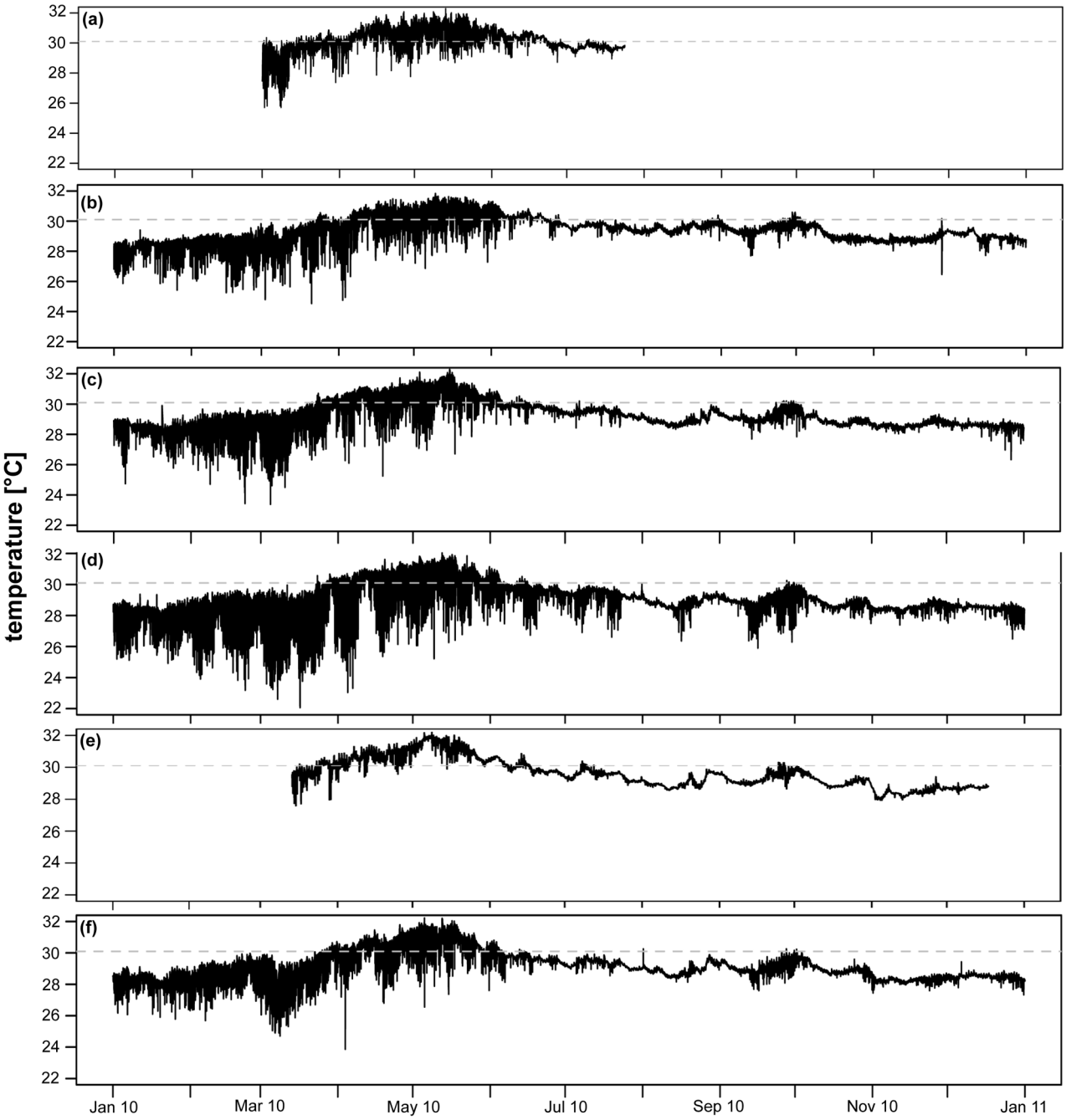

Figure S2: Temperature record for study sites during the study period. Temperature record during the bleaching year 2010 derived for six sites ((a) Racha East, (b) Racha West, (c) Bon West, (d) Tachai West, (e) Surin East and (f) Surin West) measured at 15 m water depth expect Racha East temperature record derived from 20 m water depth. Grey line indicates the bleaching threshold temperature for coral reefs in this region (30.1°C, cf. Brown et al. 1996).

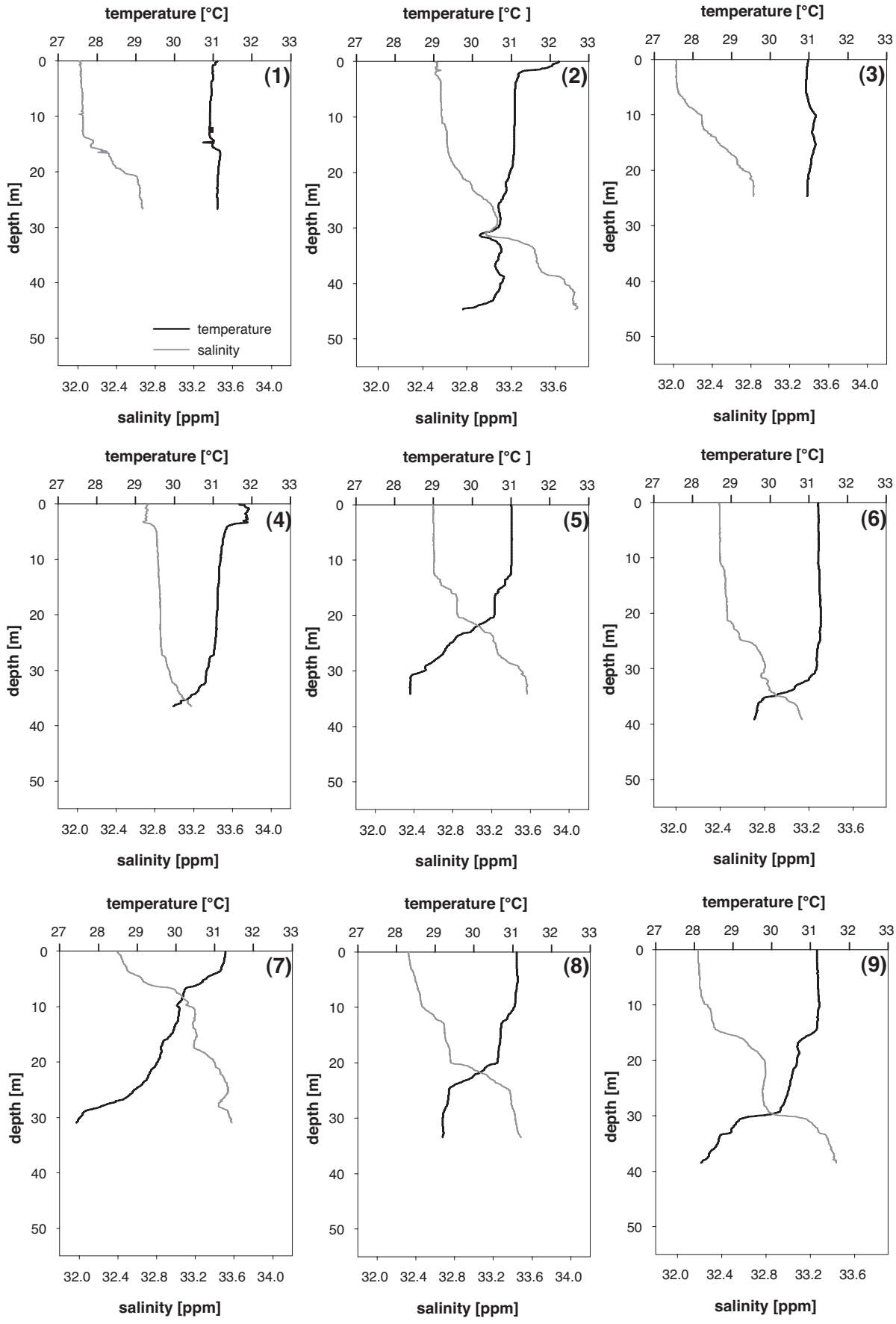

Figure S3: CTD profiles measured within the study area, Andaman Sea, Thailand. Graphs display the change of temperature (black line) and salinity (grey line) with depth. Numbers in parenthesis refer to the location the

profile was taken and corresponds to the numbers displayed in the map (Figure S3). (1)-(4) were taken at the 19th of May 2010. (5)-(8) were taken at the 22nd of May 2010. (9) was taken at the 23rd of May 2010.

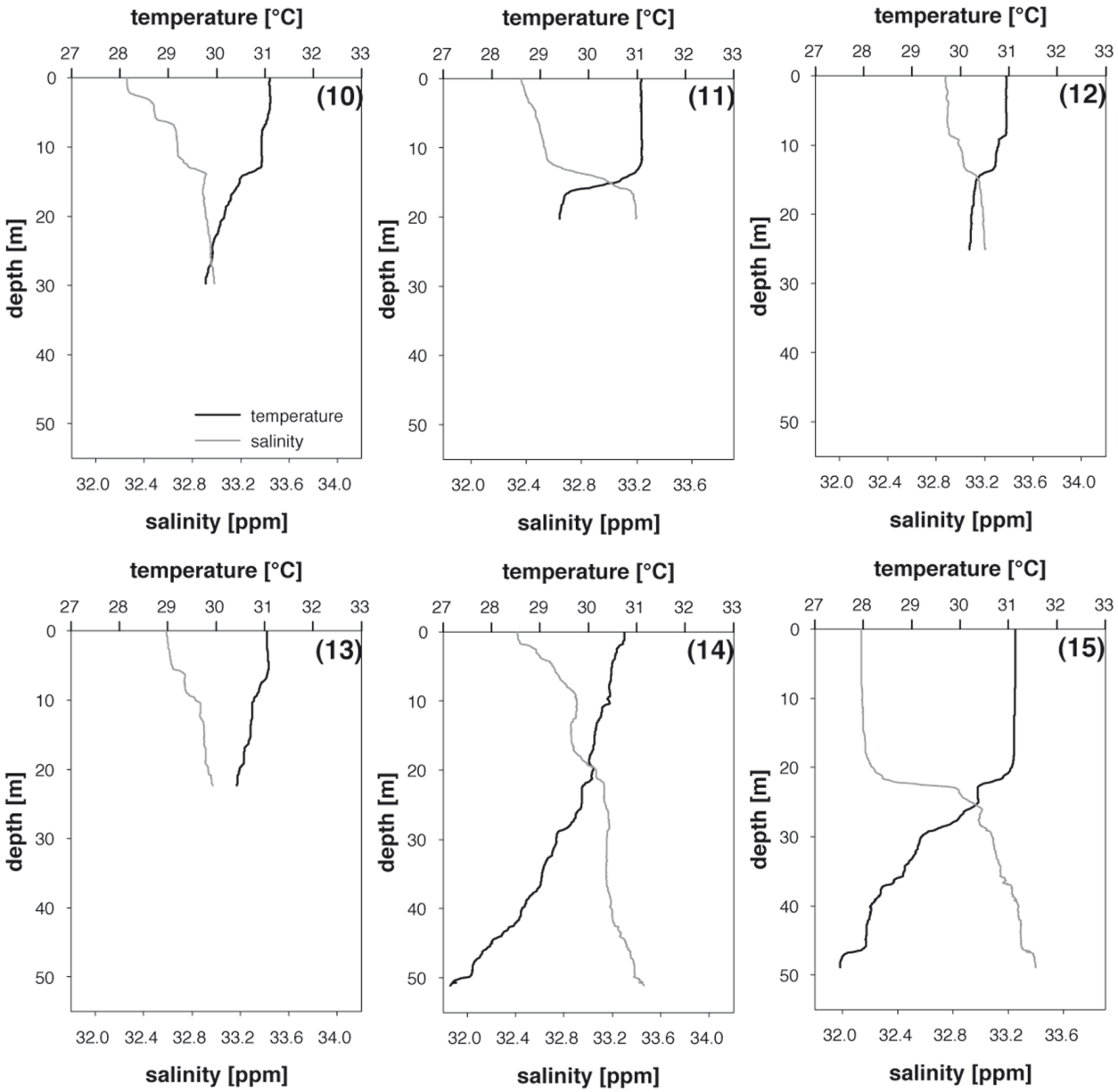

Figure S4: CTD profiles measured within the study area, Andaman Sea, Thailand. Graphs display the change of temperature (black line) and salinity (grey line) with depth. Numbers in parenthesis refer to the location the profile was taken and corresponds to the numbers displayed in the map (Figure S3). (10)-(11) were taken at the 23rd of May 2010. (12)-(13) were taken at the 24th of May 2010 and (15)-(16) were taken at the 26th of May 2010.

5.3 APPENDIX III

Supplemental figure - 2.3 Publication III:

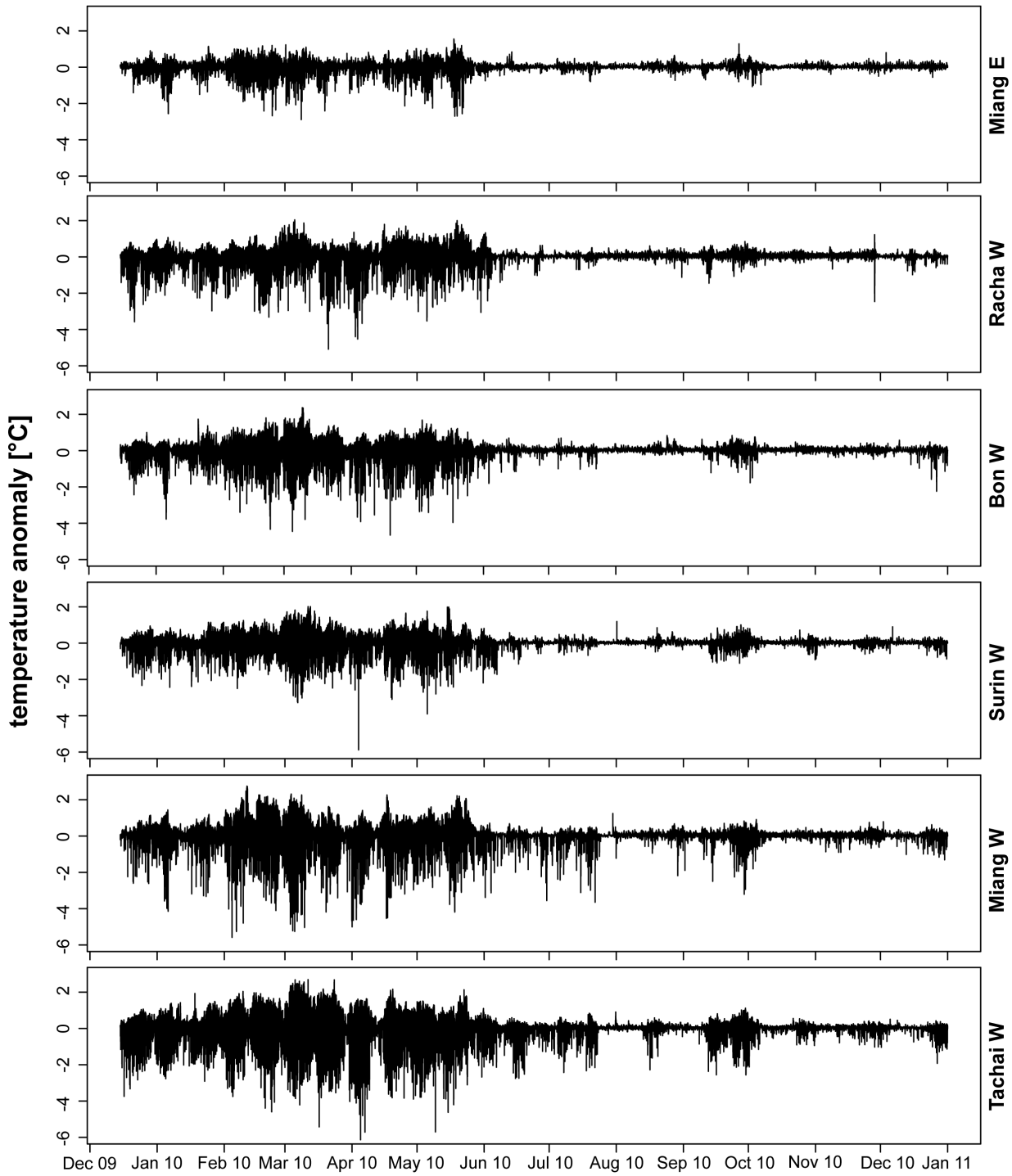

Figure S1: Temperature anomalies for the study sites. Temperature anomaly values displayed for the six study sites (Miang E, Miang W, Bon W, Tachai W, Surin W, Racha W) and one year of data collection. Temperature was recorded in approx. 15 m water depth.

ACKNOWLEDGEMENTS

„Wilhelmine Tell“ bedankt sich insbesondere bei ihrem Lehrmeister (Claudio Richter), dass er ihr gezeigt hat, wie der Bogen zu spannen ist, sich der Pfeil klar auf das Ziel zubewegt und den Apfel trifft ;). Ich möchte mich auch dafür bedanken, dass Du mir den notwendigen Freiraum gegeben hast, um sehr viele unterschiedliche Bereiche zu entdecken, und es mir ermöglicht hast, meine Forschungsvorhaben umzusetzten. Ich habe in der Zeit unter Deinen Fittichen sehr viele wertvolle Einblicke erhalten und so vieles gelernt, dass sich gar nicht alles in Worte fassen lässt! Daung da sche!

Lieber Gernot, vielen Dank, dass Du mich in die Welt der Biomineralisation eingeführt hast und ich in Deinem Lab mit den diversesten Instrumenten die wundervollen Kristallstrukturen (nicht nur) der Korallen entdecken durfte. Vielen Dank auch für die vielen wertvollen Diskussionen über Kalzifizierung, Raman und vieles mehr.

A special thanks goes to Dr. Somkiat Khokkiatiwong who supported this work in so many ways – by providing logistics and helpful staff, by discussing my work and data. Thank you very much for giving me the chance to work with you and your team in Thailand!

Another big thanks goes to Dr. Somkiats team (Nueng, Jaa, Eak, Ebb, Bab) for all their help in Thailand. In particular, I would like to thank Nueng for her effort to organize everything in Thailand for me and for making every cruise a wonderful experience.

Ich möchte mich auch bei Christian Wild für die Begutachtung meiner Doktorarbeit bedanken, sowie bei Kai Bischof und Tim Rixen, die sich kurzfristig bereiterklärt haben, als Prüfer zu fungieren.

Liebe Gertraud und Carin, ohne Euch zwei wäre vieles nicht möglich gewesen. Danke, dass Ihr mir immer mit Rat und Tat zur Seite gestanden seid, und für die viele Zeit, in der wir Ideen und Ansichten austauschen konnten. Es waren tolle 3 Jahre der Zusammenarbeit mit Euch am AWI und ich hoffe, es werden noch viele weitere Jahre folgen.

Verena, vielen Dank für Dein offenes Ohr, Deine moralische Unterstützung, die vielen Skypediskussionen über Korallenwachstum, -physiologie und -kalzifizierung und Deine vielen wertvollen Kommentare, Vorschläge und Verbesserungen meiner Arbeit.

Liebe Laura, merci beaucoup für die vielen schönen Abende und die tolle Zeit in Bremerhaven. Auch möchte ich mich für die viele Unterstützung, die ich − insbesondere in der letzten Zeit − von Dir erhalten habe, bedanken.

Dear Nan, thanks for all the great time we spent on ships, in Phuket, Bremen and Bremerhaven. I wish you all the best for your PhD at the AWI and in Hawaii and I hope we will have the time to do a cruise together again.

The Thai field trip teams of Master students and student assistants (Marc, Svenaja, Marco, Ann, Gunilla, Cesar, Patrick) made the time in Thailand on land and on sea to an unforgettable experience. Thank you so much!

Tobias, vielen Dank für Deinen Einsatz bzgl. der technischen Ausstattung auf Feldreisen und dafür, dass du mir stets mit Rat und Tat zur Seite gestanden bist, wenn mal was nicht so klappen wollte, wie es sollte!

Lieber Jürgen, vielen Dank, dass Du mit Deiner Erfahrung als Taucheinsatzleiter und mit oftmals sehr spontanen Einsätzen in Thailand immer für einen reibungslosen Ablauf der Taucheinsätze gesorgt hast.

Liebe Ruth, danke, dass Du Dir die Zeit genommen hast, meine Doktorarbeit Korrektur zu lesen.

Ulla, vielen Dank für Deine große Unterstützung am AWI!

Ich bedanke mich bei meinen Kollegen der Bentho-Pelagischen Prozesse, die mich in ihre Sektion aufgenommen und in vielen Belangen unterstützt haben.

All the Bachelor, Master and PhD students (Shobit, Chen, Chris, Steffi, Nan, Felix, Carla) that passed by the room 2400 – it's the best room in the building and it was a pleasure to share it with all of you! Thank you so much for the wonderful time we had!

Franzi und Katrin, Euch danke ich dafür, dass ihr Teile meiner Arbeit unterstützt habt, als HIWIs bzw für die Bachelorarbeit.

Weiters möchte ich mich bei jenen Personen, bei denen ich Messungen durchführen konnte, diverse Geräte verwenden durfte und die mir statistischen Beistand leisteten, vielmals bedanken: Kerstin Beyer, Ute Bock, Friedl Hinz, Johannes Freitag, Michael Seebeck, Kai-Uwe Ludwichowski, Laura Wischnewski, Stephan Frickenhaus. Vielen Dank!

Den Koordinatoren, Sprechern, Post-Docs und Doktoranden des Marie Curie Initial Training Networks Calmaro und des Graduiertenkollegs GLOMAR danke ich für die Unterstützung in Form von Organisationen von Workshops, Kursen und wissenschaftlichen Diskussionen.

Thank you ladies, Laura and Fede, for introducing me to the world of synchrotron – it was an amazing experience! I am looking forward to the next beam shifts with you and the cookie monster ;-).

Ich möchte mich auch bei meiner Familie und meinen Freunden bedanken, die immer ein offenes Ohr hatten und mich in meiner Berufswahl immer bestärkt und auch unterstützt haben.

Die Doktorandin wurde ausgestattet von Ulla und Katie Liebert ☺!

Erklärung gemäß § 6 Abs. 5 der Promotionsordnung der Universität Bremen

(für die mathematischen, natur- und ingenieurwissenschaft- lichen Fachbereiche)

Hiermit versichere ich, dass ich

1. die vorliegende Arbeit ohne unerlaubte fremde Hilfe angefertigt habe,
2. keine anderen als die von mir angegebenen Quellen und Hilfsmittel benutzt habe und
3. die den benutzen Werken wörtlich oder inhaltlich entnommenen Stellen als solche kenntlich gemacht habe.

Bremen, den 28.08.2012

Marlene Wall